VOLUME 32 | SUPPLEMENT 2 | MARCH 2019

MODERN PATHOLOGY

USCAP 2019

ABSTRACTS

HEMATOPATHOLOGY
(1234-1434)

USCAP 108TH ANNUAL MEETING

UNLOCKING YOUR INGENUITY

MARCH 16-21, 2019

National Harbor, Maryland
Gaylord National Resort & Convention Center

Published by
SPRINGER NATURE
www.ModernPathology.org

USCAP Creating a Better Pathologist
AN OFFICIAL JOURNAL OF THE UNITED STATES AND CANADIAN ACADEMY OF PATHOLOGY

EDUCATION COMMITTEE

Jason L. Hornick, Chair
Rhonda K. Yantiss, Chair, Abstract Review Board and Assignment Committee
Laura W. Lamps, Chair, CME Subcommittee
Steven D. Billings, Interactive Microscopy Subcommittee
Shree G. Sharma, Informatics Subcommittee
Raja R. Seethala, Short Course Coordinator
Ilan Weinreb, Subcommittee for Unique Live Course Offerings
David B. Kaminsky (Ex-Officio)
Aleodor (Doru) Andea
Zubair Baloch
Olca Basturk
Gregory R. Bean, Pathologist-in-Training
Daniel J. Brat
Ashley M. Cimino-Mathews
James R. Cook
Sarah M. Dry
William C. Faquin
Carol F. Farver
Yuri Fedoriw
Meera R. Hameed
Michelle S. Hirsch
Lakshmi Priya Kunju
Anna Marie Mulligan
Rish Pai
Vinita Parkash
Anil Parwani
Deepa Patil
Kwun Wah Wen, Pathologist-in-Training

ABSTRACT REVIEW BOARD

Benjamin Adam
Michelle Afkhami
Narasimhan (Narsi) Agaram
Rouba Ali-Fehmi
Ghassan Allo
Isabel Alvarado-Cabrero
Christina Arnold
Rohit Bhargava
Justin Bishop
Jennifer Boland
Elena Brachtel
Marilyn Bui
Shelley Caltharp
Joanna Chan
Jennifer Chapman
Hui Chen
Yingbei Chen
Benjamin Chen
Rebecca Chernock
Beth Clark
James Conner
Alejandro Contreras
Claudiu Cotta
Timothy D'Alfonso
Farbod Darvishian
Jessica Davis
Heather Dawson
Elizabeth Demicco
Suzanne Dintzis
Michelle Downes
Daniel Dye
Andrew Evans
Michael Feely
Dennis Firchau
Larissa Furtado
Anthony Gill
Ryan Gill
Paula Ginter
Tamara Giorgadze
Raul Gonzalez
Purva Gopal
Anuradha Gopalan
Jennifer Gordetsky
Rondell Graham
Alejandro Gru
Nilesh Gupta
Mamta Gupta
Krisztina Hanley
Douglas Hartman
Yael Heher
Walter Henricks
John Higgins
Mai Hoang
Mojgan Hosseini
Aaron Huber
Peter Illei
Doina Ivan
Wei Jiang
Vickie Jo
Kirk Jones
Neerja Kambham
Chiah Sui (Sunny) Kao
Dipti Karamchandani
Darcy Kerr
Ashraf Khan
Rebecca King
Michael Kluk
Kristine Konopka
Gregor Krings
Asangi Kumarapeli
Alvaro Laga
Cheng-Han Lee
Zaibo Li
Haiyan Liu
Xiuli Liu
Yan-Chun Liu
Tamara Lotan
Anthony Magliocco
Kruti Maniar
Jonathan Marotti
Emily Mason
Jerri McLemore
Bruce McManus
David Meredith
Anne Mills
Neda Moatamed
Sara Monaco
Atis Muehlenbachs
Bita Naini
Dianna Ng
Tony Ng
Ericka Olgaard
Jacqueline Parai
Yan Peng
David Pisapia
Alexandros Polydorides
Sonam Prakash
Manju Prasad
Peter Pytel
Joseph Rabban
Stanley Radio
Emad Rakha
Preetha Ramalingam
Priya Rao
Robyn Reed
Michelle Reid
Natasha Rekhtman
Michael Rivera
Michael Roh
Andres Roma
Avi Rosenberg
Esther (Diana) Rossi
Peter Sadow
Safia Salaria
Steven Salvatore
Souzan Sanati
Sandro Santagata
Anjali Saqi
Frank Schneider
Jeanne Shen
Jiaqi Shi
Wun-Ju Shieh
Gabriel Sica
Deepika Sirohi
Kalliopi Siziopikou
Lauren Smith
Sara Szabo
Julie Teruya-Feldstein
Gaetano Thiene
Khin Thway
Rashmi Tondon
Jose Torrealba
Evi Vakiani
Christopher VandenBussche
Sonal Varma
Endi Wang
Christopher Weber
Olga Weinberg
Sara Wobker
Mina Xu
Shaofeng Yan
Anjana Yeldandi
Akihiko Yoshida
Gloria Young
Minghao Zhong
Yaolin Zhou
Hongfa Zhu
Debra Zynger

1234 Flow Cytometric Assessment of CD10 as a Surrogate for Immunohistochemistry in Cell of Origin (COO) Subtyping of Diffuse Large B-cell Lymphoma (DLBCL)

Daniel Abbott[1], Luis Carrillo[2], Steven Kroft[3], John Astle[3], Ashley Cunningham[4], Alexandra Harrington[2]
[1]Medical College of Wisconsin Affiliated Hospitals, Milwaukee, WI, [2]Milwaukee, WI, [3]Medical College of Wisconsin, Milwaukee, WI, [4]Medical College of Wisconsin, Oconomowoc, WI

Disclosures: Daniel Abbott: None; Luis Carrillo: None; Steven Kroft: None; Ashley Cunningham: None; Alexandra Harrington: None

Background: COO subtyping is required at diagnosis of DLBCL by the 2016 WHO classification. This is most commonly performed by the Hans algorithm, which utilizes immunohistochemistry (IHC). Some laboratories routinely use flow cytometry (FC) for assessment of CD10 expression, but this method has not been formally validated as a surrogate technique for the purposes of COO subtyping.

Design: Diagnostic DLBCL cases with accompanying FC studies were retreived over a 10 year period, yielding 111 cases. These were evaluated by either 4- (26 cases) or 8-color (85 cases) FC using antibodies to CD5, CD10, CD19, CD20, CD23, CD38, FMC-7, and surface immunoglobulin in most cases. CD10 expression was assessed as the percentage of events exceeding a 2% isotypic control threshold. CD10 expression by IHC was assessed as the percentage of positive staining cells. Per the Hans algorithm, cases with at least 30% of cells staining were considered to be CD10 positive by IHC.

Results: There were 63 men and 48 women (age range 26-90 years, median 67 years). The most common locations were soft tissue (n=35; 32%), lymph nodes (n=22; 21%), and brain (n=11; 10%). FC demonstrated a clonal B-cell population in all cases, which constituted 0.04-87.6% of events (median 8.8%). CD10 IHC and FC showed a strong positive correlation (r=0.864; Figure 1). CD10 FC ROC curve showed an area under the curve (AUC) of 0.957+/-0.018 with a 95% confidence interval (CI) of 0.921-0.992 (p<0.001; Figure 2). An optimal cut-off value for CD10 positivity based on FC was determined to be >15% of events (89.4% sensitivity, 86.7% specificity compared to IHC). Based on this cut-off value, 59 cases (53%) were positive by both FC and IHC and 39 cases (35%) were negative for both FC and IHC. There were 13 discordant cases (12%), of which 6 were IHC negative/FC positive and 7 were IHC positive/FC negative (Table 1).

Table 1. Discordant cases between FC and IHC (n=13)

CD10 FC(%)	CD10 IHC(%)
4.1	35
4.9	85
7.9	45
8.2	55
11.9	70
12.4	75
14.1	75
16.1	5
16.3	2
17.3	1
32.1	1
47.7	1
88.7	5

Figure 1 - 1234

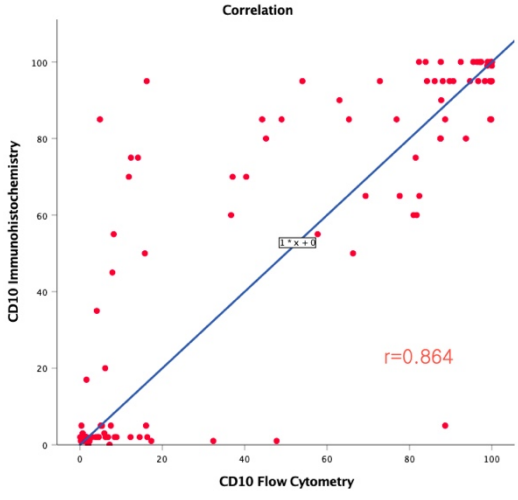

Figure1. Correlation between CD10 immunohistochemistry and CD10 flow cytometry. (n=111; r=0.864)

Figure 2 - 1234

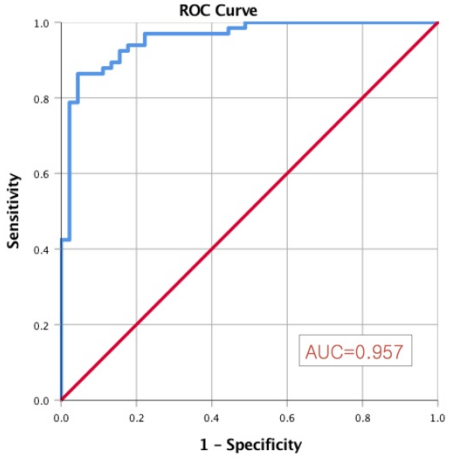

Figure2. CD10 flow cytometry receiver operating characteristic (ROC) curve (AUC=0.957+/−0.018; 95% CI, 0.921−0.992, p<0.001)

Conclusions: Our findings demonstrate that CD10 assessment by FC and IHC are strongly correlated in DLBCL. However, using an optimized FC cutoff, 12% of cases were discordant. Laboratories that routinely employ FC in lieu of IHC for assessment of CD10 should be aware that these methods are not entirely comparable for the purposes of COO subtyping.

1235 Presence of t(14;18)(q32;q21)/IGH-BCL2 Imparts Worse Prognosis in Grade 3B Follicular Lymphoma

Mustafa Abdulrazzaq[1], Valentina Fabiola Sangiorgio[2], Roberto Miranda[1], Tariq Muzzafar[1], Joseph Khoury[1], L. Jeffrey Medeiros[1], Ali Sakhdari[3]
[1]The University of Texas MD Anderson Cancer Center, Houston, TX, [2]Istituto Europeo di Oncologia, Milan, Italy, [3]Houston, TX

Disclosures: Mustafa Abdulrazzaq: None; Valentina Fabiola Sangiorgio: None; Roberto Miranda: None; Tariq Muzzafar: None; Joseph Khoury: None; L. Jeffrey Medeiros: None; Ali Sakhdari: None

Background: Follicular lymphoma (FL) grade 3B has clinical, immunophenotypic and genetic features that are distinct from other FL varieties, and it is considered more closely related to diffuse large B-cell lymphoma (DLBCL). The t(14;18)(q32;q21)/*IGH-BCL2* is a hallmark of FL, present in 80-90% of low-grade cases but in only ~50% of grade 3B FL. In DLBCL, recent studies have shown a poorer prognosis for patients with germinal-center B-cell like (GCB-like) DLBCL that harbor t(14;18)(q32;q21)/*IGH-BCL2* compared to patients with GCB-like DLBCL without this translocation (Nature Medicine, 2018, N Engl J Med 2018); however, the prognostic significance of t(14;18)(q32;q21)/*IGH-BCL2* in patients with grade 3B FL remains unknown. In this study, we assessed the t(14;18)(q32;q21)/*IGH-BCL2* status in grade 3B FL patients and correlated the findings with clinical, morphologic and genetic data.

Design: We searched our institutional database for all patients with grade 3B FL treated between [06/2001 – 01/2018] and on whom the t(14;18)(q32;q21)/*IGH-BCL2* was known through conventional cytogenetics and/or fluorescence in situ hybridization. Clinical and laboratory data were obtained through electronic medical record reviews.

Results: The study group included 78 patients [median age: 58 years (range: 12 – 81), 40 men and 38 female]. The t(14;18)(q32;q21)/*IGH-BCL2* was detected in 38 patients (**group A**) and absent in 40 patients (**group B**). There were 21 men and 17 women in group A and 19 men and 21 women in group B. The median age at diagnosis for patients in group A was 60 years (range: 37 – 78) and in group B was 57 years (range: 12 – 81). In groups A and B, 8 (21%) and 2 (5%) patients showed focal areas of low-grade FL (p=0.04) whereas DLBCL was identified in 24 (65%) and 20 (50%) patients in groups A and B, respectively (p=0.26). BCL2 expression was present in 100% (33/33) of group A and 61% (22/36) of group B (p=0.001). The median follow-up for groups A and B was 44 months (range: 0 - 198) and 42 months (range: 1.5 – 237), respectively. The median overall survival for group A was 161 months and not reached for group B (figure 1). The median progression-free survival for groups A and B were 66 and 92 months, respectively (figure 2).

Figure 1 - 1235

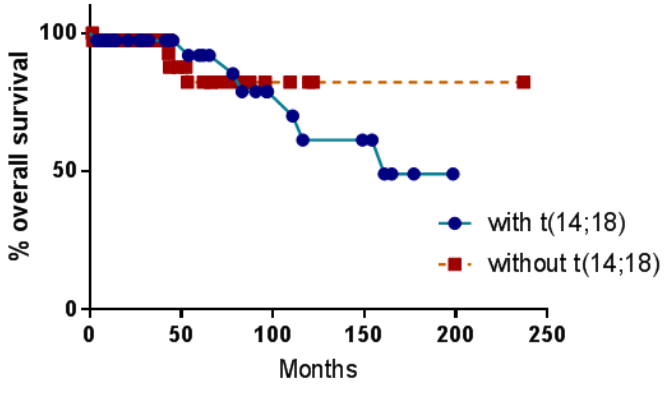

Figure 2 - 1235

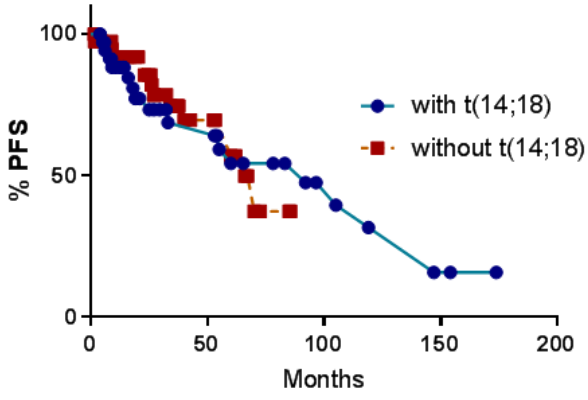

Conclusions: t(14;18)/*IGH-BCL2* was seen in 49% of grade 3B FL cases in this cohort. The presence of t(14;18)/*IGH-BCL2* is associated with the presence of a low-grade FL component and strong BCL2 expression and there appears to be a trend toward worse overall and progression-free survival.

1236 Use of Children's Oncology Group (COG)-Validated Minimal/Measurable Residual Disease Flow Cytometry (MRD-FC) for Adults with B-lymphoblastic leukemia (B-ALL): An Institutional Experience

Brooj Abro[1], Cara Shirai[2], Yi-Shan Lee[3], John Frater[1], Marianna Ruzinova[3], Anjum Hassan[2], Yvette Kudlinski[2], Barbara Weddle[2], Friederike Kreisel[1]
[1]Washington University, St. Louis, MO, [2]Washington University in St. Louis, St. Louis, MO, [3]Washington University School of Medicine in St. Louis, St. Louis, MO

Disclosures: Brooj Abro: None; Cara Shirai: None; Yi-Shan Lee: None; John Frater: None; Marianna Ruzinova: None; Anjum Hassan: None; Yvette Kudlinski: None; Barbara Weddle: None; Friederike Kreisel: None

Background: Our institution routinely employs COG-validated B-ALL MRD-FC for the detection of MRD in adults. Here, we compare aberrant antigen expression in adult B-ALL to pediatric B-ALL and assess the frequency of immunophenotypic shifts in patients (pts) with multiple MRD-FC. Also, we report on adjustments to the assay to include antigens amenable to immunotherapy.

Design: Antibodies used in the COG-validated assay were CD19, CD20, CD10, CD38, CD9, CD45, CD58, CD13/CD33, CD34, CD71, and CD3. A fourth tube with CD22 and CD123 was added to the panel to assess for immunotherapy suitability. At least 1 million events per tube were acquired. Data were acquired on Beckman Coulter NAVIOS flow cytometers, and Kaluza software was used for analysis. The Different-from-Normal analysis approach was employed, and the proportion of leukemia cells was calculated as % of mononuclear cells. Fisher's exact test to compare proportions was used for all statistical analyses.

Results: 289 bone marrow aspirates were submitted for MRD-FC in a 14-month period. Of these, 78 cases from 44 pts showed residual disease (27%; 34 adults and 10 children) ranging from 0.01% to >90% with 43 cases (55%) showing levels <5%. 14 adults and 4 children had multiple MRD-FC performed. Frequency of aberrant CD19 (27% vs. 56%, p=0.04), CD20 (40% vs. 6%, p=0.02), and side scatter (SS) (53% vs. 25%, p=0.05) expression were significantly different between adult and pediatric cases (shown respectively), while abnormal CD10 (94% vs. 88%, p=0.6), CD38 (77% vs. 63%, p=0.3), CD58 (69% vs. 75%, p=0.7), CD9 (92% vs. 88%, p=0.6), CD34 (79% vs. 81%, p= 1.0), CD45 (52% vs. 69%, p= 0.3), and CD13/CD33 (16% vs. 18%, p=0.7) expression did not differ between the two groups. All cases were positive for CD22, while ~50% were positive for CD123 (47% vs. 50%, p=1.0). Over-expression was the most common immunophenotypic aberrancy for CD10, CD58, and CD34; under-expression was more common for CD38, CD9, and CD20. Furthermore, 15/18 pts with multiple MRD-FC had at least 1 immunophenotypic shift; the most common were CD20 and CD19 (both 7/18, 39%) and CD58 (5/18 pts, 28%).

Conclusions: We show the COG-validated assay can be successfully applied to the broader adult population and can be used to measure any extent of disease burden. Also, inclusion of additional markers (CD22 and CD123) for clinical decision-making increases therapeutic options for pts. Finally, we observe the frequencies of CD19, CD20, and SS aberrancies differ between adult and pediatric B-ALL.

1237 Differential expression of DNA damage response (DDR) genes between Follicular lymphoma (FL) and Diffuse Large B-cell Lymphoma (DLBCL)

Ariz Akhter[1], Adnan Mansoor[1], Etienne Mahe[1], Meer-Shabani Taher-Rad[2], Carolyn Owen[1], Douglas Stewart[1]
[1]University of Calgary, Calgary, AB, [2]University of Calgary/Calgary Laboratory Services, Calgary, AB

Disclosures: Ariz Akhter: None; Adnan Mansoor: None; Etienne Mahe: None

Background: Defective DDR can promote genetic instability while heightened DDR can compromise therapeutic efficacy of DNA damaging drugs. Inhibitors of DNA repair molecules have proven beneficial in the treatment of BRCA1 and 2 associated breast and ovarian cancers. ('via the process termed 'synthetic lethality). Although DNA repair mechanisms are fundamental for B cell development, information on DDR activity in lymphoma is sparse. The objective of this pilot project was to investigate the gene expression pattern (GEP) for various molecules linked with DDR in a large series of DLBCL samples in comparison with FL; to determine whether the principles of synthetic lethality may also be applicable for the management of common lymphomas.

Design: nCounter PanCancer Pathway panel by Nanostring technologies was employed to determine GEP utilizing RNA from diagnostic biopsies (FFPE) in a large cohort (n=152) of follicular lymphoma (FL) and diffuse large B-cell lymphoma (DLBCL) samples. Normalized logarithmic data was analyzed for Hierarchical clustering exploiting strict statistical filters (p-value < 0.01, a false-discovery rate q-value < 0.01, fold change >2.5).

Results: Hierarchical clustering defined distinct pattern of GEP between DLBCL and FL samples (Fig. 1&2) in relation to DDR pathways and apoptosis genes. A total of nine DNA repair genes were highly expressed in DLBCL compared to FL (Table1). No correlation was observed between GEP for DDR pathway genes and cell of origin (ABC vs. GCB subtypes) in DLBCL samples. Majority of genes connected with apoptosis were suppressed among DLBCL samples in comparison to FL.

Gene	p-value	q-value	Fold change
FEN1	2.17E-35	5.78E-34	3.2
POLD1	1.90E-49	1.63E-47	3.7
BRCA1	4.24E-33	9.94E-32	2.6
CDC25A	1.17E-32	2.44E-31	4.1
CHEK1	6.15E-39	2.27E-37	4.0
E2F1	1.44E-37	4.12E-36	4.6
FANCA	8.05E-24	7.99E-23	3.9
PCNA	3.59E-50	3.47E-48	3.7
RAD51	1.71E-32	3.23E-31	6.5

Figure 1 - 1237

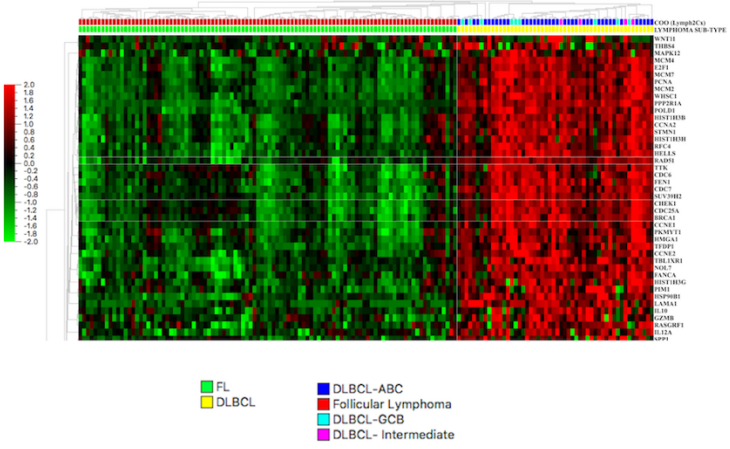

Figure 2 - 1237

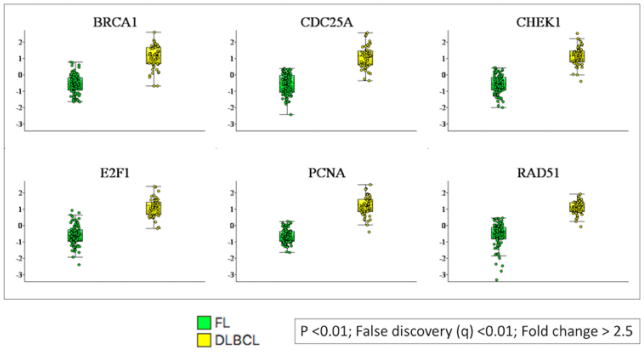

Conclusions: Our data show that numerous DDR molecules involving the checkpoint kinase (Chks) pathway genes are over-expressed in DLBCL, without correlation with COO subtype. Our data provide support for investigating the inclusion of inhibitors of DNA repair molecules to current DLBCL protocols to exploit synthetic lethality.

1238 A Simple Flow Cytometry Algorithm Incorporating CD177 to Predict Myelodysplastic Syndrome

Khaled Alayed[1], Howard Meyerson[2]
[1]King Saud University, Case Western Reserve University, University Hospitals/Case Medical Center, Aurora, OH, [2]University Hospital Case Medical Center, Cleveland, OH

Disclosures: Khaled Alayed: None; Howard Meyerson: None

Background: Previously we reported decreased CD177 on granulocytes correlates with MDS. The aim of the study was to determine whether CD177 and other FC parameters could be used to develop a simple FC algorithm for MDS diagnosis to improve upon previous FC scoring methods for MDS such as the Ogata score.

Design: 100 patients with MDS and 94 controls (patients >50 years old with cytopenia and no evidence of MDS on bone marrow biopsy) were identified by review of electronic medical records. Bone marrow samples were retrospectively evaluated for 12 FC parameters associated with MDS including CD177 and those based on previous studies by Ogata and the IMDSFlow Working Group. Parameters were: [1] myeloblast cluster size (CD34+CD117+ %), [2] myeloblast CD45 expression (mean fluorescent intensity (MFI) of CD45 on myeloblasts/lymphocytes), [3] CD177+ (%) on CD16+CD11b+ granulocytes, [4] CD10 level (granulocyte CD16+CD11b+(%)/CD10+(%)), [5] granulocyte CD56 expression (>10%), [6] granulocyte side scatter (SSC) (mean SSC granulocytes/lymphocytes), [7] abnormal granulocyte profile based on CD11b/CD13/CD16 expression, [8] monocyte CD56 expression (>10%), [9] B-progenitor- cluster size (CD10+CD19+CD34+(%) of total CD34+), [10] erythrocyte CD71 MFI, [11] erythrocyte CD71 CV and [12] erythrocyte CD36 CV. Multivariate logistic regression analysis was performed comparing MDS vs control. Parameters that maintained a $p < 0.05$ were chosen to develop a FC based algorithm for MDS. Cases from the cohort were then reclassified using the proposed FC scheme to determine sensitivity and specificity.

Results: In multivariate analysis, all 4 Ogata parameters (myeloblast-cluster size, myeloblast CD45 expression, decreased granulocyte SSC, decreased B-progenitor cluster size) as well as low CD177 and decreased CD71 MFI were significant. To create a diagnostic FC algorithm, these six FC markers were used to build an additional logistic regression model using specified cut-off values with weighted significance for each marker. CD71 MFI was of borderline significance (p = 0.06) upon this re-evaluation and was removed from schema. Based on remaining 5 parameters a simple algorithm was generated summarized in Figure 1. Application of the system to the study cases revealed a sensitivity of 90% (95% CI 82-95%) with a specificity of 94% (95% CI 87-98%).

Figure 1 - 1238

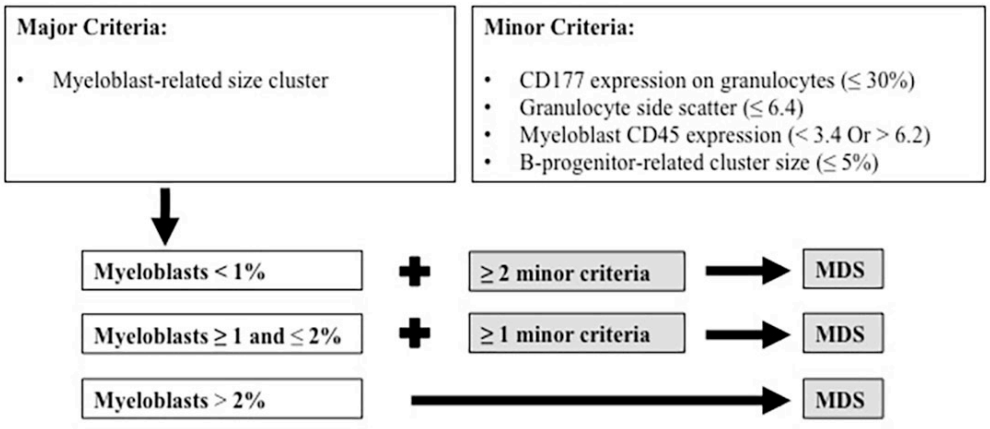

Conclusions: We developed a simple bone marrow FC algorithm incorporating CD177 and the Ogata parameters with high sensitivity and specificity for the diagnosis of MDS.

1239 Concurrent Gene Mutations Differ in SF3B1 Mutated MDS, MDS/MPN and AML

Andrew Alexander[1], Yi-Hua Chen[2], Juehua Gao[2]
[1]Northwestern University Feinberg School of Medicine, Chicago, IL, [2]Northwestern Memorial Hospital, Chicago, IL

Disclosures: Andrew Alexander: None; Yi-Hua Chen: None; Juehua Gao: None

Background: Splicing factor *SF3B1* mutation is present in 20-30% of myelodysplastic syndrome (MDS) and myelodysplasia/myeloproliferative neoplasm (MDS/MPN), particularly those with ring sideroblasts (RS), and rare (~5%) acute myeloid leukemia (AML). In this study, we compared the morphologic and genetic features of various types of myeloid neoplasms carrying *SF3B1* mutations.

Design: Searching the database in our institution, we identified 21 cases of SF3B1 mutated myeloid neoplasms (12 p.K700E, 6 p.K666N, 1 p.D781G, 1 p.R625C and 1 p.K700delinsQQE), including 11 MDS, 5 MDS/MPN and 5 AML. The morphologic features, the results of targeted next generation sequencing and cytogenetics were evaluated.

Results: Morphologic review showed RS in 11/11 of MDS, 5/5 MDS/MPN and 3/5 AML cases. The *SF3B1* mutated MDS consisted of 7 MDS-RS-multilineage dysplasia, 2 MDS-RS-single lineage dysplasia and 2 MDS with excess blast-1. Five of 11 MDS carried sole *SF3B1* mutation, and 5 of 6 remaining cases had additional *TET2* mutations. The *SF3B1* mutated MDS/MPN included 2 MDS/MPN-RS-thrombocytosis (T), 1 diagnosed as CMML and 2 MDS/MPN, NOS. Both MDS/MPN-RS-T harbored *JAK2* mutations, and the CMML case with RS had a *CBL* mutation. Both cases of *SF3B1* mutated MDS/MPN, NOS, presented with neutrophilia, and one case had *CSF3R* mutation. The *SF3B1* mutated AML included 3 AML with MDS-related changes, 1 AML with t(3;3) and 1 acute myelomonocytic leukemia. Genetic profiling of the AML cases identified additional mutations in all cases including tumor suppressor gene *RUNX1* (3/5), cell signaling (*FLT3* 3/5, *RAS* 1/5, *JAK2* 1/5), methylation (*TET2* 1/5, *DNMT3A* 2/5, *IDH2* 1/5), and transcriptional factor *GATA2* (2/5). Cytogenetic abnormalities, including del(20q) or del(7q), were detected in 5 of 11 MDS, but in none of the MDS/MPN cases.

Conclusions: The concurrent gene mutations in SF3B1 mutated MDS, MDS/MPN and AML differ significantly. In our series, MDS cases are characterized by either sole SF3B1 mutation or with concurrent TET2 mutation. In addition to the known category of MDS/MPN-RS-T, we identified 2 cases diagnosed as MDS/MPN, NOS, that had RS, neutrophilia and SF3B1 mutation, and one CMML case that had RS, monocytosis and SF3B1 mutations. Thus, the category of MDS/MPN-RS-T may need to expand to include cases with neutrophilia or monocytosis in addition to cases with thrombocytosis. Acquisition of additional mutations in tumor suppressor, cell signaling, methylation or transcriptional factors are associated with SF3B1 mutated AML.

1240 Reproducible Morphologic Features of Molecularly Defined Subgroups of Peripheral T-Cell Lymphoma, Not Otherwise Specified (PTCL-NOS)

Catalina Amador[1], Timothy Greiner[1], Karen Tatiana Galvis Castro[2], Lynette Smith[1], Tayla Heavican[1], Andreas Rosenwald[3], German Ott[4], Francesco D'Amore[5], Anja Mottok[6], Andrew Feldman[7], Sarah Ondrejka[8], Elías Campo[9], Julie Vose[1], Dennis Weisenburger[10], Wing Chung Chan[11], Javeed Iqbal[12]
[1]University of Nebraska Medical Center, Omaha, NE, [2]Hospital Universitario Fundación Santa Fe de Bogotá, Bogota, Colombia, [3]Wuerzburg, Germany, [4]Robert-Bosch-Krankenhaus, Stuttgart, Germany, [5]Aarhus University Hospital, Aarhus, Denmark, [6]University of Ulm, Ulm, Germany, [7]Mayo Clinic, Rochester, MN, [8]Cleveland Clinic, Cleveland, OH, [9]Hospital Clinic Barcelona, University of Barcelona, Barcelona, Spain, [10]City of Hope National Medical Center, Duarte, CA, [11]Pasadena, CA, [12]University of Nebraska Medical Center and on behalf of the LLMPP and I-PTCL Consortium, Omaha, NE

Disclosures: Catalina Amador: None; Timothy Greiner: None; Karen Tatiana Galvis Castro: None; Lynette Smith: None; Tayla Heavican: None; Andreas Rosenwald: None; German Ott: None; Francesco D'Amore: None; Anja Mottok: None; Andrew Feldman: None; Sarah Ondrejka: None; Elías Campo: None; Julie Vose: *Consultant*, Celgene Corporation; Dennis Weisenburger: None; Wing Chung Chan: None; Javeed Iqbal: None

Background: Using gene expression profiling (GEP), we previously defined two major molecular subgroups PTCL-GATA3 and PTCL-TBX21 in PTCL-NOS. PTCL-GATA3 and PTCL-TBX21 are characterized by high expression of *GATA3* and *TBX21*and their target genes, respectively. We then generated an immunohistochemistry (IHC) algorithm that matched the molecular subclassification with high accuracy. The objective of this study was to describe the morphologic and immunophenotypic characteristics of PTCL-GATA3 and PTCL-TBX21.

Design: TMAs were constructed from 53 cases of PTCL-NOS (20 PTCL-GATA3 and 33 PTCL-TBX21) subclassified by GEP (HG-U133 Plus2, n=32) or by the IHC algorithm (n=21). As expected, PTCL-GATA3 showed worse overall survival than PTCL-TBX21 ($p<0.01$). TMA sections were stained with CD3, CD4, CD8, TIA1, granzyme B and the algorithm antibodies (GATA3, TBX21, CXCR3, and CCR4). Two hematopathologists independently evaluated the morphologic features and immunostains. A cytotoxic phenotype was defined as the expression of one or more cytotoxic markers (TIA1 and granzyme B). The Fisher's exact and Kappa statistic tests were used to calculate the differences between groups and interrater agreement, respectively.

Results: PTCL-GATA3 was commonly characterized by a monotonous pattern; either sheets of intermediate-sized cells with abundant cytoplasm (14/20, 70%) or clusters/sheets of large cells (4/20, 20%). PTCL-TBX21 was characterized by a polymorphous inflammatory pattern with variably-sized neoplastic cells interspersed in an inflammatory background (22/33, 66%) or displayed a Lennert lymphoma pattern (3/33, 9%). The Lennert pattern was only observed in PTCL-TBX21. The morphological patterns were significantly associated with their corresponding PTCL subgroup ($p<0.01$). Strong inter-rater agreement was observed between pathologists in assessing morphologic patterns (kappa statistic= 0.86, 95% CI: 0.71-1.0). PTCL-GATA3 cases were predominantly CD4+/CD8- (72%) and less frequently CD8+/CD4- (11%). In PTCL-TBX21, the CD4+/CD8- and CD8+/CD4- phenotypes were found at similar frequencies (48% and 41%, respectively). CD4/CD8 double positive and negative cases were uncommon in both subgroups. The cytotoxic phenotype was more frequently associated with PTCL-TBX21 compared to PTCL-GATA3 (50% vs. 10%, $p<0.01$).

Conclusions: We have now defined distinctive morphologic features of the two molecular subgroups of PTCL-NOS and provide practical information that is reproducible and could be useful in clinical practice.

1241 Abnormal Immature B-lymphoblast Population in MDS and Non-CML MPN: Diagnostic Implications

Jeeyeon Baik[1], Wenbin Xiao[1], Priyadarshini Kumar[2], Maria Arcila[1], Yanming Zhang[1], Mikhail Roshal[1]
[1]Memorial Sloan Kettering Cancer Center, New York, NY, [2]New York, NY

Disclosures: Jeeyeon Baik: None; Wenbin Xiao: None; Priyadarshini Kumar: None; Maria Arcila: None; Yanming Zhang: None

Background: Mixed lymphoid/myeloid blast populations have been well described in the context of acute leukemia and chronic myeloid leukemia (CML). Presence of abnormal B lymphoblast in the context of myelodysplastic syndrome (MDS) and non-CML myeloproliferative neoplasms (MPN) has not been systematically described. We analyzed such cases in our practice.

Design: Five cases of MDS and non-CML MPN with abnormal immature B cell populations in the bone marrow have been identified through natural language search of pathology database at a major cancer center. Cases were reviewed by at least two hematopatholgists. The abnormal lymphoid blast populations were detected by flow cytometry and confirmed by immunohistochemistry when possible clinicopathologic features were reviewed.

Results: The diagnoses were MDS (N=3) and MPN (N=2). The clinical characteristics are listed in Table 1. There were 4 male and 1 female with age ranging from 65-74 years old. 4 patients had blasts less than or equal to 5% in the marrow and 1 patient had 12%. The abnormal immunophenotype of the immature B-lymphoblasts detected by flow cytometry is shown in Figure 1. The abnormal immature B-cell population was detected at low level at diagnosis (0.043-3.6%). Only 1/5 patients progressed to B-ALL (patient 5), while in remaining

patients the clone remained stable. The cases were genetically heterogeneous. In patient 5 flow cytometry sorted cell populations showed that although granulocytes and myeloid blasts shared the same mutations of JAK2 V617F, the abnormal B-lymphoblasts lacked the mutation suggesting derivation from a different clone. Evaluation of additional four patients will be presented.

	Patient 1	Patient 2	Patient 3	Patient 4	Patient 5
Gender	M	F	M	M	M
Age @ Dx	72	65	69	71	74
Diagnosis	MDS with fibrosis	MDS	MDS	MPN (early-PMF)	MPN (PV)
CBC					
WBC (k/uL)	2.9	2.2	10.4	41.7	13.2
				Basophilia	Eosinophilia/Basophilia
Hb (g/dL)	8.2	8.4	10.8	8.3	14.4
PLT (k/uL)	30	148	188	547	104
PB blasts	0	0	0	0	7%
BM blasts	<5%	<5%	5%	5%	12%
BM (myeloid blasts of WBC by flow)	0.9%	1.1%	4.2%	5.9%	0.55%
BM (abnormal Immature B by flow)	0.22%	0.078%	0.043%	0.087%	10%
Karyotype	Normal	Normal	Normal	45,XY,-18[20]	Normal
Molecular profile	ASXL1 exon12 p.H782fs (c.2343dupG)	1. ASXL1 exon12 p.G646Wfs*12 (c.1934dupG) 2. IDH2 exon4 p.R140Q (c.419G>A) 3. MPL exon10 p.S505N (c.1514G>A) 4. U2AF1 exon6 p.Q157P (c.470A>C)	1.DNMT3A exon9 p.C351Afs*56 (c.1051delT) 2. KDM6A exon22 p.G1077E (c.3230G>A) 3. SETBP1 exon4 p.D868N (c.2602G>A) 4. U2AF1 exon2 p.S34F	1. JAK2 exon14 p.V617F (c.1849G>T)(VAF: 98.3%) 2. TP53 exon8 p.R283P (c.848_849delinsCT)	1. JAK2 exon14 p.V617F (c.1849G>T) (VAF: 3.1%) 2. NOTCH1 exon34 p.Q2444L (c.7331A>T) *

Figure 1 - 1241

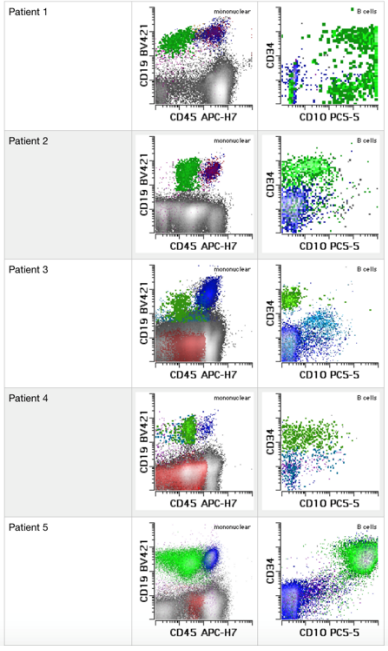

Conclusions: This is the first case series describing an abnormal immature B-cell population in MDS and non-CML JAK2 mutated MPN. Progression to frank B-ALL appears uncommon, although longer follow up is needed. Our sequencing studies on sorted populations suggest that the immature B-lymphoblasts may be clonally unrelated to the myeloid neoplasm in at least some cases, although more studies are needed to confirm these findings. The significance of the abnormal immature B-lymphoblasts in the setting of MDS and MPN warrants further investigation.

1242 TdT+ Acute Myeloid Leukemia is enriched for mutations of RUNX1, BCOR, and ASXL1

Nathanael Bailey[1], Eric Carlsen[2], Matthew Wild[2], Yen-Chun Liu[1], Miroslav Djokic[3]
[1]University of Pittsburgh School of Medicine, Pittsburgh, PA, [2]University of Pittsburgh Medical Center, Pittsburgh, PA, [3]University of Pittsburgh, Pittsburgh, PA

Disclosures: Nathanael Bailey: None; Eric Carlsen: None; Matthew Wild: None; Yen-Chun Liu: None; Miroslav Djokic: None

Background: While most frequently associated with lymphoblastic neoplasia, TdT is occasionally expressed by blasts in acute myeloid leukemia (AML) and is routinely evaluated by flow cytometric analysis in suspected cases of acute leukemia. AML with mutated *RUNX1* is a provisional entity in the revised WHO 2016 classification. Previous reports have suggested that *RUNX1*-mutated AML exhibits upregulation of TdT, but the predictive value of TdT expression in AML for *RUNX1* mutation deserves further study.

Design: 133 newly diagnosed AML patients excluding cases of acute promyelocytic leukemia with *PML-RARA* fusion were identified from 2017 and 2018 for which both TdT expression and mutational data were available. Mutational analysis using amplicon target enrichment of 37 genes recurrently mutated in myeloid neoplasia was performed. TdT reactivity was determined by flow cytometry in all cases (monoclonal mouse anti-human TdT conjugated to FITC, Supertechs, Bethesda, MD). To determine positivity, the expression of TdT on blasts was compared to internal lymphocyte controls. Cases with more than 10% TDT+ blasts were considered to be TdT-positive.

Results: The male/female ratio was 1.25 and the median age was 67. 30 of 133 (23%) patients had TdT expression on blasts (range 11% to 92%, median 31%). TdT expression was associated with *RUNX1* (10/16 cases, p=0.0003), *BCOR*(9/12 cases, $p=7x10^{-5}$), *BCORL1* (5/8 cases, p=0.02), and *ASXL1* (10/22 cases, p=0.01) mutations. 15 of 22 patients with either *RUNX1* or *BCOR* mutations had TdT positivity ($p=5x10^{-7}$). TdT expression was inversely correlated with *NPM1* (0/31 cases, p=0.0001) mutations. No significant correlation between TdT+ cases and other mutations or recurrent translocations was identified. The positive predictive value of TdT positivity for *RUNX1* mutation was 33%, while the negative predictive value was 94%. There was no significant difference in overall survival between the TdT+ and TdT- cases.

Conclusions: This study confirmed that TdT expression in AML is strongly associated with *RUNX1* mutations and identified correlations between TdT expression and mutations in the transcriptional corepressors *BCOR* and *BCORL1* and the epigenetic regulator *ASXL1.* Mutations in these genes have been associated with poor outcome in AML, though no significant survival differences were seen between TdT+ and TdT- AML cases in this retrospective, heterogeneously treated cohort. Absence of TdT expression is predictive for *RUNX1* negativity, but it cannot substitute for mutational analysis.

1243 Diagnostic Utility of CD200 Immunohistochemistry in Distinguishing EBV-Positive Diffuse Large B-Cell Lymphoma from Classical Hodgkin Lymphoma

Christopher Batuello[1], Emily Mason[2]
[1]Vanderbilt University, Spring Hill, TN, [2]Vanderbilt University Medical Center, Nashville, TN

Disclosures: Christopher Batuello: None; Emily Mason: None

Background: Epstein-Barr virus-positive diffuse large B-cell lymphoma, not otherwise specified (EBV+ DLBCL) is a heterogeneous disease that may resemble classical Hodgkin lymphoma (CHL) both morphologically and immunophenotypically. Many cases of EBV+ DLBCL are composed of large abnormal B cells embedded in a polymorphous background, and neoplastic cells may show CD30 expression and downregulation of CD20. Differentiating between EBV+ DLBCL and CHL is critical, as they are treated with distinct therapies and carry different prognoses. Previous studies have shown that Reed-Sternberg (RS) cells in CHL express CD200, while CD200 is negative in diffuse large B-cell lymphoma, not otherwise specified (DLBCL NOS). The pattern of CD200 expression in EBV+ DLBCL is unknown. Therefore, we examined CD200 expression in EBV+ DLBCL and evaluated its diagnostic utility in the differential diagnosis with CHL.

Design: CD200 immunohistochemistry was performed on archival material from 16 cases of CHL (5 EBV+, 10 EBV-, 1 unknown), 10 cases of EBV+ DLBCL, and 7 cases of DLBCL NOS (Leica Bond-Max, 1:150 following antigen retrieval, AF2724, R&D Systems). Staining pattern and intensity (0-3+ scale) were recorded.

Results: CD200 positivity was seen in RS cells in 15/16 cases (94%) of CHL, predominantly in a strong (3+, 12/15) and diffuse (13/15, >50% of cells) membranous and Golgi staining pattern. In contrast, CD200 was negative in 7/10 cases (70%) of EBV+ DLBCL; the 3

positive cases showed 1-2+ staining in <50% of lesional cells. All cases of DLBCL NOS were negative for CD200, consistent with previous reports. The single case of CD200-negative CHL was EBV-positive, HIV-associated, and refractory to CHL-directed therapy, raising the possibility that it, in fact, represented EBV+ DLBCL.

Conclusions: CD200 may be a useful immunophenotypic marker in differentiating EBV+ DLBCL from CHL, with negative to partial/weak staining favoring a diagnosis of EBV+ DLBCL and strong diffuse staining favoring CHL.

1244 Frequency and Significance of TdT Expression in Large B-cell Lymphomas

Shweta Bhavsar[1], Sarah Gibson[2], Erika Moore[3], Steven Swerdlow[4]
[1]University of Pittsburgh Medical Center, Pittsburgh, PA, [2]University of Pittsburgh School of Medicine, Scottsdale, AZ, [3]University Hospitals Cleveland Medical Center, Cleveland, OH, [4]University of Pittsburgh School of Medicine, Pittsburgh, PA

Disclosures: Shweta Bhavsar: None; Sarah Gibson: None; Erika Moore: None; Steven Swerdlow: None

Background: TdT expression is generally associated with lymphoblastic (LyB) or sometimes blastic myeloid neoplasms; however, it has been rarely described in mature large B-cell lymphomas (LBL) including very recently. Its frequency in LBL, the specific settings in which it occurs, the clinical implications and its other pathologic and molecular associations, and the relationship of these cases to B-LyB lymphomas (LyBL) remain to be better defined.

Design: 259 LBL (M:F 153:104, 21-98 years) with *BCL2, BCL6 & MYC* FISH studies, IHC stains at least for CD20, CD3, CD10, BCL6, IRF4/MUM1, BCL2, MYC, Ki-67, had successful TdT stains performed. All cases were reviewed for cytologic findings (DLBCL/intermediate with Burkitt features/ blastoid), phenotype and extent and distribution of TdT+ cells. Cases with prominent TdT expression were investigated in greater detail including review of prior biopsies and clinical associations.

Results: TdT IHC was negative in 78% biopsies, showed only rare positive cells (often in uninvolved areas) in 16%, had some irregularly scattered positive cells in 3% and showed more prominent staining in 6/259 cases (2%) although the proportion of TdT+ cells varied (table 1). These 6 Tdt+ cases appeared blastoid although with some larger cells and prominent nucleoli in some cases. TdT staining was often weaker than in typical LyBL.The proportion of TdT+ cells was higher in the CD20- areas in cases with variable CD20 staining. The 6TdT+ cases all had MYC(>70%) & BCL2(>70%) coexpression. 5/6 cases had a germinal center (GC) phenotype (Hans algorithm), with 1 case NGC type but only at the TdT+ relapse. 4/6 cases were CD10+.In case #3 the pattern of the CD10 staining was similar to CD20. 2 cases showed a switch of light chain expression during the course of disease (Case 3, before TdT+ diagnosis) and Case 4 at the time of TdT+ diagnosis (case 3 tested for clonality showed the same clone).

Case No.	1	2	3	4	5	6
Age (yrs.)/ Sex	67/F	62/F	55/M	72/F	77/F	62/F
Biopsy Site	Chest wall	Gluteal mass	Knee	Groin mass	Inguinal LN	Pretibial skin
Initial diagnoses on prior biopsies	DLBCL with some High grade features	HGBL,NOS*	Follicular lymphoma 1-2/3 -->LBCL with High grade features-->DHL	DHL	none	HGBL,NOS
TdT in prior biopsies	Negative	Positive	Neg./Neg./Neg.	Negative	NA	Negative
Initial treatment	R-CHOP x5	hyper-CVAD X1 and R-EPOCH x 4	R-CHOP x6--> R-EPOCH--> RDHAP, RICE	R-CHOP x5	R-CHOP x6	hyper-CVAD X1 and R-EPOCH x 4
Initial course	Disease Progression	Disease Progression	Disease Progression	Disease Progression	NA	Relapse after CR
TdT positive diagnoses	THL	DHL (*BCL2*- R)	DHL (*BCL2*- R)	DHL (*BCL2*- R)	DHL (*BCL6*- R)	HGBL,NOS (*MYC*-R only)
Time after initial diagnoses	4 mo.	4 mo.	4mo./4mo./5mo.	14 mo.	NA	9 mo.
TdT staining pattern	10-30% pos. cells	Large areas with 60-70% pos. cells, some areas with 20%	>50% positive cells in CD20 neg. areas	20-30% pos. cells in the CD20 neg. areas, scattered pos. cells in the CD20+ areas	10-20% pos. cells, more in CD20 neg. areas	Scattered pos. cells
CD20	Negative	Negative	Variable	Variable	Variable	Positive
Light chain	ND	Lambda	ND	Kappa	SIg negative	Kappa
Additional Treatment	RICE	RICE, R-DHAP, Radiation	Symptomatic treatment	RICE	NA	RICE, GDP
Outcome	Died of disease	Died of disease	Died of disease	Died of disease	Died of disease	Alive - undergoing Chemotherapy for relapse
Follow up after TdT+ diagnosis	0.2 mo.	2mo.	2mo.	2mo.	8mo.	5mo.
* FISH studies failed on this specimen. Follow up time for this patient from time of 2nd fully studied biopsy.						
M- male, F- female, NA- Not applicable, ND- Not done, mo.- Months, LN- Lymph node, DLBCL- Diffuse large B-cell lymphoma, HGBL,NOS- High grade B-cell lymphoma, Not otherwise specified, THL- Triple Hit Lymphoma (*MYC/BCL2* & *BCL6*- R),DHL- Double Hit Lymphoma, CR- Complete remission						

Figure 1 - 1244

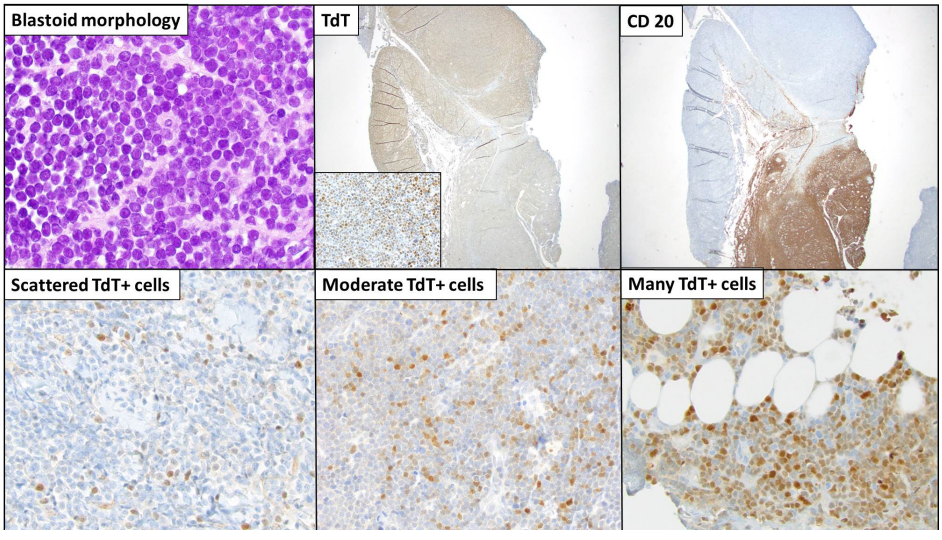

Conclusions: The frequency of TdT positivity in LBL is very low, is at least commonly seen in cases with *MYC* rearrangements mostly together with *BCL2* or less often *BCL6* rearrangements and they have a high grade morphologic appearance.TdT+ cases often followed TdT negative LBL and were found in patients who had a poor outcome. Nevertheless, these cases had varied features that suggested they were not typical lymphoblastic neoplasms. Further molecular genetic analysis of these cases is in progress.

1245 Correlation of TP53 Aberrations with P53 Staining and Outcomes in Large B-Cell Lymphomas

Shweta Bhavsar[1], Nidhi Aggarwal[1], Erika Moore[2], Svetlana Yatsenko[1], Steven Swerdlow[3]
[1]University of Pittsburgh Medical Center, Pittsburgh, PA, [2]University Hospitals Cleveland Medical Center, Cleveland, OH, [3]University of Pittsburgh School of Medicine, Pittsburgh, PA

Disclosures: Shweta Bhavsar: None; Nidhi Aggarwal: None; Erika Moore: None; Svetlana Yatsenko: None; Steven Swerdlow: None

Background: *TP53* abnormalities are often associated with an adverse prognosis in lymphoid neoplasms; however, its impact on large B-cell lymphomas (LBL) & correlation with other features remain to be better defined. Also the possibility that LBL with *TP53 & MYC* abnormalities should be considered a type of double-hit lymphoma has been raised. To explore whether p53 staining is a surrogate for *TP53* abnormalities in LBL, to assess the prognostic implications of *TP53*abnormalities & to further assess the concept of *TP53/MYC* double hit lymphomas, LBL were investigated with IHC, molecular & cytogenetic FISH studies & the results correlated with clinicopathologic parameters.

Design: 302 LBL with MYC*, BCL2 & BCL6* FISH studies were stained for p53. P53 IHC was assessed as in fig 1 & grouped into p53 low/intermediate (cat. 1-3) & high (4). *TP53* molecular analyses using NGS was performed on cases selected from each of the p53 IHC categories with classical cytogenetics (CCG) &/or *TP53* FISH used in cases with potential copy number abnormalities (CNA). Clinical parameters were recorded. Cases studied at relapse were not included in the survival data.

Results: *TP53* aberrations were identified in 36/87 successfully studied LBL & were most frequent in cases with high p53 staining (fig 1) (mut. with CNA- 18, mut. only–10, CNA only-8). 26/28 mutations were located in the DNA binding domains (Exon 5-8) with a median VAF of 61%. High p53 IHC staining, present in 18/87 cases had a sensitivity of 50% for a *TP53* aberration (64% for *TP53* mut.) & a specificity of 98% for either *TP53* aberration or mut. Neither high p53 staining nor *TP53* aberrations showed significant survival differences in the subset of cases with molecular studies; however, high p53 staining was associated with an adverse prognosis in the entire cohort (p=0.04). An adverse impact with *TP53* aberrations was, however, seen among patients with MYC>40% (p=0.03), high IPI scores with MYC>40% (p=0.01) & HGBL,NOS (p=0.04). Significant prognostic implications were not found in the subsets defined by MYC & BCL2 coexpression; *MYC, BCL2 & BCL6* FISH studies; cell of origin or high Ki-67.

Proportion of cases with *TP53* aberrations		
	***TP53* aberrations**	***P* values**
p53 Immunohistochemistry		
Cat. 1/2/3 (absent/intermediate staining) (68)	26%	**<0.0001**
Cat. 4 (strong diffuse staining)(19)	95%	
2016 WHO Classification		
DLBCL (47)	49%	**NS**
DHL/THL (16)	25%	
HGBL,NOS (18)	44%	
Cytogenetic groups		
MYC & *BCL2* &/or *BCL6* R (16)	25%	**NS**
MYC-R only (10)	50%	
No *MYC*-R (61)	44%	
Phenotypic features		
MYC <40% (35)	31%	**NS**
MYC ≥40% (47)	49%	
Clinical features		
De novo (62)	37%	**NS**
Secondary (13)	62%	
Relapse (12)	42%	
Cat. = Category, R=rearrangement, NS = not significant		

Figure 1 - 1245

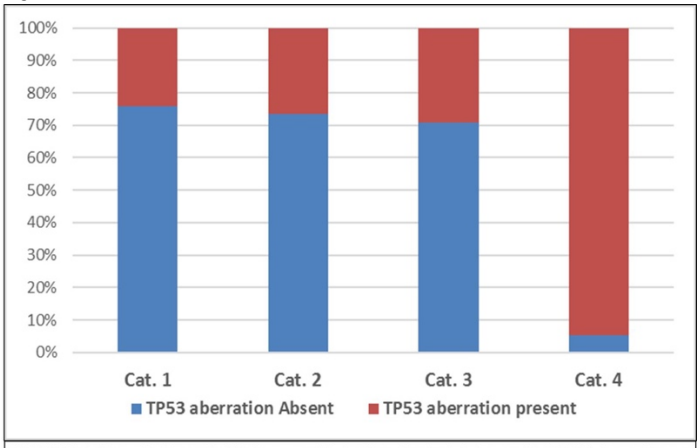

FIGURE 1. Correlation of p53 immunohistochemical staining with *TP53* aberrations

Cat.1 (n = 29) - <5% positive cells
Cat.2 (n = 15) - <20% moderate/strong positive cells, some with more weakly positive cells,
Cat.3 (n = 24) - Usually >50% weak and moderately positive cells with <20% strongly positive cells
Cat.4 (n = 19) - >95% strongly positive cells

Figure 2 - 1245

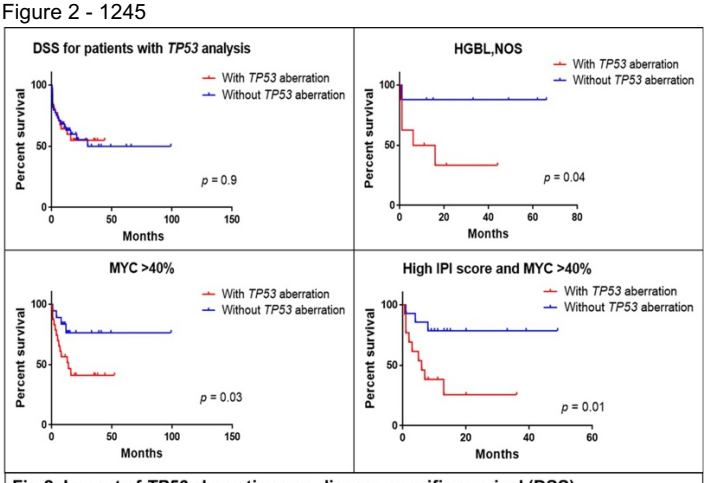

Fig.2: Impact of *TP53* aberrations on disease specific survival (DSS)

*DSS for patients with *TP53* analysis (87) should be interpreted with caution because while it did not suggest a difference between the two groups, a significant difference in survival for P53 strong expression was only found when the entire cohort was analyzed (n=302, p=0.04). It was not found when the subset studied for *TP53* was investigated. The latter is proportionally enriched in cases totally lacking p53 expression.

Conclusions: Strong diffuse p53 immunostaining is highly suggestive of a *TP53* mutation in LBL; however, it is not a sensitive screen. P53 expression is associated with an adverse prognosis in LBL but more strikingly *TP53* aberrations combined with high MYC expression identify patients with very aggressive disease, even among those with a high IPI score, as do *TP53* aberrations in HGBL,NOS

1246 Expression of Immunocheckpoint Molecules in the Microenviroment of Primary Mediastinal B-cell Lymphoma

Juraj Bodo[1], Aaron Gruver[2], Lisa Durkin[1], Xiaoxian Zhao[1], Timothy Holzer[2], Philip Ebert[2], Andrew Schade[3], Eric Hsi[1]
[1]Cleveland Clinic, Cleveland, OH, [2]Eli Lilly & Co., Indianapolis, IN, [3]Eli Lilly & Co., Fishers, IN

Disclosures: Juraj Bodo: None; Aaron Gruver: *Employee*, Eli Lilly and Company; Lisa Durkin: None; Xiaoxian Zhao: None; Timothy Holzer: None; Philip Ebert: *Employee*, Eli Lilly and Company; Andrew Schade: *Employee*, Eli Lilly and Company; Eric Hsi: *Grant or Research Support*, Abbvie; *Grant or Research Support*, Eli Lilly; *Advisory Board Member*, Seattle Genetics; *Advisory Board Member*, Celgene

Background: Effectiveness of antitumor activity can be suppressed by a number of factors, such as anti-inflammatory antigen presentation by tumor-associated macrophages (TAMs), functionally suppressed macrophages, which decrease the effectiveness of T-cell-mediated antitumor activity, or the loss of effector functions through T cell exhaustion. Primary mediastinal B-cell lymphoma (PMBCL) is a lymphoma that is known to manipulate its microenvironment through altering expression of immune checkpoint molecules such as PDL1/2 and HLA molecules. To further characterize the diversity of the PMBCL microenvironment, we investigated the expression and interactions of multiple immune molecules in the PMBCL tumors.

Design: TIM-3, GAL9, IDO1, LAG-3, VISTA and B7H3 immunohistochemistry staining was quantified using Aperio ImageScope software. TIM3/CD3, TIM3/CD68, and GAL9/IDO1 double immunoflourescent staining was performed to confirm cellular localization of these proteins. Images were analyzed with the Image-Pro Plus software (Media Cybernetics; Silver Spring, MD). RNA sequencing analysis was applied to acquire the expression profiles from 9 PMBCL samples.

Results: The 29 PMBCL (14 females, 15 males) cases were identified and analyzed. Median age was 41 (range 22 – 58 years). Double fluorescence staining showed an interaction between GAL9 and its receptor, TIM-3, and a strong correlation ($p<0.001$) between their expression. TIM-3 expression was observed on T-cells, but the majority was detected on macrophages. CD68, CD163, and CD206 staining confirmed that TIM-3 positive macrophages have a TAM phenotype. Furthermore, RNA sequencing revealed a correlation ($p<0.05$) between IL-10 (an anti-inflammatory cytokine produced by TAM) and TIM-3 levels. GAL9 levels also strongly correlated with expression of immunomodulatory enzyme IDO1 in macrophages. T-cells also frequently expressed LAG3, VISTA, and B7-H3 inhibitory immune checkpoint molecules. Spearman Rank Order Correlation analysis of immunohistochemical data revealed very strong correlations ($p<0.0001$) between the expression of TIM-3 and IDO1, or LAG3.

Conclusions: Multiple immune evasion mechanisms appear to be relevant in PMBL. In addition to the PDL1/2 expression and downregulation of HLA molecules, our findings provide new insight into additional immune checkpoint molecules are worth investigating as therapeutic targets. These include the immune checkpoint molecules TIM-3 and LAG3 as well as IDO1.

1247 Immunohistochemistry for p53 Might Lead to Prompter Treatment in TP53-Mutated Acute Myeloid Leukemia

Leonardo Boiocchi[1], Andrew Crabbe[1], Andrew Brunner[1], Amir T. Fathi[1], Robert Hasserjian[1], Valentina Nardi[1]
[1]Massachusetts General Hospital, Boston, MA

Disclosures: Leonardo Boiocchi: None; Andrew Crabbe: None; Andrew Brunner: None; Amir T. Fathi: *Consultant*, Celgene; *Consultant*, Takeda; *Advisory Board Member*, Jazz; *Consultant*, Boston Biomedical; *Consultant*, Takeda; Robert Hasserjian: None; Valentina Nardi: None

Background: Mutations in TP53 have a significant adverse prognostic effect in acute myeloid leukemia (AML) in terms of progression-free and overall survival. Patients with TP53 mutations respond poorly to conventional induction chemotherapy regimens for AML and there is evidence supporting the use of alternative regimens, like decitabine. NGS-based tests are currently part of the initial workup of AML in most institutions. Although the NGS results could inform treatment, they are usually not available before 1-2 weeks, after the AML treatment has been initiated. In this study wanted to assess whether p53 immunohistochemistry (IHC), which is usually available within 1 day of the bone marrow sample, could be a reliable surrogate for TP53 mutational status, potentially more rapidly informing therapeutic decisions.

Design: Seventy-eight consecutive cases of AML with NGS-based molecular testing results available were stained for p53 by IHC. Only cells with intense (3+) nuclear p53 expression were considered positive. All cases were reviewed by two pathologists and the number of p53+ cells assessed.

Results: The study cohort included 46 de novo AML (59%), 24 AML following other myeloid neoplasms (33%) and 8 therapy-related AML (TR-AML; 10%) (M:F=48:30; mean age: 65.2 years). Twelve cases showed mutation in TP53 (15%; 3 de novo AML; 3 secondary; 6 TR-AML). Eleven (92%) of the TP53-mutated cases showed p53+ cells (range: 15-95%; median 40%) and only 1 case was negative. In all cases p53+ cells were morphologically identified as blasts. In TP53 wild-type AML cases the median percentage of p53+ cells was 2.4% (range:0-40%). Analysis of the ROC curve for p53 staining showed that 10% was the ideal positivity cut-off (sensitivity 92%; specificity 97%) to identify TP53-mutated cases. Fisher's exact test confirmed a significant association between >10% p53+ cells and presence of TP53 mutations ($p<0.001$). p53 staining and TP53-mutation variant allele frequency correlated when considering the whole cohort ($p<0.001$; Pearson correlation factor: 0.67), but not among the 12 TP53-mutated cases ($p=0.54$).

Conclusions: A threshold of 10% p53+ cells by IHC could predict TP53-mutational status with high sensitivity and specificity. Our results suggest that IHC could rapidly provide essential information and potentially influence the clinical management of the 10-15% of AML with TP53 mutation. p53 IHC could be useful in assessing all new AML cases in which the presence of a TP53 mutation could affect up-front therapy choices.

1248 Lymphoplasmacytic Lymphoma Associated with Diffuse Large B-Cell Lymphoma: Progression or Divergent Evolution?

Macarena Boiza Sánchez[1], Cristina Chamizo Muñoz[1], Rebeca Manso Alonso[1], Rocío Salgado[2], Elham Askari[1], José Carlos Rivero Vera[3], Socorro María Rodríguez Pinilla[1], Miguel Ángel Piris Pinilla[1], Federico Rojo[4]
[1]Hospital Fundación Jiménez Díaz, Madrid, Spain, [2]Fundación Jiménez Díaz, Madrid, Madrid, Spain, [3]Hospital U de GC Dr Negrín, Las Palmas de Gran Canaria, Spain, [4]Madrid, Spain

Disclosures: Macarena Boiza Sánchez: None; Rebeca Manso Alonso: None; Rocío Salgado: None; José Carlos Rivero Vera: None

Background: Lymphoplasmacytic lymphoma (LPL) is an indolent mature B-cell neoplasm composed of small lymphocytes, plasmacytoid lymphocytes and plasma cells, with involvement of the bone marrow, usually associated with a monoclonal gammopathy.

At least 90% of LPLs carry on the MYD88 L265P mutation, an adaptor protein that mediates toll and interleukin-1 receptor signalling. 10% of LPLs develop diffuse large B-cell lymphoma (DLBCL).

We have had the opportunity of reviewing 7 cases where LPL and DLBCL were diagnosed in the same patient, comparing the results of genomic analysis in both samples.

Design: We conducted a research of patients diagnosed with LPL and DLBCL during the last 20 years in our hospital. Their clinical and analytical information was compiled and a review of the histological and immunochemistry slides was performed, in order to confirm the diagnoses.

From the paraffin samples, we analyzed BCL2, BCL6 and c-MYC translocations by FISH, MYD88 L265P mutation and IgH rearrangements (sequences FR1, FR2, FR3) by PCR. A mutational study was performed by NGS, using a 38-gene B-cell lymphoma customized Illumina panel and the OCA oncopanel.

Results: In the last 20 years 7 patients were identified with both LPL y DLBCL. There were 3 men and 4 women with ages between 36 and 104 years (mean 75 years).

The LPL component was always diagnosed in the bone marrow, with extension to lymph nodes (2 cases) and to cavum (1 case). The high-grade component proved to be an activated subtype DLBCL in all patients, with nodal involvement and additional infiltration of the jaw (1 case) and central nervous system (1 case).

Both components were simultaneously diagnosed, at the same time, in 5 patients. In one case the LPL appeared 2 years before the DLBCL. In another case, the high-grade component was discovered 4 years before the LPL. In 6/7 cases, both samples shared the MYD88 L265P mutation: this suggesting both B-cell clones have a common origin.

IgH FR1, FR2, FR3 analysis showed overlapping IgH rearrangements in two cases, and striking differences in five cases.

Mutational study was evaluable in three cases (both samples), all of which displayed shared and divergent mutations, this confirming a common clonal origin and divergent differentiation.

Conclusions: LPL and DLBCL association seems to represent in most cases a pattern of a common clonal origin, MYD88 mutated, showing divergent evolution.

1249 Epstein-Barr Virus prevalence in classic Hodgkin lymphoma is predicted by histologic subtype and not race or ethnicity a multiethnic U.S. cohort

Rachel Bolanos[1], Amie Hwang[2], Chun Chao[3], Christopher Flowers[4], Sheeja Pullarkat[5], Jose Aparicio[2], Sophia Wang[6], Karen Mann[7], Leon Bernal-Mizrachi[4], Joo Song[8], Christian Steidl[9], Imran Siddiqi[10], Wendy Cozen[1]
[1]University of Southern California, Los Angeles, CA, [2]Keck School of Medicine of University of Southern California, Los Angeles, CA, [3]Kaiser Permanente Southern California, Pasadena, CA, [4]Emory University, Atlanta, GA, [5]La Canada, CA, [6]City of Hope National Medical Center, Duarte, CA, [7]Grady Health System, Atlanta, GA, [8]City of Hope Medical Center, Duarte, CA, [9]British Columbia Cancer Agency, Vancouver, BC, [10]University of Southern California Keck School of Medicine, Los Angeles, CA

Disclosures: Rachel Bolanos: None; Amie Hwang: None; Chun Chao: None; Sheeja Pullarkat: None; Jose Aparicio: None; Sophia Wang: None; Karen Mann: None; Leon Bernal-Mizrachi: None; Joo Song: None; Christian Steidl: *Consultant*, Seattle Genetics; *Consultant*, Roche; *Grant or Research Support*, Tioma; *Grant or Research Support*, Bristol-Meyers Squibb; *Consultant*, Juno; Imran Siddiqi: None; Wendy Cozen: None

Background: Epstein-Barr virus (EBV) is present in a varying proportion of classical Hodgkin lymphoma (cHL) tumors. We examined the distribution of EBV expression in formalin-fixed paraffin-embedded (FFPE) tumor blocks from 269 multiethnic U.S. cHL cases collected as part of a larger study of tumor microenvironment in minority populations.

Design: We confirmed cHL diagnosis and histology in 269 cHL cases diagnosed from 1996-2016 provided by Kaiser Permanente Southern California, Emory University hospitals, Grady Health, City of Hope National Medical Center, University of California Los Angeles and the University of Southern California hospitals. Immunostain results were available for the majority of cases. EBER was assessed using *in situ* hybridization and scored as negative, positive in Hodgkin Reed/Sternberg (HRS) cells or positive in the surrounding normal infiltrate. Patient data included histological subtype, race/ethnicity (Hispanic, African American, Asian, non-Hispanic white), age at diagnosis, gender and anatomic site was collected. Multiple logistic regression was conducted to assess the relationship between the demographic and clinical data and EBV status.

Results: Race data was available for 200 cases (African American=44, non-Hispanic white=46, Hispanic=100, Asian=9 and mixed race=1). 123 were female (61.5%). Age at diagnosis ranged from 5-84 years (mean age=37). EBV prevalence in HRS cells by subtype was 0/8 for lymphocyte depleted(LD), 21/46 (45%) for mixed cellularity(MC) 1/3 (33%) for lymphocyte rich(LR), 32/136 (24%) for nodular sclerosis(NS), and 4/7 for not otherwise specified(57%). As expected, histologic subtype was a statically significant predictor of EBV tumor status (p=.0015), even when adjusted for age, sex, and race/ethnicity (p= 0.049). Among NS cases, tumor cell prevalence of EBV was similar in African Americans and Hispanics (~21%) and not significantly different from that of non-Hispanic whites (32%). However, there was a much higher prevalence of EBV in HRS cells in African American (86%) compared to Hispanic and non-Hispanic white (33-38%) MC cases, not explained by HIV/AIDS. Interestingly, 8/103 (8%), 1/25 (4%) and 1/3 (33%) EBV-negative NS, MC and LR cases, respectively, had EBV present in non-malignant lymphocytes but not in HRS cells.

Conclusions: Histologic subtype was the strongest predictor of EBV tumor positivity in this set of cHL tumors. Unlike previous reports, EBV-positive tumors were similar across race/ethnicity, except for African American MC cases.

1250 A Geospatial Analysis Of Risk Factors in Myeloid Leukemias with Monocytic Differentiation

Kelly Bowers[1], Timothy Haithcoat[1], Eileen Avery[2], Chi-Ren Shyu[1], Richard Hammer[2]
[1]University of Missouri, Columbia, Columbia, MO, [2]University of Missouri, Columbia, MO

Disclosures: Kelly Bowers: None; Timothy Haithcoat: None; Eileen Avery: None; Chi-Ren Shyu: None; Richard Hammer: None

Background: Myeloid leukemias with monocytic differentiation includes acute monoblastic and monocytic leukemia (AMoL), acute myelomonocytic leukemia (AMML), and chronic myelomonocytic leukemia (CMML). The epidemiology and risk factors of some leukemias are known, however there is little study for these subtypes of leukemia, particularly CMML. To explore risk factors and oncogenesis, this study uses multifactorial geospatial techniques in conjunction with individual clinical and socioeconomic data to evaluate the individual characteristics, incidence, and regional distribution of monocytic-type leukemia

Design: Retrospective chart review was performed on a local cohort of confirmed AMoL, AMML, and CMML from 2013 to 2018. Data included home address, demographics, and clinical and laboratory features. Using geospatial analysis, cases were geocoded by home address then aggregated to the zip code level to compare the distribution against multiple accepted and proposed risk factors for leukemia. Results were compared to multi-state data via the Surveillance, Epidemiology, and End Results (SEER 18) dataset.

Results: Our local cohort included 381 leukemias and demonstrated increased frequency of monocytic-types (5% AMML, 3.7% AMoL, and 8.4% CMML). Local (state) age-adjusted rates compared to national (SEER) rates show increased total number of leukemias (13.77 to 13.53), increased AMoL (4.5 to 3.88), and dramatically increased AMML (2.19 to 0.25). Geospatial evaluation mirrors these findings, with incidence and prevalence rates higher than those reported in the literature and in places over 10-times higher than expected (Figure 1). The findings suggest multiple potential factors may contribute to increased risk, including proximity to electric transmission lines (Figure 2), radon, and brownfields.

Figure 1 - 1250

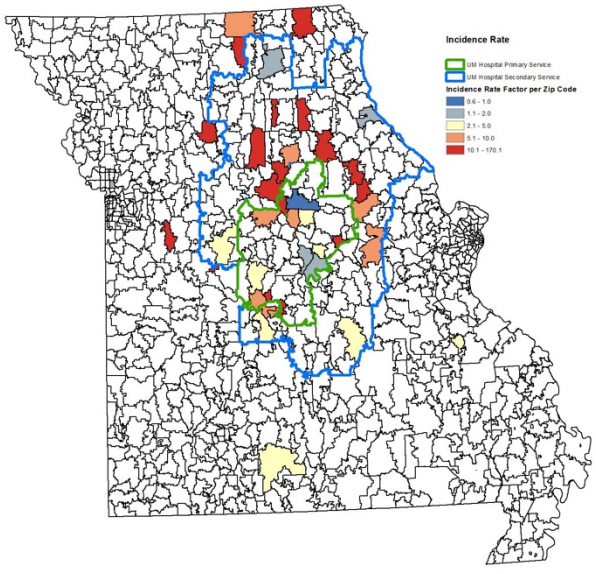

Figure 2 - 1250

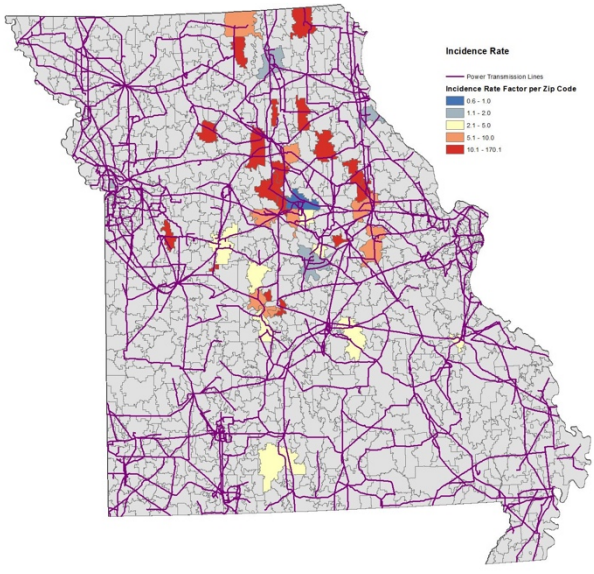

Conclusions: To our knowledge, this study is the first comprehensive analysis of risk factors using geospatial distribution of CMML, AMML and AMoL. Our results show increased incidence of monocytic-type leukemias and a distribution associated with potential environmental risk factors. Our study highlights the utility of geospatial tools for visualizing complex interactions of individuals and environment, which can our improve understanding of oncogenesis. Geospatial techniques are suited for multifactorial layering of complex big data in cancer research. This preliminary study used local data and future research is planned with larger regional and national cancer database data.

1251 Flow Cytometric Analysis of CSF Identifies Malignancy in Paucicellular Specimens with Bland Cytology

Daniel Boyer[1], Steven Weindorf[2], Timothy Miller[1]
[1]University of Michigan, Ann Arbor, MI, [2]University of Michigan, Ypsilanti, MI

Disclosures: Daniel Boyer: None; Steven Weindorf: None; Timothy Miller: None

Background: Flow cytometry (FC) is commonly performed on cerebrospinal fluid (CSF) to diagnose CNS involvement by hematolymphoid neoplasms; however, the vast majority of ordered CSF FC tests are negative for abnormal cells. Prior studies of the value of adding FC to cytology evaluation of CSF have yielded variable findings on the sensitivity of these techniques and different recommendations for optimal use of FC on CSF specimens. In the absence of standard guidelines, opinions about when to perform FC on CSF vary among the pathologists and clinicians at our institution.

Design: Archived FC results at Michigan Medicine were searched for CSF specimens collected from 1/1/2007-5/30/2016. The FC results were coded as positive, suspicious, negative or uninterpretable. FC results were correlated with cytologic diagnosis, clinical history and fluid WBC count.

Results: FC and cytology results were reviewed for 1941 consecutive CSF specimens. 256 were FC+ (13% of total), and these included 151 with suspicious or positive cytology (59% concordant), 25 atypical and 80 negative. 1652 (85%) were FC(-) or uninterpretable, and these included 109 with suspicious or positive cytology, 54 atypical and 1489 negative (90% concordant). The frequency of FC+ results correlated positively with the fluid WBC count (see Chart). Surprisingly, 3% of specimens with 0 WBC/uL were FC+. Even after removing specimens for new or treated acute leukemia from the analysis, 46/959 specimens (5%) with < 5 WBC/uL were FC+.

Figure 1 - 1251

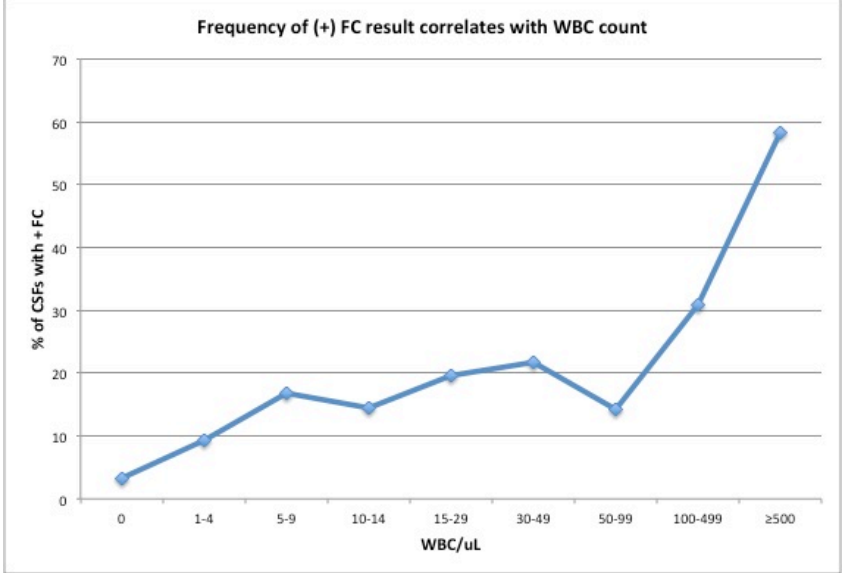

Conclusions: In this large series, 13% of CSF FC specimens were positive for hematolymphoid malignancy. If FC had been reserved only for specimens with at least atypical cytology, 31% of the FC+ specimens would not have been run. A positive FC result is more likely in specimens with at least 5 WBC/uL, but there is no minimum cellularity threshold. The rate of positivity plateaued between 5 cells/uL and 99 cells/uL, and increased rapidly above 100 cells/uL. Although careful review of cytology together with clinical history may help to reduce "wasteful" FC testing of CSF, bland cytology or paucicellularity does not always portend a negative FC result.

1252 Post-Transplant Lymphoproliferative Disorders (PTLDs) Arising in Solid Organ and Bone Marrow Transplant Recipients Show Cytogenetic Findings That May Reflect Underlying Biology

Miguel Cantu[1], Susan Mathew[2], Genevieve Crane[1], Wayne Tam[3], Ethel Cesarman[3], Amy Chadburn[3]
[1]New York-Presbyterian/Weill Cornell Medical Center, New York, NY, [2]Weill Cornell Medicine, New York, NY, [3]Weill Cornell Medical College, New York, NY

Disclosures: Miguel Cantu: None; Susan Mathew: None; Genevieve Crane: None; Wayne Tam: None; Ethel Cesarman: None; Amy Chadburn: None

Background: Post-transplant lymphoproliferative disorders (PTLDs) arise in the setting bone marrow (BMT) and solid organ (SOT) transplantation. Molecular analysis has shown that non-destructive (ND) PTLDs are polyclonal, while polymorphic (P-PTLD) and monomorphic (M-PTLD, B or T cell origin) PTLDs are usually monoclonal. Furthermore, M-PTLDs often contain oncogene or tumor suppressor gene alterations. BMT PTLDs, usually NDs and P-PTLDs, are thought to occur due to a lack of immune surveillance and are often associated with a poor outcome, while SOT PTLDs, which can be ND, P-PTLD or M-PTLD, show more variable clinical behavior and may regress following immunosuppression reduction. Only limited karyotypic information on PTLDs has been reported. Thus, the pathogenesis and behavior of PTLDs, based on cytogenetic findings has not been extensively studied.

Design: 14 PTLDs (1 ND, 4 P-PTLD, 8 M-PTLD, 1 T-PTLD) were studied by conventional cytogenetics; in 9 cases limited FISH studies were preformed as per standard laboratory procedures.

Results: Multiple genetic abnormalities were detected in 7/8 SOT M-PTLDs, the most common of which involved chromosome 11 (deletions/additions; 6/8, all B) and chromosome 18 (5/8, all B). In 4/5 cases extra copies of chromosome 18 were present, confirmed by FISH in 2. The remaining 2 SOT-PTLDs had specific translocations: t(8;14) in an EBV negative M-PTLD and t(16;18) in an EBV+ P-PTLD. Normal karyotypes were seen in 3/5 BMT PTLDs (1 ND, 1 P-PTLD, 1 M-PTLD) and 1 P-PTLD had t(4;14) with +9. The remaining BMT P-PTLD arose in the setting of recurrent T cell lymphoma. This P-PTLD was associated with a complex karyotype, including t(14;14), suggesting the genetic changes were from the T cell process. Other common genetic abnormalities in the 14 cases included 14q32 abnormalities in 4, del(7q)/-7 in 3 and del(17p)/abnormal 17 in 3 cases. Outcome was known in 10 patients; >50% of SOT M-PTLD patients with a complex karyotype have died.

Transplant Type, EBV Status, Morphology, Cytogenetics and Outcome in 14 PTLDs

	ND	P-PTLD	MB/T-PTLD	Diagnosis < 1 Year Post Transplant	<3 Chromosomal Abnormalities	≥3 Chromosomal Abnormalities	# Died (n=10)
BMT EBV+	1	3	1	4/5	5	0	1/2
SOT EBV+	0	1	4	1/5	1	4	3/4
SOT EBV-	0	0	4	0/4	1	3	1/4

Conclusions: PTLDs in BMT recipients are often EBV+, occur shortly after transplant and have non-complex karyotypes, findings consistent with development of EBV-driven lesions due to a lack of T cell immune response. M-PTLDs in SOT recipients usually have complex karyotypes, often involving chromosomes 11 and 18. These lesions, even if EBV+, appear driven by genetic changes, suggesting less response to immune modulation and requiring similar treatment to that used for aggressive lymphomas in immunocompetent patients for disease resolution.

1253 A Series of Splenic Epithelial Cysts

Timothy Carll[1], Peter Pytel[2], Tatjana Antic[1], John Hart[1], Lindsay Alpert[1]
[1]University of Chicago, Chicago, IL, [2]University of Chicago Medicine, Chicago, IL

Disclosures: Timothy Carll: None; Peter Pytel: None; Tatjana Antic: None; John Hart: None; Lindsay Alpert: None

Background: Splenic epithelial cysts (SECs) are rare lesions mostly discussed in case reports that are defined by a squamous or mesothelial lining. They generally manifest in the 2nd-3rd decades of life, mostly in women. Their etiology is poorly understood, but two major theories claim that they might originate from invagination of the mesothelium, which may undergo squamous metaplasia, or represent endodermal sinus inclusions. The differential diagnosis of SEC includes pseudocysts, parasitic cysts, and cystic vasoformative lesions. SECs are generally managed by surgical intervention, depending on cyst size and symptomology. Partial splenectomy is preferred to total splenectomy to preserve immunity against capsular organisms. In this case series, we describe four examples of large SECs occurring in young women.

Design: A search for splenic lesions in the departmental archive revealed four cases of SEC from 2005-2018. The patient demography, clinical history & management, imaging studies, gross & microscopic pathology as well as immunohistochemistry were reviewed.

Results: Four cases were identified. All patients were young females (13-21 years, mean 17.25) who presented with symptoms related to cyst rupture or mass effect. Radiologic studies revealed a large (11.7-29.0 cm) unilocular cyst in each case. The patients underwent splenic fenestration or total splenectomy (see Table 1). In one case, a postoperative complication of abscess formation occurred. Gross examination of each resection specimen demonstrated disrupted splenic tissue with a dominant cyst lined by a white-tan, fibrotic and trabecular lining. The cyst contents were purulent in one case and serosanguinous/hemorrhagic in the remaining cases. In all cases, the residual splenic parenchyma and capsules were without gross abnormality.

Histopathologic examination revealed a stratified squamous lining in all cases, with focal hyperkeratosis. In two cases, flaky intraluminal keratinaceous debris was noted. There was variable fibrosis underlying the squamous epithelium. The residual splenic parenchyma was without abnormality. Immunohistochemical staining for ER & PR were negative in the lining epithelium in all tested cases. WT-1 was focally positive while calretinin was uniformly negative.

Age (yrs)	Gender	PMHx	Symptoms	Size	Management
13	F	None	Pain, nausea/vomiting, renal obstruction	29 cm	Fenestration; complicated by abscess
21	F	None	Hemoperitoneum (traumatic rupture)	13.7 cm	Total splenectomy; no complications
18	F	Congenitally absent uterus	Pain, nausea/vomiting	15.1 cm	Fenestration; no complications
17	F	None	Pain, nausea/vomiting	11.7 cm	Total splenectomy; no complications

Figure 1 - 1253

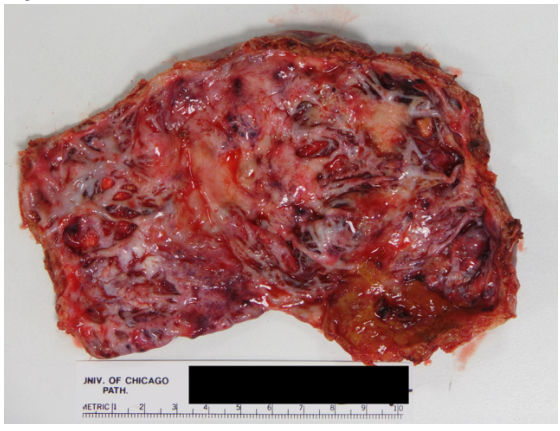

Figure 2 - 1253

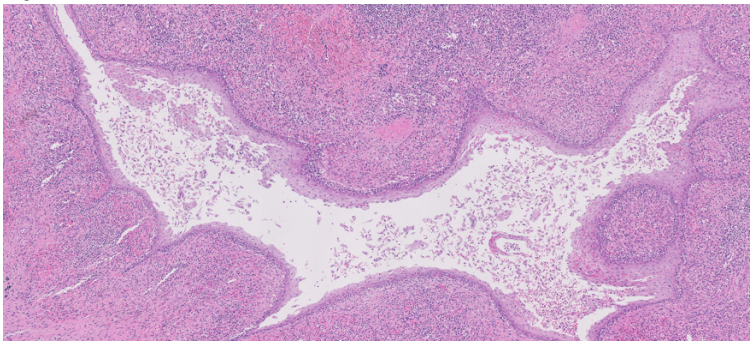

Conclusions: SECs appear to occur almost exclusively in young women both in our series and in the medical literature. The cysts in our series were noted to be significantly larger than most previously described, and all had exclusively squamous linings.

1254 Clinicopathologic And Genetic Characterization of Hypocellular Acute Myeloid Leukemia

Eric Carlsen[1], Nathanael Bailey[2], Matthew Wild[1], Nidhi Aggarwal[1], Yen-Chun Liu[2]
[1]University of Pittsburgh Medical Center, Pittsburgh, PA, [2]University of Pittsburgh School of Medicine, Pittsburgh, PA

Disclosures: Eric Carlsen: None; Nathanael Bailey: None; Matthew Wild: None; Nidhi Aggarwal: None; Yen-Chun Liu: None

Background: Hypocellular acute myeloid leukemia (hypo-AML) is infrequent compared to AML with normal or increased cellularity. The literature suggests variable cut-offs for deeming a case hypocellular, with many reports using a cellularity threshold of 20% and some reports using 40%. Overlapping biologic and phenotypic features between hypo-AML and hypoplastic myelodysplastic syndrome (MDS) have been speculated, and as a result, cases of hypo-AML can pose diagnostic challenges. Despite the prognostic and therapeutic importance of mutation analysis in AML, the mutation profile in hypo-AML has not been well studied. We aim to characterize hypo-AML and its common mutations in comparison with non-hypo-AML, particularly for genes frequently mutated in MDS.

Design: 25 cases of AML with bone marrow cellularity (BMC) <20% (AML-20), 12 cases with BMC 20-40% (AML-40) and 129 cases with BMC >40% (AML>40) were identified. Clinical records and pathology material were reviewed. NGS mutation analysis using amplicon target enrichment of coding and non-coding regions of 37 genes recurrently mutated in myeloid neoplasms was performed on cases with available material.

Results: Patients with AML-20 or AML-40 are older than those with AML>40 (mean 71, 70 vs 62; p<0.05). They also present with lower white counts, lower hemoglobin, and lower blast counts (both in peripheral blood and marrow) (p<0.05). The incidence of prior myeloid neoplasms is not significantly different among the groups. The majority of the AML-20 and AML-40 cases demonstrate decreased M:E ratios and dyspoiesis. No significant difference in survival is noted among groups. 0/15 AML-20 cases but 33/116 AML>40 cases have NPM1 mutations (p=0.01); this trend persists when limited to elderly patients (>60 y/o) to exclude confounding (p=0.06). A high percentage of hypo-AML cases have genetic lesions associated with MDS (19/37 cases or 51% with MDS-defining chromosomal abnormalities or spliceosome mutations), but this does not reach statistical significance when compared to AML>40.

Conclusions: Hypo-AML appeared to be associated with older age and more profound cytopenia but patient survival was similar. A high percentage of the hypo-AML cases demonstrate morphologic and genetic features with an MDS phenotype. The mutational landscapes of hypo-AML and non-hypo-AML appear different even after eliminating the age confounding factor. These findings emphasize potential differences between hypo-AML and non-hypo-AML and warrant further investigation.

1255 Distinct Patterns of Antigen Expression on Peripheral Blood (PB) Myeloblasts By Flow Cytometry (FC) At Diagnosis of Adult B-Lymphoblastic Leukemia/Lymphoma (B-ALL): A Pitfall in the Differential Diagnosis with Mixed Phenotype Acute Leukemia (MPAL)

Luis Carrillo[1], John Astle[2], Ashley Cunningham[3], Alexandra Harrington[1], Steven Kroft[2]
[1]Milwaukee, WI, [2]Medical College of Wisconsin, Milwaukee, WI, [3]Medical College of Wisconsin, Oconomowoc, WI

Disclosures: Luis Carrillo: None; John Astle: None; Ashley Cunningham: None; Alexandra Harrington: None; Steven Kroft: None

Background: The diagnosis of MPAL requires detailed and accurate flow cytometric immunophenotyping. In the context of B-lymphoblastic leukemia/lymphoma (B-ALL), the finding of an additional aberrant myeloblast (MB) population of any size warrants a diagnosis of MPAL according to the current WHO classification. MPAL diagnosis, in turn, implies an adverse outcome and creates uncertainty regarding appropriate treatment. We have anecdotally observed mildly expanded peripheral blood (PB) MB populations at diagnosis of B-ALL that showed distinct immunophenotypic features compared to normal circulating CD34(+) cells, and sought to study this phenomenon systematically.

Design: We identified 28 adult cases of B-ALL diagnosed by PB FC over 10 years. The blasts were characterized by 4- (4 cases) or 8-color (24 cases) flow cytometry for the following antigens in most cases: CD1a, CD2, CD3, CD4, CD5, CD7, CD8, CD10, CD11b, CD13, CD14, CD15, CD16, CD19, CD20, CD22, CD33, CD34, CD36, CD38, CD45, CD56, CD64, CD79a, CD117, CD123, HLA-DR, MPO, and TdT. The percentage of MBs (of total events) and patterns of antigen expressions were compared with those of PB CD34(+) myeloid progenitor cells in 11 PB control cases. A difference in antigen expression was defined as a ¼ log shift compared to controls.

Results: B-ALL patients included 21 men and 11 women with a median age of 43 years (range, 18-86) at initial diagnosis. A PB MB population was detectable in all B-ALL cases, and constituted 0.03-0.75% of events (median 0.16%) vs 0.01-0.13% (median 0.04%) in the control group (p=0.003). Compared to controls, the circulating MBs often showed differences in expression intensity for CD13, CD33, CD34, CD45, CD38, CD117, or HLA-DR (Table). No asynchronous expression of maturation antigens or cross-lineage antigen expression was observed.

Table. Myeloblasts antigen expression differences

	CD13	CD33	CD34	CD38	CD45	CD117	HLA-DR
Normal	14/27	7/25	14/28	1/26	16/28	20/28	13/28
Overexpressed	1/27	0	14/28	0	7/28	2/28	3/28
Under-expressed	12/27	18/25	0	25/26	5/28	6/28	12/28

Conclusions: FC detects a small population of reactive MBs in the PB at diagnosis in all adult B-ALL cases, often in mildly increased numbers compared to normal. The MBs show immunophenotypic differences compared to controls in varying proportions of cases for all antigens normally present on MBs. The patterns of alteration are mostly, but not entirely consistent with a less mature MB phenotype, suggesting release of earlier stage MBs from marrows involved by B-ALL. Awareness of these antigenic shifts is important to avoid over-diagnosing MPAL. Notably, asynchronous expression of maturation antigens and cross-lineage antigen expression were not observed, assisting in the differential diagnosis.

1256 Comparison between Next Generation Sequencing (NGS) and FISH in the Detection of Rearrangements in Large B-cell Lymphomas (LBCLs)

Daniel Cassidy[1], Kyle White[2], Deukwoo Kwon[3], Carmen Casas[4], Sandra Sanchez[5], Offiong Ikpatt[6], Jennifer Chapman[7], Francisco Vega[5]
[1]Miami, FL, [2]Lake Worth, FL, [3]University of Miami, Miller School of Medicine, Miami, FL, [4]UMH/JMH, Miami, FL, [5]University of Miami/Sylvester Cancer Center, Miami, FL, [6]UMH, Miramar, FL, [7]University of Miami, Miller School of Medicine, North Miami, FL

Disclosures: Daniel Cassidy: None; Kyle White: None; Deukwoo Kwon: None; Carmen Casas: None; Sandra Sanchez: None; Offiong Ikpatt: None; Jennifer Chapman: None; Francisco Vega: None

Background: LBCLs are a group of lymphoid neoplasms with a heterogeneous and complex molecular milieu. The molecular makeup of each tumor has prognostic relevance. Currently, LBCLs are further stratified into diffuse LBCL and high grade BCL with MYC and BCL-2 and/or BCL-6 rearrangements and their diagnosis relies on cytogenetic tests. FISH is the gold standard to identify these rearrangements. NGS has become more readily available and cost-efficient; as such, the number of cases sent for NGS is increasing. We currently send all newly diagnosed LBCLs for both FISH and NGS. It has been previously demonstrated that different FISH probes spanning various lengths of the region of interest, 8q24, allow for the detection of different MYC breakpoints. It is expected then that certain breakpoints are missed by FISH, depending on the probe used. In theory, this limitation should be abrogated by the sequencing available using NGS. This is a comparison of FISH and NGS with regards to detection of the aforementioned rearrangements. Should the sensitivities be comparable or even superior for NGS, it may be practical and cost-effective to perform only NGS on these specimens.

Design: We have collected 35 cases of LBCL for which we currently have NGS data. FISH was performed using Vysis probes, including BCL-6 and MYC dual color break apart probes, IGH/BCL-2 dual color dual fusion probe, and IGH/MYC/CEP8 tri-color dual fusion probe. NGS was performed at Foundation Medicine using a hybrid-capture based technique.

Results: The most common mutations were those involving: *BCL2* (54%), *TNFRS14* (34%), *CREBBP* (23%), *CDKN2A* (23%), and *BCL*-6 (20%). The sensitivity and PPV of NGS in detecting BCL-2 and BCL-6 rearrangements were 100%. The sensitivity of NGS in detecting MYC rearrangements was only 50% with a NPV of 88%. NGS detected two BCL-2 and one MYC rearrangement that were missed by FISH. In three instances, FISH detected non-IGH/MYC rearrangements that were not detected by NGS.

Conclusions: Our data suggest that, in the majority of cases, NGS and FISH are concordant. However, there are instances in which standalone testing for either NGS or FISH would result in failure to detect rearrangements. Importantly, three of the six failures would have led to the misclassification of cases as DLBCL, NOS rather than “double-hit” lymphomas. We are continuing to build this database; however, at this time, we cannot recommend the use of standalone NGS for detection of rearrangements in LBCLs.

1257 Blast to plasmacytoid dendritic cell ratio is predictive of progression in low grade myelodysplastic syndromes

Alexander Chan[1], Natasha Lewis[2], Jeeyeon Baik[3], Maria Arcila[3], Yanming Zhang[3], Virginia Klimek[3], Mikhail Roshal[3], Wenbin Xiao[3]
[1]Memorial Sloan Kettering Cancer Center, Chicago, IL, [2]New York, NY, [3]Memorial Sloan Kettering Cancer Center, New York, NY

Disclosures: Alexander Chan: None; Natasha Lewis: None; Jeeyeon Baik: None; Maria Arcila: None; Yanming Zhang: None; Wenbin Xiao: None

Background: Myelodysplastic syndrome (MDS) is a clonal, pre-leukemic stem cell disorder characterized by decreased blood counts due to ineffective hematopoiesis. Plasmacytoid dendritic cells (PDC) are type I interferon-producing cells that also derive from stem cells. Flow cytometry (FC) can quantify PDC using expression of CD123 and HLA-DR. Our prior study showed decreased PDC in acute myeloid leukemia (AML), and that blast/PDC ratio predicted clinical behavior in AML including relapse and progression free survival. In this study we evaluated if depletion of PDCs in MDS predicted clinical outcomes

Design: 200 patients with new MDS diagnoses and available FC data were identified. We examined bone marrow FC data at diagnosis for blast and PDC percentages. MDS with excess blasts 1 and 2 (MDS-EB1/EB2) were designated high grade, while MDS with isolated del5q, single lineage dysplasia (MDS-SLD) and multilineage dysplasia (MDS-MLD) were designated low grade. We used CD34 or CD117 to quantify blasts, CD123 and HLA-DR to quantify PDC, and calculated blast/PDC ratio.

Results: As expected, blasts were higher in high-grade MDS compared to low-grade MDS by FC (median 5.2% vs 0.97%, $p < 0.0001$, Table 1). PDC proportion was lower in high grade MDS versus low grade (0.07% vs 0.17%, $p < 0.0001$, figure 1A). Blast/PDC ratio was higher in high grade MDS compared to low grade (69.2 vs 4.9, $p < 0.0001$, figure 1B). In patients with low grade MDS, those who progressed to higher grade MDS or AML showed a significant increase in blast/PDC ratio (21.87 vs 3.93, $p < 0.0001$), despite absence of difference in blast count by morphology (3.5% vs 3.0%, $p = 0.3408$). Using receiver operator curve statistics, we chose a blast to PDC ratio cutoff of 20 to evaluate progression free survival (PFS) (sensitivity 50%, specificity 93.85%). In the low grade MDS cohort, those with blast to PDC ratio >= 20 showed a median PFS of 234 days compared to 926 days in patients with a ratio < 20 (HR 4.45, 95% CI 1.27 to 15.63,

p < 0.0001, figure 1D). In the entire cohort, patients with ratio >= 20 had shorter PFS compared to those with ratio < 20 (HR 1.78, 95% CI 1.18 to 2.69, p = 0.0075, figure 1C).

	Del5q	SLD / RS-SLD	MLD / RS-MLD	EB1	EB2	Low Grade	High Grade
Blast % Median (IQR - Interquartile Range)	0.85 (0.93-2.03)	0.78 (0.52-1.03)	0.98 (0.37-1.7)	3.1[a] (2-6.4)	8.9[b] (3.9-13.65)	0.97 (0.39-1.6)	5.20 (2.5-9.9)
PDC % Median (IQR)	0.39 (0.18-0.56)	0.19 (0.13-0.29)	0.16 (0.06-0.30)	0.073[c] (0.035-0.2)	0.066 (0.026-0.165)	0.17 (0.067-0.32)	0.07 (0.032-0.195)
Blast/PDC Ratio Median (IQR)	2.79 (1.54-4.9)	2.929 (1.59-8.17)	5.47 (2.82-15.87)	44.0[d] (15.63-92)	113.6[e] (45.82-258.2)	4.94 (2.54-12.94)	69.23 (25.06-151.4)
	p < 0.0001[f]					p < 0.0001[g]	

a. p < 0.0001 for blast % of EB1 vs. MLD/RS-MLD
b. p < 0.0001 for blast % of EB2 vs. EB1
c. p = 0.0059 for PDC % of EB1 vs. MLD/RS-MLD
d. p < 0.0001 for blast/PDC ratio of EB1 vs. MLD/RS-MLD
e. p = 0.0002 for blast/PDC ratio of EB2 vs. EB1
f. p < 0.0001 for the differences in blasts, PDCs and blast/PDC ratio, comparing all subtypes
g. p < 0.0001 for the differences in blasts, PDCs and blast/PDC ratio, comparing high vs. low grade MDS

Figure 1 - 1257

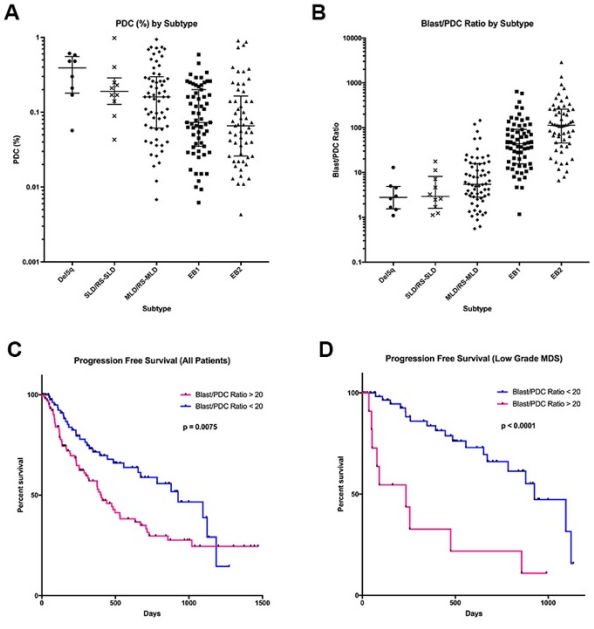

Conclusions: Our study shows that blast/PDC ratio identifies a subset of patients with high risk of progression. The effect was strongest in low grade MDS. Further studies are ongoing to characterize the clinicopathologic features of this subset of low-grade MDS including IPSS-R.

1258 MYC Partner Matters: MYC-IGH is Associated with Inferior Survival in De Novo High-Grade B-cell Lymphomas with MYC and BCL2 and/or BCL6 Rearrangements

Rahman Chaudhry[1], Abdullah Alsuwaidan[2], Prasad Koduru[3], Franklin Fuda[3], Rolando Garcia[3], Mingyi Chen[3], Flavia Rosado[4], Jesse Jaso[3], Hung Luu[3], Hsiao-Ching Li[3], Prapti Patel[3], Madhuri Vusirikala[3], Navid Sadeghi[3], Syed Rizvi[3], Praveen Ramakrishnan Geethakumari[3], Neil Desai[3], Robert Collins[3], Weina Chen[3]
[1]University of Texas Southwestern, Plano, TX, [2]University of Texas Southwestern Medical Center, Pittsburgh, PA, [3]University of Texas Southwestern Medical Center, Dallas, TX, [4]University of Texas Southwestern, Dallas, TX

Disclosures: Rahman Chaudhry: None; Abdullah Alsuwaidan: None; Prasad Koduru: None; Franklin Fuda: None; Rolando Garcia: None; Mingyi Chen: None; Flavia Rosado: None; Jesse Jaso: None; Hung Luu: None; Hsiao-Ching Li: None; Prapti Patel: *Speaker*, Celgene; *Advisory Board Member*, Celgene; Madhuri Vusirikala: None; Navid Sadeghi: None; Syed Rizvi: None; Praveen Ramakrishnan Geethakumari: None; Neil Desai: None; Robert Collins: None; Weina Chen: None

Background: High-grade B-cell lymphomas (HGBL) with *MYC* and *BCL2* and/or *BCL6* rearrangements, so-called "double/triple-hit lymphoma" (DTHL), are generally aggressive lymphomas. While extensively studied recently, many questions remain as to which factors have prognostic values. In this study, we analyzed the clinicopathologic features of such cases in an attempt to improve risk stratification among the DTHL.

Design: A search of an institutional database from 2000 to 2017 yielded 85 cases of large B-cell lymphomas (LBCL) that were further divided by 2016 WHO into the following groups: 39 cases of DTHL, 33 MYC^{neg} DLBCL, and 13 SHL/LBCL (non-BL). All cases were examined for *MYC*, *BCL2* and *BCL6* by FISH. The clinicopathologic features, including morphology, MYC-IHC, GC, DE, therapeutic regimens and overall survival (OS) were assessed and compared (Table 1). $p < 0.05$ was considered significantly different. Abbreviations are presented in the notes in Table 1.

Results: Of the DTHL, 29 cases were *de novo* and 10 transformed from low grade lymphoma. Of the *de novo* cases, 24 cases were DLBCL and 5 BCLU by morphology; alternatively, 17 DTHL-*MYC-IGH* and 12 DTHL-*MYC-non-IGH* by *MYC*partner. There was no significant difference in age, sex, MYC-IHC and DE among these subgroups except DHL-*BCL6* was less likely to be GC. At a median follow-up of 19 months (range 0.2 to 133) with most patients treated with intensive regimens, OS in transformed DTHL was inferior to *de novo* DTHL (10 vs. 53 months, $p < 0.05$) (Fig. A). Of the *de novo* DTHL, DTHL-*MYC-IgH* had a tendency toward a short OS compared to DTHL-*MYC-non-IgH* (Fig. B). While there was no difference in OS among *de novo* DTHL, MYC^{neg} DLBCL and SHL/LBCL (Fig. C), OS was shorter in DTHL-*MYC-IgH* compared to DTHL-*MYC-non-IgH, MYC^{neg}* DLBCL and SHL/LBCL ($p < 0.05$, Fig. D and Table 1). The status of morphology, DTHL-*BCL2 vs. -BCL6*, GC, DE and MYC-IHC had no effect on OS.

Table 1. Clinicopathologic Features of Large B-cell Lymphomas (LBCL)

	Age/Sex (year-M/F)	MYC-IHC*	GC*	DE*	Median survival(months)	Therapies (intensive**)
Transformed DTHL (n=10)	64 (7M/3F)	5/7 (71%)	9/10 (90%)	5/7 (71%)	10	4/9
***De novo* DTHL (n=29)**	63 (17M/12F)	22/24 (92%)	23/28 (82%)	19/22 (86%)	53	22/24
***De novo* DTHL-*MYC-IgH* (n=17)**	63 (11M/6F)	13/14 (93%)	13/17 (76%)	11/14 (79%)	51	
De novo DTHL-*MYC-non-IgH* (n=12)	63 (6M/6F)	9/10 (90%)	10/11 (91%)	8/8 (100%)	Undefined	
***MYC^{neg}* DLBCL (n=33)**	58 (20M/13F)	12/30 (40%)	19/32 (59%)	12/28 (43%)	133	4/29
SHL/LBCL (n=13)	39 (7M/6F)	4/5 (80%)	7/7 (100%)	2/6 (33%)	undefined	8/11

Of DTHL, 27 cases as DTHL-*BLC2*, 12 DHL-*BCL6*, and 6 THL

*: presented as positive cases/total cases (%); MYC-IHC = or > 40% as positive; Han's algorithm for GC and non-GC; DE, double expressor phenotype [positive for IHC of BCL2 (= or > 50%) and MYC (= or > 40%)]

**: intensive therapies including EPOCH-R, or hyper-CVAD or RICE

Abbreviations:

HGBCL, high-grade B-cell lymphomas; DTHL, HGBCL with *MYC* and *BCL2* and/or *BCL6* rearrangements [(so-called "double/triple-hit" lymphomas (DTHL)]; SHL, B-cell lymphoma with *MYC* rearrangement but without *BCL6* or *BCL2*rearrangement; DHL, double hit lymphoma; THL, triple hit lymphoma; Burkitt lymphoma, BL; DLBCL, diffuse large B-cell lymphoma; BCLU, B-cell lymphoma, unclassifiable, with features intermediate between BL and DLBCL; *MYC*^{neg} DLBCL, DLBCL without *MYC* rearrangement; LBCL, lymphomas of medium to large cell size including DLBCL and BLCU; GC, germinal center B-cell like phenotype; FISH, Fluorescence in situ hybridization; R-CHOP, rituximab, cyclophosphamide, doxorubicin, and vincristine; EPOCH-R, dose adjusted etoposide, prednisone, vincristine, cyclophosphamide, doxorubicin, and rituximab; hyper-CVAD, hyperfractionated cyclophosphamide, vincristine, doxorubicin, and prednisolone; RICE, rituximab, ifosfamide, carboplatin and etoposide

Figure 1 - 1258

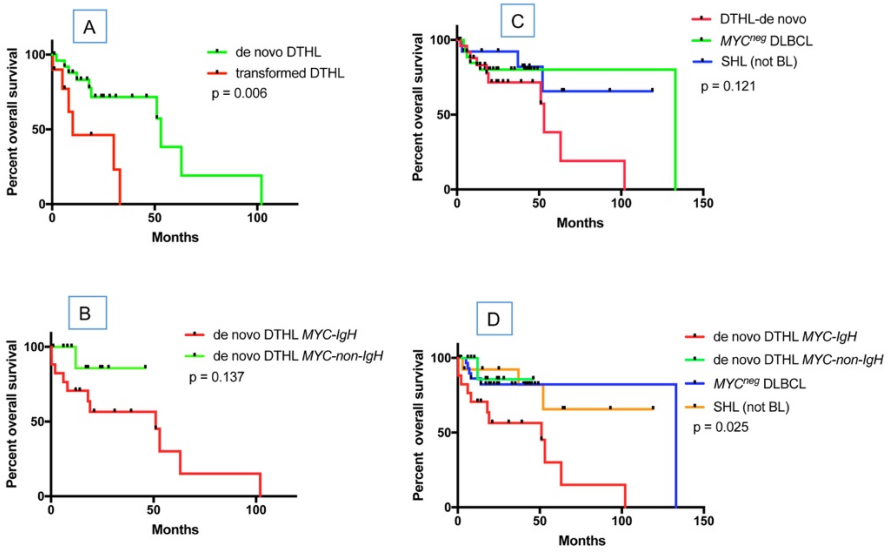

Conclusions: Our retrospective study highlights the heterogeneity among the DTHL with regard to morphology, phenotype, genotype and clinical outcomes. Importantly, DTHL transformed from low grade lymphoma has a dismal survival. Of the *de novo* DTHL, survival is affected by *MYC* partner with an inferior survival in DTHL-*MYC-IgH*. These findings may improve risk stratification by identifying those patients who may benefit from intensive treatment. Future prospective studies including *MYC* partner on light chain genes are needed for validating our results and exploring molecular pathogenesis.

1259 Is Hyperdiploidy Favorable in Adult B-Lymphoblastic Leukemia?

Zhining Chen[1], Sa Wang[1], Shimin Hu[1], Shaoying Li[1], Zhenya Tang[1], Gokce Toruner[1], L. Jeffrey Medeiros[1], Guilin Tang[1]
[1]*The University of Texas MD Anderson Cancer Center, Houston, TX*

Disclosures: Sa Wang: None; Shimin Hu: None; Shaoying Li: None; Henya Tang: None; L. Jeffrey Medeiros: None; Guilin Tang: None

Background: B-lymphoblastic leukemia (B-ALL) with hyperdiploidy (chromosomal number 50-65) is a common and favorable cytogenetic subgroup in pediatric (pedi) B-ALL, typically without translocations or other structural abnormalities. Hyperdiploidy in adult B-ALL is much less frequent and not well studied and prognostic importance of hyperdiploidy is controversial.

Design: We searched our database for patients with B-ALL who were diagnosed and managed at our institution from 2006 to 2018. Cases with a chromosome number between 50-65 and without monosomy or recurrent translocations were included. Clinicopathologic and laboratory data were collected. Cases were arbitrarily divided into 4 subgroups based on the number of structural abnormalities: hyper0, hyper1, hyper2, and hyper3, corresponding to 0, 1, 2, and 3 or more structural abnormalities, respectively.

Results: A total of 1205 patients (187 pedi and 1018 adults) with B-ALL were found, of which 78 had a hyperdiploid karyotype, including 45 (4.4%) adults and 33 (17.6%) pedi patients (p<0.0001). Overall, the adult group had a much more unfavorable outcome than the pedi group (median survival: 42 months vs. undefined, p=0.0029, Fig 1A). In addition, the adult group more frequently had additional structural abnormalities: the number of patients with hyper0, hyper1, hyper2, and hyper3 were 15, 6, 8, 16 in adult group and 13, 9, 3, 8 in pedi group, respectively. In pedi patients, additional structural abnormalities (regardless of number) in hyperdiploidy did not affect overall

survival (OS) (p=0.4851). In the adult group, patients with hyper0 and hyper1 showed a similar favorable OS, but adults with hyper2/3 showed an inferior OS compared with patients with hyper0/1 (33 months vs. undefined, p=0.0008) (Fig 1B). Adult patients with hyper0/1 (n=21) had a comparable and favorable OS as pedi with hyper0/1 (n=22) (undefined vs. undefined, p=0.7026, Fig 1C), but adult patients with hyper2/3 (n=24) showed a much worse OS comparing to pedi patients with hyper2/3 (n=11) (33 months vs. undefined, p=0.0002) (Fig 1D)

Figure 1 - 1259

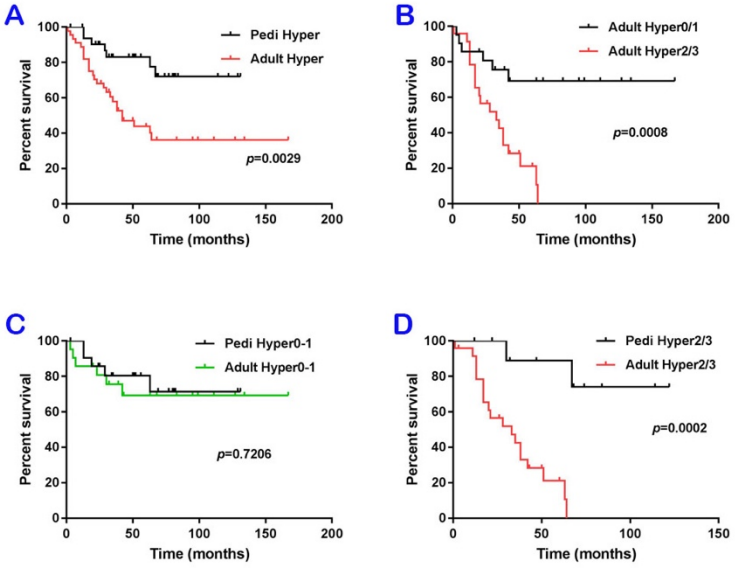

Conclusions: Hyperdiploidy is less infrequent and is an overall unfavorable cytogenetic subgroup in adult B-ALL patients compared with pediatric patients. Hyperdiploidy in adult B-ALL is more often associated with additional structural abnormalities; two or more structural abnormalities convey inferior outcomes which likely contribute to the less favorable outcome of adults with hyperdiploidy B-ALL.

1260 The clinicopathological investigation of EBV-positive T/NK-cell lymphoproliferative diseases and the construction of the prognostic nomogram for hemophagocytic lymphohistiocytosis

Zihang Chen, West China Hospital, Sichuan University, Chengdu, China

Disclosures: Zihang Chen: None

Background: EBV-positive T/NK-cell lymphoproliferative diseases (EBV-T/NK-LPD) are a spectrum of disease including chronic active EBV infection of T/NK-cell type (CAEBV-T/NK-LPD) and systemic EBV-positive T-cell lymphoma of childhood (STLC), which are always accompany with hemophagocytic lymphohistiocytosis (HLH) and in bad outcome. Additionally, it is difficult to tell them from infectious mononucleosis of T/NK-cell type (IM-T/NK) at very beginning.

Design: The cases with primary diagnosis of EBV-T/NK-LPD form January 2013 to December 2016 were reviewed based on the diagnostic criteria metioned in revised 4th edtion of WHO classification of tumours of hematopoietic and lymphoid tissue (2016) to include the cases with the diagnosis of IM-T/NK, CAEBV-T/NK-LPD and STLC. The relevant data were collected for analysis and construction of prognostic nomogram.

Results: Of the 51 cases of EBV-T/NK-LPD, the mean age was 30.22 years (ranged, 7-77 y), and male to female ratio was 2:1, including 9 cases of IM-T/NK, 28 cases of CAEBV-T/NK-LPD, and 14 cases of STLC. For clinical characteristics, the difference between IM-T/NK-LPD and CAEBV-T/NK-LPD or STLC showed significant elevated peripheral blood leucocyte (P=0.003). For histopathology, STLC was more in monomorphic morphology, while all IM-T/NK cases were polymorphic. For immunophenotype, the EBER-ISH positive rate of STLC was significantly higher than that of IM-T/NK-LPD or CAEBV-T/NK-LPD (P=0.031), and IM-T/NK was more than CAEBV-T/NK-LPD and STLC in CD4/CD8>1 (P=0.011). Univariate analysis showed that splenomegaly (P=0.003), anemia (< 82g/L, P< 0.001), with HLH (P=0.047), indicates poor prognosis; while NK-cell type suggests a good prognosis (P=0.016). Multivariate analysis showed that hemoglobin < 82g/L (HR, 4.504;95%CI, 1.586-12.788; P=0.005) is independent the risk factors. The prognostic nomogram of HLH was constructed based on 3 factors (course, CD4/CD8 and erythrophagocytosis) The calibration curve showed a high coincidence index in the validation cohort (C-index, 0.825).

Figure 1 - 1260

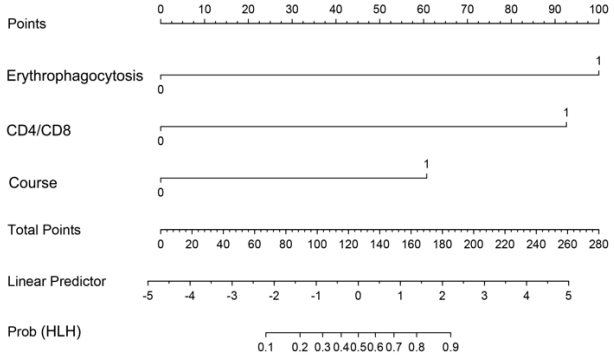

Figure 2 - 1260

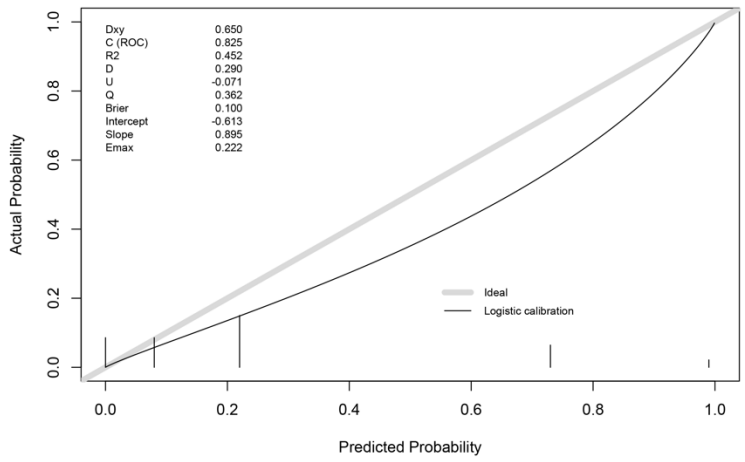

Conclusions: Increased white blood cell counts, polymorphic appearance, and extensive CD8+T lymphocytes proliferation suggest the diagnosis of IM-T/NK-LPD. Anemia (hemoglobin < 82g/L) indicates poor prognosis of patients with EBV-T/NK-LPD. The prognostic nomogram of HLH has relatively high prediction accuracy and strong stability, and it may provide the hint for diagnosis and clinical intervention.

1261 Study of immature cytoplasmic CD3, CD7 and TdT positive T-cell population in post chemotherapy patient and their implication for T-cell acute lymphoblastic leukemia minimal residual disease detection

Xiuxu Chen[1], Wei Cui[2], Da Zhang[3]
[1]University of Kansas Medical Center, Kansas City, KS, [2]University of Kansas Medical Center, Shawnee, KS, [3]Kansas University Medical Center, Kansas City, KS

Disclosures: Xiuxu Chen: None; Da Zhang: None

Background: T-cells are developed from hematopoietic stem cells in the bone marrow migrate to the thymus to complete their maturation into functional T cells. The cytoplasmic CD3 (cCD3), CD7 and TdT positive immature T-cells are usually absent in the bone marrow. Thus cCD3, TdT and other T-cell markers have been used in detect T-cell acute lymphoblastic leukemia (T-ALL) minimal residual disease (MRD). However, cCD3 and TdT positive cells are also present in normal or regenerating bone marrow. This cell population may create an issue and diagnostic pitfall in T-ALL MRD detection after chemotherapy.

Design: We followed 7 patients who had an acute myeloid leukemia and performed T-ALL MRD flow cytometry panel start at post chemotherapy day 28 at the University of Kansas Medical Center. The patient's flow cytometry data and clinical outcome were analyzed to determine the range of cCD3 and TdT positive cells in post chemotherapy bone marrow biopsy specimens and their implications in T-ALL minimal residual disease detection.

Results: Among the 7 AML patients status post chemotherapy at day 28, T-ALL MRD flow cytometry studies showed cCD3 and TdT positive cells are ranged from 0.01 to 4% of the total cells. We followed the patient who had 4% cCD3 and TdT cells at post chemotherapy day 28 in a series T-ALL MRD study. The cCD3 and TdT cells dropped to 2.6% at day 37, then 0.4% at 2 months and down to 0% at 4 months and remained undetectable at 5 months. None of these patients progress to T-ALL upto the current following up date.

Conclusions: The case study is small, we are expanding our study. Low levels of cCD3 and TdT positive cells are present in post chemotherapy regenerating bone marrow and detectable by flow cytometry. These immature T-cells can create a diagnostic pitfall in T-ALL MRD detection, Extra caution should be taken when interpret T-ALL MRD especially at post chemotherapy day 28.

1262 Clinicopathologic Characteristics and Novel Biomarkers of Aggressive B-Cell Lymphomas in the Nasopharynx

Po-Han Chen[1], Dennis O'Malley[2], Mina Xu[3]
[1]Yale University, New Haven, CT, [2]O'Malley Medical Consulting, Dana Point, CA, [3]New Haven, CT

Disclosures: Po-Han Chen: None; Dennis O'Malley: None; Mina Xu: None

Background: The most common nasopharyngeal lymphoma in the United States are B-cell non-Hodgkin lymphomas, accounting for 75% of all cases. Relatively little is known about the clinicopathologic features of these cases. In this study, we characterize a multi-institutional cohort of aggressive B-NHL primary to the nasal/nasopharyngeal area. We compare and contrast EBV positive versus EBV negative cases and evaluate expression of SSTR2, CD30 and PD-L1, potential markers for targeted therapeutics.

Design: We retrieved 53 cases of aggressive B-NHL, including 48 Diffuse Large B-cell Lymphomas (DLBCL), 2 Burkitt lymphomas, 2 high-grade B-cell lymphomas and 1 plasmablastic lymphoma, from the two institutions. Cases with prior or concurrent systemic lymphoma were excluded. Diagnoses were made according to current WHO criteria. In all cases available, staining was performed for in situ EBV (EBER), CD30, SSTR2 and PD-L1. The response to initial therapy, disease-free interval, and survival at two- and five-year follow-up were used as primary outcome data.

Results: Thirteen out of all 50 cases (26%) were EBV positive. No significant difference was found between EBV+ and EBV- cases in terms of age, proliferation index or cell-of-origin classification by Hans criteria for DLBCL (**Table**). Average expression of CMYC by IHC was higher for EBV- than EBV+ cases (45% vs 15%), while no significant difference is found in CMYC translocation by FISH (15% versus 10%, respectively). CD30 expression was more frequent in EBV+ than in EBV- cases (3/5 vs 1/17). Six of 15 (40%) cases tested were positive for SSTR2. Seven of 14 (50%) cases tested demonstrated expression of PD-L1 within tumor cells; the two EBV+ DLBCL tested showed substantial PD-L1 reactivity. The three EBV+ patients with available outcome data died within one year of diagnosis; in contrast, the EBV- cases show survival rate of 100% (8/8) and 83% (5/6) at two- and five-year follow-up, respectively.

Table: Characteristics of EBV+ and EBV- Nasopharyngeal B-NHL

Characteristics	EBV+ (n=12)	EBV- (n=41)
Average age at diagnosis	62	65
Ki-67 Proliferative Index (% positivity)	73.6	84.8
CMYC IHC (% positivity)	15	45
CMYC translocation by FISH (% cases)	10	15

Conclusions: The aggressive B-NHLs of the nasopharynx show differences between EBV+ versus EBV- cases. The association of EBV+ cases with expression of CD30 and PD-L1 is particularly informative for targeted therapies. This data corroborate with previous studies of PD-L1 expression in virus-associated B-cell malignancies. A significant number of cases expressed SSTR2, which could render them susceptible to somatostatin analogue and peptide receptor radionuclide therapies. Finally, EBV negativity predicted an improved prognosis.

1263 Tumor Associated Antigen Expression Profiles and Clinical Significance in Relapsed Multiple Myeloma Patients

Betty Chung[1], Yuelan Ren[2], Shivani Mukhi[3], Ann Leen[4], Premal Lulla[5]
[1]Houston Methodist Hospital, Houston, TX, [2]Houston Methodist Research Institute, Houston, TX, [3]Baylor College of Medicine, Sugar land, TX, [4]Texas Children's Hospital, Houston, TX, [5]Baylor College of Medicine, Houston, TX

Disclosures: Betty Chung: None; Yuelan Ren: None; Shivani Mukhi: None; Ann Leen: *Primary Investigator*, Marker Therapeutics; Premal Lulla: None

Background: Multiple myeloma (MM) remains incurable and patients frequently relapse despite combination chemotherapy, prolonged maintenance, and autologous stem cell transplantation. Adoptive transfer of T lymphocytes with native TCRs specific for cancer-antigens has demonstrated efficacy in treating patients with advanced hematological and solid malignancies. Therefore the purpose of this study is to describe the expression patterns of a cohort of myeloma-associated antigens that have been shown to elicit robust T lymphocyte responses *ex vivo*.

Design: Expression profiles of MAGE-A4, NY-ESO1, PRAME, SSX-2, and survivin were evaluated by immunohistochemical stains and scored for intensity and percentage of CD138-dual stained plasma cells in eleven relapsed MM patients (4 women, 7 men; median age: 53 years). Patient disease characteristics and eventual outcomes to subsequent lines of therapy were annotated and will be presented using descriptive statistics.

Results: All five TAAs were found to be expressed with variable intensity proportions of positive cells in this cohort of patients validating that these are MM-associated antigens. MAGE-A4, NY-ESO1, PRAME, SSX-2, and survivin expression was found in 100%, 64%, 55%, 9%, and 73% of patients, respectively. The median number of MM cells in each patient that expressed each TAA was 50% and ranged from zero to >75% of MM cells for PRAME, MAGE-A4, NY-ESO1, and survivin and was 5% for SSX-2 with a range of zero to <10% of MM cells. Overall, each patient's tumor expressed an average of 2.2 TAAs per patient.

Conclusions: MAGE-A4, NY-ESO1, PRAME, SSX-2, and survivin are commonly expressed in relapsed MM patients and are suitable targets for adoptive T cell transfer therapies. The interpatient and intra-tumor variability in the expression of each antigen would indicate that an approach that targets multiple TAAs p.p1 {margin: 0.0px 0.0px 8.0px 0.0px; text-align: justify; font: 11.0px 'Trebuchet MS'; color: #000000; -webkit-text-stroke: #000000} span.s1 {font-kerning: none}simultaneously would be most broadly applicable and could minimize tumor immune escape. Our method of co-staining with CD138 can accurately identify and quantify the expression of TAAs within MM cells.

1264 Lymphomatoid papulosis type E with subcutaneous tissue infiltration and prominent rimming

Fina Climent[1], Jan Bosch[2], Rosa Penin[1], Maria Pané[1], Itziar Salaverria[3], Maria Del Mar Varela Rodriguez[4], Cristina Muniesa[1], Octavi Servitje[1]
[1]Hospital Universitari de Bellvitge, L'Hospital de Llobregat, Spain, [2]Hospital de Bellvitge, L'Hospitalet de Llobregat, Spain, [3]Hospital Clinic of Barcelona, Barcelona, Spain, [4]ICO, Hospitalet de Llobregat, Spain

Disclosures: Fina Climent: None; Jan Bosch: None; Maria Del Mar Varela Rodriguez: None

Background: Lymphomatoid papulosis (LyP) type E is a rare variant of LyP. The infiltrates of atypical cells are angiocentric and angiodestructive and may simulate aggressive lymphomas such as extranodal T/NK-cell lymphoma, cutaneous gamma/delta T-cell lymphoma and anaplastic large cell lymphoma. We detail the clinicopathological and molecular features of 5 cases with the goal of identifying a pattern of infiltration previously unreported in the literature.

Design: The main clinical data were retrieved from the patient's records. Hematoxylin and eosin stained slides and corresponding immunohistochemistry were analyzed and molecular biologic assays were performed.

Results: Our series is comprised of 3 females and 2 males, with a median age of 58 years (range: 37-70).

All 5 cases had clinical manifestations, presenting as nodules that rapidly evolved into large ulcerations (diameter 1 to 7cm)(Fig. 1). One patient showed involvement of tongue as debut manifestation, while the other 4 initially developed lesions on the skin. The prognosis was excellent. The patient with oral disease debut subsequently presented skin involvement. One case developed Mycosis fungoides during patient follow-up.

In all cases, morphology showed dermal angiocentric infiltrates of pleomorphic cells with hemorrhage, necrosis and ulceration. An epidermotropic infiltrate was seen in 2 out of 3 cases with available epidermis. The subcutaneous tissue was affected in the 5 cases and in 3 of them the histological features included rimming of adipocytes by neoplastic lymphocytes. The neoplastic cells were positive for CD30 (100%) (Fig. 2), CD8 (60%), CD4 (40%) and TIA1 (60%). EBERs, EMA and ALK1 were negative. Monoclonal TCR gene rearrangements were found in 4 cases. Rearrangements of the IRF4/DUSP22 locus on 6p25.3 were absent in all 5 cases analyzed by FISH.

Figure 1 - 1264

Figure 2 - 1264

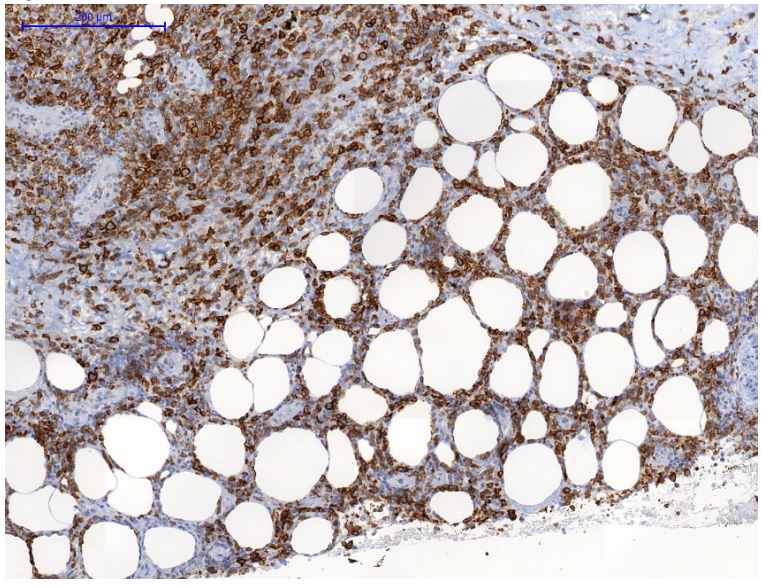

Conclusions: We are describing a new pattern of subcutaneous tissue infiltration previously unreported in LyP type E, with neoplastic cells rimming hypodermic adipocytes. The identification of rimming should prompt differential diagnosis with subcutaneous panniculitic-like T-cell lymphoma.

1265 Copy Neutral Loss of Heterozygocity (CN-LOH) study with Oncoscan demonstrates recurrent abnormalities involving chromosomes 9,13, and 17

Adam Cloe[1], Victoria Bedell[2], Joo Song[3], Raju Pillai[2], Dennis Weisenburger[2], Young Kim[2]
[1]Los Angeles, CA, [2]City of Hope National Medical Center, Duarte, CA, [3]City of Hope Medical Center, Duarte, CA

Disclosures: Adam Cloe: None; Joo Song: None; Young Kim: None

Background: Blastic plasmacytoid dendritic cell neoplasm (BPDCN) is a rare and aggressive hematologic malignancy that is derived from plasmacytoid dendritic cell precursors. It is often associated with complex cytogenetic abnormalities. Next generation sequencing studies demostrated many point mutations including NRAS, ATM, MET, KRAS, IDH2, KIT, APC, RB1, VHL, BRAF, MLH1, TP53, and RET in varying degree from 3% to 27% in one recent study. Another recent study with whole exome sequencing showed many point mutations including TET2, ASXL1, NPM1, NRAS, IKZF1-3, ZEB2, HOXB9, and UBE2G2. However examination of copy-neutral loss of heterozygosity (CN-LOH) has not been systemically studied in BPDCN.

Design: After searcing BPDCN cases in our institution, we identified 12 cases with usuable formalion fixed paraffin embeded tissue (FFPE) and studied copy neutral los of heterozygocity (CN-LOH) with OncoScan FFPE Assay Kit, which provides cancer gene coverage of about 900 cancer genes ranging from 50Kb to 125Kb, geneome wide coverage outside of the ~900 cancer genes and genome wide LOH with resulution of 3Mb-10Mb. 240K single nucleodie polymorphism (SNP) probes used for copy number (CN) detection. Probes are single stranded. There are 3 copies of each allele on the array. SNP is located in the Gap Fill position. Size of probes: Genomic part of molecular inversion probe (MIP) is 40-70nt and the tag is 25 nt. It also provides 74 SNP probes for somatic mutations (SM) detection.

Results: The OncoScan study demonstrates recurrent abnormalities involving chromosomes 9,13, and 17.Two cases has single loss of chromosome 9, One case with single loss of chromosome 13, One case with single loss of chromosome 17, Two cases with loss of chromosome 9 and 13, Two cases with loss of chromosome 13 and 17. Loss of varying length of chromose 13 is most common, occuring 6 of 12 cases, which includes loss of BRCA2, LHFP, FOXOP1, LCP1, and RB1 genes. In addition, it showed somatic mutations involving MTAP/CDKN2A, PTEN, KRAS, and ETV6.

Conclusions: In conclusion, our study demonstrates recurrent CN-LOH involving chromsome 9, 13, and 17 in high frequencies. This new finding adds another important insight to the pathogenesis of BPDCN, which has multiple abnormalities of genes, mainly point mutations, shown by whole exom sequencing and targeted ultra-deep sequencing.

1266 Characterization of MPL Mutations in Myeloid Malignancies

Ryan Craig[1], Kristin Karner[2], Jay Patel[3]
[1]Salt Lake City, UT, [2]University of Utah, Salt Lake City, UT, [3]University of Utah/ARUP Laboratories, Salt Lake City, UT

Disclosures: Ryan Craig: None; Kristin Karner: None

Background: Myeloproliferative neoplasms (MPN) are clonal diseases of the hematopoietic system that lead to hypercellularity of the bone marrow and peripheral blood and consist primarily of polycythemia vera (PV), essential thrombocythemia (ET), primary myelofibrosis (PMF), and chronic myeloid leukemia (CML). JAK2 and CALR mutations are associated with MPNs. The MPL gene, known as the thrombopoietin receptor, is also implicated in MPNs, although at a lower frequency. We sought to further characterize this association.

Design: We analyzed a series of cases submitted to a large reference laboratory for myeloid mutation panel of 58 genes by massively parallel sequencing (n=23,812). All cases with MPL mutations were identified and were further evaluated by submitted diagnosis, specific mutation, and variant allele frequency (VAF).

Results: Of the 23,812 cases submitted for NGS myeloid panel, 89 had MPL mutations (0.4% of all cases). The most common submitted diagnoses were MPN, not further classified (22%), PMF (21%), acute myeloid leukemia (AML) (12%), myelodysplastic syndrome (MDS) (11%), ET (8%), and PV (2%). No MPL mutations were detected in aCML, CEL, or CNL. The most common mutations include: W515L (58%), W515K (14%), S505N (12%), W515R (7%), W515S(5%), and Leu511fs (2%). Interestingly, the Leu511fs mutation was found in a patient with MDS and low VAF (8-12%), who never showed features of MPN, suggesting this rare mutation may have a different phenotype. We detected low-level mutations down to a variant allele frequency (VAF) of 1.5%, near the assay limit of detection, in cases of MDS, MPN, PV, ET, PMF, and AML (Table 1). The majority of cases had mutations in MPL alone (81%) but some were co-mutated with JAK2 (15%) or CALR (4%).

	Median VAF	VAF Range
MDS	17%	3.0-92%
MPN	30%	6.7-89%
PV	4.8%	2.6-7%
ET	16%	5.6-66%
PMF	46%	4.4-89%
AML	33%	1.9-91%

Conclusions: MPL mutations may be seen in various myeloid malignancies, although we most commonly identified them in MPNs including PMF and ET, as well as a few cases of AML, but none were seen in aCML, CEL, or CNL. The most common mutation was the W515L variant (52%) with others detected at lower frequencies. 19% of cases with MPL mutation showed co-mutation with either JAK2 or CALR. NGS testing found several cases with MPL mutation VAFs near the limit of detection of 1.5%. The case with the lowest VAF is in a patient with persistent thrombocytosis (930k/uL at presentation) and splenomegaly undergoing hydroxyurea therapy, suggesting that it is possible to have a clinically significant phenotype with a VAF as low as 1.5%.

1267 Marginal Zone Lymphoma in HIV: Unique Site Predilection and Frequent Association with Synchronous or Metachronous Aggressive B-Cell Lymphomas

Genevieve Crane[1], Wayne Tam[2], Daniel Knowles[3], Amy Chadburn[2]
[1]New York-Presbyterian/Weill Cornell Medical Center, New York, NY, [2]Weill Cornell Medical College, New York, NY, [3]Weill Cornell Medicine, New York, NY

Disclosures: Genevieve Crane: None; Wayne Tam: None; Daniel Knowles: None; Amy Chadburn: None

Background: Immunosuppression in the setting of HIV is associated with increased risk of non-Hodgkin lymphoma of 60-200-fold depending on treatment status. This risk is predominantly due to aggressive B-cell lymphomas, which are often associated with Epstein-Barr virus (EBV) infection. However, HIV/AIDS patients also have an increased risk of more indolent non-Hodgkin lymphomas of approximately 14-fold. These have been less extensively investigated. Given the recent finding by multiple groups of EBV+ marginal zone lymphomas (MZL) in patients with other forms of immune suppression (solid organ transplant, iatrogenic, congenital and age-related) which appear to show an indolent course, we wanted to further characterize MZL arising in the setting of HIV.

Design: The pathology archives at a single institution were searched from 1/1995 to 9/2018 to identify patients with a history of HIV/AIDS and subsequent diagnosis of MZL. Where available, clinical history was collected and additional staining performed to assess EBV-association and latency status.

Results: Eleven patients with HIV and a diagnosis of MZL were identified ranging in age from 7 (congenital HIV infection) to 62 years (Table). These were predominantly extranodal (9/11), 3 of which presented in the nasopharynx (Fig 1). Both cases of gastric MALT lymphoma were *H. pylori*-associated. EBV+ cells varied, but were predominantly scattered (<1% to 10%, Fig 2) with one case showing

more diffuse EBV-positivity. Strikingly, 6/11 patients had synchronous (2 patients, Fig 2) or metachronous (4 patients) aggressive B-cell cell lymphomas. DNA available from 2 patients with metachronous lesions demonstrated that they were not clonally related.

Clinical and Pathologic Features of MZL Arising in the Setting of HIV

		MZL		Secondary			
Age	**Sex**	**Site**	**EBER**	**Site**	**Diagnosis**	**Timing from MZL Dx (yrs)**	**Other**
47	M	Nasopharynx	10%	Lymph node (inguinal)	DLBCL (EBV+)	0.3	Processes not clonally related
48	M	Parotid	<1%				Not on retroviral therapy; Hepatitis C+
62	M	Prostate	Neg				Rising PSA; inguinal lymphadenopathy
43	M	Nasopharynx	Neg				Ear with bloody discharge for 5 years prior (Fig 1)
7	F	Lymph node (inguinal)	Diffuse	Lymph node (inguinal)	CHL (EBV+)	3.4	Congenital HIV infection; CHL not clonally related
36	M	Stomach	5%	Stomach	DLBCL	Synchronous	H. pylori+; Hepatitis C+, Fig 2 (A, B)
52	M	Lung	10%	Lung	DLBCL	Synchronous	Fig 2 (C, D)
61	F	Stomach	ND				Gastritis, melena
53	M	Lymph node (cervical)	ND				
38	M	Widespread	ND	Parotid	DLBCL	-1.4 (prior)	Found dead; Diffuse MZL involvement including leptomeninges and skull base, Negative for DLBCL at autopsy
55	M	Nasopharynx	ND	Orbit	DLBCL	0.2	

Figure 1 - 1267

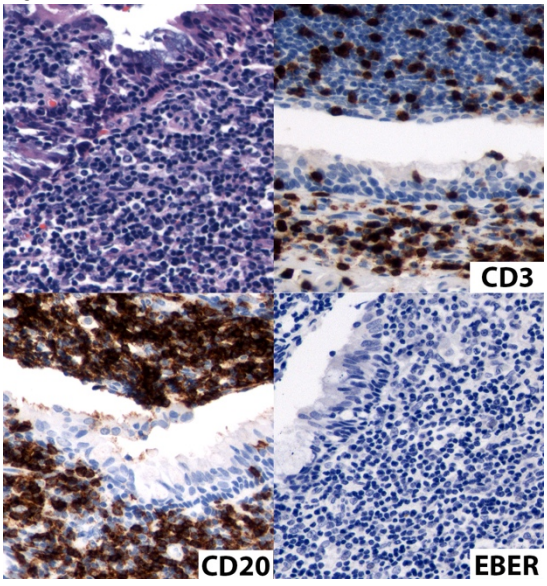

Figure 2 - 1267

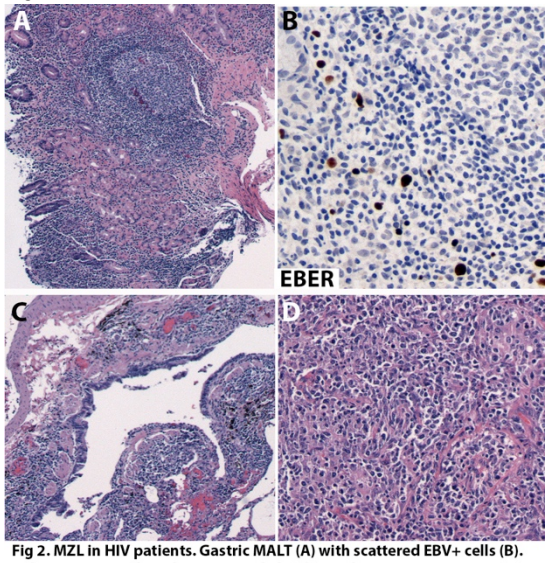

Fig 2. MZL in HIV patients. Gastric MALT (A) with scattered EBV+ cells (B). Pulmonary MALT lymphoma (C) with focal transformation to DLBCL (D).

Conclusions: MZL in the setting of HIV has several unique features. We confirm the unusual site distribution, including 3 in the nasopharynx, as suggested by prior small series. EBV may be reactivated in this setting, but at least a subset are EBV-associated as seen in other forms of immune suppression. However, in contrast to the typically indolent course described for these cases, one patient demonstrated a clinically aggressive MZL which secondarily involved the CNS without evidence of a transformed component at autopsy. In addition, 6/11 patients with HIV and MZL had concurrent or separate diagnoses of diffuse large B cell (DLBCL) or classical Hodgkin lymphoma (CHL). Overall, these findings suggest the presence of MZL may correlate with particularly increased risk of aggressive lymphoma in the HIV population.

1268 Clonal Populations in HIV-Associated Reactive Lymph Nodes Rarely Develop into High Grade Lymphoma

Genevieve Crane[1], Wayne Tam[2], Joelle Racchumi[3], Amy Chadburn[2]
[1]New York-Presbyterian/Weill Cornell Medical Center, New York, NY, [2]Weill Cornell Medical College, New York, NY, [3]Weill Cornell Medicine, New York, NY

Disclosures: Genevieve Crane: None; Wayne Tam: None; Joelle Racchumi: None; Amy Chadburn: None

Background: Reactive lymph nodes in HIV-positive patients contain clonal B cell populations (J Exp Med 1986; 165:2049). However, whether these clonal populations evolve into high grade B cell lymphoma (HG-BNHL), and thus can predict lymphoma evolution, or represent residual disease from previously treated HG-BNHL, which may represent a focus of recurrence, has not been determined. Furthermore, whether these clonal populations in HIV-associated reactive lymph nodes are related to Epstein Barr virus (EBV) infection, as in PTLDs, or KSHV/HHV8 infection is also not clear.

Design: 30 specimens from 13 HIV+ men (age 27-72 years; 2-3 specimens / pt) who had reactive (16) and malignant (14) lymphoid lesions were examined by PCR analysis (BIOMED-2 IGH and IGK assays, InvivoScribe). The lymphomas were classified as per the 2016 WHO classification. In cases with sufficient material, evaluation for the herpesviruses, HHV8/KSHV (IHC, ORF 73; Advanced BioTechnologies) and EBV (ISH, EBER; Leica), was performed.

Results: The HIV-associated HG-BNHLs included: 10 diffuse large cell lymphomas, 3 primary effusion lymphoma (PEL)/extracavitary PELs, 1 plasmablastic lymphoma, 1 Burkitt lymphoma and 1 BNHL, NOS. All the HG-BNHLs contained clonal B cell populations. In the 1 patient with 2 HG-BNHLs, separated by 24 mo, identical clones were seen. Clonal B cell populations were seen in 9/16 (56%) reactive lymphoid lesions 0.5 - 24 months prior to development of HG-BNHL (6 cases) or 1 - 99 months after HG-BNHL diagnosis (3 cases). The B cell clones in 8 of the reactive proliferations were different than in the patient's HG-BNHL, however, in 1 case identical clonal populations were present in the reactive and HG-BNHL (14 mo separation). Five clonal reactive lesions (6/8; 75%) and 3/6 (50%) non-clonal lesions were associated with at least one herpesvirus infection (EBV+ and/or HHV8/KSHV+) in the cases with sufficient material for testing.

Conclusions: While the incidence of monoclonal B cell populations in HIV-associated reactive lymph nodes is high (56%), the presence of identical clones in reactive lesions and HG-BNHLs is low (1/14 cases; 7%). Thus, the presence of a B cell clone in an HIV reactive lymph node is not associated with a high risk of developing lymphoma. However, there is a trend for clonal populations in HIV reactive lymph nodes to be seen in association with herpesvirus infections suggesting that these clonal populations likely represent an immune response and not malignant transformation.

1269 An RNA-Sequencing Assay to Identify Cell of Origin, Gene Rearrangements, and Hotspot Mutations in Diffuse Large B-Cell Lymphoma

Rory Crotty[1], Krista Hu[2], Abel Licon[3], Josh Haimes[4], Valentina Nardi[1], Abner Louissaint[1]
[1]Massachusetts General Hospital, Boston, MA, [2]Massachusetts General Hospital, Charlestown, MA, [3]Archer, Boulder, CO, [4]ArcherDx, Boulder, CO

Disclosures: Rory Crotty: None; Krista Hu: None; Josh Haimes: None; Valentina Nardi: None; Abner Louissaint: None

Background: Diffuse large B-cell lymphoma (DLBCL) is an aggressive, high-grade malignancy. At a molecular level, DLBCL displays a wide variety of translocations and driver gene mutations, which are associated with two distinct cell-of-origin (COO) categories - the germinal center B-cell subtype (GCB) and the activated B-cell subtype (ABC). Full characterization of the genetic landscape of DLBCL can require performance of multiple time-consuming assays. We developed a one-step RNA-based assay to determine COO and to detect common important translocations.

Design: We compiled a series of 42 cases of DLBCL diagnosed at our institution between 2010 and 2016. Each case underwent anchored multiplex PCR-based RNA sequencing of a series of 76 genes off formalin-fixed paraffin-embedded tissue, using a custom Archer panel. Gene fusions, rearrangements, and hotspot mutations were identified, and each case was subclassified by COO. Findings were then compared against immunohistochemistry (IHC), karyotype, and FISH results for each case.

Results: Of 42 cases, 13 were subclassified as ABCs, 26 as GCBs, and 3 were unclassified. Two of the unclassified cases were EBER-positive. Comparison to IHC COO classification demonstrated discordance in 12 cases. The remaining 30 cases were fully concordant.

All discordant cases were classified ABC by IHC and GCB or unclassified by our assay (see Table 1). Analysis of individual mutations supported the assay's call over IHC in at least 3 of 12 discordant cases, suggesting an accurate COO call in at least 33 of 42 cases overall (78.5%). Orthogonal testing is pending to verify the discordant cases.

The assay also detected seven of ten confirmed BCL6 rearrangements, of which three had not been previously identified by karyotyping. Two of three previously identified BCL2 rearrangements were detected by the assay. The assay also successfully identified two of four MYC rearrangements, one of which had not been demonstrated by karyotype, leading to a diagnosis of double-hit lymphoma.

Case	Assay COO	IHC COO	Mutation Profile Favors	Most Frequently Mutated Genes
1	GCB	ABC	ABC	*CREB3L2, LRMP, TIMP1, KMT2A*
2	GCB	ABC	GCB	*SERPINA9, STIL, MLF1, CD44*
3	Unclassified	ABC	ABC	*CREB3L2, CTLA4, CCDC50, CD44*
4	GCB	ABC	ABC	*CCDC50, EXOC2, LRMP, CDKN2A*
5	GCB	ABC	GCB	*SERPINA9, EXOC2, PDCD1LG2, CD44, FUT8*
6	GCB	ABC	GCB	*SERPINA9, CCDC50, PDCD1LG2, DENND3*
7	GCB	ABC	ABC	*TPKB, PDCD1LG2, CD44, CREB3L2*
8	GCB	ABC	ABC	*CREB3L2, E2F2, DENND3, CCND3*
9	Unclassified	ABC	ABC	*CREB3L2, E2F2, STIL, PDCD1LG2*
10	GCB	ABC	ABC	*PDCD1, CCDC50, SERPINA9, ALK, MYD88*
11	GCB	ABC	ABC	*CREB3L2, SERPINA9, NOTCH1, PAICS*
12	Unclassified	ABC	ABC	*PDCD1LG2, LRMP, DENND3, CD44, CCDC50*
Table 1 - Most commonly mutated genes in each discordant case. COO - cell of origin. ABC - activated B-cell phenotype. GCB - germinal-center B-cell phenotype.				

Conclusions: This assay offers a single method for COO classification in DLBCL, detection of hotspot mutations, and identification of most BCL2, BCL6, and MYC rearrangements, including cryptic rearrangements not previously identified. It permits comparable overall efficacy to classification by IHC, karyotype and FISH, and could significantly simplify and streamline the diagnostic process in DLBCL.

1270 IRTA-1 Expression in Low Grade B-Cell Lymphomas with Marginal Zone Differentiation

Joanna Dalland[1], Justin Koepplin[1], Karen Rech[2]
[1]Mayo Clinic, Rochester, MN, [2]Rochester, MN

Disclosures: Joanna Dalland: None; Justin Koepplin: None; Karen Rech: None

Background: Given that marginal zone lymphoma (MZL) generally shows a non-specific phenotype, classification of a low grade B-cell lymphoma (LGBCL) as MZL requires exclusion of other entities. IRTA-1 has been previously reported as a potential specific marker for MZL, however, other LGBCLs can show marginal zone differentiation (MZD), most commonly follicular lymphoma (FL). We investigated the expression of IRTA-1 in LGBCLs with MZD to evaluate the specificity of this marker for MZL.

Design: Our institutional archives were searched from 1992-2018 to identify cases of LGBCLs with MZD. All cases were reviewed to confirm the diagnosis and presence of MZD. Cases without morphologic features of MZD were excluded. 21 cases were identified including 1 mantle cell lymphoma (MCL), 19 follicular lymphoma (FL) and 1 post-transplant lymphoproliferative disorder (PTLD). In situ hybridization studies were performed on formalin fixed paraffin embedded sections using probes for IRTA-1 mRNA (Advanced Cell Diagnostics, Newark, CA).

Results: 15 cases (71%) were positive for IRTA-1 involving both nodal and extranodal sites, with expression localized in the areas of MZD (Figure 1). Case 14 showed marked MZD with an equivocal phenotype expressing CD20, BCL2, patchy BCL6 and IRTA-1; classification as FL was favored given the demonstration of BCL2 rearrangement by FISH. Case 15 showed marked MZD with an equivocal phenotype expressing CD20, partial BCL6, and IRTA-1; classification as FL was favored given the demonstration of BCL6 rearrangement by FISH. One case of FL in the tonsil (case 9) showed patchy IRTA-1 positivity located predominantly around the tonsillar crypts.

Table 1. IRTA-1 Expression in LGBCL with MZD				
	Diagnosis	Site	Immunophenotype	IRTA1
1	MCL with MZD	LN, groin	CD5, cyclin D1 (SOX11 negative)	+
2	FL grade 1 with MZD	Parotid	CD10, BCL2, BCL6	+
3	FL grade 1 with MZD	LN, posterior neck	CD10, BCL2, BCL6	+
4	FL grade 1 with MZD	LN, neck	CD10, BCL2, BCL6	+
5	FL grade 1 with MZD	LN, neck	CD10, BCL2, BCL6	+
6	FL grade 1-2	Parotid	CD10, BCL2, BCL6	+
7	FL grade 1-2 with MZD	LN, groin	CD10, BCL2, BCL6	+
8	FL grade 2 with MZD	LN, suboccipital	BCL2, BCL6	+
9	FL grade 2 with marked MZD	Tonsil	CD10, BCL2, BCL6	+
10	FL grade 2 with marked MZD	Soft tissue, forehead	CD10, BCL2, BCL6	+
11	FL grade 2 with MZD	LN, neck	CD10, BCL2, BCL6	+
12	FL grade 3a with plasmacytic differentiation	LN, supraclavicular	BCL2, BCL6	+
13	FL grade 3a (pediatric follicular lymphoma variant) with MZD	Soft tissue, submental	CD10, BCL2, BCL6	+
14	FL with marked MZD	LN, submandibular	BCL2, BCL6	+
15	FL with MZD	LN, axillary	BCL6	+
16	FL grade 1 with MZD	LN, axillary	CD10, BCL2, BCL6	-
17	FL grade 1 with MZD	LN, axillary	CD10, BCL2, BCL6	-
18	FL grade 1 with MZD	LN, axillary	CD10, BCL2, BCL6	-
19	FL grade 1 with slight MZD	LN, neck	CD10, BCL2, BCL6	-
20	FL grade 1 with MZD	LN, groin	CD10, BCL2, BCL6	-
21	PTLD, monomorphic type (MZL-like with plasmacytic differentiation)	Soft tissue, arm	BCL2, BCL6	-

Figure 1 - 1270

Figure 1. IRTA-1 Positive FL grade 1 with MZD

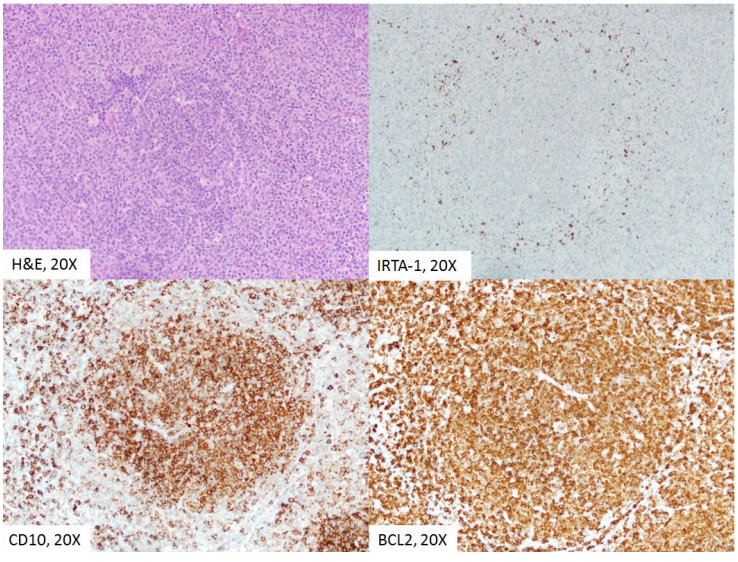

Conclusions: IRTA-1 expression alone should not be used to classify a LGBCL as MZL, as this marker is frequently expressed in areas of MZD in other LGBCLs. In particular, the differential diagnosis between FL with MZD and MZL remains difficult given their phenotypic overlap.

1271 Increased Complexity of t(11;14) FISH Patterns in Plasma Cell Neoplasms Versus Mantle Cell Lymphoma

Joanna Dalland[1], Reid Meyer[1], Kathryn Pearce[1], Rebecca King[1], Rhett Ketterling[1], Linda Baughn[1]
[1]Mayo Clinic, Rochester, MN

Disclosures: Joanna Dalland: None; Reid Meyer: None; Kathryn Pearce: None; Rebecca King: None; Rhett Ketterling: None; Linda Baughn: None

Background: Both plasma cell neoplasms (PCN) and mantle cell lymphoma (MCL) can show t(11;14)(q13;q32) often resulting in cyclin D1 overexpression. In some cases, it can be difficult to morphologically distinguish between these entities in the bone marrow (BM) since PCN with t(11;14) are often CD20+ with lymphoplasmacytic cytology while MCL can rarely have plasmacytic differentiation. We investigated the difference in FISH patterns in these two entities to evaluate for possible differentiating characteristics.

Design: We identified 605 cases from either formalin-fixed, paraffin embedded tissue (FFPE) or fresh BM specimens with a positive t(11;14) by fluorescence *in situ* hybridization (FISH) using the *CCND1/IgH* (Abbott Molecular) probe set. Data including the number of individual *CCDN1* and *IGH* signals along with the number of fusion signals was collected. The "typical" FISH pattern was defined as 3 total *CCDN1* signals, 3 total *IGH* signals, and 2 total fusion signals giving rise to a balanced t(11;14) translocation. Any deviation from the "typical", balanced t(11;14) translocation was defined as an "atypical" pattern, including both gain of fusion signals and unbalanced/complex abnormalities. Groups were compared using two-tailed Fisher's exact statistical analysis.

Results: We identified 326 cases of MCL with t(11;14) (275 FFPE specimens; 51 BM specimens) and 279 cases of PCN with t(11;14) (56 FFPE specimens; 223 bone marrow specimens). One PCN FFPE specimen showed amplification of the fusion signal. In both FFPE and BM specimens, there were a significantly higher proportion of cases that showed an atypical FISH pattern in PCN compared to MCL (53%versus 27%, p<0.0001).

Table 1. Distribution of FISH Patterns

		Typical Pattern	Atypical Pattern	Total
MCL	FFPE	197 (72%)	78 (28%)	275
	BM	41 (80%)	10 (20%)	51
	Total	**238 (73%)**	**88 (27%)**	**326**
PCN	FFPE	21 (37%)	35 (63%)	56
	BM	110 (49%)	113 (51%)	223
	Total	**131 (47%)**	**148 (53%)**	**279**

Figure 1 - 1271

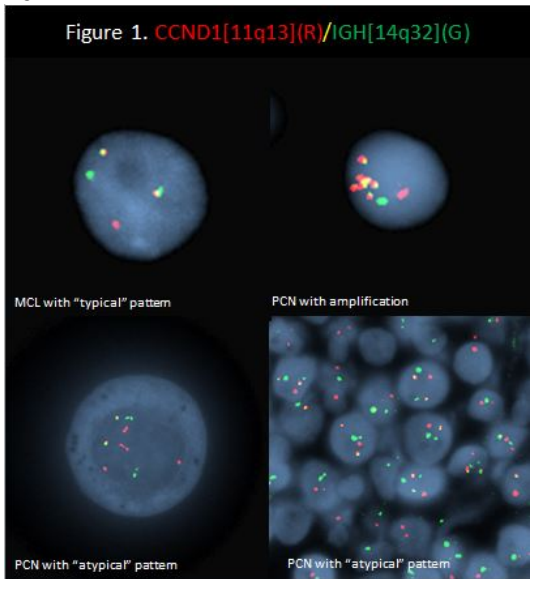

Conclusions: PCN more often have a complex t(11;14) FISH pattern compared with MCL, suggesting differences in the genomic mechanisms underlying these rearrangements in plasma cells as compared with B cells. This may be a useful feature to aid the pathologist in distinguishing the two entities when faced with morphologically challenging tissue biopsies or low level BM infiltrates.

1272 Study of the Expression of DAXX and ATRX Proteins in Follicular Lymphoma and Diffuse Large B Cell Lymphoma

Siddhartha Dalvi[1], Hassan Sheikh[2], Rubina Cocker[3], Judith Brody[4], Kalpana Reddy[5], Peihong Hsu[6], Xinmin Zhang[7], Silvat Sheikh-Fayyaz[8]

[1]Glen Oaks, NY, [2]Hofstra Northwell School of Medicine, Hempstead, NY, [3]North Shore University Hospital, Lake Success, NY, [4]Northwell Health, New Hyde Park, NY, [5]Northwell Health, Garden City, NY, [6]LIJ Medical Center / Northwell Health, New Hyde Park, NY, [7]New York, NY, [8]Donald and Barbara Zucker School of Medicine at Hofstra/Northwell, Roslyn, NY

Disclosures: Siddhartha Dalvi: None; Hassan Sheikh: None; Judith Brody: None; Kalpana Reddy: None; Peihong Hsu: None; Xinmin Zhang: None; Silvat Sheikh-Fayyaz: None

Background: DAXX (death-domain associated protein) functions as either pro-apoptotic or anti-apoptotic protein depending on cell type and cellular location. ATRX (alpha thalassemia/mental retardation syndrome X linked) belongs to the SWI/SNF family of chromatin remodeling proteins. Recent studies have shown that DAXX and ATRX function as tumor suppressors in solid tumors by interacting with one another and by regulating chromatin remodeling. However, their functions in tumorigenesis are controversial and their expression pattern in follicular lymphoma (FL) and diffuse large B cells lymphoma (DLBCL) have not been reported.

Design: This cohort includes 23 cases of follicular lymphoma (FL) and 15 cases of diffuse large B cell lymphoma (DLBCL). The cellular location and intensity (weak, moderate, strong) of immunohistochemical staining and the percentage of positive cells were recorded for each case. In FL, the number of cells with strong DAXX expression were counted in five representative high power fields independently by four hematopathologists. In addition, other parameters including histological grading and Ki-67 proliferation index were reviewed for FL cases.

Results: Both DAXX and ATRX show diffuse and strong staining in all the DLBCL cases. They are differentially expressed in FL cases, with negative or weak staining for ATRX and moderate to strong staining for DAXX. DAXX shows two staining intensities in FL, strong and moderate. We counted the number of strong DAXX cells in five representative follicles at high power field to get the average for each case. Of the 23 cases of FL, 16 were low grade (1-2) and 7 were high grade (3A-3B). Using a cut-off of 100 darkly staining cells per HPF (40X) (DAXX index), there was a 100% correlation with high grade FL and DAXX index of more than 100 (7 of 7 cases). Of the 16 cases of low grade FL, 9 cases have DAXX index of less than100 (69% correlation) and 5 cases had a DAXX index more than 100. However, 4 of these 5 discordant cases had a high Ki-67 proliferation index, with an overall 94% correlation of DAXX index with prognosis.

Correlation of DAXX index with grade and Ki-67 proliferation index in FL

	No. of cases	High grade	Low grade	% Discordant
DAXX >100 Ki-67 >20	11	7	4	17.4%
DAXX <100 Ki-67 <20	9	0	9	0%
DAXX >100 Ki-67 <20	1	0	1	4.3%
DAXX <100 Ki-67 >20	2	0	2	8.7%
Total Cases	23		Total %	30.4

Conclusions: Our findings show that counting cells with strong DAXX expression has a predictive value for FL grading. Secondly, DAXX and ATRX are strongly expressed in DLBCL but differentially expressed in FL, which can be useful for differentiating FL and DLBCL in small biopsies such as needle core biopsies

1273 Genetic and Immunophenotypic Differences between Acute Leukemias with Expression of T-Cell and Myeloid Markers and Correlation with Minimal Residual Disease

Katelyn Dannheim[1], Erdyni Tsitsikov[1], Jon Aster[2], David Dorfman[3], Elizabeth Morgan[3], Jacqueline Garcia[4], Andrew E. Place[5], Olga Weinberg[6]

[1]Boston Children's Hospital, Boston, MA, [2]Brigham and Women's Hospital, Boston, MA, [3]Brigham and Women's Hospital, Boston, MA, [4]Dana-Farber Cancer Institute, Boston, MA, [5]Dana-Farber/Boston Children's Cancer and Blood Disorder Center, Boston, MA, [6]Children's Hospital Boston, Boston, MA

Disclosures: Katelyn Dannheim: None; Erdyni Tsitsikov: None; Jon Aster: None; David Dorfman: None; Elizabeth Morgan: None; Jacqueline Garcia: None; Andrew E. Place: None; Olga Weinberg: None

Background: T-cell acute lymphoblastic leukemia (T-ALL), early T precursor lymphoblastic leukemia (ETP), T/myeloid mixed phenotype acute leukemia (MPAL), and acute undifferentiated leukemia (AUL) can all co-express T-cell markers with markers of myeloid lineage and can thus pose a diagnostic challenge. Little is known about how these entities compare in regards to non-lineage-defining markers or genetic abnormalities nor the occurrence of minimal residual disease (MRD) in each group.

Design: Cases were identified from the pathology databases of Boston Children's Hospital and Brigham and Women's Hospital with available flow cytometric data, cytogenetic findings, next generation sequencing, and clinical information. Multiple analyses were performed using student's t-test and one-way ANOVA to compare the incidence of common genetic abnormalities and the variation of immunophenotype between each diagnostic group, as well as to assess incidence of MRD detected by flow cytometry after one month of therapy.

Results: We identified 44 T-ALLs, 27 ETPs, 8 T/Myeloid MPALs, and 6 AULs cases. Genetic variations included a higher incidence of 11q23 (MLL) amplification (p=0.0041) in AUL and lower incidence of 9p21.3 (CDKN2A) deletions in all groups when compared to T-ALL (p=0.0005). Several cytogenetic abnormalities occurred in T/Myeloid MPAL that were not seen in other groups, including del(1)(p13p22), add(7)(p13), add(10)(p13), and add(14)(q32) (all p<0.05). Molecular aberrations unique to AUL included mutations of *ASXL1, ATM, BCOR, IDH2, PDGFRB, PTPN11, SETBP1, SMARCB1*, and *SRSF2*, as well as trisomy 13 and add(21)(p11.2) (all p<0.05). Significant findings in marker expression identified in the flow cytometric data analysis are listed in Table.

The incidence of MRD did not vary significantly among the groups, however a higher rate of MRD was associated with TP53 mutations (p=0.0205) in the entire cohort and NRAS (p=0.0142) mutations in T-ALL. Detectable MRD was seen at a lower frequency in cases that expressed CD5, CD8, CD11b, and TdT (all p<0.05). In non-T-ALL cases, expression of CD33 (p=0.0066) and CD56 (p=0.0268) were also associated with less MRD. Within T-ALL alone, a lower incidence of MRD was associated with expression of sCD3 (p=0.0365).

	T-ALL (n=44)	ETP (n=27)	T/Myeloid MPAL (n=8)	AUL (n=6)	p Value*
%Male	83.30%	74.10%	36.40%	84.10%	0.1851
Age at Diagnosis [Median(Range)]	10 (1-57)	23 (6-80)	21 (12-70)	60 (29-80)	<0.0001
MRD Positive (patients with MRD data)	9 (n=34)	9 (n=20)	2 (n=3)	3 (n=5)	0.2275
Marker expression [Percent Positive Cases(Cases Measured)]					
CD2	73.17% (41)	30.43% (23)	100% (4)	33.33% (6)	0.0009
CD4	59.09% (44)	4% (25)	ND	50% (2)	<0.0001
CD5	95.45% (44)	48.15% (27)	16.67% (6)	16.67% (6)	<0.0001
CD7	100% (44)	100% (27)	100% (6)	60% (5)	<0.0001
CD8	70.45% (44)	0% (25)	0% (5)	ND	<0.0001
CD10	57.14% (42)	19.05% (21)	0% (2)	0% (6)	0.0016
CD13	7.14% (42)	36% (25)	50% (6)	16.67% (6)	<0.0001
CD33	2.38% (42)	48.15% (27)	66.67% (6)	66.67% (6)	<0.0001
CD34	34.09% (44)	81.48% (27)	83.33% (6)	83.33% (6)	0.0001
CD117	14.63% (41)	36% (25)	66.67% (6)	66.67% (6)	0.0039
HLA-DR	9.76% (41)	63.63% (22)	66.67% (6)	66.67% (6)	<0.0001
Tdt	95.24% (42)	56% (25)	100% (5)	ND	<0.0001

T-ALL, T-cell acute lymphoblastic leukemia; ETP, early T precursor lymphoblastic leukemia; MPAL, mixed phenotype acute leukemia; AUL, acute undifferentiated leukemia; ND, no data

*Results were considered significant at p<0.05

Conclusions: There are several potential genetic and immunophenotypic differences that might be helpful in distinguishing ETP, T/Myeloid MPAL, and AUL from T-ALL, and providing prognostic clues in regards to incidence of minimal residual disease.

1274 Detection of B-Cell Clonality in FFPE Tissue Microarrays Using Ultrasensitive RNA In Situ Hybridization

Chelsey Deel[1], David Czuchlewski[1], Karen Buehler[2], Mohammad Vasef[1]
[1]University of New Mexico, Albuquerque, NM, [2]TriCore Reference Laboratories, Albuquerque, NM

Disclosures: Chelsey Deel: None; David Czuchlewski: None; Karen Buehler: None; Mohammad Vasef: None

Background: Demonstration of clonality is an important tool to differentiate lymphoma from reactive lymphoid hyperplasia. Flow cytometry represents a sensitive method for reliable detection of clonality in B-lymphoid neoplasms. However, flow cytometry requires fresh tissue and does not allow for concurrent assessment of morphology. Other conventional techniques that are suitable for FFPE tissues, including immunohistochemistry and in situ hybridization, are useful in detecting cytoplasmic light chain restriction in plasma cell neoplasms and B-cell proliferations with plasmacytoid differentiation but lack sensitivity to capture surface immunoglobulin light chain restriction in the vast majority of B cell neoplasms. In this study, we evaluated the potential utility of an ultrasensitive RNAscope method in the detection of B-cell clonality in FFPE tissue microarrays (TMAs) constructed from CLL cases with known surface light chain expression based on prior flow cytometric analysis.

Design: TMAs including 27 known CLL/SLL and 2 transformed CLL cases were analyzed for light chain expression using RNAscope (Advanced Cell Diagnostics, Newark, CA) with single color detection. Briefly, 4µm tissue sections were mounted on positively charged glass slides, deparaffinized in Xylene, rehydrated with graded alcohol, treated with hydrogen peroxidase, boiled in citric buffer, and incubated with protease followed by hybridization with target probes. Hybridization signals were detected as brown staining with hematoxylin counterstain.

Results: Cases were reviewed and classified as kappa-restricted, lambda-restricted, or mixed by 3 pathologists before correlating with the prior flow cytometry results. Light chain restriction was identified in 24 out of 29 (83%) cases including kappa restriction in 13 and lambda restriction in 11 cases. Prior flow cytometric analysis was available in 25 out of 29 cases. Concordance with flow cytometry was observed in 20 out of 21 (95%) cases. Of the 5 remaining cases, 4 showed no staining, and one (4%) showed discordance. The discordant case showed mixed staining by RNAscope but kappa light chain restriction by flow cytometry. In addition, excellent reproducibility was demonstrated among the 3 pathologists who reviewed the cases (86%).

Figure 1 - 1274

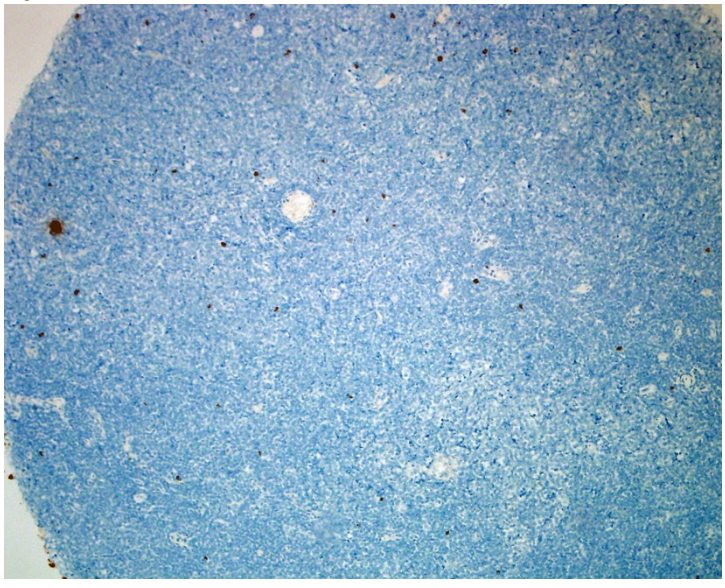

Figure 2 - 1274

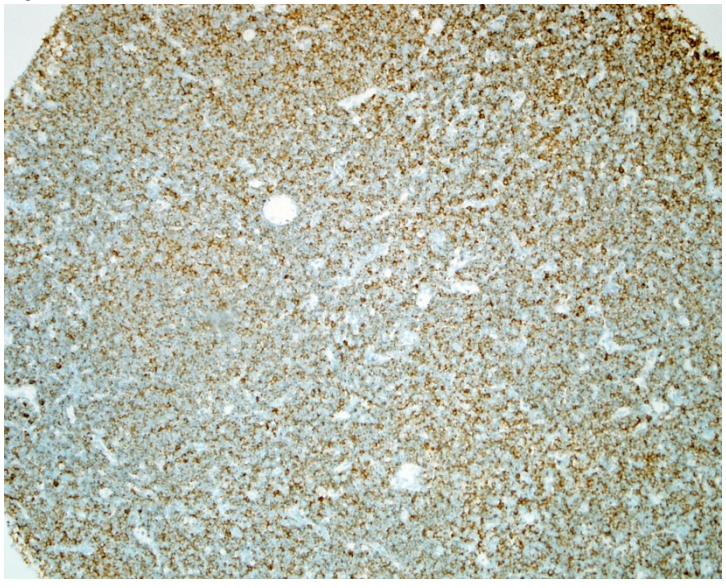

Conclusions: Ultrasensitive RNA in situ hybridization represents a robust, sensitive tool for the assessment of B-cell clonality in cases where no fresh tissue is available for flow cytometry.

1275 Assessment of PD-L1, PD-L2 And JAK2 in Classical Hodgkin Lymphoma Using Immunohistochemical (IHC) And Copy Number Analysis By Fluorescence In-Situ Hybridization (FISH)

Hany Deirawan[1], Ali Gabali[2], Radhakrishnan Ramchandren[3]
[1]Detroit Medical Center/Wayne State University, Detroit, MI, [2]Wayne State University/Karmanos Cancer Center, Farmington, MI, [3]Wayne State University School of Medicine, Detroit, MI

Disclosures: Hany Deirawan: None; Ali Gabali: None; Radhakrishnan Ramchandren: None

Background: In relapsed and refractory Hodgkin lymphoma (HL), immune check point inhibition by anti-PD1 antibodies is an indicated and efficacious treatment. The genes for PDL1 and PDL2 (both Ligands for PD1) are located adjacent to each other on chromosome 9p24 and are downstream of the JAK2 gene which has been implicated in PDL1 upregulation. Immunohistochemistry (IHC) is commonly used to assess the expression of these genes. Whether the expression pattern depicted by IHC can predict the corresponding genetic alterations and provide clinically meaningful indicators has not been studied.

Design: 20 newly diagnosed classical HL cases were selected and evaluated for Reed Sternberg (RS) cells PDL1 (using two clones), PDL2 and JAK 2 expression using IHC. RS cells were scored for staining intensity (IS; 0, +1, +2 and +3) and proportion of positive RS cells (proportion score, PS). High scores were designated based on an IS >2+ and PS > 25 %. Evaluation was done by two blinded hematopathologists. FISH analysis of the corresponding genes was evaluated in 100 RS cells per sample. A ratio comparing the centromeric signal of chromosome 9 (CEP9) and PDL1, PDL2 and JAK was obtained. When cells within a tumor samples demonstrated 2 or more differing copy number alterations the tumor was classified by the largest copy number subpopulation.

Results: Expression of PDL1 by IHC was found in 19/20 (95%) cases regardless of the antibody used. However, a high degree variability in staining intensity and PS score was observed between the 2 tested clones suggesting infidelity in antibody affinity or interpretation (fig.1). PDL1 and PDL2 were coexpressed in 70% of cases. JAK2 positivity was noted in all cases. Copy number alterations by FISH were identical for *PDL1* and *PDL2*. RS had heterogeneous gene alterations within the same tumor (fig.2). Interestingly, majority of samples demonstrated some degree of *PDL1* relative copy loss of and 25% of cases (n=5) exhibited 10% or more copy loss. There was no association between *PDL1* copy number and IHC IS or PS scores (p=0.26).

Figure 1 - 1275

Patient	PD-L1 IHC (22C3)	PD L1/2 FISH	% Relative Loss
1	2+	Disomy	10
2	3+	Disomy	0
3	2+	Disomy	13
4	2+	Copy Gain	2
5	3+	Disomy	18
6	2+	Amplification	0
7	3+	Disomy	2
8	2+	Copy Gain	13
9	0	Disomy	16
10	1+	Polysomy	1
11	2+	Polysomy	3
12	3+	Copy Gain	0
13	1+	Polysomy	3
14	2+	Disomy	5
15	3+	Disomy	9
16	1+	Polysomy	1
17	3+	Copy Gain	1
18	2+	Polysomy	7
19	1+	Amplification	2
20	2+	Polysomy	8

IHC Analysis	Any Intensity	High Intensity 2+/3+	High PS ≥ 25%
PD-L1 (22C3) n=20	19/20 (95%)	15/20 (75%)	16/20 (80%)
PD-L1 (H-130) n=20	19/20 (95%)	0/20 (0%)	2/20 (10%)
PD-L2 n=20	14/20 (70%)	4/20 (20%)	0/20 (0%)
JAK2 n=20	20/20 (100%)	12/20 (60%)	3/20 (15%)

PD-L1 Gene Alteration	High IHC Intensity by 22C3	High IHC PS by 22C3
Disomy n= 8	7/8 (87 %)	6/8 (75 %)
Polysomy n = 6	3/6 (50 %)	4/6 (66 %)
Copy gain n = 4	4/4 (100 %)	**4/4 (100 %)**
Amplification n = 2	1/2 (50 %)	**2/2 (100 %)**

Figure 2 - 1275

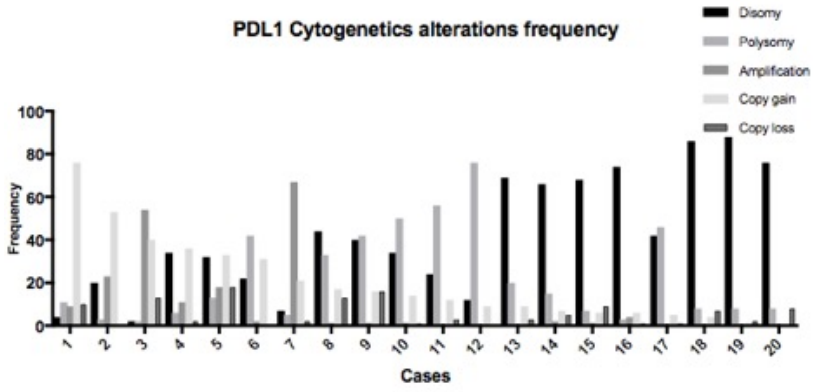

Conclusions: *PDL1* shows significant genetic alterations in HL. Analysis of PDL1 expression pattern by IHC have a high degree of variability and does not correlate with copy number changes. PDL2 and JAK2 expression is also not a reliable surrogate for PDL1 gene status. FISH assessment may offer a better insight to underlying tumor biology. Correlation with clinical outcome and response to PD1-PDL1 axis blockade is underway.

1276 CD36 Is a Leukemia Stem Cell Chemoresistance Gene and Confers an Adverse Prognosis in Acute Myeloid Leukemia

Monica del Rey Gonzalez[1], Omar Habeeb[1], Alec Stranahan[2], Wenhou Hu[3], Sean Devlin[3], Cynthia Liu[4], Arnaldo Arbini[1], Christopher Park[1]
[1]NYU School of Medicine, New York, NY, [2]Weill Cornell Medicine, New York, NY, [3]Memorial Sloan Kettering Cancer Center, New York, NY, [4]NYU Langone Health, New York, NY

Disclosures: Monica del Rey Gonzalez: None; Omar Habeeb: None; Alec Stranahan: None; Wenhou Hu: None; Sean Devlin: None; Cynthia Liu: None; Arnaldo Arbini: None; Christopher Park: None

Background: Leukemia stem cells (LSC) in acute myeloid leukemia (AML) are thought to represent the therapy-resistant subset of leukemia cells that mediate disease relapse. We previously showed that CD36, a transmembrane glycoprotein that mediates fatty acid uptake, confers resistance to different chemotherapeutic drugs in blast crisis chronic myeloid leukemia cells. We have performed gene expression profiling on LSC-enriched populations (CD34+CD38-) from paired diagnosis: day 14 post-induction therapy samples from 10 AML patients and identified CD36 as a significantly upregulated transcript following chemotherapy. The aims of this study were to investigate whether CD36 regulates AML responses to induction therapy and/or predicts overall survival (OS).

Design: The role of CD36 in AML blast function was assessed in CD36 shRNA knockdown (KD) HL60 cells as well as WT and CD36 KO MLL-AF9+ mouse AML by measuring effects on proliferation, apoptosis and cell cycle, as well as responses to anthracycline or cytarabine induced cell death. The mean fluorescence intensity (MFI) of CD36 expression from 50 AML samples was determined and correlated with response to therapy. TCGA and ECOG 1900 AML datasets were evaluated to determine the correlation between CD36 mRNA expression and OS.

Results: Comparison of AML LSCs before and after induction chemotherapy showed that CD36 mRNA is induced approximately 2-fold ($p<0.05$). CD36 KD in human AML cell lines or deletion of CD36 in mouse LSCs resulted in significantly reduced cell growth, higher levels of apoptosis, as well as decreased quiescence compared to controls. Moreover, CD36 KD and MLL-AF9 KO cells were sensitized to daunorubicin, but not cytarabine, treatment ($p<0.01$). Patients not having achieved morphologic remission at D14 (blasts >5%) showed a trend towards a higher frequency CD36+ blasts and statistically significant higher CD36 expression at diagnosis than those achieving remission ($p=0.02$). Moreover, higher levels of CD36 mRNA expression was associated with worse outcomes in both the TCGA and ECOG 1900 cohorts.

Conclusions: Overexpression of CD36 as assessed by mRNA levels or flow cytometry is an indicator of poorer responses to chemotherapy and shorter OS in AML. Assessment of CD36 expression at the time of diagnosis by flow cytometry represents a simple method to provide prognostically relevant information in AML patients.

1277 Improved Recognition of Hematogones from Precursor B-cell Acute Lymphoblastic Leukemia by a Single Tube Flow Cytometric Analysis

Michelle Don[1], Washington Lim[2], Brian Cox[2], Qin Huang[2], Sumire Kitahara[3], Jean Lopategui[3], Serhan Alkan[4]
[1]Los Angeles, CA, [2]Cedars-Sinai Medical Center, Los Angeles, CA, [3]Cedars-Sinai Medical Center, West Hollywood, CA, [4]Cedars-Sinai Medical Center, Beverly Hills, CA

Disclosures: Michelle Don: None; Washington Lim: None; Brian Cox: None; Sumire Kitahara: None; Jean Lopategui: None; Serhan Alkan: None

Background: Hematogones (HG) are normal precursor lymphoid cells. Immunophenotypic analysis of HG by flow cytometry (FC) typically shows expression of dim CD45, CD10, CD34, CD19, TdT and variable CD20. However, this phenotype may be seen in precursor B-cell acute lymphoblastic leukemia (pre B-ALL), which is problematic in distinguishing pre B-ALL from HG. Studies suggest FC analysis using these markers as useful for differentiation; however, in our experience this limited panel is insufficient. Studies also show CD58 is commonly expressed in pre B-ALL but not in HG, however CD58 as a single marker is limited when expressed at lower levels. To improve diagnostic accuracy, we generated a 7 color antibody panel including: CD10, CD19, CD45, CD38, CD34, CD58 and CD81 to assess the feasibility of a single tube panel and provide an approach to distinguish HG from pre B-ALL.

Design: 50 cases including 18 pre B-ALL (diagnostic, residual/relapsed cases) and 32 HG cases were analyzed by 7 color FC. A single tube with CD10 FITC/CD58 PE/CD19 ECD/CD38 PC5/CD34APC/CD81PB/CD45 PC7 was run simultaneously with standard acute leukemia panels analyzing phenotypic expression and mean fluorescent intensity (MFI) for each marker. Results were correlated with BM histologic findings and ancillary studies: FISH, molecular, cytogenetic and chimerism analysis.

Results: HG typically showed bright CD38, moderate (mod) CD19, mod CD10, variable CD20, bright CD81, dim to no CD58; while pre B-ALL showed weak to mod CD38, mod to strong CD19, mod to strong CD10, dim to no CD81 and mod CD58. B-ALL cases had an average MFI of 25.9 for CD81 and 137.1 for CD58. HG cases had an average MFI of 71.6 for CD81 and 38.1 for CD58 (figure 1). Utilizing phenotypic expression patterns and intensity of these markers, reliable separation of leukemia from HG was achieved, except in 2 borderline cases where correlation with ancillary studies was necessary.

Figure 1 - 1277

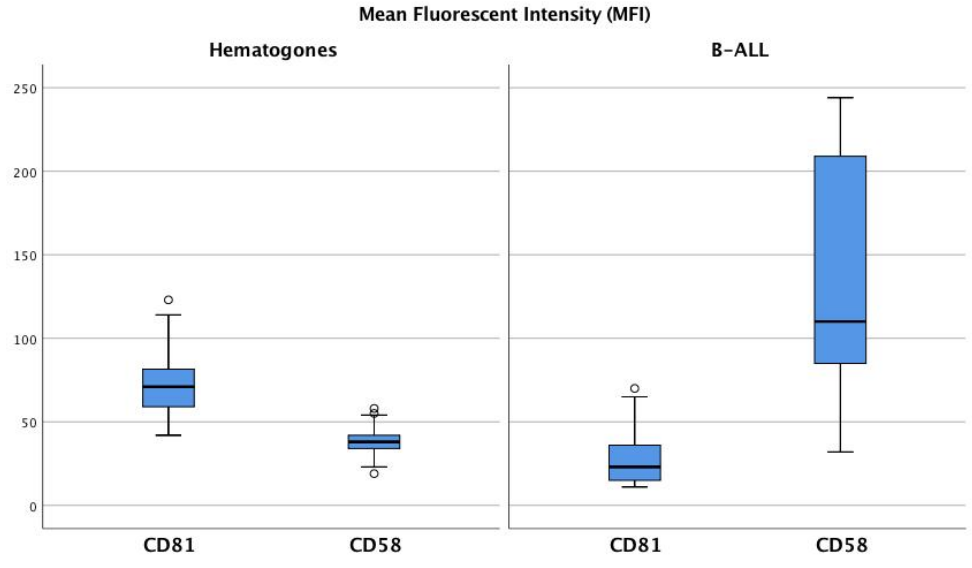

Conclusions: A 7 color FC with the above markers provides dependable separation in differentiating HG from pre B-ALL. In such cases with a CD19/CD10/bright CD38 population, we recommend using MFI for CD58 and CD81 (high CD58/low CD81 favoring leukemia). In rare cases of HG and pre B-ALL overlap, additional ancillary studies are helpful. Inclusion of these markers is recommended in routine BM samples for pre-B-ALL evaluation, especially post treatment samples, to prevent misdiagnosis. The aforementioned antibody panel in a single tube could cut costs while improving patient care.

1278 Novel Activating Mutations in CSF1R and Additional Kinases with Therapeutic Implications in Histiocytic Neoplasms

Benjamin Durham[1], Jennifer Picarsic[2], Estibaliz Lopez-Rodrigo[1], David Hyman[1], Eli Diamond[1], Omar Abdel-Wahab[1]
[1]Memorial Sloan Kettering Cancer Center, New York, NY, [2]Children's Hospital of Pittsburgh of UPMC, Pittsburgh, PA

Disclosures: Benjamin Durham: None; Jennifer Picarsic: None; Omar Abdel-Wahab: None

Background: Genomic analyses of Langerhans cell histiocytosis (LCH) and Erdheim-Chester disease (ECD) have revolutionized our understanding of these disorders as clonal hematopoietic malignancies driven by MAP kinase signaling. Nonetheless, the genetic alterations across histiocytoses (juvenile xanthogranuloma (JXG), Rosai-Dorfman disease (RDD), and histiocytic sarcoma (HS)) have not been comprehensively evaluated. Moreover, although histiocytoses usually occur as sporadic disorders, familial clustering has been documented, but germline genetic causes are unknown. Here we performed comprehensive genomic analyses of 222 patients with diverse histiocytic neoplasms, including monozygotic twins.

Design: We performed whole exome sequencing (WES) of skin lesions and fingernails from monozygotic twins with JXG. We also sequenced 93 ECD (42%), 61 LCH (27%), 50 JXG (23%), 12 RDD (5%), and 6 HS (3%) lesions using WES and targeted DNA and RNA sequencing (**Fig. 1A-B**).

Results: We identified in-frame deletions in *CSF1R* (*CSF1R*^{Y546_K551del}) in the JXG lesions of both twins that were absent in fingernails. Interestingly, 8 patients had *CSF1R* mutations, most commonly *CSF1R*^{Y546_K551del}, which conferred cytokine-independent growth in Ba/F3 cells and sensitized these cells to inhibition by the CSF1R-specific inhibitors pexidartinib and BLZ945. Furthermore, novel mutations in *CSF3R, KIT, ALK, MET, JAK3, RAF1*, *MAP2K2*, as well as a *RET* fusion were discovered (in addition to previously described mutations in *BRAF*^{V600E}, *MAP2K1*, *N/KRAS*, and *ARAF*, as well as fusions in *BRAF, NTRK1,* and *ALK*) (**Fig. 1A-E**). As evidence of the direct therapeutic implications of these findings, an *ALK*-rearranged ECD patient required therapy with crizotinib that resulted in profound therapeutic improvement, as well as patients with novel kinase mutations treated with a MEK1/2 inhibitor (**Fig. 2A-D**).

Figure 1 - 1278

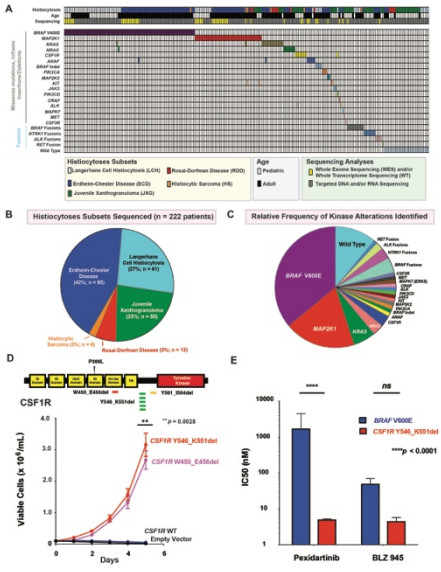

Figure 2 - 1278

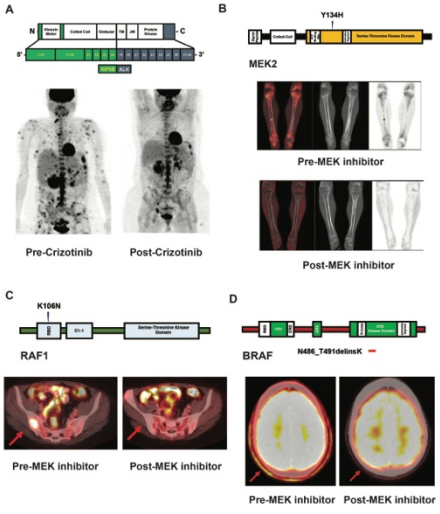

Conclusions: Here we identify activating mutations in *CSF1R*, the receptor tyrosine kinase (RTK) required for monocyte/macrophage development, and other novel activating RTK alterations in histiocytoses, many of which have direct therapeutic importance (**Fig. 2**). In addition, the discovery of somatic, activating *CSF1R* mutations in identical twins with histiocytosis suggests the possibility that tissue-resident macrophages may serve as a cell-of-origin of histiocytoses.

1279 Whole Exome Sequencing of Secondary Histiocytic / Dendritic Sarcoma Reveals Alterations in the RAS Pathway and Epigenetic Modifiers

Caoimhe Egan[1], Justin Lack[2], Liqiang Xi[3], Stefania Pittaluga[4], Elaine Jaffe[1], Mark Raffeld[5]
[1]National Cancer Institute/NIH, Bethesda, MD, [2]Frederick National Laboratory for Cancer Research, Frederick, MD, [3]National Cancer Institute/National Institutes of Health, Bethesda, MD, [4]Washington, DC, [5]National Cancer Institute, Bethesda, MD

Disclosures: Caoimhe Egan: None; Liqiang Xi: None; Stefania Pittaluga: None; Elaine Jaffe: None; Mark Raffeld: None

Background: Histiocytic sarcoma and sarcomas with dendritic cell differentiation (HDS) are uncommon malignant neoplasms often with an aggressive clinical course that may occur in association with another hematologic malignancy or mediastinal germ cell tumor (secondary HDS, sHDS). Previous mutational analysis on small numbers of HDS cases has shown a high frequency of BRAF V600E mutations as well as alterations in other RAS pathway/RASopathy-associated genes including KRAS, MAP2K1 and PTPN11. We performed whole exome sequencing on a cohort of 16 sHDS to better characterize the mutational alterations that occur in this rare tumor.

Design: Sixteen cases of sHDS were identified from institutional files. Seven cases were previously published. Histologic and immunophenotypic review confirmed the diagnosis in each case. DNA was extracted from FFPE, and whole exome sequencing was performed on Illumina HiSeq platforms. Variant calling was performed with MuTect2 and annotated using the Ensembl Variant Effect Predictor (VEP v88). Variants were selected using a "tumor only" model based on functional prediction algorithms, population allele frequencies, "expected" variant allele frequencies, and annotated gene ontology terms from dbNSFP v 3.5a. Copy number was estimated from the exome sequencing data using CNVkit (v0.8.5).

Results: The 16 cases comprised histiocytic sarcoma (n=15) and Langerhans cell sarcoma (n=1) and were associated with follicular lymphoma (n= 6), B-ALL (n=2), T-ALL (n=4), CLL/SLL (n=2), aggressive B-cell lymphoma (n=1) and PTCL (n=1). We identified a high frequency of genetic alterations within the RAS-MAPK pathway and RASopathy genes (n=7/16), with variations identified in KRAS (n=4/16), BRAF (n=2/16) and NF1 (n=1/16). Mutations in CREBBP were identified in 5/6 cases associated with follicular lymphoma (FL). Other recurrently mutated epigenetic modifiers included KMT2D (n=5/16) and SETD2 (n=3/16). Copy number analysis showed losses of 9p/CDKN2A in 9 cases, including most cases associated with known FL (n=5/6).

Conclusions: Alterations in RASopathy-associated / RAS pathway genes and epigenetic modifiers are present in a significant number of sHDS. Our results provide further insight into the molecular alterations occurring in sHDS and suggest that certain patients with the condition may benefit from treatment with targeted therapy.

1280 Bilateral Bone Marrow Trephine Biopsies Are Not Necessary in the Diagnosis of Pediatric Acute Leukemias

Lindsey Ellis[1], Katsiaryna Laziuk[1], Stephanie Wells[2], Richard Hammer[3]
[1]Columbia, MO, [2]WIlliam Woods University, Fulton, MO, [3]University of Missouri, Columbia, MO

Disclosures: Lindsey Ellis: None; Katsiaryna Laziuk: None; Stephanie Wells: None; Richard Hammer: None

Background: Acute leukemias (AL) account for up to 30% of neoplasms in children under 19 years of age[1]. Bone marrow aspiration is considered the gold standard for the diagnosis of AL[2,3,4]. However, guidelines do not exist for ASP vs bone marrow trephine biopsy (BMBX) in the pediatric population. Bilateral BMBX continues to be performed in the diagnosis of AL in children. But, the risks of BMBX often outweigh the benefits in children[5,6]. To our knowledge, the use of bilateral BMBX in the diagnosis of AL has not been evaluated in pediatric patients.

Design: 32 cases of bilateral bone marrow evaluation performed at University of Missouri Health Care from Jan 1, 2011 to Feb 5, 2018 in patients under 21 years of age for initial diagnosis or follow-up of AL were reviewed. The peripheral blood film (PB), bilateral aspirate smears (ASP), bilateral core sections (BX), bilateral clot sections (CS), and flow cytometric analysis were independently reviewed by two hematopathologists. For each case, it was determined which preparations were predictive of the correct final diagnosis and then ranked.

Results: The combination of PB, ASP and CS was diagnostic in 30/32 (94%).Flow cytometric analysis of bone marrow ASP showed 100% positive predictive value (PPV) and was ranked first. BMBX ranked second with no difference between left and right (86% and 87%). Bilateral ASP and paraffin-embedded CS showed a PPV of 79-80%. PB film was least predictive (66%) (Table 1). In3 cases, a BX only was diagnostic: 2 were negative for AL post-therapy and only 1 was a new diagnosis of AL.

Table 1. Predictive value of differing preparation types in the diagnosis of Acute Leukemia in the pediatric population

Preparation	Trials	Predictive Percentage	N	Rank
Flow Cytometry	31	100%	0	**1**
Blood Film	29	(.34)=**66%**	10	**6**
Left Aspirate	30	(.20)=**80%**	6	**4***
Left clot	30	(.20)=**80%**	6	**4***
Left Biopsy	30	(.134)=**86%**	4	**3**
Right Aspirate	30	(.20)=**80%**	6	**4***
Right Clot	29	(.21)=**79%**	6	**5**
Right biopsy	31	(.13)=**87%**	4	**2**

Conclusions: Bilateral BMBX is routinely performed in pediatric patients for AL but no guidelines exist in the pediatric population. Our study shows flow cytometric analysis of the ASP or PB has a PPV of correct diagnosis of AL in 100% of cases. BMBX, ASP, CS, and PB film were less predictive in that order. In only 1 case of new AL was BX essential for diagnosis. However, BX may be more useful to confirm an absence of disease. Our data suggests that BMBX usually is not necessary for the initial diagnosis of acute leukemia in children, and may be more valuable in evaluating for post treatment response/relapse. Bilateral BMBX appear to be unnecessary, with no significant difference in diagnosis based on specimen laterality. In summary, bilateral BMBX for the diagnosis of AL in the children is not diagnostically necessary. With the use of flow cytometric analysis, bone marrow ASP with immunophenotyping is the gold standard.

1281 Molecular Profiling by Next Generation Sequencing Defines Primary Mediastinal Large B-cell Lymphoma Lacking Characteristic Features

Lauren Eversmeyer[1], Sonam Prakash[2], Jessica Van Ziffle[2], Yi Xie[2], Linlin Wang[2]
[1]San Francisco, CA, [2]University of California, San Francisco, San Francisco, CA

Disclosures: Lauren Eversmeyer: None; Sonam Prakash: None; Jessica Van Ziffle: None; Yi Xie: None; Linlin Wang: None

Background: Primary mediastinal large B-cell lymphoma (PMBL) is defined as a large B-cell lymphoma predominantly limited to the mediastinum with characteristic features including compartmentalizing fibrosis, intermediate cell size, clear cytoplasm, expression of CD23 and CD30, and commonly lack of surface immunoglobulin. Common genetic alterations in PMBL affect specific molecular pathways including JAK-STAT and NF-kappaB. The clinical distinction from diffuse large B-cell lymphoma, NOS (DLBCL) involving the mediastinum can be challenging as DLBCL can show overlapping morphologic and immunophenotypic features. Given the significant difference in clinical treatment of PMBL versus DLBCL, we explore the use of molecular profiling to diagnose PMBL in cases that are ambiguous between PMBL and DLBCL.

Design: Three cases were reviewed (2 left neck mass biopsies and 1 mediastinum mass resection). Clinical, histologic and immunophenotypic features were collected. PMBL was suspected in all cases but definite diagnosis could not be made. Next generation sequencing (NGS) was subsequently used to identify affected molecular pathways for definite diagnosis. Formalin-fixed paraffin-embedded blocks of tumor and normal tissue (if available) from each patient was retrieved from the UCSF Pathology Archives and genomic DNA was prepared. Targeted sequencing using UCSF 500 gene panel was performed, with data analysis using open source or licensed software for alignment to the human reference sequence UCSC build hg19 (NCBI build 37) and variant calling.

Results: All cases are women (31, 34, 63 years-old) with a mediastinum mass (8.5 or 10 cm) +/- a neck mass (3 or 6 cm). Periceliac/gastrosplenic lymph nodes are involved in one case. All cases show either no or scant compartmentalizing fibrosis, medium to

large tumor cells with nuclear pleomorphism, and necrosis (present in two cases). CD23 is negative in one case. Given these collective findings, a definite diagnosis of PMBL cannot be rendered in these cases. NGS in each case demonstrates somatic alterations mostly affecting JAK-STAT signaling (SOCS1, STAT6 or JAK2) or NF-kappaB pathway (TNFAIP3 or NFKBIE). The combination of mutations and variations seen collectively supports a diagnosis of PMBL in all three cases.

Conclusions: This study demonstrates that NGS to detect JAK-STAT signaling and NF-kappaB pathway can help diagnose PMBL in cases lacking characteristic features. An additional cohort of cases has also been submitted for targeted NGS.

1282 Bone marrow dEMI - Digital Erythroid Maturation Index can precisely identify erythroid maturation

Jiayun Fang[1], Matthew Leavitt[2], Srikanth Ragothaman[3], Spencer Hayes[4], David Wingate[4], Rajan Dewar[5]
[1]University of Michigan Hospitals, Ann Arbor, MI, [2]LUMEA, Salt Lake City, UT, [3]University of Michigan, Ann arbor, MI, [4]Brigham Young University, Provo, UT, [5]Ann Arbor, MI

Disclosures: Jiayun Fang: None; Matthew Leavitt: *Major Shareholder*, LUMEA; Srikanth Ragothaman: None; Spencer Hayes: None; David Wingate: None; Rajan Dewar: None

Background: Erythroid maturation assessment by morphology is limited by imprecision and inter-observer variability and thus not widely used. Digital pathology is emerging as a crucial tool to assist pathologists by precisely measuring cellular and sub-cellular components. We developed a digital pathology tool called dEMI - Digital Erythroid Maturation Index to assess erythroid maturation in bone marrow aspirates and core biopsies.

Design: 21 consecutively obtained bone marrow specimens with aspirates and E-Cadherin & Glycophorin A immunostains were utilized for this study. In this study we compare 3 techniques to assess erythroid maturation: 1) dEMI - Digital Erythroid Maturation Index calculated from a training set of ~400 erythroid images, preclassified by an expert pathologist into 4 maturation stages (pro-, basophilic, poly- and orthochromic normoblasts). The image processing algorithm segmented the cytoplasm, nucleus, and nucleolar regions and assigned scores to RGB intensity of cytoplasmic regions. The algorithm could successfully separate the 4 stages with minimal overlap between stages 1 and 2, pro- and basophilic normoblasts (Fig 1). 2) Immuno-EMI was calculated from digitally scanning Gly-A and E-Cad and creating a ratio of E-Cad/GlyA. A ratio of >3 was considered immature and <3 was mature (Fig 2). 3) The dEMI and Immuno-EMI was compared to the gold standard pathologist's morphologic assessment. Weighted scores were assessed for individual cases, and on a 4 point scale, a score of <2.5 was considered immature and >2.5 was mature.

Results: Consecutively obtained biopsies carried the following diagnoses: AML staging (n=7), MDS (4), Lymphoma staging (3), Myeloproliferative neoplasm (2), Erythroid leukemia (2), CLL (2), B-ALL (1), PCM (1). Of the 21 cases, 29% of cases were left shifted by weighted scores and 26% were left shifted based on immuno-EMI. There was overall concordance between the techniques on 75% of cases. With a cut-off of E-Cad/Gly-A=3, there was a statistically significant agreement between the methods (Cohen's kappa of 0.4, signifying fair level of agreement). While dEMI calculation for individual disease categories varied and were limited by numbers within each category, significantly the two erythroid leukemia received dEMI scores of 1.1 and 1.98 and Immuno-EMI of 5.2 and 6.42, indicating immaturity assessed by the digital algorithm.

Figure 1 - 1282

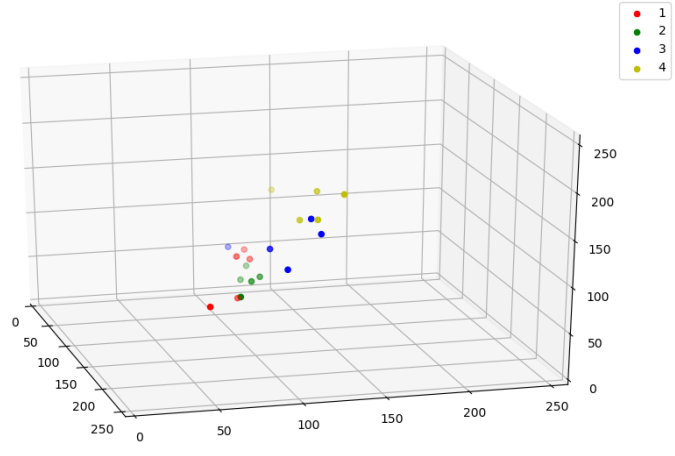

Figure 2 - 1282

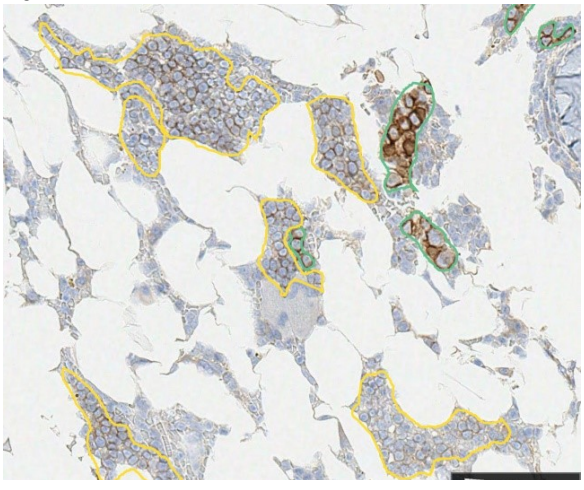

Conclusions: A Digital Erythroid Maturation Index can be useful to classify erythroid cells in bone marrows.

1283 Utility of Flow Cytometry in Distinguishing Subtypes of Aggressive B-cell Lymphomas

Taliya Farooq[1], Garry Wang[2], Bachir Alobeid[1], Govind Bhagat[3], David Park[3]
[1]New York-Presbyterian/Columbia University Medical Center, Manhattan, NY, [2]New York-Presbyterian/Columbia University Medical Center, New York, NY, [3]Columbia University Medical Center, New York, NY

Disclosures: Taliya Farooq: None; Garry Wang: None; Govind Bhagat: None; David Park: None

Background: Double/triple-hit lymphomas (D/THL) are aggressive B-cell lymphomas (ABL) with MYC and BCL2 and/or BCL6 rearrangements. Rapid identification of D/THL is critical given the poor response of these tumors to standard chemoimmunotherapy. Although immunohistochemistry plays a central role in defining characteristic features of D/THL, there is no consensus on which ABL should undergo requisite genetic studies. Flow cytometry (FC) studies on D/THL are limited and show conflicting results. Furthermore, FC studies frequently do not distinguish between DHL and THL. Hence, we sought to determine if FC could discriminate between ABL depending on their BCL2, BCL6 and MYC rearrangement status.

Design: The pathology database at a single institution was searched from 2008 to 2018 for cases of ABL with concurrent flow cytometry and FISH studies for BCL2, BCL6 and MYC rearrangements. Clinical, morphological, IHC and cytogenetic/FISH data were reviewed for all cases. A total of 21 D/THL (8 THL, 8 BCL2-DHL, 5 BCL6-DHL); 19 MYC only (SHL); 17 BCL6 only (BCL6); 5 BCL2 only (BCL2); and 12 triple-negative (TN) cases were identified. Evaluation of widely-used FC markers, including CD10, CD19, CD20, CD38, and CD45 was performed and relative intensities of each marker determined by comparison to either normal germinal center (GC) B cells or non-GC B cells depending on the cell-of-origin according to the Hans' algorithm.

Results: FC results of ABL are summarized in Table 1 with representative flow plots in Figure 1.

1. MYC-rearranged ABL frequently showed bright CD38

2. THL and BCL2-DHL frequently showed dim/absent CD20, bright CD10, and dim FMC7; uniform bright CD10 was seen only in THL.

3. BCL6-DHL and BCL6 cases largely showed absent CD10.

4. Non-MYC rearranged ABL did not show a unique immunophenotypic profile with the possible exception of dim CD20.

	THL	BCL2-DHL	BCL6-DHL	SHL	BCL2	BCL6	TN
CD19 dim/absent	50%	25%	40%	21.0%	80%	29.4%	25%
CD20 dim/absent	87.5%	62.5%	60%	57.1%	60%	42.8%	41.6%
CD10 bright	100%[A]	87.5%	0%[B]	55.5%	40%	0%	50%
CD38 bright	85.7%	100%	80%[C]	85.7%	25%	87.5%*	50%
HLA-DR very bright	16.7%	50%	25%	9.1%	25%	64.3%	58.3%
FMC7 dim/absent	83.3%	83.3%	50%	70%	75%	28.5%	54.5%
CD45 dim	14.2%	14.2%	40%	36.8%	0%	17.6%	0%
sIg light chain absent	25%	12.5%	20%	5.2%	20%	17.6%	8.3%

A. 62.5% (uniform bright expression)

B. 20% (normal CD10 expression)

C. 60% with brighter expression than normal GC B cells

*** nearly all cases dimmer than normal GC B cells**

Figure 1 - 1283

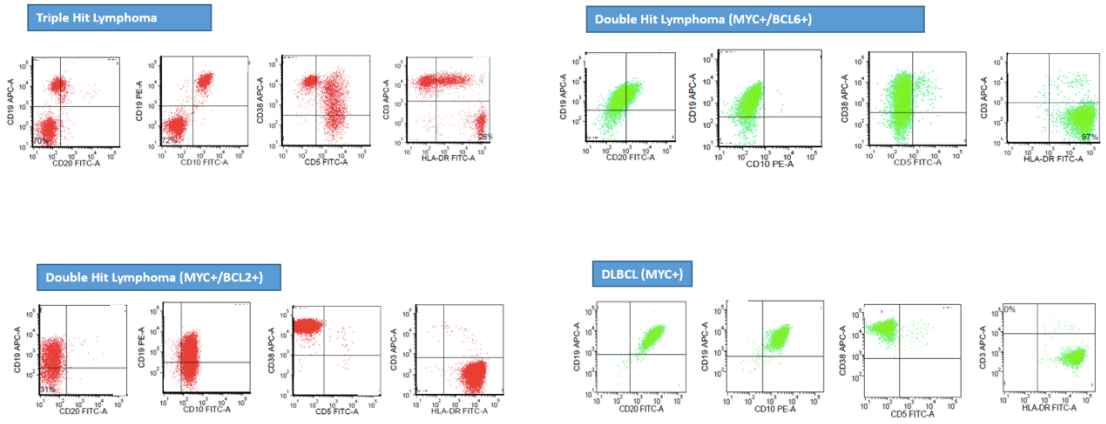

Conclusions: The current study is one of the largest in assessing the role of FC in distinguishing between DH and THL as well as MYC and non-MYC rearranged ABL. To the best of our knowledge, this is the first FC study showing frequent immunophenotypic similarities between BCL2-DHL and THL aside from previously reported CD10 expression. In addition, a distinguishing feature of THL is uniform bright CD10 expression which has not been described. Finally, our study highlights the utility of FC in predicting the relevant genetic abnormalities in ABL.

1284 Phospho-STAT5 (pSTAT5) Staining is Observed at High Frequency in Ph-like ALL with ABL Class Rearrangements: Potential Utility in Screening for Ph-like ALL

Shiraz Fidai[1], Charles Van Slambrouck[2], Sandeep Gurbuxani[1]
[1]University of Chicago, Chicago, IL, [2]Advocate South Suburban Hospital, Hazel Crest, IL

Disclosures: Shiraz Fidai: None; Charles Van Slambrouck: None; Sandeep Gurbuxani: None

Background: B-lymphoblastic leukemia, *BCR-ABL1*-like (Ph-like ALL) shows gene expression profile indistinguishable from B-lymphoblastic leukemia with t(9;22)(q34.1;q11.2); *BCR-ABL1* (Ph+ ALL). In contrast to Ph+ ALL, genomic landscape of Ph-like ALL is complex and includes over 60 rearrangements involving 15 kinase or cytokine receptor genes. Clinically validated flow cytometry can be used to detect CRLF2 expression (due to *CRLF2* rearrangements) on leukemic blasts to identify Ph-like ALL in ~50% of patients. However, genetic changes that constitute the remaining 50% of cases are numerous, can be cryptic, and require use of complex genetic tools for diagnosis. Low density arrays for screening of gene expression profile exist but are not available for clinical use. Therefore, identifying clinically useful surrogate markers that can predict an underlying Ph-like genotype will provide a powerful tool to triage this relatively uncommon subtype of ALL for appropriate genetic testing.

The majority of kinase and cytokine receptor alterations converge on two pathways: *JAK*-family member signaling or *ABL*-signaling. Both *JAK* and *ABL* class fusions result in phosphorylation of STAT5 at Tyr694 and activation of STAT5. We therefore hypothesize that expression of phospho-STAT5 (pSTAT5) can potentially be used as surrogate marker for Ph-like ALL.

Design: 10 Ph-like ALL, 3 Ph+ ALL, and 1 hyperdiploid B-ALL cases were collected. Immunohistochemical stain for pSTAT5 was performed on B-5 fixed bone marrow core biopsies using commercially available antibody (CST, clone C11C5) with antigen retrieval at alkaline pH. Nuclear staining of erythroid precursors and adipocytes served as an internal positive control. 10% or more stiaing in leukemic blasts scored as positive. Positive staining was further divided into 10%, 10- 50%, or >50%.

Results: Phospho-STAT5 nuclear staining observed in 5/10 Ph-like ALLs, 3/3 Ph+ ALLs. Hyperdiploid B-ALL was Negative. Of the 5 positive Ph-like ALLs, 3/5 had *ABL* class, and 2/5 had *JAK* class alterations.

Case #	Age at Diagnosis	Sex	UCM Presentation	Genetics	IKZF1 Deletion	Phospho-STAT5 Staining
1	20	M	De Novo	*RCSD1-ABL2*	Yes	Positive, >50%
2	28	M	De Novo	*NUP214-ABL1*	Yes	Positive, >50%
3	34	F	Relapse	*CRLF2-P2RY8*	Yes	Negative
4	3	F	De Novo	*CRLF2-P2RY8*	Not Done	Negative
5	51	M	De Novo	*CRLF2-IGH*	Yes	Positive, 10%-50%
6	61	M	Relapse	*CRLF2-IGH*	Not Done	Positive, 10%-50%
7	15	M	De Novo	*CRLF2-P2RY8*	Yes	Negative
8	20	M	De Novo	*CRLF2-IGH*	No	Negative
9	68	M	Relapse	*BCR-PDGFRB*	Yes	Positive, 10%
10	1	M	De Novo	*CRLF2-IGH*	No	Negative
11	1	M	De Novo	Hyperdiploid	Not Done	Negative
12	36	F	De Novo	*t(9;22)*	No	Positive, >50%
13	46	F	De Novo	*t(9;22)*	Yes	Positive, >50%
14	54	M	Refractory	*t(9;22)*	Not Done	Positive, 10%

Conclusions: Our preliminary studies show that nuclear p-STAT5 staining is observed at high frequency in the Ph-like ALL with ABL class rearrangements. p-STAT5 immunostaining can therefore potentially complement CRLF2 expression by flow cytometry to provide a critical screening tool to triage cases for resource heavy genetic studies. Additional ongoing studies in the laboratory will assess sensitivity, specificity and predictive value of positive and negative results.

1285 Clinicopathologic Features of Peripheral T-Cell Lymphoma from Sub-Saharan Africa

Megan Fitzpatrick[1], Shahin Sayed[2], Zahir Moloo[2], Drucilla Roberts[1], Abner Louissaint[1], Aliyah Sohani[1]
[1]Massachusetts General Hospital, Boston, MA, [2]Aga Khan University Hospital, Nairobi, Kenya

Disclosures: Megan Fitzpatrick: None; Shahin Sayed: None; Zahir Moloo: None; Drucilla Roberts: None; Abner Louissaint: None; Aliyah Sohani: None

Background: Peripheral T-cell lymphomas (PTCL) are heterogeneous, clinically aggressive and rare neoplasms relative to B-cell lymphomas. The difference in distribution of PTCL subtypes by geographic location and ethnic group is thought to be caused by etiologic factors including viral exposure and genetic predisposition. Such differences are well documented in the Americas, Europe and Asia, however, there is limited data from sub-Saharan Africa (SSA), and a shortage of resources needed for full subclassification. We sought to uncover clinicopathologic features of PTCL in a SSA cohort.

Design: We identified 23 cases of PTCL received in consultation from 3 countries in SSA between 2012-2018: Kenya (n=17), Uganda (n=4) and Botswana (n=2). Clinical data was provided by the referring pathologist. PTCL subtype and immunophenotype were based on slide review. The diagnosis was made by a hematopathologist in all cases per the 2017 WHO Classification.

Results: Median age was 46 years (range 12-81) with a M:F ratio of 7:3. Most cases were nodal (70%). Nearly all cases (22/23, 96%) required additional stains in our laboratory for subclassification. NOS was the most common subtype (n=13, 57%), followed by systemic anaplastic large cell lymphoma (sALCL, n=4, 17%), angioimmunoblastic T-cell lymphoma (AITL, n=3, 13%), extranodal NK/T-cell lymphoma (ENKTL, n=2, 9%) and cutaneous ALCL (n=1, 4%). Among PTCL-NOS, CD7 was the T-cell antigen most commonly lost, followed by CD5, and 5/11 cases expressed CD30. All sALCL occurred in young males and 3/4 were ALK+. All AITL cases occurred in older patients and expressed T-follicular helper antigens, with 2/3 showing CD21+ follicular dendritic cell expansion. Both ENKTL cases occurred in young females and were CD56+ and EBV+ by EBER ISH. The cutaneous ALCL case occurred in association with granulomatous inflammation suspected to represent coexisting mycobacterial infection.

Figure 1 - 1285

Table 1. Clinicopathologic characteristics of PTCL

	Overall (n=23)*	PTCL-NOS (n=13)	sALCL (n=4)	AITL (n=3)	ENKTL (n=2)
Sex, n (%)					
Male	16 (70%)	8 (62%)	4 (100%)	3 (100%)	0 (0%)
Female	7 (30%)	5 (39%)	0 (0%)	0 (0%)	2 (100%)
Median age (range)	46 (12-81)	52 (26-74)	23 (12-40)	68 (45-81)	25 (24-25)
Location, n (%)					
Nodal	16 (70%)	10 (77%)	3 (75%)	3 (100%)	0 (0%)
Extranodal	7 (30%)	3 (23)	1 (25%)	0 (0%)	2 (100%)
IHC, n (%)					
CD4+	8/13 (62%)	5/8 (63%)	2/3 (67%)	n/a	0/1 (0%)
CD8+	1/7 (14%)	1/6 (17%)	n/a	n/a	0/1 (0%)
CD20+	1/23 (4%)	1/13 (8%)	0/4 (0%)	0/3 (0%)	0/2 (0%)
CD2-/Loss	4/16 (25%)	2/9 (22%)	2/2 (100%)	0/2 (0%)	0/2 (0%)
CD3-/Loss	7/22 (32%)	2/13 (15%)	3/4 (75%)	0/2 (0%)	1/2 (50%)
CD5-/Loss	9/20 (45%)	5/13 (39%)	1/1 (100%)	0/3 (0%)	2/2 (100%)
CD7-/Loss	7/9 (78%)	6/8 (75%)	n/a	1/1 (100%)	n/a
CD25+	1/3 (33%)	1/3 (33%)	n/a	n/a	n/a
CD15+	0/8 (0%)	0/5 (0%)	0/1 (0%)	0/2 (0%)	n/a
CD30+	9/18 (50%)	5/11 (46%)	3/3 (100%)	0/2 (0%)	0/1 (0%)
CD56+	2/6 (33%)	0/4 (0%)	n/a	n/a	2/2 (100%)
ALK+	3/16 (19%)	0/7 (0%)	3/4 (75%)	0/2 (0%	0/2 (0%)
EBER ISH+	2/11 (18%)	0/7 (0%)	n/a	0/2 (0%)	2/2 (100%)
EMA+	2/8 (25%)	1/4 (25%)	1/1 (100%)	0/2 (0%)	n/a
PD1+	2/3 (67%)	n/a	n/a	2/3 (67%)	n/a
BCL6+	1/5 (20%)	0/2 (0%)	n/a	1/2 (50%)	0/1 (0%)
CD10+	2/10 (20%)	0/6 (0%)	0/1 (0%)	2/2 (100%)	0/1 (0%)
CD21+ FDC Hyperplasia	2/5 (40%)	0/2 (0%)	n/a	2/3 (67%)	n/a

*: Includes clinicopathologic data of primary cutaneous ALCL case

Figure 2 - 1285

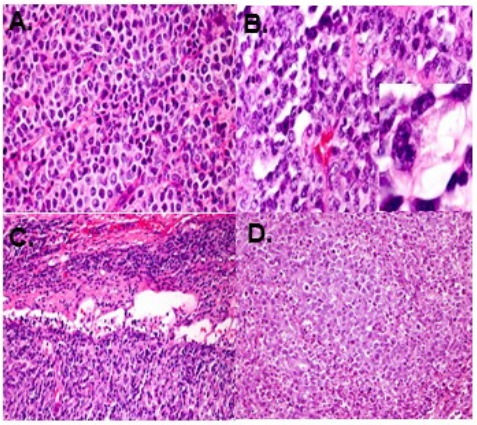

Figure 1: Morphology of PTCL. A) PTCL-NOS. B) ALK+ ALCL with characteristic hallmark cells. C) AITL with patent subcapsular sinus. D) ENKTL.

Conclusions: We describe a series of PTCL from SSA, an underrepresented population in large-scale lymphoma studies. All cases could be classified by current WHO criteria, with PTCL-NOS being the most common subtype. Age and sex were consistent with previously reported data, apart from 2 ENKTL cases, which occurred in young females. The diagnosis of PTCL requires extensive ancillary testing, which may not be available in low-resource areas including much of SSA. As the burden of lymphoma rises globally, well-equipped pathology services are critical to ensure diagnostic accuracy and optimal patient care.

1286 Pediatric-Type Follicular Lymhpoma Lacks N-Glycosylation Sites and Positive Antigen Selection Despite Ongoing Somatic Hypermutation

Leonie Frauenfeld[1], Julia Steinhilber[1], Itziar Salaverria[2], Elías Campo[3], Elaine Jaffe[4], Irina Bonzheim[1], Falko Fend[5], Leticia Quintanilla-Fend[6]

[1]University of Tuebingen, Tübingen, Germany, [2]Barcelona, Spain, [3]Hospital Clinic Barcelona, University of Barcelona, Barcelona, Spain, [4]National Cancer Institute/NIH, Bethesda, MD, [5]University Hospital of Tuebingen, Tuebingen, Germany,[6]University of Tuebingen, Tuebingen, Germany

Disclosures: Leonie Frauenfeld: None; Julia Steinhilber: None; itziar salaverria: None; Elías Campo: None; Elaine Jaffe: None; Irina Bonzheim: None; Falko Fend: None; Leticia Quintanilla-Fend: None

Background: Pediatric-type follicular lymphoma (PTFL) is a t(14;18) negative FL with distinctive clinicopathological features. PTFL has a specific genetic and mutational profile distinct from other NHL including conventional FL (cFL). However, the immunogenetic features of PTFL including IGV-gene usage, somatic hypermutation (SHM) and evidence for antigen selection are unknown. cFL t(14;18)+ are known to frequently acquire N-glycosylation motifs during SHM, a mechanism substituting for antigen-induced BCR signaling. The aim of this study was to investigate the immunogenetic features of PTFL to gain insights in the pathogenesis of the disease.

Design: Thirty-eight well characterized PTFL cases were subjected to NGS-based clonality analysis on the Ion Torrent PGM platform. NGS libraries were amplified using the LymphoTrack® DX *IGH* FR1 Assay, DX *IGH* FR2 Assay or DX *IGK* Assay (invivoscribe, San Diego, CA). Raw data were analyzed with LymphoTrack® DX *IGH*Visualization software. All sequences were also evaluated with IMGT/V-Quest. Sequences covering the whole IGV-gene were evaluated for evidence of antigen selection by BASELINe software.

Results: Of the 38 cases only 29 were informative. IGHV-gene usage was similar to that of the normal, circulating B-cell population with VH3 genes most commonly found (17/27 cases), followed by VH1 (5/27), VH4 (4/27), VH5 (1/27) and VH2 (1/27). IGK usage showed mainly VH3 subgroup (2 cases). As expected, 28/29 cases showed SHM (<97% identity to the germline) of the V-gene. N-glycosylation (Asn-X-Ser/Thr) motifs were identified in only 3/29 (10%) cases. However, only two of the three samples originated during SHM, one was found in the CD3 region, and the other in the FR3 region. The last one represented a germline variants located in FR3, a highly conserved area of the V-gene. There was no overrepresentation of specific V-genes indicating lack of auto-antigen selection. A potential role for antigen selection was investigated in all 27 cases, without evidence for positive selection of the clonal population. Ongoing somatic hypermutation was present in all 10 analyzed cases.

Figure 1 - 1286

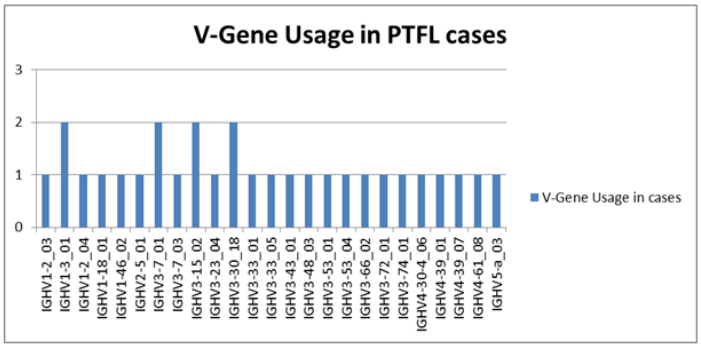

Conclusions: PTFL is a distinct type of FL. We now demonstrate that in contrast to *BCL2*+ cFL, PTFL lacks N-glycosylations motifs and positive antigen selection, two important mechanisms for BCR signaling activation. Further studies are needed to understand whether these distinct immunogenetic features might explain the indolent and self-limiting behavior of this disorder.

1287 Interplay of Various Cytokines and Immune Cells in Kikuchi Fujimoto Disease

Pallavi Galera[1], Julie Alejo[1], Racquel Valadez[1], Theresa Davies-Hill[1], Elaine Jaffe[2], Stefania Pittaluga[3]
[1]National Cancer Institute/National Institutes of Health, Bethesda, MD, [2]National Cancer Institute/NIH, Bethesda, MD, [3]Washington, DC

Disclosures: Pallavi Galera: None; Julie Alejo: None; Racquel Valadez: None; Theresa Davies-Hill: None; Elaine Jaffe: None; Stefania Pittaluga: None

Background: Kikuchi-Fujimoto disease (KFD) is a reactive lymphadenitis, histologically showing paracortical expansion with a T cell infiltrate($CD8^+$>$CD4^+$), clusters of plasmacytoid dendritic cells (pDCs)($CD123^+$/$CD68^+$/$CD4^+$/$TCF4^+$) admixed with karyorrhectic bodies and crescentic histiocytes($CD68^+$/MPO^+). Our objective was to analyze the interactions between innate immune cells and other components of cellular immunity utilizing a novel technique of RNA detection in tissue sections. RNAscope permits the detection of cytokines and chemokines in-situ.

Design: Cases diagnosed as either KFD or reactive lymphadenitis with pDC accumulation (Reactive LAD) in which material was available for further testing were retrieved from the archives of hematopathology consultation service at NCI/NIH. The number of pDCs were comparable in both cohorts. The immunohistochemical (IHC) panel included antibodies against CD3, CD20, CD4, CD8, CD68, CD123, MPO, ID2, TCF4, PD1, PDL1 and SLAM7. Dual IHC was done against ID2 & TCF4, ID2 & CD123 and ID2 & CD68. RNAscope targeting POLR2A, IFNγ, CXCL9, CXCL10, IL12A, IL18, IL10 & SLAM7 was performed.

Results: The study cohort included 8 cases of KFD and 2 cases of reactive LAD. The KFD cases were predominantly females with a median age of 26.5 years. The clinico-pathologic findings are detailed in Table 1.

IHC stains identified large clusters of CD123+ pDCs surrounding the necrosis in the proliferative stage of KFD, with fewer pDCs in the necrotic stage. In a subset of KFD cases pDCs were positive for PDL1, whereas in the reactive LAD they were negative. TCF4 was expressed in pDCs and was mutually exclusive of ID2, by dual IHC. SLAM7 was positive in pDCs by both techniques in all evaluable cases.

RNAscope detected IFNγ expression (same distribution as CD3+ T-cells) in all stages of KFD suggesting a Th1 environment. A high level of expression of CXCL9 and CXCL10 (downstream chemokines from IFNγ) was identified in the subcapsular sinuses and interfollicular areas. IL18 expression had a similar distribution as the CD68+ histiocytes. Expression of IFNγ, CXCL9, CXCL10 and IL18 was higher in KFD in comparison to reactive LAD.

Table 1.				
Case #	**Pathological Diagnosis**	**Age/Sex**	**Site**	**Clinical History**
1	KFD- Proliferative Stage	39/M	Axillary LN	HIV+, Solitary LAD
2	KFD- Proliferative & Necrotic Stage	22/F	Cervical LN	Solitary LAD
3	KFD-Necrotic Stage	26/F	Cervical LN	Tender Solitary LAD
4	KFD- Proliferative Stage	28/F	Axillary LN	Tender Solitary LAD with fever, chills and fatigue
5	KFD-Necrotic Stage	14/M	Mesentric LN	Solitary LAD with FUO & 21 lbs wt loss
6	KFD-Necrotic Stage	46/F	Axillary LN	B/L Breast Ca. with sentinel LN Bx
7	KFD-Necrotic Stage	22/F	Axillary LN	Multiple site LAD
8	KFD-Necrotic Stage	27/M	Cervical LN	Solitary LAD with anemia & leukopenia
9	PTGC with pDC clusters	9/F	Cervical LN	Recurrent Solitary LAD
10	Reactive hyperplasia with pDC clusters	16/F	Submandibular LN	Solitary LAD

Conclusions: Our data suggests that a Th1 environment with increased IFNγ, CXCL9 and CXCL10 is vital in pathogenesis of KFD. It shows that in spite the accumulation of pDCs in reactive LAD Th1 response was not elicited, further highlighting the difference in the milieus of the two conditions and suggesting a different stage of pDC activation in the two conditions.

1288 Plasma Cell Immunophenotypic Abnormalities as Predictors of Progression in Patients with Monoclonal Gammopathy of Undetermined Significance and Smoldering Plasma Cell Myeloma

Pallavi Galera[1], Xiaoping Sun[2], Constance Yuan[3], M. Stetler-Stevenson[1], Ola Landgren[4], Dickran Kazandjian[1], Irina Maric[5]
[1]National Cancer Institute/National Institutes of Health, Bethesda, MD, [2]CC/NIH, Bethesda, MD, [3]National Institutes of Health/National Cancer Institute, Bethesda, MD, [4]Memorial Sloan Kettering Cancer Center, New York, NY, [5]National Institutes of Health, Bethesda, MD

Disclosures: Pallavi Galera: None; Xiaoping Sun: None; Constance Yuan: None; Ola Landgren: *Grant or Research Support*, Celgene; *Grant or Research Support*, Amgen; *Grant or Research Support*, Janssen; *Grant or Research Support*, Takeda; *Grant or Research Support*, Glenmark; Dickran Kazandjian: None; Irina Maric: None

Background: Plasma cell myeloma (MM) is consistently preceded by a precursor state, monoclonal gammopathy of undetermined significance (MGUS) or smoldering myeloma (SMM). The annual rate of progression for MGUS is 1% and for SMM is 10% in the first 5 years. Biomarkers that may predict progression to MM are limited. Over the years, studies have proposed clinical and genetic risk factors to predict progression. Histopathological features and immunophenotypic profiles of plasma cells in relationship to risk for progression to symptomatic myeloma in MGUS/SMM have not been systematically investigated.

Design: 50 MGUS and SMM patients enrolled in the NIH natural history study of myeloma precursor disease were studied. Bone marrow samples from 29 non-progressors and 21 progressors were reviewed retrospectively. Cases were analyzed by immunohistochemistry (IHC) using CD138, CD20, CD56, CD117, cyclin D1. Expression of CD19, CD45, CD20, CD117 and CD56 was also assessed by multiparameter flow cytometry (MFC). IHC and MFC aberrancy scores were determined by the number of aberrant plasma cell markers in each case. Cases were segregated into two groups based on low (MFC: ≤ 4 aberrant markers; IHC: ≤ 2 aberrant markers) and high aberrancy scores.

Results: Baseline marrow involvement by CD138 positive plasma cells was significantly higher in progressors (Fig 1A). Plasma cell expression of CD20 (by IHC and MFC; Fig 1B) and CD117 (by MFC) significantly correlated with progression. Percent of cases with detectable aberrant expression of CD20 increased with increase in plasma cell burden (Fig 1C). Interestingly, there was no significant correlation between CD20 and Cyclin D1 expression in progressors. Expression of multiple abnormal markers significantly correlated with

progression (Fig 1D). Plasma cells in 7/21 (33%) progressors and only 1/29 (3%) non-progressors were positive for three or more abnormal markers by IHC. Strikingly, IHC cases triple positive for CD20, CyclinD1 and CD56 were present only in progressors.

Figure 1 - 1288

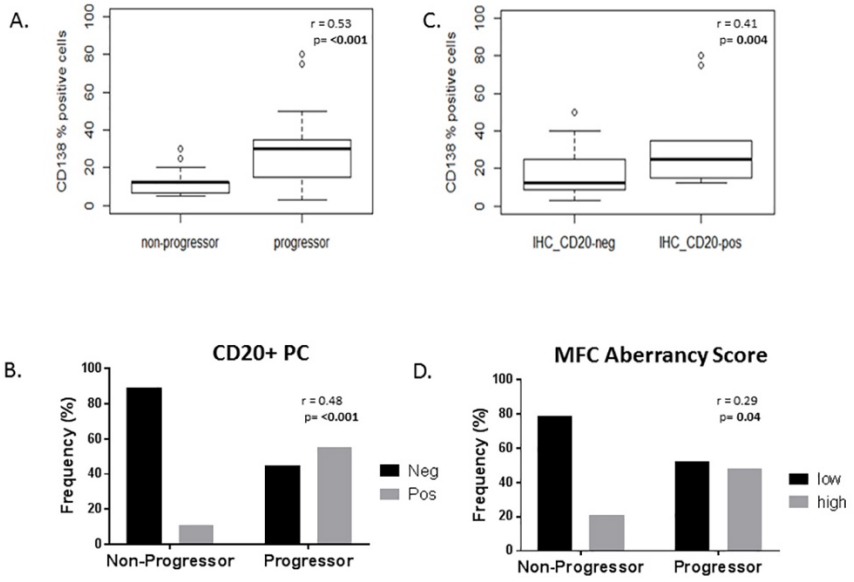

Conclusions: High number of plasma cell immunophenotypic aberrancies in myeloma precursor disease (MGUS/SMM) correlates with progression. Interestingly, plasma cell CD20 expression in precursor disease is an independent predictor of progression. Plasma cell immunophenotyping in precursor disease should be routinely performed as it can be helpful in identifying patients with a higher risk of progression that may warrant closer follow up.

1289 Sensitive and Ultra-Rapid BRAF V600E Mutation Assessment in Hairy Cell Leukemia From Stained Smear Slides, Blood and Bone Marrow Without Pre-Extraction

Edwin Gandia[1], Maria Arcila[1], Khedoudja Nafa[1], Caleb Ho[1], Mikhail Roshal[1], Paulo Salazar[1], Roger Chan[1], Daniela Elezovic[1], Ivelise Rijo[1]
[1]Memorial Sloan Kettering Cancer Center, New York, NY

Disclosures: Edwin Gandia: None; Maria Arcila: *Speaker*, Biocartis; *Speaker*, Raindance; Khedoudja Nafa: *Speaker*, Biocartis; Caleb Ho: None; Paulo Salazar: None; Roger Chan: None; Daniela Elezovic: None; Ivelise Rijo: None

Background: Hairy cell leukemia (HCL) is a rare mature B-cell malignancy characterized by leukemic hairy cells harboring the BRAF V600E mutation in virtually all cases. Establishing the BRAF mutational status has important diagnostic and therapeutic implications in this setting but may be challenging due to characteristic paucity of circulating tumor cells in peripheral blood (PB) and scarcity of aspirate material associated with extensive bone marrow (BM) fibrosis. BM biopsies are also generally unsuitable for testing due to decalcification processes. In this study we explore the clinical utility and performance characteristics of the Idylla system for ultra-rapid assessment of BRAF V600E on PB and BM aspirates involved by HCL.

Design: HCL cases submitted for routine assessment of BRAF V600E were selected. Testing was performed using an integrated, real-time PCR-based system (Idylla - Biocartis). Assay performance was assessed on scraped material from stained BM aspirate smears, as well as pre-extracted tissue and extracted DNA from PB and BM aspirates collected in EDTA. Results were compared to concurrent clinical BRAF testing by MSK-IMPACT, digital PCR and/or Sanger sequencing with locked nucleic acid probes.

Results: 31 samples were studied (17 smears, 6 unextracted liquid samples (2 PB, 4 BM), 8 extracted DNA samples). Overall, we achieved 100% accuracy in mutation detection compared to the reference methods with excellent reproducibility. Sensitivity studies showed a limit of detection of 1% and 2% variant frequency (VF) with 200ng and 50ng DNA input, respectively. Minimal input studies performed on extracted DNA, showed $\geq$10ng (~2,000 cell equivalents) were required to consistently detect a mutation known to be present at 5% VF. The Technical hands on time averaged 5 minutes and time from set up to instrument report generation was 90 minutes.

Conclusions: The Idylla system allows ultra-rapid, accurate and sensitive assessment of BRAF V600E mutation status in HCL. The system performs equally well on scant, stained material as well as pre and post extraction tissue from peripheral blood and bone marrow aspirates. This rapid assessment allows the incorporation of mutation status information together with initial morphologic and immunophenotypic assessment for rapid patient triaging and treatment decisions.

1290 Cyclin D1 Protein is Overexpressed in Rosai-Dorfman Disease

Sofia Garces Narvaez[1], Mario Marques Piubelli[2], Sheila Siqueira[3], Vathany Sriganeshan[4], Ana Medina[4], Amilcar Castellano-Sánchez[5], Robert Poppiti[4], Joseph Khoury[6], Shaoying Li[6], Jie Xu[7], Beenu Thakral[6], Karan Saluja[8], Meenakshi Bhattacharjee[9], Juan Carlos Garces[10], L. Jeffrey Medeiros[6], C. Cameron Yin[6]
[1]Mount Sinai Medical Center, Miami, FL, [2]University of São Paulo, São Paulo, NA, Brazil, [3]São Paulo, SP, Brazil, [4]Mount Sinai Medical Center, Miami Beach, FL, [5]Florida International University, Miami Beach, FL, [6]The University of Texas MD Anderson Cancer Center, Houston, TX, [7]Houston, TX, [8]UT Health Science Center at Houston, Houston, TX, [9]University of Texas Houston, Houston, TX, [10]Instituto Oncológico Nacional Dr Juan Tanca Marengo, Guayaquil, Ecuador

Disclosures: Sofia Garces Narvaez: None; Mario Marques Piubelli: None; Sheila Siqueira: None; Vathany Sriganeshan: None; Ana Medina: None; Amilcar Castellano-Sánchez: None; Robert Poppiti: None; Joseph Khoury: None; Shaoying Li: None; Jie Xu: None; Beenu Thakral: None; Karan Saluja: None; Meenakshi Bhattacharjee: None; Juan Carlos Garces: None; L. Jeffrey Medeiros: None; C. Cameron Yin: None

Background: Rosai-Dorfman disease (RDD) is a histiocytic disorder shown to carry kinase-activating mutations in genes encoding for the MAPK/ERK pathway in up to 30% cases. Cyclin D1 expression by immunohistochemistry (IHC) has been proposed as a surrogate marker of aberrant MAPK/ERK signaling activation in neoplasms including hairy cell leukemia and Langerhans cell histiocytosis. Using IHC, this study aimed to determine the level of cyclin D1 expression in the histiocytes of RDD.

Design: The study included 35 formalin-fixed paraffin-embedded tissue samples from 30 patients with RDD. Thirty lymph node samples from patients with reactive sinus histiocytosis were used as controls. IHC for cyclin D1 was performed in all cases and IHC for p-ERK was done in most cases. Cases were considered positive if staining was present in >5% lesional cells.

Results: The study group included 14 men and 16 women (median age: 36 years [range, 4-72]). Fifteen patients had extranodal disease alone, 8 nodal disease alone, and 7 had a combination of both. Extranodal disease sites included soft tissue (n=6), nasopharynx (n=5), duramater (n=3), orbit (n=2), breast (n=2) and brain (n=2). Ten had multifocal disease. Histologically, all cases showed features typical of RDD including many large S100-positive histiocytes, a subset of which exhibited emperipolesis. Nuclear cyclin D1 expression was detected in lesional histiocytes of 31/35 (89%) RDD samples, and in sinus histiocytes of 23/30 (77%) reactive lymph nodes. However, there were substantial differences in the extent and intensity of cyclin D1 expression between the two. (Table 1) RDD more frequently showed moderate/strong cyclin D1 expression (97% vs. 13%, *P*=<0.0001) with expression in >50% of lesional histiocytes (83% vs. 7%, *P*=<0.0001) compared to reactive sinus histiocytosis. p-ERK was positive in 5/24 (21%) cases of RDD, all of which coexpressed cyclin D1. No significant p-ERK expression was noted in sinus histiocytes of 10 reactive lymph nodes tested.

Figure 1 - 1290

Table 1. Summary and Comparison of Cyclin D1 Expression by Rosai-Dorfman Disease and Reactive Sinus Histiocytosis

	RDD (n/N [%])	Reactive sinus histiocytosis (n/N [%])	*P*-value
Percentage of histiocytes with expression*			<0.0001
<5	4/35 (11)	7/30 (23)	
5-25	1/35 (3)	15/30 (50)	
25-50	1/35 (3)	6/30 (20)	
>50	29/35 (83)	2/30 (7)	<0.0001
Intensity			<0.0001
Weak	1/31 (3)	20/23 (87)	
Moderate	10/31 (3)	3/23 (13)	
Strong	20/31 (64)	0/23 (0)	<0.0001

*Cases were considered positive if staining was present >5% of lesional histiocytes.

Conclusions: Cyclin D1 protein is overexpressed in RDD histiocytes. We theorize that cyclin D1 upregulation with subsequent cell cycle progression promoting clonal proliferation might be a common end-point for the development of RDD. At least in a subset of cases, upregulation of cyclin D1 most likely represents the downstream effects of MAPK/ERK constitutive activation. However, the absence of p-ERK coexpression in a proportion of cases suggests the role of alternative signaling pathways possibly bypassing ERK1/2.

1291 Posttransplant Lymphoproliferative Disorders (PTLD) in Argentina: A 20 -year single center study

Hernan Garcia- Rivello[1], Dana Kohan[2], Federico Jauk[3], Melina Pol[4], Marina Bonanno[5], Victoria Otero[6], Monica Makiya[4]
[1]Hospital Italiano Bs As, IMTIB, IUHI DA Patologia, Buenos Aires, Argentina, [2]Hospital Italiano Bs As Argentina, Buenos Aires, Argentina, [3]Buenos Aires, Argentina, [4]Hospital Italiano de Buenos Aires, Buenos Aires, Argentina, [5]Hospital Italiano de Bs As, Buenos Aires, Argentina, [6]Hospital Italiano de Buenos Aires, Instituto Universitario del Hospital Italiano, Buenos Aires, Argentina

Disclosures: Hernan Garcia- Rivello: None; Dana Kohan: None; Federico Jauk: None; Melina Pol: None; Marina Bonanno: None; Victoria Otero: None; Monica Makiya: None

Background: Post-transplant lymphoproliferative disorders (PTLD) comprise a heterogeneous group of lymphoid proliferations that present after a transplant in 1-2% of organ recipients.

The World Health Organization (WHO) 2017 updated the PTLD categories as Non-Destructive PTLD, Polymorphic PTLD, Monomorphic PTLD and Hodgkin-like PTLD . Most PTLD are caused by Epstein- Barr Virus (EBV) infected lymphocytes inadequately regulated by suppressor cytotoxic T lymphocytes due to the immunosuppressive treatment.

Design: The objective of this study is to describe the cases of PTLD diagnosed at Hospital Italiano de Buenos Aires, Argentina) between 1998 and 2018, in terms of morphological, immunophenotypic characterization according to the WHO 2017 criteria and to study the prevalence of EBV. Data of all cases diagnosed as PTLD in our hospital were obtained from the institutional data center. Histological material was obtained from archive. Immunohistochemical techniques were performed to reclassify the cases according to the WHO criteria with the following antibodies: CD20, CD3,CD10,Bcl6, MUM1,Bcl2, CMYC, LMP1, Ki67, CD4, CD8, CD30,CD15, CD45 (ACL), PAX5, CD79a,CD138 and HHV8.

RNA In situ hybridization for EBERs was performed to detect EBV in the tissue.

Results: The study population comprises 40 patients, 20 of whom were female patients and 20 were male patients. Fifty % of the patients were pediatric and 45% were adults.

The age range was 1 to 73 years (mean 27.4 +/- 22.4 years). 50% (n=20) of the transplants were hepatic, 47.5% (n=19) renal and 2,5% (n=1) lung transplantation . The localization of the tumors was heterogeneous, mainly involving lymph nodes (37.5%).

Regarding the histological pattern, the vast majority of PTLDs were of B cell phenotype.

We found that 2.5% were Non-Destructive PTLD, 60% were monomorphic PTLD, 27.5% were Polymorphic PTLD and 10% were classic Hodgkin lymphoma- PTLD.

The monomorphic PTLD types we found were Diffuse Large B Cell lymphomas (66.6%, n=16), Burkitt lymphomas (16,6%, n=4)), Plasmablastic lymphomas (8,3%, n=2), Plasmacytic lymphoma (4.2% , n=1) and Peripheral T cell lymphoma, CD4+ (4.2%, n=1). The prevalence of EBV was 62.5% (n= 25 cases).

Figure 1 - 1291

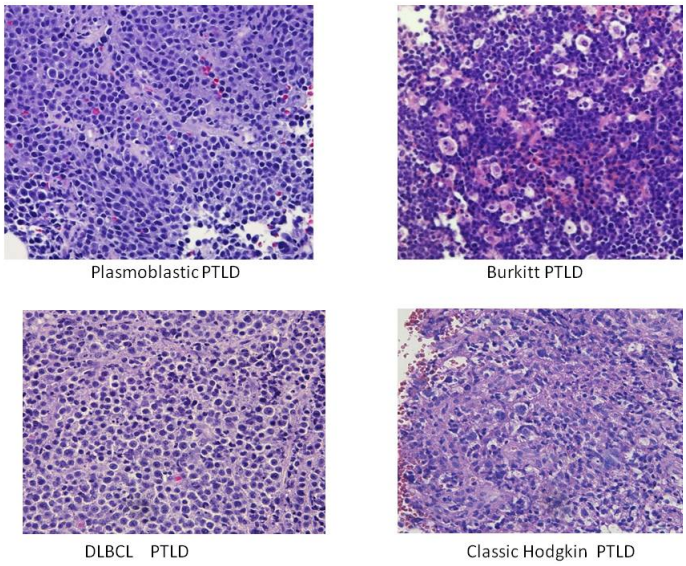

Figure 2 - 1291

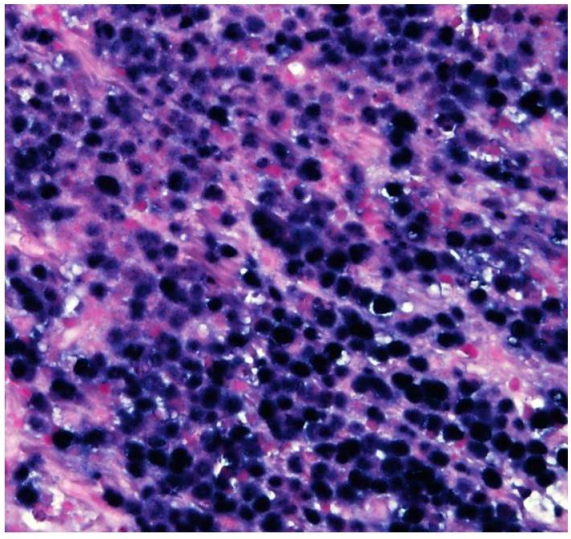

Conclusions: In conclusion, the data of our series are consistent with previous reportes in international series regarding morphological classification and EBV virus status.

Futher research well be needed to study the etiology of EBV negative cases.

1292 Lymphoplasmacytic Lymphoma/Waldestrom Macroglobulinemia: Characterization of Bone Marrow Infiltration Patterns and Mutational Profile by Targeted NGS

Julia Garcia-Reyero[1], Nerea Martinez[2], Ainara Gonzalez[2], Marcela Urquieta Lam[3], Andres Insunza[3], Sonia Gonzalez de Villambrosia[3], Santiago Montes-Moreno[3]
[1]HUMV/IDIVAL, Santander, Spain, [2]IDIVAL, Santander, Spain, [3]Hospital Universitario Marqués De Valdecilla, Santander, Spain

Disclosures: Julia Garcia-Reyero: None; Nerea Martinez: None; Ainara Gonzalez: None; Marcela Urquieta Lam: None; Andres Insunza: None; Sonia Gonzalez de Villambrosia: None; Santiago Montes-Moreno: None

Background: Lymphoplasmacytic lymphoma/Waldestrom Macroglobulinemia (LPL/WM) is defined by the combination of a LPL with an IgM monoclonal paraprotein. MYD88L265P somatic mutation has been found to be the driver mutation in the majority of cases. The aim of this study was to describe the characteristics of the bone marrow infiltration found in a series of clinically defined LPL/WM and to perform targeted NGS for the identification of additional somatic mutations in candidate genes relevant for lymphoma pathogenesis.

Design: We have reviewed a series of 39 bone marrow biopsies from 30 patients with a clinical diagnosis of LPL/WM (26 cases) or MGUS (4 cases). All 30 patients had a IgM component (mean 2.35 gr/dL, range 0.35-6.47 gr/dL). Bone marrow infiltration characteristics by morphology, IHC, FCM and allele-specific real-time PCR for the detection of MYD88L265P mutation were analyzed. Targeted exonic amplicon-based NGS of 36 lymphoma-related genes was performed in 21 samples.

Results: LPL/WM bone marrow biopsies were characterized by a paratrabecular infiltration pattern (21 samples, 54%), combined with either patchy (9 samples, 23%) or nodular (7 samples, 18%) interstitial patterns. The other 18 samples (46%) showed a non-paratrabecular pattern with interstitial involvement.

Bone marrow quantification of B cells by IHC showed invariably higher values than by FCM (median 20% (range 0-80%) by IHC vs 6.5% (range 0-62%) by FCM, p value of the mean difference <0.05). 22 out of 26 LPL/WM cases (84%) were positive for MYD88L265P mutation. Median Variant Allele Frequency of the mutated LPL cases was 0.1 (range 0.03-0.43). One out of 4 IgM-MGUS cases was positive with a VAF of 0.45%. In addition to MYD88L265P mutation, recurrent mutations were found in NOTCH2 (2 cases). Other mutated genes were PRDM1 (2 cases), KMT2D, MYC and ID3 (1 case each). MYD88L265P negative cases had mutations in KMT2D, ID3 and NOTCH2.

Figure 1 - 1292

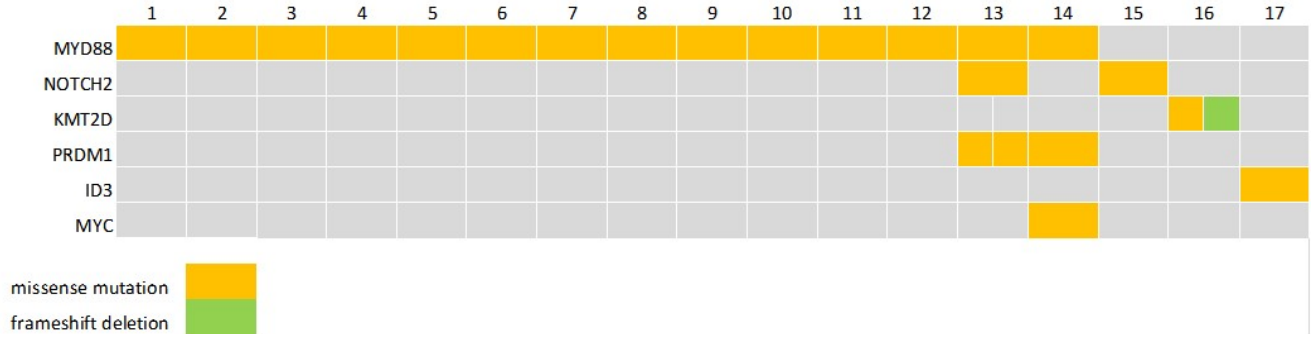

Conclusions: A combined paratrabecular and interstitial bone marrow infiltration pattern is the most common feature found in LPL/WM bone marrow biopsies. In addition to MYD88L265P, somatic mutations in KMT2D, NOTCH2 and PRDM1 might be relevant genetic events in a fraction of LPL/WM.

1293 Pitfall: Kappa Light Chain Restricted B Lymphocyte Clone in Treated Myeloma Patients, an Artifact Secondary to Daratumumab (Anti-CD38) Monoclonal Antibody Therapy

Sharon Germans[1], Valerie Juarez[2], Franklin Fuda[2], Flavia Rosado[1], Mingyi Chen[2], Weina Chen[2]
[1]University of Texas Southwestern, Dallas, TX, [2]University of Texas Southwestern Medical Center, Dallas, TX

Disclosures: Sharon Germans: None; Valerie Juarez: None; Franklin Fuda: None; Flavia Rosado: None; Mingyi Chen: None; Weina Chen: None

Background: Plasma cell myeloma is an incurable malignancy of clonal plasma cells. Recent success in immunotherapeutic strategies has altered the landscape of myeloma treatment. Daratumumab (DARA) is an anti-CD38 IgG kappa monoclonal antibody that has shown efficacy in refractory myeloma. However, DARA brought with it new challenges in post-therapeutic laboratory assessment including therapeutic antibody interference with serum protein electrophoresis and serum immunofixation electrophoresis assays. Here, we report an additional interference identified in post-therapeutic flow cytometry (FC) analysis related to bound DARA on normal B-cell progenitors known as hematogones (Hgs).

Design: 21 patients with refractory plasma cell myeloma (13 men, 8 women, ages 30-77) received DARA (2016-2018) with follow up BM hematogones > 0.10% (range 0.10-5.3%). FC was performed using 4 or 10 color antibody panels (BD FASCCanto) and analyzed by cluster analysis (Cytopaint software). Panels included CD5, CD10, CD19, CD20, CD34, CD38, CD45, CD56, Ig light chain kappa and lambda. Pretreatment and post-DARA follow up bone marrow FC samples were analyzed for persistent disease and hematogones.

Results: 100% of post-DARA treated cases showed negative staining for CD38 on all cells in the specimen (figure 1). In addition, 100% of cases also showed a kappa light chain staining artifact on 100% of hematogones (figure 1). The artifact was reproducible using different antibody tube designs with different anti-Kappa clones and fluorochromes (figure 2). Fluorescence-minus-one (FMO) tubes showed positive kappa staining on 100% hematogones (figure 2).

Figure 1 - 1293

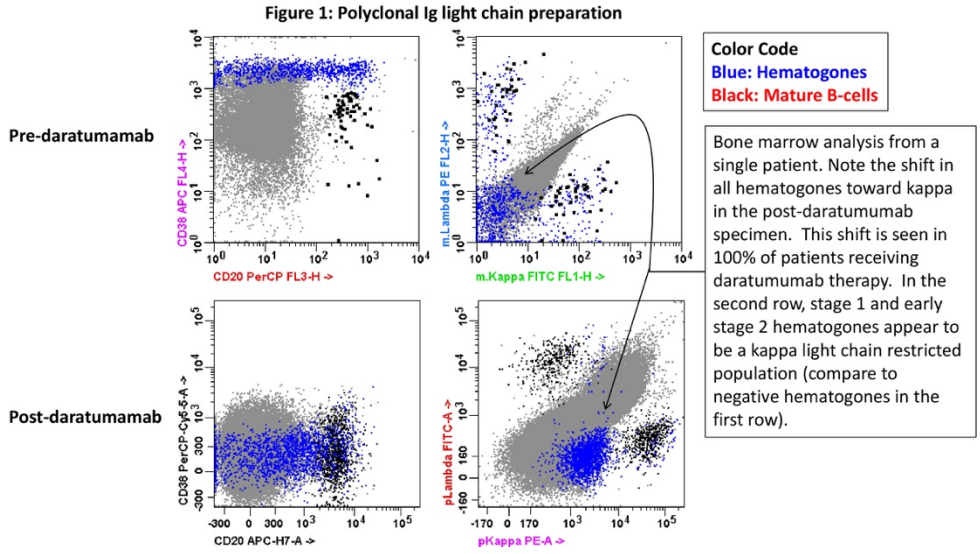

Figure 2 - 1293

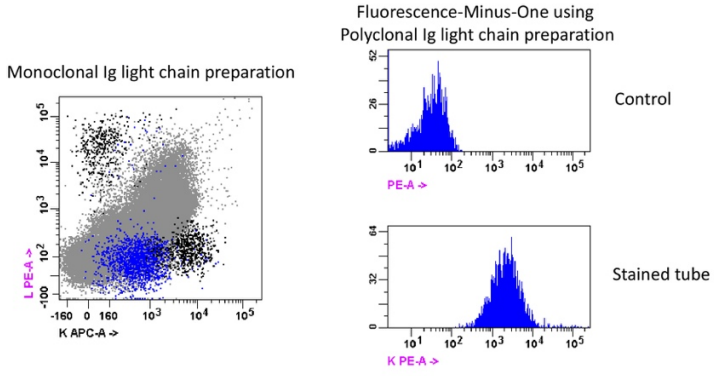

Conclusions: With the emergence of successful targeted therapies like anti-CD38 antibodies, it is important to be aware of artifactual changes that might be seen in follow up FC. Normal Hgs demonstrate a spectrum of antigen expression over 3 stages of maturation; all of which show high levels of CD38 expression. DARA binds all Hgs creating an appearance of kappa expression including on stage 1/early stage 2 Hgs, which normally lack surface Ig expression (figure 1). Hence, in the presence of DARA these Hgs appear to be a monotypic CD10(+) B-cell population. Misinterpretation of these normal cells as a CD10(+) B-cell clone can lead to unnecessary bone marrow immunohistochemical evaluation and unwarranted anxiety. Therefore, all institutions performing flow cytometry on post-DARA treated plasma cell myeloma patients need to be aware of this potentially disruptive or dangerous artifact.

1294 Philadelphia Chromosome-negative "Blast Phase" of Chronic Myeloid Leukemia

Zimu Gong[1], Mingyi Chen[2], Mina Xu[3], Wei Cui[4], Ting Zhou[5], Wei Wang[6], L. Jeffrey Medeiros[6], Shimin Hu[6]
[1]Chicago, IL, [2]University of Texas Southwestern Medical Center, Dallas, TX, [3]New Haven, CT, [4]University of Kansas Medical Center, Shawnee, KS, [5]Houston, TX, [6]The University of Texas MD Anderson Cancer Center, Houston, TX

Disclosures: Zimu Gong: None; Mingyi Chen: None; Mina Xu: None; Wei Cui: None; Ting Zhou: None; Wei Wang: None; L. Jeffrey Medeiros: None; Shimin Hu: None

Background: Chronic myeloid leukemia (CML) is characterized by *BCR-ABL1* fusion as a result of der(22)t(9;22)(q34;q11.2) (Philadelphia chromosome or Ph) and typically has a biphasic or triphasic natural history: initial chronic phase (CP), followed by accelerated phase or blast phase (BP), or both. Occasionally, CML patients may develop myelodysplastic syndrome in Ph-negative cells, which can be followed by onset of acute myeloid leukemia (AML). However, in the absence of a precedent stage of myelodysplastic syndrome and karyotyping results, the development of acute leukemia raises the issue whether this represents blastic transformation of CML or a separate disease.

Design: Patients with CML diagnosed, treated or followed over the past 20 years were retrospectively reviewed for the development of acute leukemia without Ph. Clinicopathological, genetic and follow-up data were analyzed.

Results: The study group included 6 patients: 3 men and 3 women with a median age of 58 years (range, 48-78) at initial diagnosis of CML. Five patients were diagnosed with CML-CP with P210 BCR-ABL1 and 1 CML-BP with P190. All patients received tyrosine kinase inhibitor therapy and one patient (#6) also received chemotherapy. After a median of 35 months (range, 6-187) from initial diagnosis, all patients developed acute leukemia with a myeloid phenotype: 4 were diagnosed as CML-BP and 2 as AML. The karyotypes and levels of BCR-ABL1 by FISH and qRT-PCR were shown in Table 1.

After diagnosis of Ph-negative AML, 4 patients were treated with chemotherapy, including 1 patient who received stem cell transplant (#4), and 1 treated with hydrea. The treatment was unknown in the other patient. At last follow-up, 3 patients (#1, 5, 6) died with refractory or progressive Ph-negative disease 2, 4 and 10 months after diagnosis of AML respectively, and 2 living patients had refractory (#3) or residual (#2) disease 1 and 11 months respectively. The patient who received stem cell transplant remained free of disease 65 months later.

Table 1 Karyotype and BCR-ABL1 levels at diagnosis of Ph-negative AML

#	Karyotype	FISH (%)	qRT-PCR (%)
1	46,XX[20]	0	0.05
2	47,XX,+8[20]	2	0.34
3	45,XY,-7[20]	0	NA
4	45,XY,-7[18]/45,X,-Y,t(9;22)(q34;q11.2)[2] 62% blasts	5	3.50
5	46,XY,t(11;17)(q23;q25)[20]	4	NA
6	45,XX,der(3)(q12q21)del(3)(q21q25),del(5)(q13q33),add(6)(q25),-7,add(7)(p21)[13]/45,idem,i(11)(q10)[5]/45,idem,t(5;15)(p10;q10)[2]	0	8.11

Conclusions: Ph-negative AML in patients with a history of CML is extremely rare. These patients appear to have a dismal survival similar to that of patients with blast phase of CML. Rapid FISH analysis is essential for reaching a correct diagnosis and offering appropriate therapy.

1295 CD26 and CD7 loss in peripheral blood CD4 T cells for staging of cutaneous T cell lymphoma: limitations and importance of the denominator

Bartosz Grzywacz[1], Elizabeth Courville[1]
[1]*University of Minnesota, Minneapolis, MN*

Disclosures: Bartosz Grzywacz: None; Elizabeth Courville: None

Background: According to ISCL, EORTC and WHO classifications, a CD4:CD8 ratio > 10 or expanded T cells with abnormal immunophenotype such as loss of CD7 and/or CD26 are parameters used for staging of blood cutaneous T cell lymphoma (CTCL) involvement. Recommended values are 30% CD4 positive T cells with loss of CD7 and 40 % CD4 positive T cells with loss of CD26; however, the denominator is not clearly stated, resulting in confusion in interpretation.

Design: In this IRB approved retrospective study we evaluated flow cytometry data and patient clinical history for 250 tests performed on 217 patients in the years 2011 and 2017. 8-color flow cytometry was performed using CD2, CD3, CD4, CD5, CD7, CD8, CD26, CD45. CD4+CD7- T cells and CD4+CD26- T cells were expressed as fraction of: (1) CD4 positive T cells, (2) all T cells and (3) all lymphocytes

Results: As shown in Table 1, the CD4:CD8 ratio above 10 and CD4 T cells with loss of CD7 accounting for more than 30% of T cells were findings relatively unique to CTCL patients. In contrast the proportion of CD4 T cells negative for CD26 exceeded 40% of T cells in many patients without CTCL diagnosis, nearly as many as with CTCL in this patient cohort. The entire lymphocyte population appears to be a better denominator, as it incorporates both the loss of CD26 and relative expansion of CD4 T cells seen in CTCL.

Parameter	Samples showing positive result (total n=250)	Fraction of positive samples coming from CTCL patients
CD4:CD8>10	17 (6.8%)	14/17 (82%)
CD4+CD7- T cells >30% of lymphocytes	10 (4%)	10/10 (100%)
CD4+CD7- T cells >30% of T cells	15 (6%)	15/15 (100%)
CD4+CD7- T cells >30% of CD4+ T cells	20 (8%)	16/20 (80%)
CD4+CD26- T cells >40% of lymphocytes	33 (13%)	21/33 (64%)
CD4+CD26- T cells >40% of T cells	65 (26%)	35/65 (54%)

Conclusions: Based on retrospective review of flow cytometry data we find that CD4:CD8 ratio >10 and CD4 positive T cells with loss of CD7 constituting more than 30% of total T cell population are findings relatively specific to the CTCL patients. In contrast CD4 T cells with loss of CD26 can constitute more than 40% of T cells in many patients without diagnosis of CTCL, questioning specificity of this parameter for circulating T cell lymphoma. Of note, significant subset (12 of 30) of the patients without CTCL with CD26 negative CD4 T cells above 40% had concurrent CD5 positive B cell populations with CLL/SLL like immunophenotype. Our results underscore the importance of denominator in using cut-off values for antigen loss in peripheral blood staging of CTCL, as the proportion of samples showing loss of the antigen varied considerably based on the denominator used, particularly for CD26. We feel that the advantage of using lymphocyte population as denominator is that it factors in the expansion of CD4 T cells as well as their immunophenotype.

1296 Initial optimization of a computational pathology algorithm for scoring plasma cell percentages on bone marrow biopsies

Angela Guenther[1], Fred Fu[2], Abhishek Rawat[2], Trevor McKee[2], Daniel Xia[3]
[1]Toronto, ON, [2]University Health Network, Toronto, ON, [3]University Health Network, University of Toronto, Toronto, ON

Disclosures: Angela Guenther: None; Fred Fu: None; Abhishek Rawat: None; Trevor McKee: None; Daniel Xia: None

The evaluation of reactive and neoplastic plasma cell proliferations requires accurate counts and percentages. On bone marrow biopsies and clot sections, the percentages of CD138+ plasma cells are traditionally estimated by eye. While arguably accurate, this human-based method is by definition imprecise, which can be problematic when the “true” percentage is close to an important cut-off (e.g., ~10%, at the border between MGUS and myeloma). Computational pathology can potentially assist humans in this setting by providing rapid, accurate, and precise enumerations of all positive/negative cells on the slide. Here, we describe the initial optimization of an algorithm for scoring digitized CD138-stained slides.

Design: This algorithm uses a combination of 1) computer-vision-based stain separation (e.g., of brown and blue signals), 2) threshold-based segmentation (e.g., for separating nucleated cells [more blue] from RBCs [less blue]), and 3) watershedding (e.g., for identifying individual cells within dense aggregates) to identify CD138+ and CD138- cells on digitized slides. Selected parameters for the algorithm were optimized using annotations of positive and negative cells provided by pathologists. The algorithm was then evaluated against pathologist annotations on selected images.

Results: For each CD138+ and CD138- cell counted by a pathologist, the algorithm counted on average 1.10 and 1.02 cells, respectively. On review (see Figure 1), the majority of the cells in the images identified by the pathologists were correctly segmented by the algorithm (green outline), while a minority were over-segmented (purple outline), under-segmented (red outline), or missed (no outline).

Figure 1 - 1296

Figure 1. Comparison of pathologist (red dots) and algorithm labels (outlines). Well-segmented cells are indicated by green outlines (one dot for every outlined object). Over-segmented cells are indicated by purple outlines (no dots within the outlined object). Under-segmented cells are indicated by red outlines (two or more dots within the outline). A few cells were missed (dots with no outline).

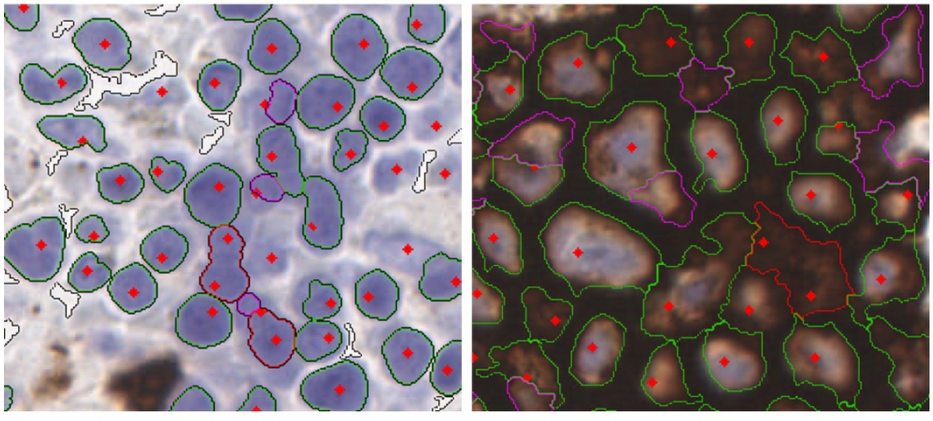

Our method shows promise; further fine-tuning is needed to minimize over- and under-segmentation of cells. A version of this algorithm may eventually contribute to precision and standardization in hematopathology, potentially by acting as a digital “second opinion” tool in selected cases (e.g., those with ~10% plasma cells).

1297 Expression of myelomonocytic markers in Langerhans cell histiocytosis

Rohit Gulati[1], Jordyn Griffin[2], Nives Zimmermann[1], Liang Cheng[2], Bradley Gibson[1], Sandeep Batra[1], Magdalena Czader[1]
[1]Indiana University, Indianapolis, IN, [2]Indiana University School of Medicine, Indianapolis, IN

Disclosures: Rohit Gulati: None; Jordyn Griffin: None; Nives Zimmermann: None; Liang Cheng: None; Bradley Gibson: None; Sandeep Batra: None; Magdalena Czader: None

Background: Langerhans cell histiocytosis (LCH) is the most common histiocytic neoplasm in children and adults. LCH is a heterogeneous disease and can originate from either epidermal Langerhans cells or from myeloid dendritic cell precursors. The latter origin is primarily supported by gene expression and experimental studies, however, reports on immunohistochemical expression of myelomonocytic markers in large LCH series are limited.

Design: We studied 75 archival LCH cases from 59 children and 16 adults (median age 8 years, range 3 weeks to 70 years). The most common location was bone (88%). 60% of patients had a single bone lesion and were treated with curettage, whereas the remaining patients with either multisystem, muti-focal bone disease or CNS-risk lesions received chemotherapy. 11 patients experienced relapse (long-term follow-up data available in 46 patients). The diagnostic and myelomonocytic markers studied by immunohistochemistry included: S100, CD1a, CD207, CD33, CD13, CD15, CD68, PGM1, CD14, CD163, myeloperoxidase, CD4 and CD2. Immunohistochemical stains were scored semiquantitatively in morphologically identified Langerhans cells (LC). A case was considered positive for an individual marker if at least 5% of LC were positive. BRAF mutational status was determined by PCR. The correlation of antigen expression to clinicopathological parameters was studied.

Results: Of all pan-myeloid markers, CD33 was most uniformly and strongly expressed followed by CD68 and CD13. 92% of cases showed CD33 antigen expression in at least 50% of LC. CD68 antigen was expressed in 86% cases with 22% showing more than 50% positive LC. Only 47% of cases expressed CD13 with rare cases being positive in more than 50% LC. Among monocytic markers, CD14 antigen expression was most prominent (positive in 88% of cases, 29% cases positive in more than 50% LC), whereas PGM1 and CD163 were positive in 48% and 68% cases, respectively. Myeloperoxidase and CD15 were negative in all cases. CD4 and CD2 were expressed in 92% and 62% cases respectively, with CD2 expressed in the minority of LC. There was no statistically significant correlation between individual marker expression and site of involvement, stage or disease recurrence.

Conclusions: As shown by immunohistochemistry, LCH shows a significant expression of myeloid and monocytic markers similar to that previously described in myeloid dendritic cells and their precursors. CD33 antigen may be a potential immunological target for treatment of LCH.

1298 IgA Plasma Cell Neoplasms Are Characterized by Shorter Long-Term Survival Than Their IgG Counterparts and Are Associated with Increased Genomic Complexity

Gabriel Habermehl[1], Megan Nakashima[2], Claudiu Cotta[2]
[1]Cleveland, OH, [2]Cleveland Clinic, Cleveland, OH

Disclosures: Gabriel Habermehl: None; Megan Nakashima: None; Claudiu Cotta: None

Background: In the medical literature IgA plasma cell neoplasms are usually discussed together with their IgG counterparts. Recent studies indicate that IgM, IgD and IgE neoplasms have clincal characteristics and behavior different that IgG tumors. This study aims to identify the features that separate the IgA neoplasms from the other gammopathies.

Design: 45 patients with M proteins characterized as IgA and 43 with IgG were identified. Data regarding their presentation, laboratory and radiologic characteristics were collected from the electronic medical record. Statistical analysis was performed in order to detect differences at presentation and in survival.

Results: At presentation, the IgA patients were slightly younger (66.5±11.3 vs. 69.2±10.7, $p<0.23$) than their counterparts. In contrast to control, the IgA group had an equal male:female ratio, was less likely to have bone lesions (12/45 vs 18/43, $p<0.14$), immunoparesis (51% vs. 63%) and the kappa/lambda ratio was more skewed towards kappa (3:1 in IgA vs. 1:0.7 in IgG). A significant difference was the number of cases with normal FISH results, 27% for IgA vs 61% for IgG ($p<0.037$). Other features of IgA and IgG PCN at presentation, including their classification as MGUS (49 vs 46%), SPCM (2% for both) and PCM (49 vs 51%) were essentially identical. The most important finding was the worse survival of IgA patients (80 vs 108 months median survival IgA vs IgG, $p<0.013$), difference which was not detectable in the first 5 years and become substantial 10 years post-diagnosis.

	IgA (n =45)	IgG (n = 43)	P Value
Age	66.5 ± 11.3	69.2 ± 10.7	0.23
Male/Female	22/23	30/13	0.07
Kappa/Lambda	34/11	25/18	0.08
Immunoparesis	23 (51%)	27 (63%)	0.27
Bone lesions	12 (27%)	18 (42%)	0.14
FISH	IgA (n=15)	IgG (n=23)	P Value
Normal	4 (27%)	14 (61%)	0.013
RB1	3 (20%)	4 (17%)	n/a
t(4;14)	4 (27%)	1 (4%)	n/a
P53	2 (13%)	1 (4%)	n/a
t(11;14)	4 (27%)	3 (13%)	n/a

Figure 1 - 1298

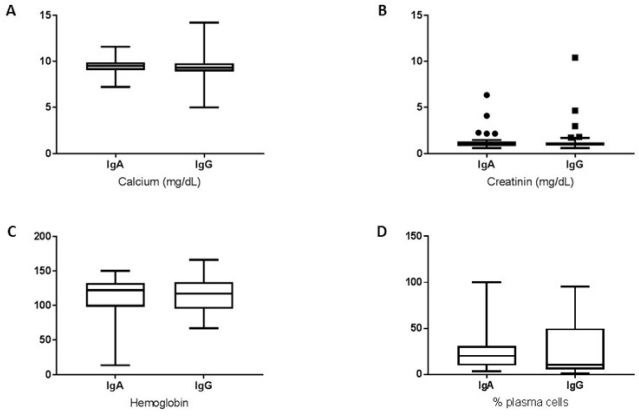

Figure 2 - 1298

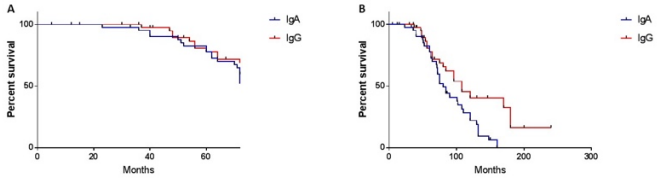

Conclusions: In conclusion, we have compared the presentation and the clinical outcome of patients presenting with IgA monoclonal gammopathies to that of patients with IgG, in an effort to decide whether IgA neoplasms should be considered in a different diagnostic category from their IgG counterparts. The major difference is the poorer survival of IgA patients, the differences from IgG becoming evident only long-term. The possible cause for this is increased genomic complexity, likely due to increased genomic instability of IgA neoplasms, as suggested by the findings of fluorescence in-situ hybridization.

1299 Bone Marrow Morphologic, MyPRS, and Mutation Correlations in Multiple Myeloma, Mount Sinai Icahn Tisch Experience

Yansheng Hao[1], Daniel Khaykin[2], Levi Machado[3], Jane Houldsworth[4], Julie Teruya-Feldstein[5]
[1]New York, NY, [2]Icahn School of Medicine at Mount Sinai, Oceanside, NY, [3]Mount Sinai Hospital, New York City, NY, [4]Icahn School of Medicine at Mount Sinai, New York, NY, [5]Mount Sinai Hospital Icahn School of Medicine, New York, NY

Disclosures: Yansheng Hao: None; Daniel Khaykin: None; Levi Machado: None; Jane Houldsworth: None; Julie Teruya-Feldstein: None

Background: Multiple myeloma is a malignant neoplasm of plasma cells with clinical and genetic heterogeneity. Recent work has shown the molecular subtypes and the 70-gene prognostic risk score (MyPRS) significantly correlate with prognosis in myeloma patients. Here, we investigated correlation of bone marrow histology and genetic alterations with MyPRS gene expression at a single academic center.

Design: 329 myeloma cases collected from 01/2017 to 05/2018. Histologic features were evaluated. Samples were analyzed for MyPRS risk score, molecular subtype and virtual karyotype through gene expression profiling. Translocation and mutation data was from FoundationOne next-generation sequencing.

Results: 329 cases included 143 female (43.5%) and 186 male (56.5%) in this studies. There was no significant difference with age (p= 0.5200), gender ratio (p=0.1500), or race distribution (p=0.4800) between the two groups. Among the 7 molecular subtypes, poor prognostic types were closely associated with high-risk group, whereas good prognostic types are associated with low-risk group (p=0.0001). Compared to low-risk cases, high-risk ones show higher marrow cellularity (p=0.0005), higher percentage of tumor cells (p=0.0155) and higher histological stage (p=0.0001). Diffuse sheet growth pattern were more associated with high-risk cases (62.8%). Immature nuclear morphology (p=0.0001), advanced fibrosis (p=0.0002) and higher mitotic index (p=0.0227) were more commonly occurred in high-risk cases. No significant difference was observed in light chain restriction (p=0.098) or percentage of different cell types in the marrow. Genetically, t(4:14), deletion of 1p, 6, 13 and gain of 1q correlated with high risk; whereas 3 gain, 7 gain, and t(11:14) correlated with low risk. A higher degree of tumor mutation burden was associated with high-risk patients (p=0.0027). The most frequent recurrent translocations were IGH-MMSET and IGH-FGFR3, significantly associated with high risk cases. Top 10% most frequent mutations, KRAS, BRAF, NRAS, DNMT3A, TET2 and CREBBP were frequently mutated in both groups whereas TP53, FGFR3 and CD36 were significantly associated with high-risk cases.

		High risk		Low risk		P value
Case #		151		178		
Age	Mean	64		65		0.52
Sex	F	71	47.02%	72	40.45%	0.15
	M	80	52.98%	106	59.55%	
Race	Aferican American	20	13.25%	21	11.80%	0.48
	Asian	4	2.65%	6	3.37%	
	White	105	69.54%	117	65.73%	
	Others	22	14.57%	34	19.10%	
Subtype	CD1	25	16.67%	16	8.99%	0.0001
	CD2	23	15.33%	63	35.39%	
	HY	16	10.67%	42	23.60%	
	LB	8	5.33%	21	11.80%	
	MF	14	9.33%	14	7.87%	
	MS	30	20.00%	16	8.99%	
	PR	34	22.67%	6	3.37%	
Infiltrating Pattern	Non-sheets	109	80.15%	145	90.06%	0.0155
	sheets	27	19.85%	16	9.94%	
Bartl stage	1	55	46.61%	99	66.89%	0.0001
	2	29	24.58%	39	26.35%	
	3	34	28.81%	10	6.76%	
Nuclear Grade	1	57	45.24%	73	49.66%	0.0001
	2	52	41.27%	72	48.98%	
	3	17	13.49%	2	1.36%	
Fibrosis	0	38	27.94%	76	46.91%	0.0002
	1	77	56.62%	80	49.38%	
	2	17	12.50%	4	2.47%	
	3	4	2.94%	2	1.23%	
Light chain	K	74	57.81%	107	67.30%	0.098
	L	54	42.19%	52	32.70%	
Tumor Mutation Burden	low	18	64.29%	32	94.12%	0.0027
	intermediate	10	35.71%	1	2.94%	
	high	0	0.00%	1	2.94%	
% cellularity of marrow		52.39		44.27		0.0005
% Plasma cell in Smear		28.35		22.14		0.0225
% Plasma cell in Bx		36.44		28.89		0.0155
Mitoses / HPF		2.27		1.37		0.0227

Conclusions: For the first time we show bone marrow histologic features, including high plasma cell volume, diffuse growth pattern, immature cell morphology, high mitotic index, and increased fibrosis, significantly correlate with MyPRS high risk disease. We also demonstrate the association of MyPRS risk stratification with specific genetic alterations.

1300 The Survival Impact of 1q+/CKS1B Depends on Background Karyotype and Del(17p)/TP53 Allelic Burden

Suyang Hao[1], Sergej Konoplev[2], Xinyan Lu[3], Shaoying Li[4], Shimin Hu[4], Jie Xu[2], Guilin Tang[4], L. Jeffrey Medeiros[4], Pei Lin[4]
[1]Houston Methodist Hospital, Houston, TX, [2]Houston, TX, [3]Chicago, IL, [4]The University of Texas MD Anderson Cancer Center, Houston, TX

Disclosures: Sergej Konoplev: None; Xinyan Lu: None; Shaoying Li: None; Shimin Hu: None; Jie Xu: None; Guilin Tang: None; L. Jeffrey Medeiros: None; Pei Lin: None

Background: Gain or amplification of 1q/CKS1B, a controversial risk factor, is not listed in the Revised International Staging System for myeloma. A recent study found amp/gain of 1q/CKS1B combined with biallelic TP53 inactivation defines a subset of “double-hit” high-risk myeloma (Walker BA, *Leukemia*, 2018). It is unknown however if the impact of “double hit” is related to the background karyotype.

Design: We compared overall survival (OS) of myeloma patients with 1q+/CKS1B, with or without concurrent del(17p)/TP53 (ΔTP53), and that of patients with del(17p)/TP53 but without 1q+/CKS1B in the context of a normal or simple karyotype (< 3 abnormalities)(NK/SK) vs. a complex karyotype (CK, ≥ 3 abnormalities). The 1q+/CKS1B and del(17p)/TP53 were detected by FISH analysis. Survival analysis was based on Kaplan-Meier and Cox or log rank.

Results: The study group included 65 patients with 1q+/CKS1B (2-100%, median 63%): 40 men and 25 women, with a median age of 69 years (range, 41-82). Of these patients, 28 had a NK/SK (NK=24, SK=4) and 34 had a CK, 3 were unknown. Nineteen (29%) also had ΔTP53 (5- 100%, median 40%). The control group included 22 patients without 1q+/CKS1B but with ΔTP53 (median 8-93, 13%). These patients were further divided into group A: 1q+/CKS1B single hit (n=46), group B: CKS1B + ΔTP53 double hit (n=19), group C: ΔTP53 with NK (n=16), group D: ΔTP53 with CK (n=6). The follow up period for patients with 1q+/CKS1B ranged from 5-80 (48 mos); 33 died with a median survival of 32 months. The OS of patients with double hit (group B) was significantly worse than those with 1q+/CKS1B alone (group A)(p =0.006). The OS of patients with 1q+/CKS1B as a whole group is similar to that of ΔTP53, but the subset of 34 patients with a CK was significantly worse. A cut off of 50% ΔTP53 signals further identified patients within the double hit subgroup (B) with a poorer survival having a median OS of 13 months (p=0.008). Furthermore, the double hit is highly correlated with a complex karyotype (p= 0.013). Within the 1q+/CKS1B group, the OS of patients with a CK is significantly worse than those with a NK/SK.

Figure 1 - 1300

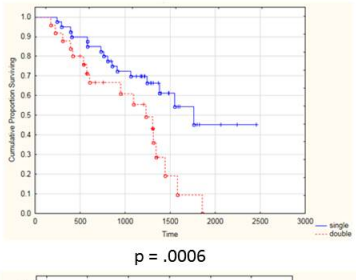

p = .0006

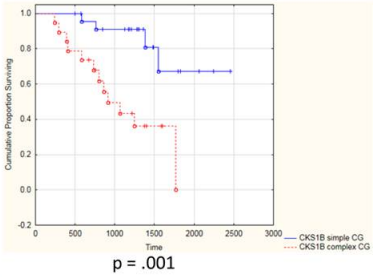

p = .001

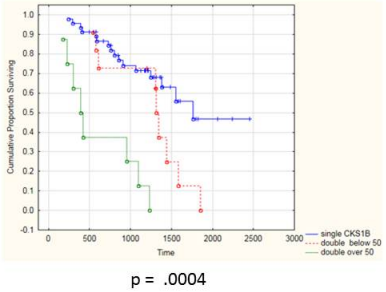

p = .0004

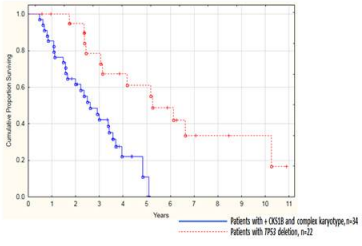

p = .001

Conclusions: The adverse impact of 1q+/CKS1B is only evident in the subgroup with a complex karyotype. The combined 1q+/CKS1B and ΔTP53 (double hit) correlate with a complex karyotype, accounting for the poor OS, and may serve as a biomarker for high risk myeloma. A threshold of > 50% ΔTP53 signals further identifies an ultra-high risk subset.

1301 The Utility of Flow Cytometry in Cerebrospinal Fluid Diagnosis

Christopher Hartley[1], Mohamed Mostafa[2], Steven Kroft[1], Alexandra Harrington[3]
[1]Medical College of Wisconsin, Milwaukee, WI, [2]Medical College of Wisconsin, Wauwatosa, WI, [3]Milwaukee, WI

Disclosures: Christopher Hartley: None; Mohamed Mostafa: None; Steven Kroft: None; Alexandra Harrington: None

Background: Several hematologic malignancies (HM) involve the central nervous system and are readily detected in the cerebrospinal fluid (CSF) via flow cytometry (FC). The sensitivity of FC makes it an attractive diagnostic tool for clinically challenging cases. Nonetheless, significant pretest factors influence the overall value of FC of CSFs. The aim of this study was to retrospectively correlate pretest variables, including morphology, with FC results on CSF specimens.

Design: CSF FC samples were retrieved from 1/1/2013 to 9/30/2015, with age, sex, FC result (4- or 8-color), history of HM, CNS imaging, and several preanalytical FC parameters collected. Cytomorphologic evaluation (CME) was performed on cytospins by a hematopathologist (AH) blinded to all but the indication for analysis, and categorized as (-), atypical, suspicious, or (+) for malignancy. Imaging results were categorized on the same ordinal scale. Stepwise multivariate logistic regression was used to compare pretest variables to the binary FC result (negative or positive for HM). A pretest index was developed by assigning points to each variable in the final model by dividing the odds ratio (OR) of each variable by the smallest OR and rounding to the nearest whole number.

Results: FC results were analyzed on 499 CSFs, with demographics, clinical findings, FC metrics, and indications listed in Table 1. Eighty-one of 499 CSFs had (+)FC (16.2%) ;157/499 were atypical or worse by CME (31.5%), of which 39.5% had (+)FC. FC and CME were concordant in 77% of cases; however, 5.8% had (+)FC/(-)CME and 60.5% (-)FC/(+)CME, including 66/375 (17.6%) with HM. FC results are summarized according to the only 2 significant pretest variables from the final multivariate model: history of HM and CME (Table 2), which both confer an 11x higher rate of (+)FC (OR of 11.4 and 11.5). As such, history of HM and CME each contribute 1 point to the pretest FC result index. Cases with a pretest index score of 2 (maximum possible) had a (+)FC result in 59 of 125 cases (47.2%). None of the 92 cases (18.4% of all cases) with a pretest index of 0 (no history of HM and negative CME) had a (+)FC result (Table 2).

Table 1: Final Bivariate Logistic Regression Model, Non-significant Variables, and Pre-Test Index

Variable	p-value	Odds Ratio	Lower 95% CI	Upper 95% CI
History of Hematologic Malignancy (75% of total cases; of these, 16% AML, 29%ALL, 16% DLBCL/BL/DHL, 9% T/NK cell lymphomas, 29% others)	<0.0001	11.42	3.43	38.1
Cytospin Morphology Atypical/Suspicious/Positive (31.5% of cases)	<0.0001	11.51	6.46	20.5
Imaging Abnormal/Suspicious/Positive (23.8% of cases)	NS	NS	NS	NS
Male Gender (M:F ratio 1.3:1)	NS	NS	NS	NS
Age (years) mean=52, range (19-98)	NS	NS	NS	NS
Hemodilute Cerebrospinal Fluid (28% of cases)	NS	NS	NS	NS
Log of Cell Count of Cerebrospinal Fluid (mean=3.74, range(0-6.74))	NS	NS	NS	NS
Volume Submitted for Flow Cytometry (mean=0.29 mL; range 0.1-1.7 mL)	NS	NS	NS	NS
Cell Viability for Flow Cytometry (%), mean=85%, range(0-100%)	NS	NS	NS	NS

Legend: NS=Not significant; AML=Acute myeloid leukemia; ALL=Acute lymphoblastic leukemia; DLBCL=Diffuse large B cell lymphoma; BL=Burkitt lymphoma; DHL=Double-hit lymphoma; NK=Natural killer.

Preflow Index: Cases with Positive Flow Cytometry

Pre-flow Index Variables	Cytospin Morphology Atypical/Suspicious/Positive	Negative Cytospin Morphology	Totals
History of Hematologic malignancy	59/125 (47.2%)	19/250 (7.6%)	78/375 (20.8%)
No History of Hematologic Malignancy	3/32 (9.3%)	0/92 (0%)	3/124 (2.4%)
Totals	62/157 (39.5%)	19/342 (5.6%)	81/499 (16.2%)

Conclusions: Together, cytospin CME (atypical or worse) and positive history of HM are exquisitely sensitive for a (+)FC result using a simple pretest index assigning 1 point to each of these parameters. However, CME was a stronger predictor of positivity than FC, having identified almost 20% more (+) CSFs in HM patients, emphasizing the importance of CME.

1302 SAMHD1 predicts poor outcomes in mantle cell lymphoma patients

Miaoxia He[1], Tao Wang[2], Shimin Zhang[3], Jianming Zheng[4], Jianmin Yang[2]
[1]Changhai Hospital, Shanghai, Shanghai, China, [2]Changhai Hospital, Second Military Medical University, Shanghai, China, [3]Joint Pathology Center, Bethesda, MD, [4]Changhai Hospital, Shanghai, China

Background: Sterile alpha motif and histidine-aspartic domain-containing protein 1 (**SAMHD1) is a deoxynucleoside triphosphate triphosphohydrolase (dNTPase), which palys an important role in tumor development and treatment. However, SAMHD1 expression and function in** mantle cell lymphoma **(MCL) has not been well-defined.**

Design: We evaluated SAMHD1 expression in 58 MCL tissue by immunohistochemistry (IHC) and SAMHD1 genetic mutations by Whole-exome sequencing (WES). And we retrospectively compared chemotherapy response and clinical outcome of SAMHD1 positive and negative MCL patients.

Results: p.p1 {margin: 0.0px 0.0px 0.0px 0.0px; text-align: justify; text-indent: 21.0px; font: 12.0px 'Times New Roman'; color: #2f2a2b} span.s1 {font: 10.5px 'Times New Roman'; color: #000000}

SAMHD1 was positive in 32/58 (55.2%) patients. Four SAMHD1 genetic mutations (**Exon 8 53A; Exon 12 A82G, 76G, A25G)** were observed in MCL patients associated amino acid substitutions (**S-Y**, **V- I, N-D**, **Y-A**). Comparison between SAMHD1 positive and negative patients revealed that the SAMHD1 positivity associated with lower chemotherapy response rate (p=0.012) and shorter overall survival (OS) (p=0.0335). Besides, MCL patients with MIPI scores between 0-5 could be divided into two groups based on SAMHD1 expression, which shown significantly different PFS (p=0.047) and OS (p=0.006).

Conclusions: SAMHD1 is expressed in the majority of MCL patients, and high expression of SAMHD1 is related to poor MCL chemotherapy response and OS. Also, exon 12 mutation of SAMHD1 was closely associated with unregulated expression and poor chemotherapy response. Therefore, SAMHD1 may be an adverse biomarker of MCL patient's chemotherapy response and outcome. We suggest that MCL risk stratification could be combined SAMHD1 with MIPI.

1303 Aurora-A and Polo-Like Kinases Are Important Diagnostic and Therapeutic Markers in Hodgkin Lymphoma and Mimics

Kathryn Hogan[1], Carlos Murga-Zamalloa[2], Girish Venkataraman[3], Daniel Schultz[1], Madhu Menon[4], Juan Gomez-Gelvez[5], Jie Yan[1], Kedar Inamdar[1]
[1]Henry Ford Health System, Detroit, MI, [2]University of Michigan, Ann Arbor, MI, [3]University of Chicago Medical Center, Chicago, IL, [4]Detroit, MI, [5]Henry Ford Hospital, Detroit, MI

Disclosures: Kathryn Hogan: None; Carlos Murga-Zamalloa: None; Girish Venkataraman: None; Daniel Schultz: None; Madhu Menon: None; Juan Gomez-Gelvez: None; Jie Yan: None; Kedar Inamdar: None

Background: Aurora-A (AA) and Polo-like kinases (PLK) are mitotic kinases that regulate the G2/M phase of the cell cycle and are implicated in the tumorigenesis of solid tumors and, recently, in B- and T-cell non-Hodgkin lymphoma (NHL). They play a key role in tumor proliferation and disease progression in highly aggressive B-NHL. They serve as indicators of disease activity and thus are attractive therapeutic targets. Expression of AA and/or PLK has not yet been assessed in Classical Hodgkin Lymphoma (CHL) and its mimics. Thus, we performed this study to assess AA and PLK expression in different CHL types and their mimics, nodular lymphocyte predominant HL (NLPHL) and primary mediastinal B-cell lymphoma (PMBL).

Design: We assessed 27 CHL, 16 NLPHL and 8 PMBLs for AA and PLK expression by immunohistochemistry. A mouse monoclonal AA-(Abcam, UK) and PLK-antibody (Cell Signaling Technologies, USA) were used. Any cytoplasmic and/or nuclear staining was considered positive. Each case was semi-quantitatively graded for percentage of positive cells (<50% and >50%) and for staining intensity (1-3+). Immunohistochemical analysis was independently performed by 2 pathologists (KMH and KVI). Statistical analysis was performed using Fisher's exact test.

Results: AA and PLK were expressed in 100% of NLPHL and 96% of CHL cases. In contrast only 37% of PMBLs were positive for AA (CHL vs PMBL, p=0.0002; NLPHL vs PMBL, p=0.0013) and PLK (CHL vs PMBL, p=0.0009; NLPHL vs PMBL, p=0.0013). In the NLPHL group, PLK but not AA correlated with higher stage disease at presentation (III and IV) (p=0.044). In CHL, AA was expressed in >50% of tumor cells in cases with higher stage and extranodal disease, however, this correlation was not statistically significant. No statistically significant differences were found either in the intensity or localization of AA or PLK within or between CHL and NLPHL cohorts. Also, there was no correlation of intensity or localization of either AA or PLK with a variety of clinical and laboratory features in CHL types and mimics.

Figure 1 - 1303

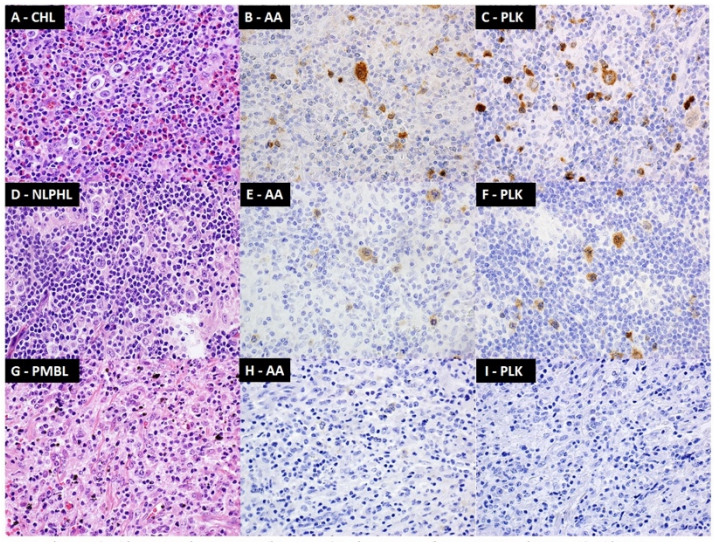

Fig. 1. a) CHL, H&E. b) CHL, AA. c) CHL, PLK-1. d) NLPHL, H&E. e) NLPHL, AA. f) NLPHL, PLK-1. g) PMBL, H&E. h) PMBL, AA. i) PMBL, PLK-1. All images at 400x.

Conclusions: AA and PLK are commonly expressed in CHL and NLPHL but not in PMBL and thus are useful markers in the distinction of CHL or NLPHL from PMBL in mediastinal location. PLK is a useful marker for prognostication of NLPHL. AA and PLK are attractive potential therapeutic targets in the treatment of CHL and NLPHL. Additional studies are underway to characterize an array of hematopoietic lesions known to overlap with CHL.

1304 High-Grade B-Cell Lymphoma is Associated with a Worse Survival than Other Aggressive B-Cell Lymphomas in HIV+ Patients

Zhihong Hu[1], Wei Wang[2], Yi Sun[2], Robert Brown[3], Xiaohong Iris Wang[4], Lei Chen[5], Md Amer Wahed[6], Nghia Nguyen[6], L. Jeffrey Medeiros[2]

[1]The University of Texas Health Science Center at Houston, Sugar Land, TX, [2]The University of Texas MD Anderson Cancer Center, Houston, TX, [3]UTHealth, McGovern Medical School, Houston, TX, [4]Bellaire, TX, [5]University of Texas Houston, Houston, TX, [6]The University of Texas Health Science Center at Houston, Houston, TX

Disclosures: Zhihong Hu: None; Wei Wang: None; Yi Sun: None; Robert Brown: None; Xiaohong Iris Wang: None; Lei Chen: None; Md Amer Wahed: None; Nghia Nguyen: None; L. Jeffrey Medeiros: None

Background: HIV infection is associated with an increased risk of developing lymphomas. The most common HIV-associated lymphomas are those with aggressive clinical behavior including Burkitt lymphoma(BL), diffuse large B-cell lymphoma (DLBCL) and others. High grade B cell lymphoma (HGBCL), a novel entity introduced in 2016 WHO revision, occurs in HIV patients but the incidence and clinicopathologic features are unknown.

Design: In this study, we retrospectively reviewed our HIV+ patients diagnosed with aggressive non-Hodgkin lymphoma during the interval of 2008-2018. The diagnosis was rendered based on the 2016 revised WHO criteria. Patients' clinical information including demographic data, treatment regimens and follow-up data were analyzed. We compared the clinicopathologic features of patients with high-grade B-cell lymphoma to patients with other aggressive non-Hodgkin lymphomas.

Results: The study included a total of 95 patients including 40 DLBCL, 21 plasmablastic lymphoma (PBL), 17 HGBCL, 10 BL, 4 primary effusion lymphoma (PEL), 2 B-lymphoblastic lymphoma (B-ALL) and 1 angioimmunoblastic T cell lymphoma (AITL). There were 81 men and 14 women with a median age of 45 years (range, 20-67). 16/17 (95%) cases had a proliferation rate of >90% by Ki67 stain; 15/15 (100%) cases had a germinal center B cell (GCB) subtype; 3/6 (50%) cases were positive for EBER; 8/16 (50%) patients had bone marrow involvement; 9/13 (69%) cases showed *MYC* rearrangement while only one case had double *MYC* and *BCL6* rearrangements by FISH; 15 patients presented with high clinical stage (III/IV). For treatment in HGBCL patients, 15/17 (88%) patients received aggressive chemotherapy. Eleven (65%) patients died with a median follow up of 10 months (range, 0-119). The median overall survival (OS) of patients with HGBCL was 8 months. When compared to patients with other types of lymphomas, HGBCL patients' survival was worse than patients with BL, DLBCL and PBL (median survival not reached) (Figure 1). Furthermore, patients with HGBCL appear to have an inferior survival than patients of DLBCL even with a proliferation rate >90%.

Figure 1 - 1304

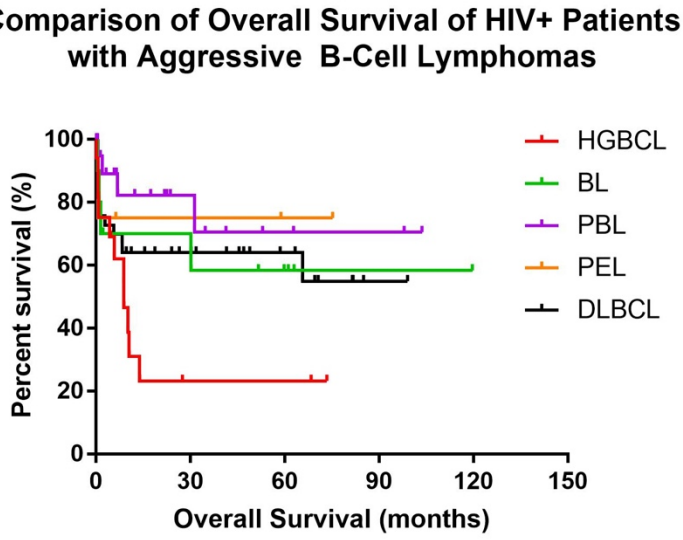

Conclusions: The mortality of HIV-associated HGBCL is high. Thus, the diagnosis of HGBCL is important for proper patient management and risk stratification of these HIV+ patients. The morphology, immunophenotype, proliferation rate and detection of *MYC* rearrangement by FISH can help to identify this entity and distinguish it from other aggressive B cell lymphomas.

1305 Extranodal NK/T-cell Lymphoma with Aberrant Expression of CD20: A Clinicopathological Study of Five Cases

Yuhua Huang[1], Jingping Yun[1]
[1]Sun Yat-sen University Cancer Center, Guangzhou, China

Disclosures: Yuhua Huang: None; Jingping Yun: None

Background: CD20 expression by immunohistochemistry was historically considered restricted to B-lineage neoplasms and CD20 is served as the target of the therapeutic monoclonal antibodies in B-cell lymphomas and leukemias. Aberrant expression of CD20 in extranodal NK/T-cell lymphoma （ENKTCL) has been rarely reported, while all instances were documented as case report rather than as study series. Due to the rarity, the frequency and clinicopathological features of this extremely rare condition have not been characterized. We aimed to evaluate CD20 immunoexpression in a large series of ENKTCL.

Design: A total of 772 cases of ENKTCL diagnosed in Sun Yat-sen University Cancer Center from March 2013 to February 2018 were included in present study. The medical record, hematoxylin and eosin-stained (H&E) and immunohistochemistry slides were retrospectively reviewed. Some necessary immunostainings and molecular assays for gene rearrangements were further performed for differential diagnosis.

Results: Aberrant membranous expressions of CD20 were identified in 5 cases among the 772 ENKTCLs, representing a detection rate of 0.65% (5/772). The patients of ENKTCL with aberrant expression of CD20 ranged from 37 to 79 years with the ratio of male to female at 3:2.The primary sites of the tumor were as follows: testis (2 cases), nasal cavity (2 cases) and skin (1 case).All these 5 cases exhibited typical morphology of ENKTCLs and showed a immunophenotype of CD3ε+/cytotoxic granules (at less two markers)+/EBER+. CD56 immunostaning was found in 4 of 5 cases (80%). The percentage of the CD20-positive tumor cells ranged from 40% to 80% with variable immunostaning intensity. All CD20-positive tumor cells were negative for CD79a, CD19 and PAX5. Interestingly, CD20 expression was detected in tumor cells both in primary site (nasal cavity) and secondary involved site (testis).

Figure 1 - 1305

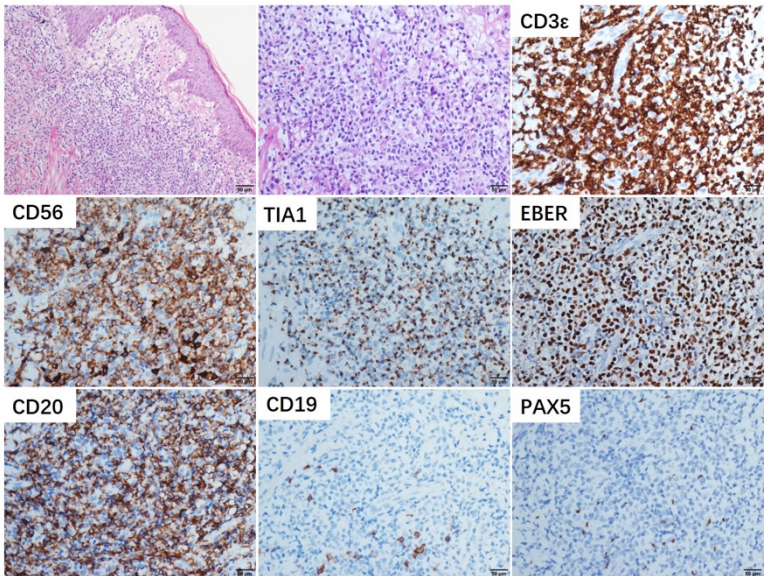

Conclusions: Aberrant expression of CD20 in ENKTCL may present a diagnostic pitfall and may be mistaken for B-lineage neoplasms, leading to misclassification and inappropriate therapy. A correct diagnosis requires awareness and recognition of this pitfall by a panel of sufficient immunostainings. The clinicopathologic significance and potential molecular mechanisms of aberrant expression of CD20 in ENKTCL merit further investigation.

1306 High Incidence and Prognostic Significance of IgH/MYC rearrangement in Plasmablastic Lymphoma

Yuhua Huang[1], Lanfang Miao[2]
[1]Sun Yat-sen University Cancer Center, Guangzhou, China, [2]Anyang Tumor Hospital, Anyang, China

Disclosures: Yuhua Huang: None; Lanfang Miao: None

Background: Plasmablastic lymphoma (PBL) is a rare aggressive B-cell non-Hodgkin lymphoma defined as a high-grade large B-cell neoplasm with plasma cell phenotype. Genetic alterations in MYC have been found in a proportion of PBL cases previously. However, clinicopathological features of PBL with IgH/MYC rearrangemen and prognostic significance of IgH/MYC rearrangement in PBL have not been characterized.

Design: IgH/MYC rearrangement were performed in 13 unpublished single-center PBLs. In addition, 91 cases of PBLs with IgH/MYC-FISH data from the literature were retrospectively reviewed. The association between IgH/MYC rearrangement and clinicopathological features and prognosis in PBLs were analyzed.

Results: The medium age of the patients with PBL was 48 years with the ratio of male to female at 4.15:1. Overall, the IgH/MYC rearrangement rate was 39.4% (41/104). The IgH/MYC rearrangement rate in HIV-positive patients (50.9%, 28/55) was significantly higher than that in HIV-negative patients (26.2%, 11/42) (p=0.014). IgH/MYC rearrangements were more common in EBER-positive (22/44, 50%) than EBER-negative (5/18, 27.8%) PBLs with borderline significance (p=0.109). No significant association was found between IgH/MYC rearrangement and other clinicopathological parameters, including age, gender, Annarbor Stage and primary tumor location. Patients with IgH/MYC rearrangement had inferior median survival (9.38 months. Vs 17.76 months, p=0.061) and 2-year OS (17% vs 37%, p=0.094). In subgroup analysis, IgH/MYC rearrangement was related to inferior OS with statistical significance (p=0.019) in HIV-positive patients. In contrast, IgH/MYC rearrangement was not significantly associated with the outcome in HIV-negative patients (p=0.499). In addition, IgH/MYC rearrangement correlated with significantly inferior OS in EBER-negative PBL (p=0.013), and was related to poorer OS in EBER-positive PBL, but the difference was not statistically significant (p=0.321).

	MYC/IgH Rearangement		
Characteristics	**Negative** **n (%)**	**Positive** **n (%)**	**p-value**
Patients	63（60.6%）	41（39.4%）	
Age			
≤48	26 (52.0%)	24 (48.0%)	0.115
>48	35 (67.3%)	17(32.7%)	
Gender			
Male	52 (62.7%)	31(37.3%)	0.299
Female	10 (50.0%)	10 (50.0%)	
Annarbor Stage			
Ⅰ/Ⅱ	11(73.3%)	4(26.7%)	0.256
Ⅲ/Ⅳ	8（53.3%）	7（46.7%）	
HIV			
Negative	31 (73.8%)	11(26.2%)	**0.014**
Positive	27 (49.1%)	28 (50.9%)	
EBER			
Negative	13 (72.2%)	5 (27.8%)	0.109
Positive	22 (50.0%)	22 (50.0%)	
Location			
Nodal	14(73.7%)	5 (26.3%)	0.196
Extranodal	49 (57.6%)	36 (42.4%)	
Surviaval (mo)			
Median (Range)	17.76 (0.5-105)	9.38 (0.3-94)	0.061

Figure 1 - 1306

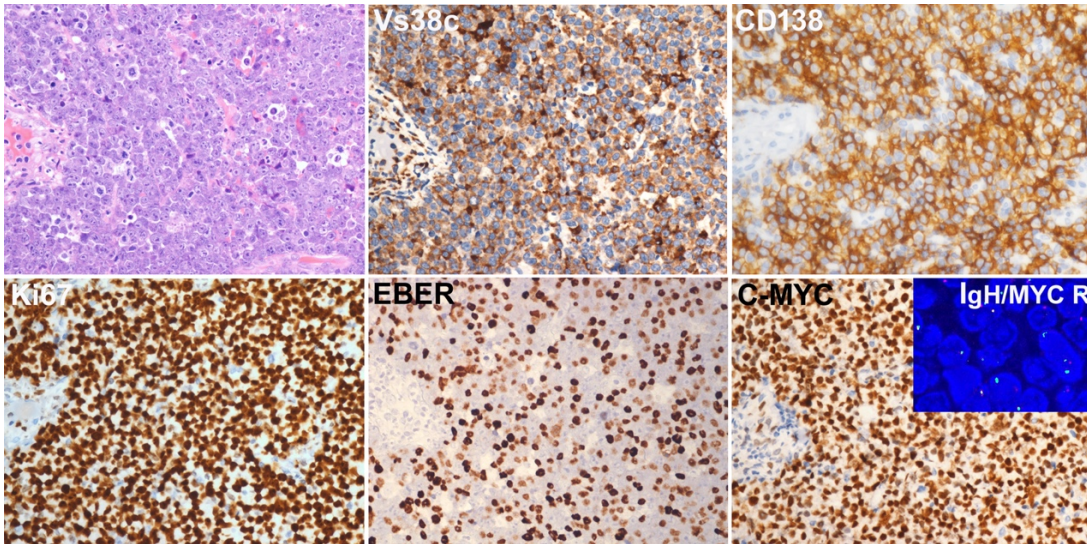

Figure 2 - 1306

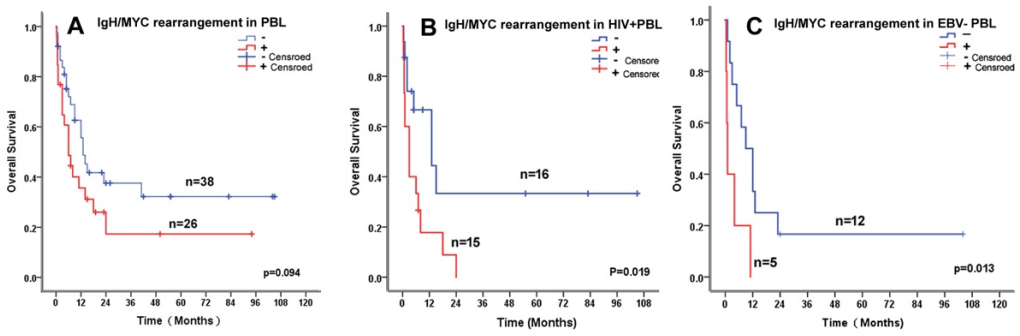

Conclusions: IgH/MYC rearrangements are frequently identified in PBLs, more common in HIV-positive cases and EBV-positive cases. In addition, IgH/MYC rearrangements related to poor outcome, and is an inferior prognostic marker in HIV-positive and EBER-negative PBLs

1307 De Novo Testicular Extranodal NK/T-cell Lymphoma: A Clinicopathologic Study of 21 Cases with Review of Additional 18 Cases in the Literature

Yuhua Huang[1], Xiao-Ge Zhou[2], Xiaolan Shi[3], Peng Zhong[4], Jingping Yun[1]
[1]Sun Yat-sen University Cancer Center, Guangzhou, China, [2]Beijing Friendship Hospital Capital Medical University, Beijing, China, [3]Liaocheng Second People's Hospital, Liaocheng, China, [4]Daping Hospital and Research Institute of Surgery, The Third Military Medical University, Chongqing, China

Disclosures: Yuhua Huang: None; Xiaolan Shi: None; Peng Zhong: None; Jingping Yun: None

Background: Although the testis is not uncommonly involved during the course of disease in both nasal and non-nasal extranodal NK/T cell lymphoma (ENKTCL), only several cases presenting initially with a testicular mass have been previously reported, which are mostly documented as case reports rather than as study series. Due to its rarity, the clinicopathologic features and the prognosis of de novo testicular ENKTCL have not been well-characterized.

Design: Clinicopathologic features of 21 cases of de novo testicular ENKTCL from three institutions, China, were retrospectively analyzed with review of additional 18 cases from the literature.

Results: Most (31/33, 93.9%) of de novo testicular ENKTCL occurred in Asian. The median age was 45 years (rang from 21 to 79 years). All patients (37/37) initially presented with testicular swelling and most patients (33/36, 91.75%) had unilateral testicular masses. Approximately 70% (21/29) of the patients presented at Ann Arbor Stage I/II. Expression of CD56 was found in 86.8% (33/38) of available cases. Interestingly, aberrant expression of CD20 was found in the tumor cells in 10.3% (4/39) of cases. Of the 30 patients with survival data, the median follow-up was 6 months (range, 0.5 to 87 months). Majority of patient (23/28, 82.1%) had subsequent extra-testicular involvement, included lymph node (8/28), skin (7/28), adrenal gland (5/28), bone marrow (5/28), spleen (5/28) and CNS (2/28); and approximately 70% (22/30) of patients died of disease during the follow-up period. The 2-year OS of the patients with de novo testicular ENKTCL was 23%, and the median survival was 9.5 months. Patients presented with B symptom was related to inferior OS with borderline significance (p=0.095). No statistical significance was found between patients with Stage I/II and Stage III/IV(p=0.783).

De novo testicular ENKTCL tends to disseminate early and should be recognized as a highly aggressive form of ENKTCL. A portion of cases show aberrant expression of CD20, accurate diagnosis, timely and optimal treatment for patients with this disease is highly important.

Figure 1 - 1307

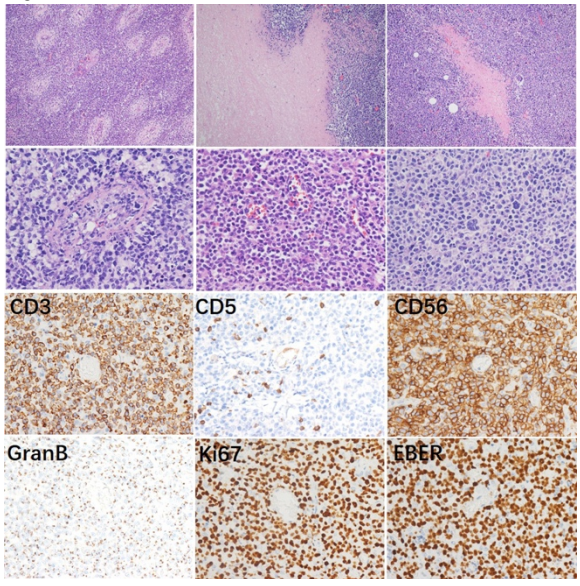

Conclusions: De novo testicular ENKTCL tends to disseminate early and should be recognized as a highly aggressive form of ENKTCL. A portion of cases show aberrant expression of CD20, accurate diagnosis, timely and optimal treatment for patients with this disease is highly important.

1308 Histopathologic and Machine Deep Learning Criteria to Predict Lymphoma Transformation in Bone Marrow Biopsies

Lina Irshaid[1], Ethan Weinberger[2], James Garritano[2], Jonathan Patsenker[2], Yuval Kluger[2], Sam Katz[2], Mina Xu[3]
[1]Yale New Haven Hospital, New Haven, CT, [2]Yale University School of Medicine, New Haven, CT, [3]New Haven, CT

Disclosures: Lina Irshaid: None; Ethan Weinberger: None; James Garritano: None; Jonathan Patsenker: None; Yuval Kluger: *Consultant*, Alexion Pharmaceuticals; *Consultant*, Genentech/Roche; *Consultant*, Corvus Pharmaceuticals; *Consultant*, Nektar/Biodesix/Pfizer/Celldex/Iovance Biotherapeutics; *Grant or Research Support*, Merck/Bristol-Myers Squibb/Apexigen; Sam Katz: None; Mina Xu: None

Background: Large cell transformation (LCT) of B-cell lymphomas such as Follicular Lymphoma (FL) occurs in 3% of patients per year, signals worse prognosis and portends more aggressive chemotherapy. In lymph node biopsies transformation is based on presence of diffuse large cell proliferation. However, even though there are no standardized criteria for LCT in bone marrow (BM), it is frequently obtained due to relative ease of procedure, low cost and low morbidity. This study uses histologic analysis and machine-learning to determine the most predictive features of LCT in BM.

Design: BM biopsies of FL patients in which LCT was clinically questioned were stratified by final clinical decision and lymph node biopsy findings. Two pathologists blinded to outcome independently scored biopsies for percent involvement, large cells, highly atypical cells, irregular lymphoid aggregates, distinct nucleoli, chromatin pattern, fibrosis and proliferation. Whole-slide Aperio scans annotated into patches with QuPath were used to train a ResNet-50 model to discriminate between small and large tumor cells and analyzed by a deep learning algorithm (Figure 1). Pathology and machine learning results were correlated with final clinical transformation outcomes.

Results: BM microscopy was predictive of clinical transformation in 86% (18/21) of cases. Four histologic features were significantly associated with clinical transformation: proportion of large cells (p=0.019), chromatin pattern (p=0.019), distinct nucleoli (p=0.0053) and proliferation index (p=0.011). The most predicitive feature was distinct nucleoli. Proportion of large cells had a correlation of 0.64 between pathologist and machine-derived estimates. Compared to pathologist-derived estimates, machine-generated quantification displayed better reproducibility and stronger correlation with final outcome data (Figure 2). Combining machine-generated values for proportion of large cells with other pathologist-derived features improved the overall prediction of transformation (ROC-AUC 0.80 vs. 0.74).

Figure 1 - 1308

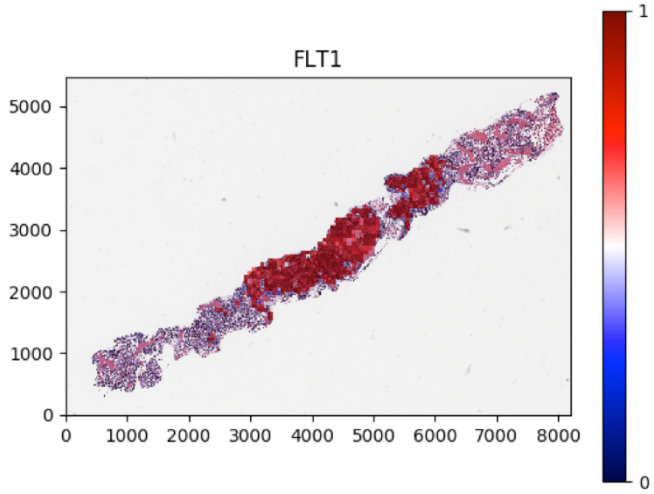

Figure 1. Annotated whole slide image of Follicular Lymphoma transformed to Diffuse Large B-cell Lymphoma used to train a machine-model to differentiate large lymphoma cells.

Figure 2 - 1308

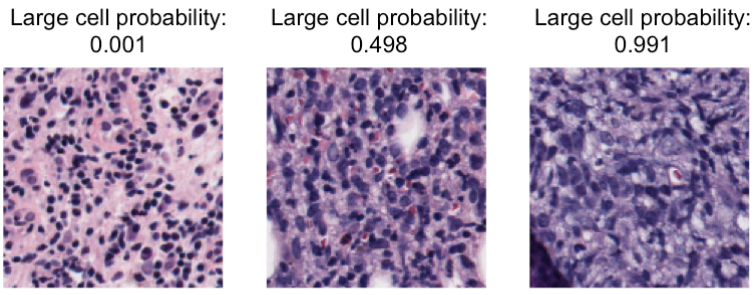

Figure 2. Patches extracted from annotated tumor regions displaying machine generated quantification of large lymphoma cells.

Conclusions: Using routine morphologic examination, proportion of large lymphoma cells, chromatin pattern, distinct nucleoli and proliferation index significantly correlated with LCT. Machine generated quantification of proportion of large lymphoma cells shows strong reproducibility and correlation with final outcome data. Augmenting pathologist estimates with machine systems may further enhance diagnostic accuracy.

1309 Rationale and Feasibility of Using a Standardized Screening Tube on the FACSCanto II and the FACSLyric

Ryan Jackson[1], Jean Oak[2], Jason Kurzer[3]
[1]Stanford University, Redwood City, CA, [2]Stanford University, Stanford, CA, [3]Stanford University School of Medicine, Mountain View, CA

Disclosures: Ryan Jackson: None; Jean Oak: None; Jason Kurzer: None

Background: Flow cytometric immunophenotyping is a powerful diagnostic tool for hematolymphoid disorders, but high reagent and labor costs limit the use of a full panel as a screen. In this study we evaluated the performance of standardized hematolymphoid screening assays on the FACSLyric versus FACSCanto II and investigated the difference in reagent utilization between the screening assay and a full immunophenotypic antibody panel.

Design: All samples were stained with an 8-color, 12-antigen screen, consisting of CD8+, Lambda, CD56+, Kappa, CD5, CD19+, TCRgd, CD3, CD38, CD20+, CD4, and CD45. B-cell lymphoma cases were additionally stained with CD23, CD10, CD79b, CD19, CD200, CD43, CD20, and CD45. Each sample was run on the BD FACSCanto II and BD FACSLyric. Data was compared to the results of a retrospective institutional review of 4-8 color panel data.

Results: Retrospective analysis reveals that 212 of 624 cases show no immunophenotypic aberrancies, with 45% of tissue biopsies and 42% of bone marrow biopsies without a prior diagnosis being negative. Prospective analysis with the screening tube on 31 specimens reveals an aberrant population in all positive cases (N = 22), with 100% agreement between FACSLyric and FACSCanto II. Use of a screening tube reduces the number of antigens evaluated for negative cases (19 to 12) while expanding the number of antigens evaluated in B cell lymphomas (10 to 11).

Conclusions: Use of a screening tube allows for cost and time savings. Adjusting target MFI values and using a standardized method during instrument setup on the FACSLyric generates equivalent results from the FACSCanto. Additionally, given that the FACSLyric has 10-color tubes and our institution serves a significant population of patients with CD10+ B-cell lymphomas or B-cell acute lymphoblastic leukemias, we adopted a drop-in system in which CD10 and CD34 are added to the 8-color tubes. We have found that the addition of these markers increases our ability to detect these disease entities without affecting the performance of the backbone panel.

1310 Anti-Zonadhesin Reactivity in Normal Splenic Sinus Lining Cells and Littoral Cell Angiomas

Nicholas Jaeger[1], Kenneth Tung[2], Daniel Hardy[3], Dennis O'Malley[4], Liang Cheng[5], Nadine Aguilera[6]
[1]University of Virginia Health System, Charlottesville, VA, [2]University of Virginia, Charlottesville, VA, [3]Texas Tech University Health Science Center, Lubbock, TX, [4]O'Malley Medical Consulting, Dana Point, CA, [5]Indiana University School of Medicine, Indianapolis, IN, [6]University of Virginia Health System, Fredericksburg, VA

Disclosures: Nicholas Jaeger: None; Kenneth Tung: None; Daniel Hardy: None; Dennis O'Malley: None; Liang Cheng: None; Nadine Aguilera: None

Background: Littoral cell angioma (LCA) is a rare splenic tumor in which the exact nature of the lining cells is uncertain. The lining cells in LCA have morphologic and immunohistochemical properties which overlap dendritic, histiocytic and endothelial origins. LCA has two cell types: flat lining cells with endothelial differentiation occurring against the basement membrane and tall lining cells with histiocyte-like differentiation. Zonadhesin (ZAN), a large sperm antigen involved in zona pellucida adhesionis, is a mosaic polypeptide that contains multiple von Willebrand D (vWD) cell adhesion domains. The third vWD domain in mice is composed of 20 partial domains, identified as D3p1 to D3p20. An antigen affinity-purified antibody to the D3p18 domain of mouse ZAN, used in a tissue microarray, identified human spleen sinuses as positive. Because LCA lining cells have some similarities to normal splenic sinuses, we attempted staining LCA with anti-D3p18 of ZAN (anti-ZAN).

Design: Thirteen cases of LCA were identified with blocks from 3 institutions and were histologically confirmed on H&E stained slides. Seven benign spleen were used for controls. Immunohistochemistry (IHC) for ERG and anti-ZAN was performed on the LCA and control cases. The staining profile of anti-ZAN was compared to ERG on the LCA and controls.

Results: The benign spleen controls demonstrated ERG nuclear staining of the sinus lining cells and anti-ZAN exhibited perinuclear cytoplasmic staining as well as basement membrane staining in all cases (6/6). In the LCA cases (Table 1), anti-ZAN IHC stains the cytoplasm in both the flat and tall lining cells in all 13 cases (4 had weak or focal positivity). The anti-ZAN IHC strongly stains the basement membranes of the sinuses in all 13 cases. ERG IHC stains the nuclei of the flat lining cells in all 13 cases (3 had weak or focal positivity), but does not stain the tall lining cells (focally positive in 1/13).

Table 1: Staining profile based on cell subtype present in littoral cell angiomas. This demonstrates that while the anti-ZAN and ERG IHC have similar staining profiles for the flat lining or basal cells of littoral cell angiomas, the anti-ZAN also stains the tall lining cells with histiocyte-like differentiation while ERG does not stain these cells.

	Flat Lining or Basal Cells (n=13)			Tall Lining or Histiocyte-like Cells (n=13)		
	Pos.	Weak & Focal	Neg.	Pos.	Weak & Focal	Neg.
Anti-ZAN	9	4	0	9	4	0
ERG	10	3	0	0	1	12

Conclusions: Littoral cell angiomas are rare splenic tumors that exhibit two types of lining cells with differing histologic and IHC features. Normal splenic sinus lining cells display similar features to the flat lining cells with endothelial differentiation of LCAs as demonstrated by the common ERG staining profile. The histiocyte-like cells of LCAs do not stain with ERG. Anti-ZAN targets both lining cell types in LCAs as well as normal sinus lining cells. Further study is necessary to determine the target of anti-ZAN in both the normal splenic sinuses and LCA lining cells.

1311 Clonal Cytopenia of Unknown Significance with Dysplasia (CCUS-D) More Closely Resembles MDS than does CCUS with No Dysplasia (CCUS-ND)

Audrey Jajosky[1], Navid Sadri[2], Kwadwo Oduro[3], Howard Meyerson[4], Ashwin Kelkar[5], Brynn FitzGerald[6], Benjamin Tomlinson[3], Erika Moore[3], Rose Beck[7]
[1]Case Western Reserve University/University Hospitals Cleveland Medical Center, Cleveland, OH, [2]Cleveland, OH, [3]University Hospitals Cleveland Medical Center, Cleveland, OH, [4]University Hospital Case Medical Center, Cleveland, OH, [5]Case Western Reserve University, Cleveland, OH, [6]Case Western Reserve University, Cleveland Heights, OH, [7]University Hospitals Cleveland Medical Center, Case Western Reserve University, Cleveland, OH

Disclosures: Audrey Jajosky: None; Kwadwo Oduro: None; Howard Meyerson: None; Ashwin Kelkar: None; Brynn FitzGerald: None; Benjamin Tomlinson: None; Erika Moore: None; Rose Beck: None

Background: Clonal cytopenia of unknown significance (CCUS) is an age-related disorder that shares features with myelodysplastic syndrome (MDS) but does not fulfill MDS diagnostic criteria. The clinical, histologic, and molecular traits of CCUS patients (pts) at greatest risk for developing MDS are not well established. We noted minimal (non-diagnostic) dysplasia was present in some CCUS pts. Therefore, we compared the clinical, pathologic, and molecular features of CCUS pts with dysplasia (CCUS-D) to CCUS pts with no dysplasia (CCUS-ND).

Design: To identify CCUS pts, we reviewed 140 bone marrow biopsies (BM bxs) with molecular testing performed over an 18-month period for persistent cytopenia(s). CBC's were recorded at the time of BM bx. Ion-semiconductor next generation sequencing was used to detect single nucleotide variants and small indels within the targeted hotspots of 30 myeloid-related genes. CCUS was defined by at least 1 unexplained cytopenia(s) and at least 1 MDS-associated mutation(s) (mt), per the 2018 NCCN guidelines, with a variant allele frequency (VAF) >2% or a clonal karyotypic abnormality in >2 metaphases. Pts with defined myeloid neoplasms were excluded. Trilineage cells were counted in BM smears, and CCUS-D was defined as >2% to <10% erythroid precursors with nuclear irregularities, >5% to <10% atypical granulocytes, or >10% atypical megakaryocytes. Granulocytes, monocytes, and blasts were examined for immunophenotypic abnormalities by FC (flow cytometry). BM histology and FC were reviewed by at least 2 pathologists. Statistical analysis was performed using Welch's *t*-tests.

Results: We identified 38 CCUS pts: 37 with myeloid mts and 1 with an abnormal karyotype. By morphology, 22 pts met criteria for CCUS-D and 16 pts were classified as CCUS-ND. Compared to CCUS-ND (**Table 1**), CCUS-D more frequently had an absolute neutrophil count <1.8 x 10^9/L (p=0.009), myeloid mts with VAF >10% (p=0.02), non-*TET2*/*DNMT3A*/*TP53* mts with VAF >10% (p=0.0005), and *SRSF2/IDH2/CBL/RUNX1* mts (p=0.01 to 0.02). No statistically significant differences were observed in the degree of anemia or thrombocytopenia, BM cellularity, M:E ratio, or FC findings.

Feature	CCUS-ND (+/total)	CCUS-D (+/total)	P-value
ANC <1.8 x 10^9/L	1/16	8/22	0.009
Platelet <100,000/uL	10/16	9/22	0.900
Hemoglobin <10 g/dL	8/16	10/22	0.704
MCV >100 fL	4/16	10/22	0.099
Hypercellular bone marrow	8/16	15/22	0.209
M:E ratio >1	1/16	3/22	0.227
Immunophenotypic abnormalities by flow cytometry	6/16	10/22	0.100
MDS mutation, VAF >10%	6/16	16/21	0.017
Non-*TET2*/*DNMT3A*/*TP53*mutation, VAF >10%	0/16	9/21	0.0005
SRSF2 mutation	0/16	5/21	0.010
IDH2, *RUNX1*, or *CBL* mutation	0/16	4/21	0.021
>1 MDS mutation	4/16	8/21	0.175

Conclusions: Among CCUS pts, the presence of sub-diagnostic dysplasia is associated with severe neutropenia, myeloid mts with VAF >10%, and non-*TET2*/*DNMT3A*/*TP53* mts, suggesting CCUS-D may represent a more immediate precursor to MDS. Long-term follow-up will indicate whether CCUS-D pts are at increased risk for developing MDS.

1312 CD38 Expression After Daratumumab Is Associated With Interval After Therapy, Bone Marrow Cellularity and Extramedullary Disease

Sarmad Jassim[1], Daniel Boyer[1]
[1]*University of Michigan, Ann Arbor, MI*

Disclosures: Sarmad Jassim: None; Daniel Boyer: None

Background: Daratumumab (Dara) is a monoclonal antibody approved for use in the treatment of multiple myeloma (MM) and targets CD38, a glycoprotein highly expressed on plasma cells (PC). PC surviving Dara are known to have decreased expression of CD38.

Because bright CD38 is a key feature to identify PC in flow cytometric (FC) analysis, we reviewed results from our FC laboratory to assess if plasma cells were accurately identified after Dara. Surprisingly, we found that the intensity of CD38 staining was highly variable after Dara therapy. To understand this phenomenon, we correlated CD38 brightness with interval after last dose, bone marrow (BM) cellularity, %PC in BM, and presence of extramedullary (EM) disease.

Design: Michigan Medicine electronic medical record was reviewed to identify patients receiving Dara and FC testing from 1/15/2015 - 08/15/2018. Dates of Dara dosing and FC testing were compared. FC data were reviewed and CD38 intensity was scored as negative (no higher than background), dim (less than normal PC but brighter than other cells in the specimen) or normal (moderate-to-bright). Biopsy reports corresponding to FC specimens were reviewed for site of biopsy (BM or EM), total cellularity of BM and % involvement by MM.

Results: 29 post-Dara FC specimens were found from 20 patients. 6 specimens were EM and 23 were BM. 13 were negative for CD38, 7 dim and 9 normal. Normal CD38 was associated with longer interval after last dose of Dara (range 35 – 749 d; mean 350 d). Interval after Dara was similar for specimens with dim (range 1 – 146 d; mean 38 d) or negative CD38 (range 1 – 223 d; mean 44 d). Specimens with dim CD38 were associated with EM sites and hypercellular BM. 3/4 BM with dim CD38 were >60% cellular, but only 4/13 BM with negative CD38 were >60% cellular. No EM specimens were CD38 negative. 6 patients had 2 or 3 BM specimens after Dara. CD38 returned to normal in 4 patients but remained negative (-) in 2 patients. 1 that remained (-) only had 69 d follow up, the other BM had a high burden of CD38(-) MM after 223 d, suggesting selection of a CD38(-) clone.

Conclusions: CD38 expression initially becomes dim or negative after Dara but returns to normal over time. Rare cases that remain negative might reflect emergence of a CD38(-) MM population. Decreased but not completely negative CD38 after Dara is associated with EM myeloma or hypercellular BM, suggesting that high burden of disease might interfere with the elimination of CD38+ cells.

1313 Bone Marrow Specimen Positive For Amyloid Not Always AL – Can be AA and ATTR

Sara Javidiparsijani[1], Maria Picken[2]
[1]Loyola University Hospital, Maywood, IL, [2]Loyola University Medical Center, Maywood, IL

Disclosures: Sara Javidiparsijani: None; Maria Picken: None

Background: Bone marrow biopsy is the method of choice for follow up/diagnosis of patients with most hematologic disorders including plasma cell dyscrasia/multiple myeloma, patients with abnormal serum/urine paraproteins and lymphomas. Meanwhile, detection of amyloid in the bone marrow can be the first evidence of concurrent amyloidosis. Majority of the bone marrow reports merely describe the presence or absence of amyloid and do not specify further characterization. We reviewed our Congo red stains in the bone marrow specimens and subcategorized the location of the amyloid deposits and its relation to type of amyloidosis and it's associated conditions.

Design: 775 bone marrow biopsies from1999-2018 were reviewed and 79 cases had positve Congo red in the marrow specimen. Slides from 21 cases (mostly consults) unavailable for review were marked NOS. The cases were subcategorized according to the location and type of amyloid. Clinical/pathological corelation was performed.

Results: 71/79 cases (89%) had AL amyloidosis. Interestingly, there were 2 cases of AA (2.5%) and 1 case (1.2%) of AT/TR amyloidosis. Five patients had insufficient data, including one highly suspicious for wild type ATTR (aka senile amyloidosis).

The M:F is 1.3:1 and the mean is 65 y/o. The% of the plasma cells in the marrow ranged 1-80% with the mean of 13.46%, median 8%.

The presence of **stromal** (ST) amyloid deposits was associated only with patients with AL- amyloidosis (4 cases of ST only, 6 with ST and vessel wall (MVW) and 6 with periosteal soft tissue (POST), MVW and ST involvement)

Non-AL amyloides were deposited in the MVW (2 AA amyloid, 1 ATTR); 1 patient with possible senile amyloidosis shows amyloid deposits in POST; all had poltypic plasma cells.

82% (65/79) of the patient have biopsy proven amyloid deposits in at least 1 other organ and (26/79) 32% has amyloid deposit in abdominal fat.

Table 1 show summary of the data.

Figure 1 - 1313

Table 1: Distribution of different types of amyloids in the marrow and other organs

Location	MVW	Stroma	MVW+ stroma	POST	POST +MVW	POST+ MVV+ST	NOS
Type	AA: 2 AL: 8 ATTR: 1 Amyloid NOS: 1	AA: 0 AL: 4 ATTR:0 Amyloid NOS: 0	AA: 0 AL: 6 ATTR:0 Amyloid NOS: 0	AA: 0 AL: 16 ATTR: 0 Amyloid NOS: 3	AA: 0 AL: 10 ATTR: 0 Amyloid NOS: 1	AA: 0 AL: 6 ATTR: 0 Amyloid NOS: 0	AA: 0 AL: 21 ATTR: 0 Amyloid NOS: 0
Concurrent* Other organ involvement	Abd fat: 4 Kidney: 5 Heart: 3 GI and liver: 2 Other: 3**	Abd fat: 2 Kidney: 1 Heart: 1 GI and liver: 1 Other: 0**	Abd fat: 1 Kidney: 1 Heart: 0 GI and liver: 0 Other: 2**	Abd fat: 7 Kidney: 1 Heart: 1 GI and liver: 1 Other: 3**	Abd fat:2 Kidney: 1 Heart: 1 GI and liver: 0 Other: 2**	Abd fat:3 Kidney: 3 Heart: 1 GI and liver: 2 Other: 0**	Abd fat:7 Kidney: 6 Heart: 1 GI and liver: 3 Other: 2**

* Some patients have more than one organ involvement

** Other organs include lymph nodes, skin, spleen, thyroid, prostate, salivary gland, lung, bone

MVW: marrow vessel wall

ST: marrow stroma

POST: periosteal soft tissue

NOS: not otherwise specified

Figure 2 - 1313

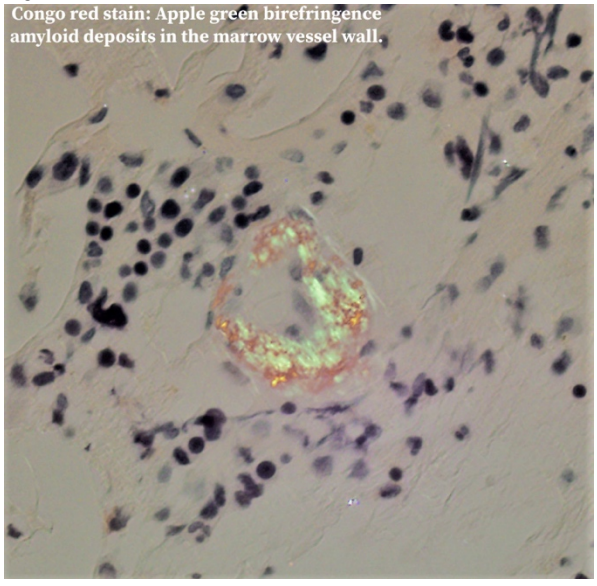

Conclusions: Confirming the nature of amyloidosis is essential in the treatment stragies of systemic amyloidosis. Application of chemotherapy or bone marrow trasplant to a patient with a nonimmunoglobulin form of amyloid would be harmful to the patient. Althugh AL amyloid is the most common type of amyloid in the bone marrow specimen, the pathologist should have high index of suspcioun for non-AL amyloidosis especially if the deposits are present in the MVW or POST. Non- AL amyloidosis may be associated with polytypic and mildly increased percentage of plasma cells, especially in AA amyloidosis.

1314 Experience with 79 Consecutive Congo Red Positive Bone Marrow Biopsy Specimens – Addressing the Definition of Organ Involvement and Reporting

Sara Javidiparsijani[1], Maria Picken[2]
[1]Loyola University Hospital, Maywood, IL, [2]Loyola University Medical Center, Maywood, IL

Disclosures: Sara Javidiparsijani: None; Maria Picken: None

Background: Progress in treatment of systemic amyloidoses has created the need for defining organ specific involvement. Thus not only the presence but also the location and the extent of amyloid deposits in various organs has been included in the definition of organ involvement. The situation with bone marrow (bm) has not been addressed. We reviewed 79 consecutive bone marrow specimens positive for amyloid by Congo red stain.

Design: Seventy nine (79) bm specimens reported as positive for amyloid were retrospectively reviewed and the location of the amyloid deposits were recorded and correlated with amyloid type; in 21 consult cases/slides no longer available for review, the location was marked NOS.

Results: The M:F was 1.3:1, age range 26- 94 years, mean age was 65 years. The % of the plasma cells in the bm ranged from 1%-80%; mean 13.46%, median 8%.

The location of amyloid depositis, divided into 7 sites, shown in table 1, was hetrogenous. Vascular deposits were common (60%) while marrow stroma was involved in only 27% but exclusively extramedullary deposits were seen in 33% of cases. Extramedullary deposits in combination with other bm sites comprised 62%.

71/79 cases (89%) had AL amyloid deposits and among them, 70% had AL-lambda and 30% had AL-kappa. There were 2 cases of AA (2.5%) and 1 case (1.2%) of ATTR amyloidosis; all with exclusively vascular deposits. 5 patients had polyclonal dposits in the bm and insufficient clinical data; including one patient with possible wild type ATTR.

Overall 65/79 patients had amyloid deposits in additional organs.

Figure 1 - 1314

Figure 2 - 1314

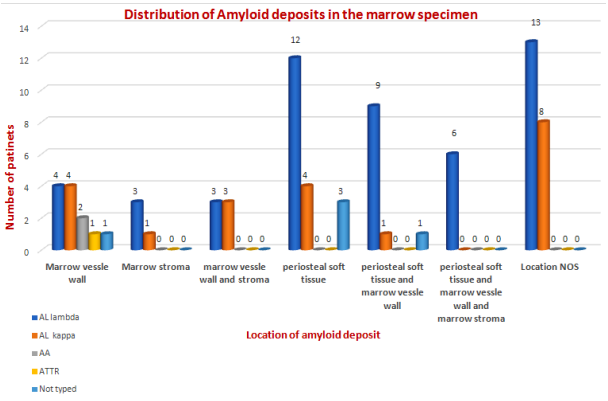

Conclusions: There is significant heterogeneity of amyloid distribution in patients with AL-amyloidosis with extramedullary/periosseous amyloid deposits being more frequent than medullary. These findings raise the need for development of a consensus definition of what constitutes marrow involvement in amyloidosis in general and in AL in particular and how it should be graded and reported.

BM reporting and grading should be limited to vascular and stromal involvement while extramedullary deposits should be reported as soft tissue involvement. Nevertheless, the latter is equally important since it may be helpful in early detection of amyloid, including the non-AL types, and thus obviate the need for invasive biopsies of the target organs.

Despite selection bias (bm biopsies primarily done for diagnosis/staging of plasma cell disorders), our data shows that other types of amylodosis can be present in the bm.

1315 5hmc Expression is an Independent Predictor of Survival in African American Patients with Multiple Myeloma

Rajeswari Jayakumar[1], Rong Xia[1], Qiang Xie[1], Raavi Gupta[1]
[1]SUNY Downstate Medical Center, Brooklyn, NY

Disclosures: Rajeswari Jayakumar: None; Rong Xia: None; Qiang Xie: None; Raavi Gupta: None

Background: Multiple myeloma (MM) is 2-3 times more common in African American (AA) population compared to Caucasians. Alterations in epigenetic pathways are currently being explored for identification of prognostic indicators in high risk patients. Studies show that mutations in epigenetic pathway (TET1, TET2, TET3, IDH1, IDH2, DNMT1, DNMT3A and DNMT3B) are associated with reduced survival in MM patients. Alteration in these genes impair hydroxylation of 5mc to 5hmc causing loss of 5hmc expression in tissues. This loss of 5hmc leads to hypermethylation thus silencing tumor suppressor genes. In this study we studied the prognostic value of 5hmc expression in bone marrow biopsy of AA patients with MM.

Design: Bone marrow biopsies from 46 consecutive cases of MM in AA patients diagnosed between 2002 and 2011 were retrieved. 5hmc immunohistochemistry was performed using rabbit anti-5hmc antibody (Active Motif, Carlsbad, CA, cat # 39769, 1:3000 dilution) and was semi quantitatively measured based on the percentage of stained plasma cells (no staining - 0; 1-10% - 1; 11 – 50% - 2; 51 – 100% - 3). Intensity of staining was graded as weak staining (1+), moderate staining (2+) and strong staining (3+). A final score was obtained by multiplying quantitative score and staining intensity which ranged from 0 to 9. All relevant clinical and laboratory parameters and overall survival data were obtained. Statistical analysis was done using Pearson correlation. Overall survival was analyzed by Kaplan- Meier curves.

Results: Age at diagnosis ranged from 39 to 76 years (Mean=60.5, M:F: 1:1.3). 18 patients were of ISS stage I, 13 were stage II and 10 were stage III at diagnosis. 24 out of 46 cases (52%) had loss of 5hmc expression (score $\leq$ 3). Multivariate analysis showed loss of 5hmc expression correlated significantly with M spike (p=0.025) but not with beta-2 microglobulin, lytic lesions, hypercalcemia, high creatinine or anemia. Patients with 5hmc score >3 had significantly better survival than those with a score of ? 3 irrespective of ISS stage (p=0.032). For all clinical stages, there was a strong trend of poor survival in patients with 5hmc score < 3.

Figure 1 - 1315

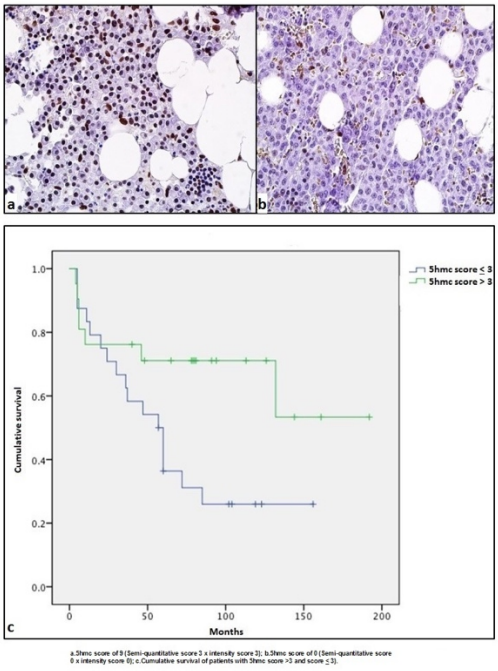

Conclusions: Loss of 5hmc correlated significantly with M-spike and poor survival in AA patients. 5hmc expression can prove to be a valuable tool to stratify risk in patients with MM and use personalized treatment options such as DNMT inhibitors in patients with high risk disease.

1316 Evaluation of CD123 as a Potential Membrane Biomarker for Normal Karyotype Acute Myeloid Leukemia

Gina Jiang[1], Maryam Pourabdollah[2], Eshetu Atenafu[3], Mark Minden[3], Hong Chang[2]
[1]University Health Network, Markham, ON, [2]Toronto, ON, [3]University Health Network, Toronto, ON

Disclosures: Gina Jiang: None; Maryam Pourabdollah: None; Eshetu Atenafu: None; Mark Minden: None; Hong Chang: None

Background: Interleukin-3 receptor α chain (IL-3Rα or CD123) is a type I cytokine receptor encoded in the pseudoautosomal region of allosomes. It is normally expressed on early hematopoietic cells to transmit the signal of interleukin-3 upon forming a heterodimer with IL-3Rß. This activates the JAK/STAT pathway necessary for hematopoiesis, which stimulates proliferation and differentiation while inhibiting apoptosis. Recent evidence suggests CD123 is frequently overexpressed in primitive leukemic stem cells, and lowly expressed by normal myeloid progenitors. Thus, CD123 is an attractive target for immunotherapy, with various antibodies having been synthesized for preclinical and clinical studies. However, there have been few studies investigating the prognostic effects of CD123 expression in normal karyotype AML (NK-AML).

Design: 231 *de novo* adult NK-AML patients from our institution were retrospectively analyzed. Patients with acute promyelocytic leukemia and patients who received transplant were excluded. CD123 expression was correlated to clinical laboratory features, event-free survival (EFS) and overall survival (OS).

Results: CD123 was expressed by cells from 39% of patients; that expression was associated with high white blood cell (WBC) count (>30 x 10^9/L), the co-expression of CD4, CD11b, CD11c, CD33, CD36, and the presence of *FLT3*-ITD and *NPM1* mutation. Univariate analysis showed high expression of CD123 (>72% of blasts) was significantly correlated with shorter EFS and OS (P = 0.013, P = 0.017, respectively). Furthermore, CD123 expression was associated with shorter EFS and OS when combined with CD36 expression (P = 0.0061, P = 0.02, respectively) or lack of CD65 expression (P = 0.038, P = 0.027, respectively). Multivariate analysis with age >60 years, *FLT3*-ITD, *NPM1* mutation, and high expression of CD123 as categorical variables revealed only age >60 years (P < 0.01, P < 0.01, respectively) and *FLT3*-ITD (P < 0.001, P < 0.01, respectively) were independent predictors of shorter EFS and OS. Interestingly, when *FLT3*-ITD was removed as a covariate, CD123 expression was an independent predictor of shorter EFS and OS (P < 0.01, P < 0.01, respectively).

Conclusions: CD123 is frequently overexpressed in NK-AML and high expression confers adverse outcome. However, it is not an independent predictor likely due to its correlation with *FLT3*-ITD.

1317 Lack of CD13 Confers Adverse Prognosis in FLT3-ITD-Negative Normal Karyotype Adult Acute Myeloid Leukemia Regardless of NPM1 Mutation Status

Gina Jiang[1], Maryam Pourabdollah[2], Eshetu Atenafu[3], Mark Minden[3], Hong Chang[2]
[1]University Health Network, Markham, ON, [2]Toronto, ON, [3]University Health Network, Toronto, ON

Disclosures: Gina Jiang: None; Maryam Pourabdollah: None; Eshetu Atenafu: None; Mark Minden: None; Hong Chang: None

Background: *FLT3*-ITD and *NPM1* are routinely tested mutations in normal karyotype AML (NK-AML). *FLT3*-ITD, regardless of *NPM1* status, is identified as a poor prognostic factor, thus, stem cell transplantation is performed when possible. However, the majority of NK-AML cases are *FLT3*-ITD-neg. *NPM1*-mut patients in this group have better prognosis and are treated similarly to those with favorable-risk cytogenetics, whereas *NPM1*-wt patients have an intermediate prognosis with standard intensive therapy. Whether these two subgroups would benefit from transplantation is still unclear and further stratification is necessary.

Design: 430 *de novo* adult NK-AML patients receiving curative intent therapy with known *FLT3*-ITD and *NPM1* status were retrospectively analyzed. Patients were categorized into four groups defined by the two molecular markers: *FLT3*-ITD/*NPM1*-mut, *FLT3*-ITD/*NPM1*-wt, *FLT3*-ITD-neg/*NPM1*-mut, and *FLT3*-ITD-neg/*NPM1*-wt. Survival outcomes were evaluated with event-free survival (EFS) and overall survival (OS).

Results: 27% of diagnostic samples were positive for *FLT3*-ITD and 43% of them subsequently received transplants. Transplant patients were associated with longer EFS and OS, within both the *NPM1*-wt ($P < 0.0001$, $P < 0.001$, respectively) and *NPM1*-mut subgroups ($P < 0.0001$, $P < 0.0001$, respectively). 73% of patients were *FLT3*-ITD-neg and 25% of them received transplants. In keeping with prior reports, transplantated patients with *NPM1*-wt had a significantly longer EFS and OS ($P < 0.0001$, $P < 0.0001$, respectively) when compared to non-transplant *NPM1*-wt patients. 47% of *FLT3*-ITD-neg non-transplant patients expressed CD34 and 13% lacked CD13. On univariate analysis, CD34 expression and lack of CD13 were both significant adverse predictors for EFS ($P = 0.034$, $P = 0.05$ respectively) and OS ($P = 0.033$, $P = 0.019$, respectively). Multivariate analysis adjusting for age (>60 years), *NPM1*-wt, lack of CD13, and CD34 expression as categorical variables revealed that lack of CD13 was an independent predictor for shorter EFS [$P = 0.027$, HR: 1.766 (95% CI:1.068–2.922)] and OS [$P = 0.016$, HR: 1.872 (95% CI:1.122–3.125)].

Conclusions: Transplantation significantly improves outcome in NK-AML patients, except those with *FLT3*-ITD-neg/*NPM1*-mut. We identified lack of CD13 to be an independent adverse predictor in *FLT3*-ITD-neg patients regardless of *NPM1* status. Further prospective studies are required to determine the possible benefit of transplantation for this CD13 negative subpopulation.

1318 Epstein–Barr Virus-positive Diffuse Large B-cell Lymphoma Features Disrupted Antigen Capture/Presentation and Hijacked T-cell Suppression

Xiang Nan Jiang[1], Weige Wang[2], Xiaoqiu Li[3]
[1]Fudan University Shanghai Cancer Center, Shanghai, Shanghai, China, [2]Shanghai, China, [3]Shanghai Cancer Center, Shanghai, China

Disclosures: Xiang Nan Jiang: None; Weige Wang: None; Xiaoqiu Li: None

Background: B-cells can function as antigen presenting cells by presenting antigens captured by the B-cell receptor (BCR) on Class II Major Histocompatibility Complex (MHCII) to T-cells. In addition, B-cells can also maintain immune homeostasis by expressing PD-L1 and suppress T-cell activity. Epstein-Barr virus (EBV) infection can disrupt B-cell function and lead to B-cell malignancies, including diffuse large B-cell lymphoma (DLBCL). Here we show that EBV-positive DLBCL (EBV+ DLBCL) has decreased BCR and MHCII expression, but over-expressed PD-L1, which may lead to immune evasion.

Design: An EBV+ DLBCL cohort (n=30) and an EBV-negative DLBCL control cohort (n=83) were established. Immunostaining of PD-L1, MHCII, MHCII Transactivator (CIITA) and pBTK were performed on automated stainer. H-score was used to denote the results of staining of PD-L1 and pBTK. Break apart and deletion of *CIITA* locus was studied by fluorescent *in situ* hybridization. Surface immunoglobulin mean fluorescent insensitivity (MFI) was detected by flow cytometry to demonstrate the level of BCR.

Results: EBV+ DLBCL showed significantly lower expression of CIITA and MHCII compared to EBV-negative DLBCL. Genetic aberrations involving *CIITA* were also more common in EBV+ DLBCL, with 23% break apart events and 6% deletion events, compared to 2% break apart and 0% deletion in EBV-negative DLBCL. In addition to the loss of antigen presenting molecules, the antigen capturing receptor, BCR, was also down-regulated in EBV+ DLBCL. Accordingly, BCR signaling was also significantly decreased in EBV+ DLBCL as denoted by the respective pBTK levels. Finally, EBV+ DLBCL showed over expression of the T-cell inhibitory ligand, PD-L1.

Conclusions: Antigen capture and presentation system were disrupted, and T-cell inhibitory molecule was hijacked in EBV+ DLBCL, which may contribute to immune escape in this high risk disease. Therapies targeting these aberrations may improve the outcome of patients with EBV+ DLBCL.

1319 Latent Membrane Protein 2A (LMP2A) Mimics B-cell Receptor (BCR) Signaling and Promotes Immune Escape in Epstein-Barr Virus (EBV)-Positive Diffuse Large B-cell Lymphoma (DLBCL)

Xiang Nan Jiang[1], Weige Wang[2], Xiaoqiu Li[3]
[1]Fudan University Shanghai Cancer Center, Shanghai, Shanghai, China, [2]Shanghai, China, [3]Shanghai Cancer Center, Shanghai, China

Disclosures: Xiang Nan Jiang: None; Weige Wang: None; Xiaoqiu Li: None

Background: EBV+ DLBCL is an aggressive malignancy that is largely resistant to current therapeutic regimens. LMP2A is expressed during different latency stages of EBV-infected B cells in which it triggers activation of cytoplasmic protein tyrosine kinases. Early studies have revealed that an immunoreceptor tyrosine-based activation motif in the cytoplasmic N-terminus of LMP2A can trigger a transient increase of the cytosolic Ca^{2+} concentration similar to that observed in activated B cells. Meanwhile, tumor cells often express PD-L1 in EBV+ DLBCL, providing a possible mechanism for immune escape. We thus explored the correlations between LMP2A expression, BCR signaling, and PD-L1 expression in EBV+ DLBCL.

Design: Two cohorts of DLBCL cases, respectively EBV-positive (n=28) and EBV-negative (n=32), were selected. LMP2A, PD-L1 and the BCR signaling-related molecule, phosphorylated form of SYK (pSYK), were immunohistochemically evaluated on formalin-fixed, paraffin-embedded tumor tissues. The expression status of LMP2A, pSYK and BCR were further validated by a flow cytometry analysis using fresh tissues from 3 EBV-positive and 5 EBV-negative DLBCL patients.

Results: The EBV-positive cases, with a median age of 61yrs, were more frequently associated with a high-risk IPI score and a non-GCB phenotype (P=0.029). Compared with EBV-negative ones, patients with EBV-positive tumors showed a worse response to the RCHOP therapy and a shorter median survival (P = 0.041). Twenty-one EBV-positive cases (75 %) expressed LMP2A, whereas none of the EBV-negative cohort expressed this protein. The expression level of pSYK was significantly lower (P = 0.0313) in EBV+ DLBCL cases than those EBV-negative ones, and the pSYK level correlated negatively with LMP2A level (P = 0.119). The expression level of PD-L1 was significantly higher (P = 0.042) in EBV+ DLBCL, which correlated positively with the LMP2A level (P=0.184). Flow cytometry confirmed the LMP2A expression in EBV+ DLBCL, which correlated with a down-regulated BCR and pSYK expression.

Conclusions: EBV+ DLBCL seems to feature an inactive BCR signaling, which may be related to the expression of LMP2A. Besides, LMP2A may function and promote the PD-L1 expression. These findings indicate that targeting immune checkpoints including PD-1/PD-L1 instead of BCR signaling molecules seems to be more reasonable and promising for the treatment of EBV+ DLBCL.

1320 Low-Blast Burden/ Hypoplastic Disease is Prevalent in NCCN Poor-Risk Acute Myeloid Leukemia Group and Has Characteristic Molecular/Genetic and Clinicopathologic Features

Ridas Juskevicius[1], Aaron Shaver[1], Adam Seegmiller[1], Jonathan Douds[2], Emily Mason[1], David Head[1]
[1]Vanderbilt University Medical Center, Nashville, TN, [2]Nashville, TN

Disclosures: Ridas Juskevicius: None; Adam Seegmiller: None; Jonathan Douds: None; Emily Mason: None

Background: The National Comprehensive Cancer Network (NCCN) poor-risk acute myeloid leukemia (AML) group as defined by cytogenetic abnormalities or by the presence of the *FLT3*-ITD mutation is characterized by poor survival overall. However, clinical and pathologic heterogeneity within the group is recognized. Some cases in this group have relatively low blast counts and bone marrow (BM) cellularity, consistent with so called hypocellular AML, which is a rare entity that is variably defined in the literature. In this study we aimed to assess the prevalence and clinicopathologic features of hypoplastic AML as defined not only by BM cellularity but also by blast burden (BB), in the NCCN poor-risk group.

Design: All patients with newly diagnosed AML meeting NCCN criteria for poor-risk disease presenting from 2008 to 2016 were identified. Clinical, demographic and laboratory data were collected. BM morphology to assess for dysplasia was reviewed by a consensus panel of three hematopathologists. BM blast percentage and cellularity were recorded, and BB was calculated (BM blast % x cellularity %). Next-generation sequencing (NGS) with a panel of 37 myeloid-associated genes was performed on all cases. Mutations were classified according to functional status.

Results: Of 100 cases included in the study, 18 patients met criteria for hypoplastic disease, defined as BM cellularity $\leq$40% and BB <20%. These cases showed a remarkably uniform mutational pattern, where receptor/kinase/*RAS* mutations and a subset of transcription mutations (*ETV6, NPM1, PHF6,* and *WT1*) were uniformly absent. *RUNX1* mutations were overrepresented (22% vs 8%), as compared to non-hypoplastic disease. There was no significant difference in the distribution of *TP53* or methylation and splicing mutations. Blast % in this group ranged from 20% to 90% with a distribution similar to non-hypoplastic AML group. There was male predominance (78% M vs 55% M) and the proportion of cases with complex karyotype was higher (67% vs 47%) within the hypoplastic disease as compared to the non-hypoplastic AML.

Conclusions: A novel approach using BM cellularity together with BB identifies distinct subset of hypoplastic AML which represents a significant subset (18%) within the NCCN poor-risk group and has relatively uniform molecular, cytogenetic and clinicopathologic features.

1321 Preliminary Evidence of a Distinctive Secretome of Neoplastic Cells in Breast Implant Associated Anaplastic Large Cell Lymphomas

Marshall Kadin[1], John Morgan[1], Nick Kouttab[1], Haiying Xu[1], William Adams[2], Patricia Mcguire[3], Caroline Glicksman[4], Alan Epstein[5], Mark Clemens[6]

[1]Roger Williams Medical Center, Providence, RI, [2]University of Texas Southwestern Medical Center, Dallas, TX, [3]Barnes Jewish Hospital/Washington University, St. Louis, MO, [4]Hackensack Meridian School of Medicine at Seton Hall, Sea Girt, NJ,[5]LAC + USC Medical Center, Pasadena, CA, [6]The University of Texas MD Anderson Cancer Center, Houston, TX

Disclosures: Marshall Kadin: None; John Morgan: None; Nick Kouttab: None; Haiying Xu: None; William Adams: None; Patricia McGuire: *Consultant*, Allergan; *Primary Investigator*, Establishment Labs; Caroline Glicksman: None; Alan Epstein: None; Mark Clemens: None

Background: Breast implant associated anaplastic large cell lymphoma (BIA-ALCL) is a rare ALK negative CD30+ T cell lymphoma which may develop around breast implants. Most patients present with an accumulation of fluid (so-called seroma) 8-10 years after implantation. We previously reported that elevated CD30 in seroma fluid is a useful screening test for BIA-ALCL. However, the nature of neoplastic cells in BIA-ALCL remains an enigma. To shed light on this enigma we undertook an immunologic analysis of cytokines in supernatants of BIA-ALCL cell cultures and malignant seromas compared to benign seromas.

Design: We analyzed 48 hour supernatants of BIA-ALCL cultures compared to cell-free media and pathologically malignant seromas of 8 patients compared to 9 benign seromas. Fluids were analyzed for 13 cytokines by flow cytometry using the Legendplex™ Human Cytokine Panel 2 (13-plex). Seromas were analyzed undiluted, diluted 1:10 and 1:100; I:10 proved to be most reproducible. Cut-off concentration for elevated cytokine level was 1000pg/ml.

Results: Our analysis reveals that neoplastic cells secrete IL-9, IL-10, IL-13 and/or IL-5 and IFNγ not detected in cell-free culture media nor in non-malignant seromas. IL-6 was elevated in most and IL-21 in few malignant as well as benign seromas, thereby not distinguishing malignant from benign seromas. Interestingly, IL-17A, whose gene transcripts are high in BIA-ALCL (Di Napoli, Mod Path, Aug. 2018) was not detected in malignant or benign seromas. Figure 1 is a heatmap showing high activity (dark green – black - red) for IL-9, IL-10, IL-13 in 8 malignant seromas and cell culture supernatants of BIA-ALCL line TLBR1, but not in 9 pathologically negative seromas. Cytokine detection correlates with concentration of malignant cells as shown for TLBR1 BIA-ALCL cells (bottom 3 rows: 1e4=10^4, 1e5=10^5, 1e6=10^6cells/ml).

Figure 1 - 1321

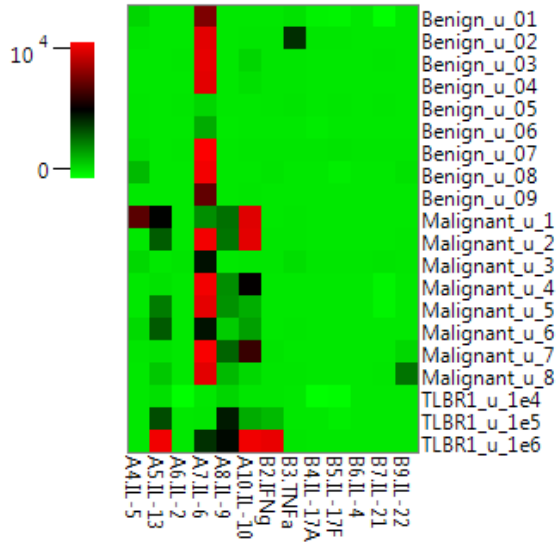

Conclusions: BIA-ALCL cells secrete distinctive cytokines not found in benign seromas. The cytokine profile and reported expression of FoxP3 (Kadin et al, Aesthet Surg J, 2016) suggests the neoplastic cells are derived from functional T cells similar to recently described Th2-like Treg cells (Halim et al., Cell Reports, 2017) in 6 of 8 cases and from Th1 cells in 1. Limitations of our study were the small number of cases and limited number of cytokines analyzed, known overlap and plasticity of T cell subsets. Ongoing studies will expand the number of cases and cytokines analyzed and correlate tumor cell phenotype with pathology and stage of disease.

1322 Unique Immature Flow Cytometric Immunophenotype Masquerading as T-Lymphoblastic Leukemia/Lymphoma Identified in Retrospective Analysis of Thymoma Specimens

Megan Ketcham[1], Lorinda Soma[2], Jonathan Fromm[1]
[1]University of Washington, Seattle, WA, [2]University of Washington Medical Center, Seattle, WA

Disclosures: Megan Ketcham: None; Lorinda Soma: None; Jonathan Fromm: None

Background: Flow cytometry is a useful tool in diagnosing mediastinal masses; however, the differential diagnosis of thymoma versus T-lymphoblastic leukemia/lymphoma (T-ALL/LBL) can be challenging. Classically, thymic tissue contains immature T-cells present at all stages of maturation whereas T-ALL/LBL displays relatively uniform antigen expression. Correlation of a few difficult flow cytometry cases, histologically diagnosed as thymoma (and initially misdiagnosed on flow as abnormal), demonstrated an uncommon T-cell immunophenotypic maturation pattern not significantly described in the clinical flow literature. We also hypothesized the microenvironment of the thymoma/thymus might also support the expansion of hematogones.

Design: A database query was performed for cases from 2004 to 2018 with a histologic diagnosis of thymoma and concurrent 10-color flow cytometric analyses (FCM; n=31) was available. For comparison, FCM of benign thymic tissue (n=9), mediastinal T-ALL/LBL (n=5), and benign lymph node tissue (n=28) cases were also reviewed.

Results: FCM was performed in 31 cases of thymoma with variable WHO histologic type. Three cases of thymoma (9.7%) that were diagnosed as abnormal by FCM demonstrated a unique T-cell maturation immunophenotype having an abundance of CD4/CD8 negative lymphocytes with bright positivity for CD7, dim positivity for CD45, and negativity for surface CD3 (mean, 18.2% of WBC; mean, 2.1% of WBC for other thymoma cases). This population blended into a CD4 positive population (spectrum) that became dual CD4/CD8 positive (figure 1A) and this pattern was present in all 3 (100%) thymoma cases misdiagnosed as T-ALL/LBL but only 3 of 28 (10.7%) flow “normal” thymoma cases (figure 1B). In contrast, none of the benign thymic cases or the cases of T-lymphoblastic leukemia/lymphoma showed this pattern (one T-ALL/LBL showed a discrete CD4/CD8 negative population without the dim/spectrum of CD4, figure 1C). The average percentage of hematogones in cases of thymoma with this unique pattern was increased (1.03%) compared to typical cases of thymoma (0.34%), benign thymic tissue (0.002%), mediastinal T-ALL/LBL (0%), and benign lymph node tissue (0.005%).

Figure 1 - 1322

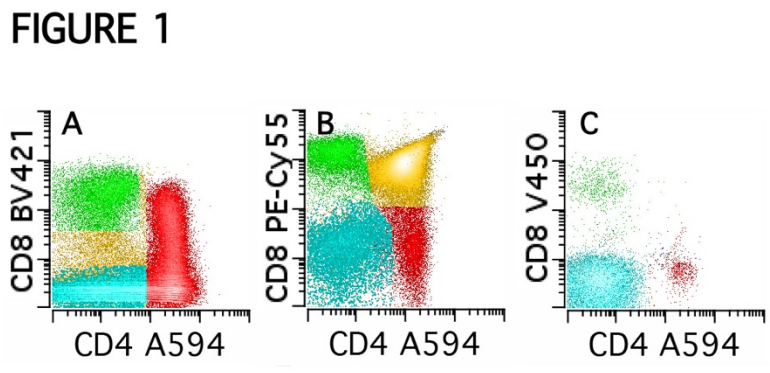

T cell maturation in thymoma and T-ALL/LBL. A) Atypical maturation in thymoma with CD4-/CD8-/CD7^{bright}/CD45^{low} continuous with CD4+ T cells. B) Typical maturation in thymoma with prominent CD4+/CD8+ maturing to mature CD4 and CD8 cells. C) T-ALL/LBL case with prominent CD4-/CD8- population without maturation to mature T cells. CD4-/CD8-/CD7^{bright}/CD45^{low} events in teal.

Conclusions: In conclusion, uncommon T-cell maturation patterns can occur in thymomas and should not be misinterpreted as T-ALL/LBL. As hematogones did not occur in our small number of T-ALL/LBL cases, their presence in mediastinal tissue samples with immature T-cells may strengthen suspicion for a diagnosis of thymoma.

1323 Indolent in situ High-Grade B-cell lymphoma with a MYC Translocation and Mutations Identified by Next Generation Sequencing

Jyoti Kumar[1], Sharon Wu[2], Alexandra Butzmann[3], James Lau[4], James Zehnder[5], Roger Warnke[4], Grant Nybakken[6], Matt Van De Rijn[7], Robert Ohgami[4]
[1]Stanford University, Los Altos, CA, [2]El Camino Hospital, Mountain View, CA, [3]Stanford University, Palo Alto, CA, [4]Stanford University, Stanford, CA, [5]Stanford University School of Medicine, Stanford, CA, [6]Santa Clara, CA, [7]Stanford University Medical Center, Stanford, CA

Disclosures: Jyoti Kumar: None; Sharon Wu: None; Alexandra Butzmann: None; James Lau: None; James Zehnder: None; Roger Warnke: None; Grant Nybakken: None; Matt Van De Rijn: None; Robert Ohgami: None

Background: High-grade B-cell lymphoma (HGBL) is a new group of aggressive, mature B-cell lymphomas. There have been rare documented cases of HGBL limited to the germinal center with preserved follicular architecture and intact mantle zone. However, in such cases, these findings were associated with aggressive lymphoma elsewhere. We report two rare cases of isolated very focal germinal center colonization with HGBL with a MYC rearrangement, similar in morphology to Burkitt lymphoma, in patients without involvement in any other location. These patients have remained without disease after surgical excision alone, and no other treatment.

Design: We identified two cases of focal, in situ involvement by a high-grade B-cell lymphoma with *MYC* gene rearrangement in patients with localized lymphadenopathy and no history of hematolymphoid disease (Table 1). We evaluated the tissue morphology, immunohistochemiscal stains, and FISH results on the lymph node specimens. Targeted next-generation sequencing (NGS) of 281 genes known to be mutated in hematolymphoid diseases of the microdissected HGBL from both patient lymph node samples was performed.

Results: Tissue sections of the lymph nodes revealed predominantly reactive follicular hyperplasia. One focal area, there were follicles that showed absence of mantle zones and loss of internal polarization of the follicles (Fig 1A) with a “starry sky” pattern. High power magnification revealed these cells to be large in size with nuclear membrane irregularities, immature/fine chromatin, and prominent nucleoli. Immunohistochemical stains identified the B-cells within these follicles are diffusely positive for CD20 (Fig 1B), dim BCL2 (Fig 1C), CD10 (Fig 1D), c-myc (Fig 1E) with a very high mitotic rate and Ki67 index >95%. Kappa and lambda protein stains show these nodules are lambda-monotypic (Fig 1F; kappa expression Fig 1G). A *MYC* translocation by FISH (Fig 1H) was seen in this focal area of atypical B-cells. Preliminary analysis of the targeted NGS from both patient lymph node samples revealed rare mutations, including ANKRD11, CSMD3, EZH2, U2AF1, CRLF2 and PCLO.

Table 1

Case	Age	Sex	Site of involvement	Clinical presentation	Treatment	Status (time of follow-up)
1	58 y	M	Right neck lymphadenopathy	Isolated adenopathy	Excision	Alive (1.5 y)
2	68 y	M	Right iliac lymphadenopathy	Incidental adenopathy during hernia repair	Excision	Alive (6 mo)

Figure 1 - 1323

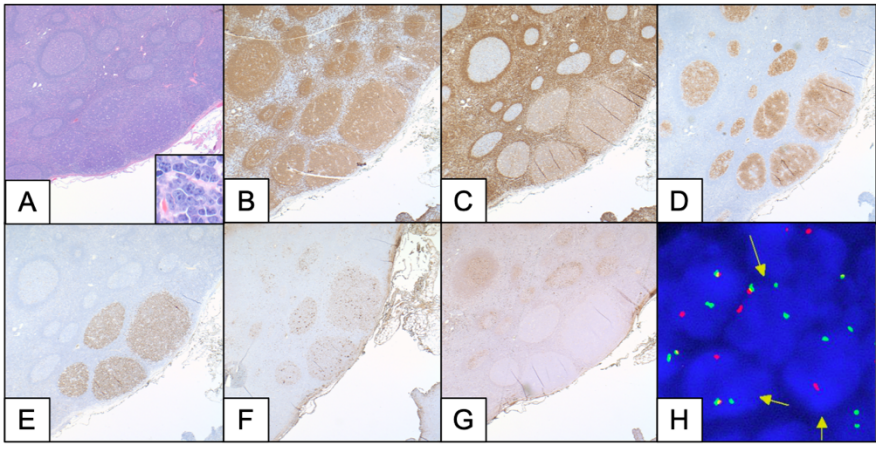

Conclusions: We report the first examples in the literature of "*in situ*" high-grade or Burkitt-like lymphoma, as characterized by the localization of *MYC* gene rearrangement in reactive-appearing germinal centers, in patients that remained without disease after surgical excision alone. Finally, we used targeted NGS to identify mutations in both cases.

1324 Performance of the Lymph2Cx Cell of Origin Classifier of Diffuse Large B-cell Lymphoma in Comparison to Two Immunohistochemical Algorithms

Katrina Lancaster-Shorts[1], Ann Crowley[2], Matthew Lunning[1], Allison Vokoun[3], Ji Yuan[1], Catalina Amador[1], Timothy Greiner[1], Kai Fu[1], Hina Qureishi[1]
[1]University of Nebraska Medical Center, Omaha, NE, [2]Nebraska Medicine, Omaha, NE, [3]Nebraska Medical Center, Omaha, NE

Disclosures: Katrina Lancaster-Shorts: None; Ann Crowley: None; Matthew Lunning: None; Allison Vokoun: None; Ji Yuan: None; Catalina Amador: None; Timothy Greiner: None; Kai Fu: None; Hina Qureishi: None

Background: Diffuse large B-cell lymphoma (DLBCL) is a heterogeneous mature B-cell neoplasm in which the cell of origin (COO) classification has prognostic and therapeutic relevance. DLBCL is divided into germinal center B-cell (GCB), non-GCB also known as activated B-cell (ABC) and intermediate/unclassified (UC) subgroups by mRNA gene expression profiling (GEP). Immunohistochemical (IHC) classification algorithms, such as Hans and Choi, were developed in lieu of GEP, which could not analyze formalin fixed paraffin embedded (FFPE) tissue. The Nanostring Lymph2Cx assay is capable of RNA gene expression profiling on FFPE tissue. Our aim was to determine the concurrence rate amongst the Hans algorithm, Choi algorithm and Lymph2Cx assay.

Design: A retrospective study from January 2017to September 2018 of 75 cases of DLBCL analyzed by the Lymph2Cx assay was performed. 70 cases had sufficient tissue for RNA extraction with a threshold of 60% tumor involvement. IHC was performed on FFPE tissue sections using antibodies for CD10, BCL6, MUM1, GCET1 and FOXP1. The concordance rates between the Lymph2Cx assay and the Hans and Choi algorithms were calculated.

Results: Of the 70 cases analyzed by Lymph2Cx, 36 cases (51%) were classified as GCB, 25 cases (36%) were classified as ABC and 9 cases (13%) were UC. The IHC classification was determined by the Hans algorithm in 70 cases and by the Choi algorithm in 36 cases. The Hans algorithm classified 37 cases (53%) as GCB and 33 cases (47%) as non-GBC. The Choi algorithm classified 14 cases (39%) as GCB and 22 cases (61%) as ABC. After excluding the UC cases by Lymph2Cx assay, 61 cases classified by the Lymph2Cx assay were compared to 61 cases classified by the Hans algorithm and 30 classified by the Choi algorithm. Overall, 54 cases of 61 (89%) classified by the Hans IHC algorithm and Lymph2Cx assay were concordant. 23 cases of 30 (77%) classified by the Choi algorithm and Lymph2Cx assay were concordant.

Conclusions: In our study, the Hans algorithm showed better concordance with the Lymph2Cx assay than the Choi algorithm, 89% and 77% respectively, which contrasts prior literature. Fewer cases studied by Choi algorithm may be a factor. Additionally, our study used whole slide tissue sections, whereas microarrays were used in previous studies. Additional review is needed to expand the IHC evaluation by Choi algorithm in our DLBCL cases and discrepancies in individual cases need to be studied.

1325 CD24 Expression in Follicular Lymphoma: An Alternative B-cell Marker in Therapy Selected, Recurrent Lymphoma

Katrina Lancaster-Shorts[1], Samuel Pirruccello[1]
[1]University of Nebraska Medical Center, Omaha, NE

Disclosures: Katrina Lancaster-Shorts: None; Samuel Pirruccello: None

Background: CD24 Expression was first described on B-cell precursors and was subsequently shown to be expressed on a number of cell types including many epithelial and mesodermal derived tissues. In B-cells, CD24 undergoes significant surface density changes during normal maturation. CD24 expression is bright on B-cell precursors and memory B-cells, dim on naïve B-cells and negative on follicle center B-cells (Figure 1), some splenic derived marginal zone cells and plasma cells. In contrast to the loss of CD24 expression in normal follicles, we had noted that a high percentage of follicle center derived lymphomas retained CD24 expression. The recent use of biologic reagents such as rituximab and CAR-T cells in lymphoma therapy have the potential to select for tumor cells that are negative for both CD19 and CD20. Once selected, these cells will be negative both by flow cytometry and immunohistochemistry. Further, anti-CD22 and anti-CD19 antibodies are also being employed in lymphoma/leukemia treatment and will similarly be associated with selection of antigen-negative tumor cells in some patients. The rapidly expanding use of antigen targeted therapies in B-cell malignancies will require application of additional B-cell-associated antigens in assessment of residual disease.

Design: We reviewed 334 patients with a diagnosis of follicular lymphoma (FL; 228), large cell lymphoma of follicular origin (59) or B-cell lymphoma of follicular origin (47) by flow cytometry from October 2012 to August 2018. Cases without a confirmed tissue diagnosis of FL or diffuse large B-cell lymphoma (DLBCL) were excluded leaving 113 patients with FL, 38 patients with CD10-positive DLBCL and 12 patients with mixed FL/DLBCL. We analyzed the percentage of patients with CD24 positive lymphomas in each of the 3 diagnostic categories.

Results: We found that CD24 expression was retained in 89% of FLs (101/113), 63% (24/38) of DLBCLs and 42% (5/12) of mixed FL/DLBCL. Five cases of CD20 negative FL were CD24 positive. An example of aberrant CD24 expression in FL is shown in Figure 2.

Figure 1 - 1325

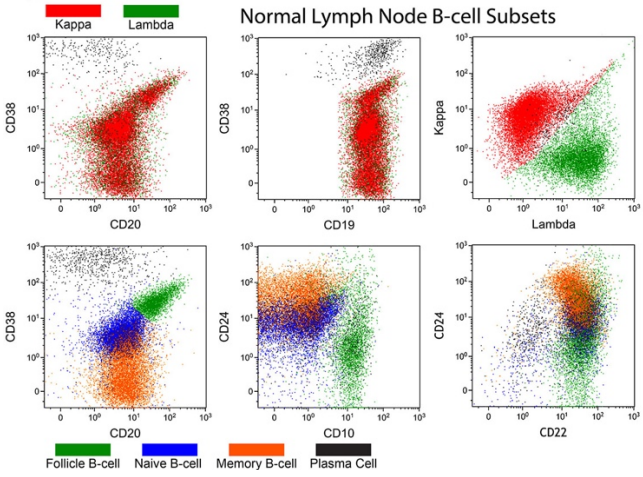

Figure 2 - 1325

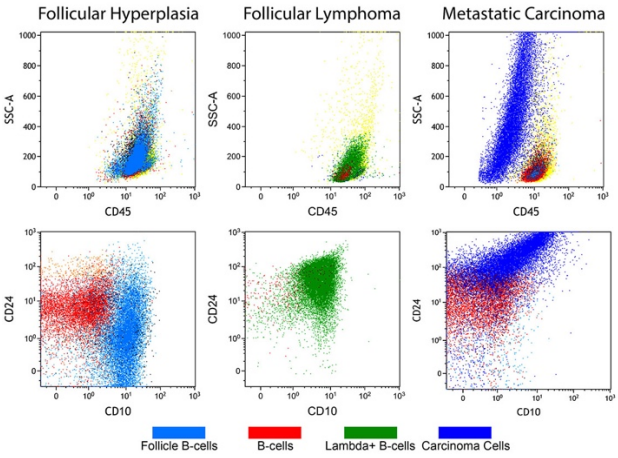

Conclusions: CD24 is aberrantly expressed in 89% of FLs and to a lesser extent in DLBCLs and mixed FL/DLBCLs, 63% and 42% respectively. Our results show the utility of aberrant CD24 expression in the identification of follicular lymphoma by flow cytometry. In the era of therapeutic targeting of B-cell antigens such as, CD19, CD20 and CD22, additional markers will be needed for the identification of disease post-therapy and CD24 is a promising marker.

1326 Patients With Immunoglobulin Amyloidosis and IgM Paraprotein Fall Into Two Distinct Disease Groups

Daniel Larson[1], Surbhi Sidana[1], Shaji Kumar[1], Patricia Greipp[1], Rong He[1], Taxiarchis Kourelis[1], Morie Gertz[1], Ellen Mcphail[1], Surendra Dasari[1], Rebecca King[1]
[1]Mayo Clinic, Rochester, MN

Disclosures: Daniel Larson: None; Surbhi Sidana: None; Shaji Kumar: None; Patricia Greipp: None; Rong He: None; Taxiarchis Kourelis: None; Morie Gertz: None; Ellen Mcphail: None; Surendra Dasari: None; Rebecca King: None

Background: Immunoglobulin (Ig) light chain amyloidosis (AL) is typically associated with abnormal non-IgM paraprotein produced by a clonal plasma cell neoplasm (PCN). However, approximately 5-7% of AL occurs in patients with an IgM paraprotein (IgM AL). IgM AL shows distinct clinical features with different organ predilection than in non-IgM cases. Our study evaluated the pathologic, cytogenetic, and proteomic features of patients with IgM AL.

Design: Patients with AL (2006-15) and IgM paraprotein were identified retrospectively from a clinical database. BM pathology was reviewed and classified based on WHO 2017 criteria. Cases were tested for *MYD88^{L265P}*, *CXCR4^{WHIM}*, FISH for t(11;14), and amyloid subtyping by mass spectrometry (MS) on archived samples.

Results: Of 1128 patients with AL, 75 (6.6%) had an IgM paraprotein (41% kappa/59% lambda). 59/75 had BM pathology material available. After BM review, cases fell into two broad categories: those with a low grade B-cell neoplasm (LGBCN) (68%) (lymphoplasmacytic lymphoma n=24, low grade B-cell lymphoma with plasmacytic differentiation, not further classifiable n=13, and LGBCL other type n=3), and those with a pure PCN (27%) (myeloma n=5, <10% clonal plasma cells (PC) n=11). 3 BM had too few clonal cells to classify. Only LGBCN had extramedullary involvement (8/40, 20%). Median BM involvement by disease was 10% for all cases and differed between the LGBCN (20%) and PCN (5%) groups. PC were positive (or partial positive) for CD19 in 15/17(88%) LGBCN and 2/7(29%) PCN, p<0.003, and for CD45 in 11/17(65%) LGBCN and 2/6(33%) PCN, p=0.2. *MYD88^{L265P}* was present in 21/25(84%) LGBCN and 0/13 PCN, p<0.0001. *CXCR4^{WHIM}* was present in 5/20(25%) LGBCN cases and 0 PCN, p=0.05. FISH for t(11;14) was positive in 10/12(83%) PCN and 0 LGBCN, p <0.0001. Amyloid was present in 45/59 BM biopsies; the remainder had amyloid in fat aspirate (n=10) or other tissue (n=4). MS showed AL-type amyloid in 14/20 cases and ALH (kappa or lambda light chain and mu heavy chain) amyloid in 8/20. ALH amyloid was identified in 7/15 (47%) LGBCL and 1/5 (20%) PCN, p=0.32. In the entire cohort, patients with LGBCN type IgM AL had inferior overall survival (OS) compared with PCN type IgM AL, 21 vs. 82 months, p=0.01.

Conclusions: Patients with IgM paraproteins and Ig amyloidosis fall into two distinct disease groups based on BM pathology: PCN and LGBCN. These groups show overall low-levels of BM involvement and have distinct molecular, cytogenetic and proteomic features as well as different OS.

1327 An analysis of mediastinal B cell lymphomas identifies metachronous occurrence of classic Hodgkin lymphoma (CHL), primary mediastinal large B-cell lymphoma (PMBL), and mediastinal gray-zone lymphoma (MGZL)

Lhara Lezama[1], Vivek Charu[2], Matthew Koo[3], Yaso Natkunam[4]
[1]San Mateo, CA, [2]Palo Alto, CA, [3]Stanford Pathology, Stanford, CA, [4]Stanford University Medical Center, Stanford, CA

Disclosures: Lhara Lezama: None; Vivek Charu: None; Matthew Koo: None; Yaso Natkunam: None

Background: Mediastinal B cell lymphomas include CHL, PMBL, and B-cell lymphoma, unclassifiable, with features intermediate between CHL and DLBCL, also known as MGZL. They are hypothesized to form a biological continuum. We provide a single institution experience of a comparative analysis of these three entities, including cases with different diagnoses at initial presentation and at relapse.

Design: A search of the pathology database yielded 154 cases (72 PMBL, 20 MGZL and 62 CHL) diagnosed since 2012. Clinicopathologic data including age, sex, immunohistochemistry (IHC), and cytogenetics were analyzed. Cases with prior or subsequent diagnoses different from the original were further studied.

Results: The median age at diagnosis and the female to male ratio were similar across the 3 groups. IHC highlighted similarities; specifically, CD30 and PAX5 expression was positive in > 90% of cases in each group and showed variability in intensity and proportion of positive cells. CD45 was lacking in almost all CHL (1/25), positive in all PMBL (27/27), and positive in 4 of 11 MGZL (4/11). CD15 was positive in similar proportions of CHL and MGZL (72%), but in only 5% of PMBL. CD20 was positive in a subset of CHL (7/57), almost all PMBL (70/71), and was less frequent in MGZL (15/19). EBV (EBER) was detected in < 25% of CHL and MGZL, and <5% of PMBL. FISH studies for MYC, BCL2 and BCL6 were negative in all cases. Most interestingly, our results showed 5 cases of MGZL that had diagnosis of CHL within 6 to 8 months prior to the MGZL diagnosis, one case of MGZL that had prior diagnosis of PMBL and one case of PMBL that had prior diagnosis of CHL. In these cases, IHC for CD79a and CD23 were particularly helpful in identifying a PMBL-like morphology.

Table 1 Clinicopathologic features of mediastinal B cell lymphomas

	CHL (N=62)	*PMBL (N=72)*	*MGZL (N=20)*
Age range	6-75	16-79	20-78
Median age	33	34	35
Male: female ratio	1:1	1:1.6	1.2:1
CD30	62/62 (100%)	67/70 (94.3%)	19/19 (100%)
PAX5	58/60 (96.7%)*	48/48 (100%)	20/20 (100%)
CD45	1/25 (4%)	27/27 (100%)	4/11 (36.4%)
CD15	43/60 (71.7%)	2/42 (4.8%)	13/18 (72.7%)
CD20	7/57 (12.3%)	70/71 (98.6%)	15/19 (78.9%)
EBER	8/38 (21.1%)	2/43 (4.6%)	3/15 (20%)
FISH MYC		0/23	0/6
FISH BCL2		0/22	0/4
FISH BCL6		0/22	0/4
History of CHL		1/72	5/20
History of PMBL			1/20

CHL classic Hodgkin lymphoma, MGZL mediastinal gray-zone lymphoma, PMBL primary mediastinal B cell lymphoma, EBER Epstein–Barr virus-encoded small RNAs, FISH fluorescence in situ hybridization

* the majority of cases showed dim expression

Conclusions: A comparative analysis of mediastinal B cell lymphomas is critical to define a possible biological continuum. Our results show high degree of overlap in clinicopathologic features and lack of specific genetic markers to aide in their separation. Additionally, our study highlighted CD45, CD20, CD15, CD79a and CD23 as helpful diagnostic tools. Importantly, we identified the existence of metachronous disease in 7 patients where the criteria for diagnosis at initial presentation and relapse were met, although they were different diagnoses. These findings provide evidence of a true biological continuum among mediastinal B-cell lymphomas and warrant further investigation to interrogate the underlying genetic events and clinical impact.

1328 Cuplike Nuclear Morphology in Pediatric B-cell Acute Lymphoblastic Leukemia is Highly Associated with IKZF1 Deletion

Weijie Li[1], Linda Cooley[1], Keith August[1], Aida Richardson[2]
[1]Children's Mercy Hospital, Kansas City, MO, [2]University of Utah/ARUP Laboratories, Salt Lake City, UT

Disclosures: Weijie Li: None; Linda Cooley: None; Keith August: None

Background: Cuplike nuclear morphologic feature (CLN) has been recognized as a distinctive morphologic finding seen in approximately 20% of acute myeloid leukemia (AML) cases. Its presence in AML is associated with a normal karyotype and the mutations of *FLT3* and/or *NPM1*genes. Its presence in acute lymphoblastic leukemia (ALL) has only rarely been reported in single case studies. Its incidence and possible association with certain ALL subtype are not known.

Design: We retrospectively reviewed 425 B-cell ALL (B-ALL) cases diagnosed in our institute over a 20-year period. Two pathologists reviewed the diagnostic peripheral blood and/or bone marrow smears separately and counted 500 blasts. The nuclei with invagination >25% of the nuclear area were considered as CLN. The findings of chromosome, fluorescence in situ hybridization (FISH) and SNP+CN microarray analyses in CLN+ B-ALL groups were compared with those of a control B-ALL group without CLN. The control group includes all the recent CLN negative B-ALL cases with results of microarray analysis and/or FISH analysis for *IKZF1*. Clinical and biological information of the cases in different groups were also compared.

Results: We identified 5 (1.2%) CLN+ B-ALL cases based on the criterion (>10% blasts with CLN) used for AML. We also identified 36 (8.5%) CLN+ B-ALL cases using cutoff >2% CLN+ blasts. Compared with the control group (69 cases), CLN+ B-ALL groups (>10% and >2%) showed significantly higher incidences of *IKZF1* deletions (100% and 76.7% vs 11.6%, $p<0.001$), detected by FISH and/or DNA microarray. Also, CLN+ B-ALL cases were more likely to have a normal karyotype (40% and 27.8% vs 10.1%, $p<0.05$). Favorable cytogenetic abnormalities including hyperdiploidy and *ETV6/RUNX1* fusion were less commonly seen in CLN+ B-ALL cases (0% and 19.4% vs 56.5%, $p<0.05$). There were no significant differences in age, gender, or diagnostic white blood cell count.

Conclusions: Our study shows that CLN is an uncommon finding in B-ALL. It is more common in B-ALL cases with a normal karyotype, and less common in those cases found to have hyperdiploidy or an *ETV6/RUNX1* fusion. More interestingly, the presence of CLN in B-ALL is highly associated with *IKZF1* deletion. To our knowledge, this is the first time this association has been reported. *IKZF1* deletion is seen in 10-15% of all pediatric B- ALL cases and is associated with a worse prognosis. Recognizing CLN may help predict the prognosis of B-ALL in patients, and may be especially useful when no cytogenetic results are available. Furt

1329 Development of an RNA In Situ Hybridization Method for the Detection of CXCL13 mRNA in AILT and Other Lymphomas

Na Li[1], Quan Zhou[2], Zhifu Zhang[1], Courtney Anderson[1], Xiao-Jun Ma[1], Robert Monroe[1]
[1]Advanced Cell Diagnostics, Newark, CA, [2]Beijing Shijitan Hospital, Capital Medical University, Beijing, China

Disclosures: Courtney Anderson: *Employee*, Advanced Cell Diagnostics, Inc; Xiao-Jun Ma: None; Robert Monroe: *Employee*, Bio-Techne

Background: Angioimmunoblastic T-cell lymphoma (AITL) is a subtype of peripheral T cell lymphoma (PTCL) within the subcategory of nodal T cell lymphomas with T follicular helper (TFH) phenotype. The differential diagnosis of AITL is complex owing to its polymorphous composition and includes benign entities as well as malignancies. CXCL13 is a chemokine that controls the organization of B cells within follicles; when expressed in T lymphocytes, the biomarker reflects a germinal center origin of the T cell (TFH phenotype). CXCL13 is one of the most useful markers in the diagnosis of AILT and, when used as part of a panel, can help differentiate AILT from other lymphomas and reactive lymphoid conditions. However, IHC antibodies for CXCL13 are not widely available, leading to challenges in the use of this biomarker for routine diagnosis. In the current study, we have developed a highly sensitive and specific RNA *in situ* hybridization (RISH) approach using the RNAscope technology to examine *CXCL13* mRNA expression in a panel of B and T cells lymphomas, including several confirmed cases of AITL.

Design: A total of 43 FFPE lymphoma samples were studied, including 16 T cell lymphomas and 27 non-T cell lymphomas, as summarized in Table 1 (annotated, deidentified tissues provided courtesy of Beijing Shijitan Hospital and reviewed for accuracy of diagnosis by an independent pathologist at ACD). For each case, separate serial sections were stained for *PPIB* (positive RNA control), *DapB* (negative control), and *CXCL13* and then scored for *CXCL13* expression.

Results: 43/43 FFPE samples passed RISH quality control. While some degree of *CXCL13* mRNA staining was observed in all lymphoma cases, reflective of the presence of scattered TFH cells, 7 AILT cases exhibited strong, diffuse expression of *CXCL13* in large numbers of cells across the tissue. 9 non-AILT T cell lymphomas and 27 B cell lymphomas showed only scattered *CXCL13*+ cells in significantly reduced numbers relative to the AILT cases.

Table 1. *CXCL13* RNA ISH in 43 lymphomas

Sample number	*CXCL13* staining pattern	Number *CXCL13*+ cells	Pathology diagnosis	Anatomical site	Age	Gender (M/F)
1	Scattered	low	Extranodal NK/T cell lymphoma (nasal type)	Right hemicolon	56	Male
2	diffuse	high	Angioimmunocell T cell lymphoma	Neck lymph node	54	Female
3	scattered	low	NK/T cell lymphoma	Nasal cavity tumor (Left)	66	Male
4	diffuse	high	Angioimmunocell T cell lymphoma	Left supraclavicular lymph node	51	Female
5	scattered	low	NK/T cell lymphoma	Right inferior turbinate tumor	29	Male
6	scattered	low	Extranodal nasal type NK/T cell lymphoma	Back tumor	39	Female
7	diffuse	high	Angioimmunocell T cell lymphoma	Left inguinal lymph node	68	Male
8	diffuse	High	Angioimmunocell T cell lymphoma	Neck lymph node	76	Female
9	scattered	low	Subcutaneous panniculitis like T cell lymphoma	Chest wall tumor	53	Male
10	scattered	low	Peripheral T cell lymphoma	Left inguinal tumor	63	Female
11	scattered	low	Enteropathy associated T cell lymphoma	Partial small intestine	75	Male
12	diffuse	high	Angioimmunocell T cell lymphoma	Left supraclavicular lymph node	65	Female
13	diffuse	high	Angioimmunocell T cell lymphoma	Right submandibular tumor	84	Female
14	diffuse	high	Angioimmunocell T cell lymphoma	Left inguinal lymph node	72	Male
15	scattered	low	Enteropathy associated T cell lymphoma	Small intestine	75	Male
16	scattered	low	T cell lymphoblastic lymphoma	Left neck	28	Female
17	scattered	low	Follicular lymphoma	Right subaxillary and anerolateral chest	51	Male
18	scattered	low	Classical Hodgkin's lymphoma mixed cellularity, MCH)	Left neck	32	Male
19	scattered	low	Diffuse large B-cell lymphoma	Right submandibular	24	Male
20	scattered	low	B-cell non Hodgkin's lymphoma	Back	66	Male
21	scattered	low	Diffuse large B-cell lymphoma (non-GCB)	Mesenteric root	72	Female
22	scattered	low	Non Hodgkin's B-cell lymphoma, lymphoplasmacytic lymphoma	Small intestine	66	Male
23	scattered	low	Castleman Disease, Plasma cell type	Right axillary lymph nodes	40	Female
24	scattered	low	Diffuse large B-cell lymphoma (non-GCB)	Right tonsil	58	Male
25	scattered	low	Adenocarcinoma	Lymph node	52	Male
26	scattered	low	Non Hodgkin's lymphoma, Diffuse large B-cell lymphoma	Right hemicolon	67	Male
27	scattered	low	B-cell lymphoma	Thigh	80	Male
28	scattered	low	Chronic lymphocytic leukemia/ Small B Lymphoid Lymphoma	Lymph node	77	Female
29	scattered	low	Small round cell tumor, Lymphoma	Right submandibular gland	42	Male
30	scattered	low	Lymphoma	Right neck+Right tonsil	54	Female
31	scattered	low	Diffuse large B-cell lymphoma	Right submandibular	66	Female
32	scattered	low	Mantle cell lymphoma	Right cheek	83	Female
33	scattered	low	Non Hodgkin's lymphoma, high grade B-cell lymphoma	Right tonsil	69	Male
34	scattered	low	Non Hodgkin's lymphoma, high grade B-cell lymphoma	Right tonsil	69	Male
35	scattered	low	Diffuse large B-cell lymphoma (non-GCB)	Right hemicolon	77	Male
36	scattered	low	Follicular Lymphoma (3A)	Left armpit	64	Male
37	scattered	low	Submental lymph node metastatic squamous cell carcinoma	Submental lymph node	50	Male
38	scattered	low	Lymph node metastatic renal clear cell carcinoma	Cervical/neck lymph nodes	72	Male
39	scattered	low	Lymph node metastatic breast invasive ductal carcinoma, Histological grade Stage 2	Left axillary lymph node	53	Female
40	scattered	low	Borderline B-cell lymphoma	Right neck+Right jaw	71	Male
41	scattered	low	Mantle Cell Lymphoma	Right parotid gland+Left jaw	67	Male
42	scattered	low	Follicular lymphoma grade 3 with diffuse large B-cell lymphoma	Left inguinal lymph nodes	73	Female
43	scattered	low	Follicular Lymphoma (IIIB type)	Left axillary	59	Female

Conclusions: We have developed a novel RISH method for the detection of *CXCL13* mRNA in FFPE tissue in lymphomas. Although *CXCL13*$^{+}$ cells were present in all lymphomas, only AITL exhibited a strong, diffuse, widespread mRNA staining pattern, reflective of the TFH phenotype of AITL. Overall, our results demonstrate that the RNAscope technology is a reliable and easy to interpret method for the detection of *CXCL13* expression in lymphomas and provides a sensitive and specific alternative to IHC for the assessment and diagnosis of AILT.

1330 Hyperleukocytosis in Pediatric B-Lymphoblastic Leukemia has a 2nd Incidence Peak in Teenage Males, Suggesting Hormone Effect as a Contributing Factor

Tian Li[1], Billy Carstens[2], Xiayuan Liang[3]
[1]*University of Colorado, Aurora, CO,* [2]*Colorado Cytogenetics Laboratory, Aurora, CO,* [3]*Children's Hospital Colorado, Aurora, CO*

Disclosures: Tian Li: None

Background: Hyperleukocytosis (≥ 100,000/mm^3) is often seen in infantile B-acute lymphoblastic leukemia (B-ALL), T-ALL, acute myelomonocytic/monocytic leukemia, and chronic myeloid leukemia. B-ALL with hyperleukocytosis confers a worse prognosis. Although the occurrence of hyperleukocytosis is not limited to infants in B-ALL, the incidence, pattern of distribution, and the potential cause in pediatric non-infantile patients have not been investigated yet. We performed a 10-year retrospective data analysis to (1) identify if there is a relationship between hyperleukocytosis and clinicopathologic characteristics and (2) provide insights on the underlying biology.

Design: Between 2009 and 2018, 444 cases of newly diagnosed ALL with age < 20 year old were identified at our institution. There were 394 cases of B-ALL, 50 T-ALL, 59 with WBC ≥ 100k, and 385 with WBC < 100k. Clinicopathologic characteristics analyzed were age, gender, WBC, CD10, percent S phase, B/T-lineage, and cytogenetics. A p-value was calculated for each comparison with a value of less than 0.05 considered statistically significant.

Results: See table and figure.

Clinicopathologic Features of Pediatric ALL with Hyperleukocytosis

B-ALL	**<1y (G1)**	**1-9 y (G2)**	**10-19 y (G3)**	**P value**
# of patients	10	279	105	
Rate of WBC ≥ 100k	4/10 (40%)	17/279 (6%)	16/105 (15.2%)	*p1* (G1 vs G2) = 0.01 *p3* (G2 vs G3) = 0.015
M:F ratio for WBC ≥ 100k M:F ratio for WBC < 100k	1:3 3:3	7:10 140:122	13:3 41:48	*p* (G3, M vs F) = 0.013
CD10- (WBC ≥ 100k)	3/4 (75%)	3/17 (17.6%)	2/16 (12.5%)	*p1* (G1 vs G2) < 0.001 *p2* (G1 vs G3) < 0.001
High S-phase (>5%) (WBC ≥ 100k)	1/4 (25%)	6/17 (35%)	8/14 (57%)	
Cytogenetics (WBC ≥ 100k)	*KMT2A*+ 4/4 (100%)	heterogenous	heterogenous	
T-ALL	**<1y**	**1-9 y**	**10-19 y**	
# of patients	1	33	16	
Rate of WBC ≥ 100k	0/1 (0%)	14/33 (42.4%)	8/16 (50%)	
M:F ratio for WBC ≥ 100k M:F ratio for WBC < 100k	0:0 0:1	12:2 17:2	7:1 5:3	

Figure 1 - 1330

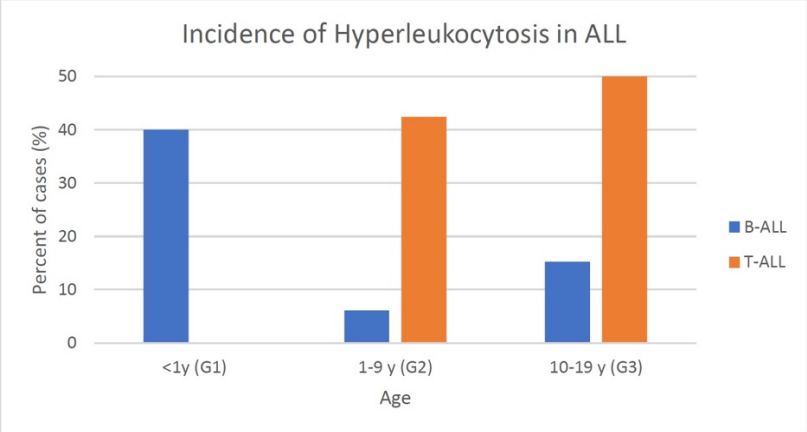

1. A high rate of hyperleukocytosis occurs not only in T-ALL and infantile B-ALL, but also occurs in B-ALL of the teenage group resulting in a bimodal distribution in B-ALL which is not seen in T-ALL.
2. Teenage patients of B-ALL with hyperleukocytosis are male predominant compared to those without hyperleukocytosis. This suggests that unlike (1) infantile B-ALL in which hyperleukocytosis is driven by *KMT2A* gene rearrangement and CD10- progenitor B-cell phenotype and (2) T-ALL in which hyperleukocytosis is driven by T-cell phenotype, teenage B-ALL with hyperleukocytosis is at least in part caused by a hormone effect - either a deleterious effect from testosterone and/or the lack of a protective effect from estrogen.

1331 HIV-Associated Plasmablastic Lymphoma: Ten-Year Experience in the Era of Highly Active Antiretroviral Therapy

Pathology Lin[1], Wei Wang[2], Nfn Aakash[3], Shimin Hu[2], Robert Brown[4], Xiaohong Iris Wang[5], Lei Chen[6], Md Amer Wahed[3], Nghia Nguyen[3], L. Jeffrey Medeiros[2], Zhihong Hu[7]
[1]UT Health Science Center at Houston, Houston, TX, [2]The University of Texas MD Anderson Cancer Center, Houston, TX, [3]The University of Texas Health Science Center at Houston, Houston, TX, [4]UTHealth, McGovern Medical School, Houston, TX, [5]Bellaire, TX, [6]University of Texas Houston, Houston, TX, [7]The University of Texas Health Science Center at Houston, Sugar Land, TX

Disclosures: Pathology Lin: None; Wei Wang: None; Nfn Aakash: None; Shimin Hu: None; Robert Brown: None; Xiaohong Iris Wang: None; Lei Chen: None; Md Amer Wahed: None; Nghia Nguyen: None; L. Jeffrey Medeiros: None; Zhihong Hu: None

Background: Plasmablastic lymphoma was originally reported in the oral cavity of HIV patients, but subsequent studies showed cases in non-oral sites and in non-HIV patients. In this study our aim was to review our experience with plasmablastic lymphomas occurring in HIV patients in the era of highly active anti-retroviral therapy (HAART).

Design: Over an interval of 10 years, we identified 95 HIV+ patients with aggressive non-Hodgkin lymphomas. From this group, we reviewed the morphologic, immunophenotypic and clinical features of cases of plasmablastic lymphoma.

Results: Plasmablastic lymphoma was diagnosed in 21 of 95 (22%) HIV associated aggressive non-Hodgkin lymphoma cases with a median age of 45 years (range, 28-60) and male predominance (M:F=20:1). Seven patients were diagnosed at time of initial HIV diagnosis and 14 diagnosed at a median interval of 7.7 months after HIV diagnosis. The median CD4 count, CD4:CD8 ratio and HIV copy number were 115/uL (range 1-393), 0.19 (range 0.01-0.40) and 90,000 (range 20-4,530,000) at time of diagnosis of PBL, respectively. 4/15 (27%) patients had disease involving bone marrow and blood. Lymph nodes (n=9, 43%), oral cavity/sinonasal mass (n=6, 29%) and rectal masses (n=5, 24%) were the most commonly involved sites. The neoplastic cells were immunoreactive for MUM-1/IRF4 (22/22 cases, 100%), CD138 (16/17 cases, 94%), CD79a (5/9 cases, 56%) and CD45 (4/8 cases, 50%). Proliferation rate is >= 90% in 18/20 (90%) and EBER was positive in all 20 (100%) cases assessed. FISH analysis was positive for *MYC* rearrangement in 2/4 (50%) and 1 had gains of BCL6 and MYC. 7/19 (37%) patients presented with stage I/II disease and 12/19 (63%) patients with stage III/IV disease. 19/21(90%) patients were treated with chemotherapy including 13 patients with EPOCH and 2 with CHOP. With a median follow-up time of 17 months (range, <1 to 103), 5/15 (33%) patients died. BM involvement had a significant impact on overall survival (OS) with a median OS of 1.9 months in patients with BM involvement (p=0.02) (Figure 1). Although patients with CD4 count <200 and elevated serum LDH level appeared to have a poorer survival, their median OS were not statistically significant from patients with higher CD4 counts and normal serum LDH level (P = 0.21 and 0.17 respectively).

Figure 1 - 1331

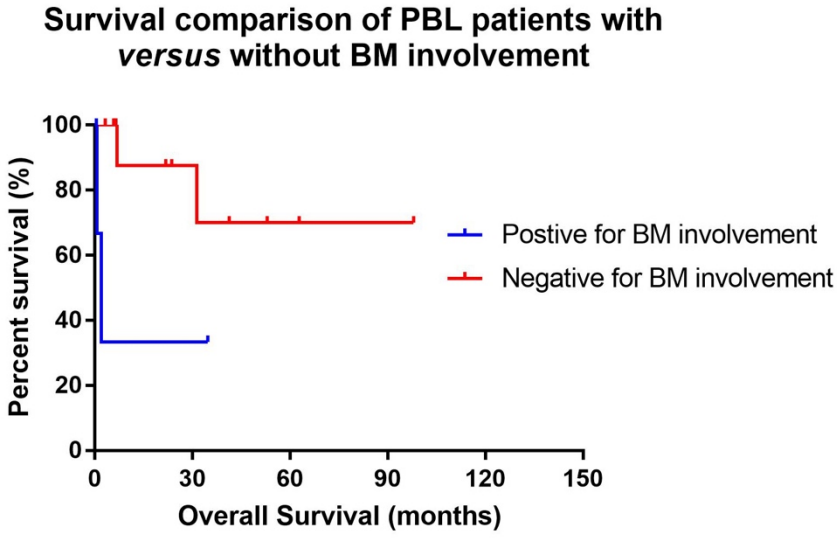

Conclusions: In HIV patients PBL is currently the second most frequent aggressive B-cell lymphoma. Lymph nodes are the most commonly involved sites. Our data suggest patients with PBL involving BM have a very poor prognosis.

1332 Two Distinct Pathways for the Development of Plasmablastic Lymphoma in the Setting of Chronic Lymphocytic Leukemia: Richter Transformation-Like Clonal Evolution and Epstein-Barr Virus Associated De Novo B-Cell Neoplasm

Catherine Luedke[1], Shimin Hu[2], Yue Zhao[1], Zenggang Pan[3], Jinming Song[4], Carlos Bueso-Ramos[2], L. Jeffrey Medeiros[2], Endi Wang[1]
[1]Duke University Medical Center, Durham, NC, [2]The University of Texas MD Anderson Cancer Center, Houston, TX, [3]Yale University School of Medicine, New Haven, CT, [4]Moffitt Cancer Center, Tampa, FL

Disclosures: Catherine Luedke: None; Shimin Hu: None; Yue Zhao: None; Zenggang Pan: None; Carlos Bueso-Ramos: None; L. Jeffrey Medeiros: None; Endi Wang: None

Background: Plasmablastic lymphoma (PBL) is unusual in the setting of chronic lymphocytic leukemia (CLL), and whether or not the event consistently represents a variant of Richter transformation needs further study.

Design: We identified 9 cases of PBL in association with CLL, and their clinicopathologic features were retrospectively analyzed.

Results: Of 9 patients, 8 were male, and 1 was female with a median age of 64 years (range: 57-77) at the time of CLL diagnosis. Of 8 cases analyzed, 6 were *IGHV* unmutated either by sequencing or surrogate testing. 8 patients had PBL diagnosed after CLL with a median interval of 76.5 months (range: 38-147), while 1 presented with concurrent disease. Of the 8 patients with preceding CLL, 7 received treatment, while the remaining patient who was asymptomatic did not. Clinical presentations of PBL included 7 with extranodal masses, 4 with pancytopenia, 3 with diffuse lymphadenopathy, 2 with lytic bone lesions, and 2 with pleural effusions. 4 of 6 cases showed bone marrow involvement and 7, with available data, exhibited residual CLL. In all cases, PBL demonstrated typical features with expression of CD138 and down-regulation of B-cell markers. All 9 cases were tested for Epstein-Barr Virus (EBV) and 2 were positive. IGH clonality testing was performed in 3 cases. CLL and PBL were found to be clonal in 2 EBV-negative cases, while they were not in 1 EBV-positive case. In addition, 4 other EBV-negative cases had concordant lambda light chain restriction between the CLL and PBL. Interestingly, one case of EBV-negative PBL was tested for MYC rearrangement and was positive. 6 patients died of their disease with a median overall survival of 2.8 months (range: 0.3-9), with the longest survival time seen in a patient with EBV-positive PBL and shorter survival times seen in those with EBV-negative PBL. The remaining 3 cases lacked adequate follow-up.

Conclusions: In the setting of CLL, PBL appears to arise via two different pathways. There are those which evolve directly from CLL via a clonally related Richter transformation and those associated with EBV that likely represent de novo aggressive B-cell neoplasms. While Richter transformation heralds a dismal outcome as seen in this series and may be driven by the acquisition of a *MYC* rearrangement, whether or not EBV-positive PBL, in the setting of CLL, predicts a relatively better prognosis remains to be seen and requires a larger cohort study.

1333 Biomarkers of Hypoxia and the Immune Microenvironment of DLBCL: HIF1a, HIF2a, and Immune Checkpoint Molecule Expression and Clinical Outcome Analysis

Vladislav V. Makarenko[1], Pallavi Galera[2], Karen Dresser[1], Benjamin Chen[3]
[1]University of Massachusetts Medical School, Worcester, MA, [2]National Cancer Institute/National Institutes of Health, Bethesda, MD, [3]UMass Memorial Medical Center, Worcester, MA

Disclosures: Vladislav V. Makarenko: None; Pallavi Galera: None; Karen Dresser: None; Benjamin Chen: *Grant or Research Support*, TESARO Inc.

Background: Hypoxia inducible factor (HIF) is a transcription factor that regulates expression of genes involved in responses to hypoxia and can modulate the tumor microenvironment. HIF1a expression in diffuse large B-cell lymphoma (DLBCL) has previously been shown to be associated with inferior survival. Similarly, immune checkpoint molecules, such as programmed cell death ligand-1 (PDL1), can modulate the immune microenvironment by downregulating T-cell activity. Expression of PDL1 in DLBCL has also been associated with inferior overall survival. HIF-dependent transcriptional pathways increasing PDL1 expression have been proposed. In this study, we hypothesized that HIF1a and HIF2a expression would correlate with immune checkpoint molecule expression in DLBCL and would be associated with inferior patient outcomes.

Design: We retrospectively identified 49 cases of DLBCL (including nodal and extranodal cases) and extracted relevant clinicopathologic data from these patients. HIF1a, HIF2a, and PDL1 immunohistochemical (IHC) analysis was performed on FFPE sections and correlated with clinical outcome data. Tumor microarray with an additional 36 DLBCL cases were evaluated for HIF1a expression by IHC as well as for proteins involved in tumor immune response by NanoString nCounter Digital Spatial Profiling (DSP) assay. This study was approved by the UMass IRB.

Results: Extranodal DLBCL represented 76% of cases. IHC staining was positive for HIF1a in 15 cases (31%) and for HIF2a in 23 cases (47%). HIF1a, but not HIF2a, expression showed strong correlation with PDL1 expression by IHC (p=0.011). Data from NanoString DSP assay showed strong positive correlation of HIF1a expression levels with PDL1, LAG3, B7-H3, but not with PD1, VISTA and TIM3 proteins in DLBCL. Patients with tumors expressing HIF1a, but not HIF2a, demonstrated inferior OS upon long term follow up (p=0.045 and 0.059, respectively).

Conclusions: HIF1a, but not HIF2a, expression strongly correlated with PDL1 and other immune checkpoint molecules (LAG3 and B7-3) and was associated with inferior patient outcome. Further studies of association between HIF1a and immune checkpoint molecules, and of possible clinical/therapeutic implications for DLBCL patients, are warranted.

1334 Comprehensive Multiplexed Protein Analysis of Immune-Related Molecules Comprising the DLBCL Immune Microenvironment

Vladislav V. Makarenko[1], Pallavi Galera[2], Karen Dresser[1], Benjamin Chen[3]
[1]University of Massachusetts Medical School, Worcester, MA, [2]National Cancer Institute/National Institutes of Health, Bethesda, MD, [3]UMass Memorial Medical Center, Worcester, MA

Disclosures; Vladislav V. Makarenko: None; Pallavi Galera: None; Karen Dresser: None; Benjamin Chen: *Grant or Research Support*, TESARO Inc.

Background: The immune host response has been shown to play an important role in the pathogenesis and clinical outcome of diffuse large B-cell lymphoma (DLBCL). Programmed cell death ligand-1 (PDL1) expression has been associated with inferior overall survival in DLBLC patients. The full composition of the DLBCL tumor immune microenvironment remains incompletely understood. In this study, we performed a comprehensive multiplexed analysis of immune-related proteins found in DLBCL tumors.

Design: 33 nodal and extranodal DLBCL cases were selected for immunohistochemical (IHC) analysis and NanoString nCounter Digital Spatial Profiling (DSP) assay. IHC analysis of PDL1, PD1, LAG3, and TIM3 were performed on FFPE tissue sections. DLBLC samples were also submitted to NanoString for their DSP assay using a 30-protein immuno-oncology panel. Data interpretation and statistical analysis were performed at UMass. The study was approved by the UMass IRB.

Results: IHC staining was positive for PD1 in 4 cases (12%), PDL1 in 13 cases (39%), TIM3 in 24 cases (73%), and LAG3 in 6 cases (18%). Strong correlation was found between IHC expression levels of PDL1, PD1, and TIM3 ($r>0.6$, $p<0.001$ for each protein) but not LAG3 ($r=0.27$, $p>0.05$). Pairwise associations between immune checkpoint proteins in DLBCL were studied using the nCounter DSP data and found strong positive correlations between PDL1 and LAG3 ($r=0.71$, $p<0.001$), PDL1 and B7-H3 ($r=0.78$, $p<0.001$), PDL1 and TIM3 ($r=0.46$, $p<0.01$), and VISTA and LAG3 ($r=0.46$, $p<0.01$). Ki67 protein level correlated with PDL1 and B7-H3 expression only ($r=0.71$ and 0.56, respectively, $p<0.001$). Phosphorylated STAT levels were associated with high expression of PDL1, TIM3, and B7-H3 ($r>0.6$, $p<0.001$ for each protein). AKT expression correlated with PDL1 and VISTA ($r>0.55$, $p<0.001$ for each protein). Proteins levels of CD44, b-catenin, b-2-microglobulin, and PTEN were also found to correlate strongly with PDL1 expression.

Conclusions: A comprehensive protein-level analysis of the immune microenvironment of DLBCL reveals coordinated expression of several therapeutically-relevant immunomodulatory molecules. Further studies are required to elucidate causative links for the observed protein expression patterns, as well as potential clinical and therapeutic implication of these findings.

1335 Juvenile Myelomonocytic Leukemias with CBL or Canonical RAS-Pathway Mutations Are Morphologically and Immunophenotypically Different

Rachel Mariani[1], Shanxiang Zhang[2], Shunyou Gong[3]
[1]Columbus, OH, [2]Indiana University School of Medicine, Indianapolis, IN, [3]Ann & Robert H. Lurie Children's Hospital of Chicago, Chicago, IL

Disclosures: Rachel Mariani: None; Shanxiang Zhang: None; Shunyou Gong: None

Background: Juvenile myelomonocytic leukemia (JMML) is a myelodysplastic/myeloproliferative neoplasm occurring in infancy and early childhood. Differing clinical behaviors are recognized between cases with *CBL* and canonical RAS-pathway gene (RAS-p) mutations; we have also observed differences in aspects of bone marrow morphology and immunophenotype. Here we describe abnormal findings in megakaryocyte morphology and myeloblast immunophenotypes in cases of JMML with RAS-p mutations as compared to cases with *CBL* mutations. We also found statistically-significant differences in various laboratory parameters between these two groups.

Design: A retrospective search for cases within the past 13 years meeting current WHO diagnostic criteria of JMML identified 9 patients with either *CBL* or RAS-p mutations who had adequate material available. Mutations were detected by either massively parallel or targeted sequencing. Bone marrow morphology and available corresponding flow cytometry dot plots were reviewed. Laboratory data were collected.

Results: *CBL* mutation was present in 3 patients and the remaining 6 had mutations of RAS-p. Megakaryocytes in cases with RAS-p, but not *CBL*, mutations were abnormal in morphology and numbers (Figure 1). Patients with *CBL* mutations presented with lower HgF levels (p=0.007), lower absolute monocyte counts (p=0.009), lower bone marrow blast counts (p=0.029), and lesser degrees of thrombocytopenia (p=0.032) and leukocytosis (p=0.003) than patients with RAS-p mutations (Table 1). Per flow cytometry analyses, there was no immunophenotypic abnormality in myeloblasts of the *CBL*-mutated group (Figure 2a, 2b), however CD7 expression was found in 4 of 5 patients with RAS-p mutations (Figure 2c, 2d).

Table 1. Bone marrow and laboratory findings at diagnosis.

			Megakaryocytes				Laboratory Parameters				
	Gene	**Age (yrs)/ sex**	**Morphology**	**Distribution**	**Numbers**	**Myeloblast %/ Aberrant antigen expression**	**WBC (k/μL)**	**Absolute monocyte count (k/μL)**	**Absolute platelet count (k/μL)**	**HbF (%)**	**Hb (g/dL)**
Patient 1	*CBL*	1.9/ F	Normal	Normal	Normal	3.0/ No	8.5	2.79	95	3.3	9.8
Patient 2	*CBL*	1.6/ F	Normal	Normal	Normal	1.0/ No	14.2	2.49	146	1.1	11.9
Patient 3	*CBL*	0.75/ F	Normal	Normal	Normal	1.8/ No	21.9	2.60	178	2.4	10.7
Patient 4	*NF1*	7.0/ F	Abnormal lobation, nuclear hyperchromasia	No core biopsy performed	No core biopsy performed	14.8/ No	16.1	1.77	61	15.8	8.4
Patient 5	*PTPN11*	0.23/ M	Normal	Normal	Normal	8.9/ CD7+	49.8	8.96	36	47.0	9.9
Patient 6	*PTPN11, KRAS*	3.9/ M	Occasional monolobation	Normal	Decreased	3.7/ CD7+	28.6	5.15	37	17.6	6.6
Patient 7	*PTPN11*	0.2/ M	Occasional monolobation	Normal	Decreased	3.3/ Flow cytometry not performed	44.0	5.67	31	39.5	9.4
Patient 8	*RRAS, JAK3*	3.7/ F	Normal	No core biopsy performed	No core biopsy performed	2.8/ CD7+	32.3	7.30	69	56.5	8.8
Patient 9	*PTPN11*	1.8/ M	Abnormal lobation, nuclear hyperchromasia	Focal clustering	Normal	3.0/ CD7+ (partial)	29.2	4.30	29.2	40.3	9.1
		p=0.104				*p=0.029	*p=0.003	*p=0.009	*p=0.032	*p=0007	p=0.079

Figure 1 - 1335

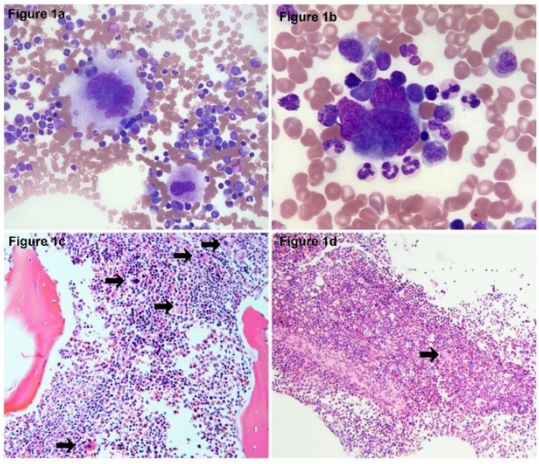

Megakaryocytes with hypolobation (Figure 1a; Patient 4) and other abnormal nuclear lobation (Figure 1b; Patient 9) in patients with RAS-p mutations. In patients with *CBL* mutations, megakaryocytes (black arrows) are present in normal numbers (Figure 1c; Patient 3) whereas patients with RAS-p mutations demonstrated significantly decreased numbers (Figure 1d; Patient 6).

Figure 2 - 1335

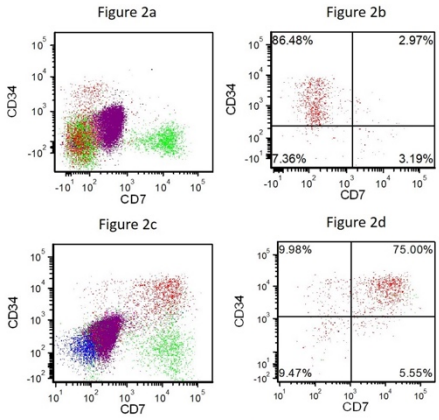

Representative flow cytometry dot plots from patients 1 (Figures 2a and 2b) and 9 (Figures 2c and 2d). The myeloblasts from patient with *CBL* mutation do not demonstrate CD7 positivity (Figure 2a – viable events & 2b – CD34+CD19- myeloblasts only), whereas the myeloblasts express CD7 in a patient with *PTPN11* mutation (Figure 2c – viable events & 2d – CD34+CD19- myeloblasts only). Gate colors used in Figures 2a and 2c: blasts including hematogones – red; granulocytes – violet; monocytes – pink; lymphocytes – green; erythroids – blue.

Conclusions: According to the current WHO, no specific immunophenotypic abnormalities are found in JMML. Although few cases have been reported with abnormal myeloblast immunophenotypes, notably aberrant CD7 expression, a genotype association has not been described. As JMML is a myelodysplastic/myeloproliferative neoplasm, dysplasia may be present however is more often observed in granulocytic and/or erythroid lineages. Our data suggest that JMML with *CBL* and RAS-p mutations differ in morphology and immunophenotypes. These findings may also provide a role for flow cytometry as a diagnostic tool in the diagnosis and monitoring of residual disease and emphasize the importance of careful bone marrow morphologic examination in JMML.

1336 Detection of Myeloid Targeted Mutations in Patients with Plasma Cell Neoplasm and Accompanying Cytopenia Is Useful for a Diagnosis of Concomitant or Secondary Myeloid Neoplasms

Brian Martens[1], Jose Rodriguez[2], Yuanyuan Lu[3], Yun Seongseok[2], Jinming Song[4], Ling Zhang[5]
[1]University of South Florida, Bradenton, FL, [2]H. Lee Moffitt Cancer Center & Research Institute, Tampa, FL, [3]University of South Florida, Tampa, FL, [4]Moffitt Cancer Center, Tampa, FL, [5]Tampa, FL

Disclosures: Brian Martens: None; Yuanyuan Lu: None; Ling Zhang: None

Background: Concomitant or secondary myeloid neoplasms (sMNs) have been seen in patients with plasma cell myeloma (PCM). Patients often present with refractory cytopenia (CP) that requires a bone marrow biopsy (BMBx) in conjunction with cytogenetic/molecular studies to characterize the disease process. Emerging data shows the importance of NGS myeloid targeted mutations for accurate diagnosis of clonal myeloid disorders. However, the landscape of somatic mutations in PCM alone vs PCM with CP has not been well studied.

Design: Patients who were diagnosed with PCM and followed-up for refractory CP (2014-18) were retrospectively identified by chart review. BMBxs along with 54-myeloid targeted genes were reviewed. Patients are divided to 3 groups: no myeloid diseases (group 0), diagnostic sMNs (group 1) and suspicious for but not diagnostic for sMNs (group 2). Kaplan-Meier curves and Log rank test were used to estimate overall survival (OS) comparing these 3 subgroups. Statistically significant is defined $p<0.05$.

Results: 108 PCM patients with CP and suspicious for sMNs were included. Mutations were identified in 18/55 patients (32.3%) in group 0, 22/24 patients (91.6%) in group 1, and 14/29 patients (48.3%) in Group 2 ($p<0.001$). Excluding overt PCM, the mutation rate was higher in group 1 and 2 ($p<0.01$). A summary of the 3 groups is found in Table 1. The most common mutation was *TP53*. Patients in group 1 showed more non-statistically significant *RUNX1* mutations or $\geq$3 mutations when compared with the others (p=0.161). The median OS rates were 38.9%, 36.4% and 7.1% for group 0, 1 and 2 (p=0.063). Analysis showed no OS difference in patients with/without myeloid mutation as a whole (p=0.11) or in each group (p=0.092, 1.0, and 1.0 for group 0, 1, and 2, respectively). Follow up NGS studies on 5 patients (group 2) who were mutated but non-diagnostic of sMNs showed 1 free of mutation/disease, 3 carried on the similar mutations but not diagnostic for sMNs, and one transformed to AML.

Table 1 summary of the subgroup patients' demographic data, disease status, and mutations status.

	Group 0 **(no myeloid neoplasm)** **n=55**	**Group 1** **(diagnostic myeloid neoplasm)** **N=24**	**Group 2** **(equivocal myeloid neoplasm)** **n=29**
Age, median (range)	68 (37-89)	70 (39-87)	66 (42-79)
Gender (M:F ratio)	32:23	18:6	19:10
Hemoglobin (g/dL), median (range)	9.6 (6.8-14.5)	10.8 (7.7-12.9)	10.1 (6.9-14.0)
ANC (x 10^9/uL), median (range)	1920 (0-23580)	1750 (150-18710)	2060 (120-11550)
Platelets (x 10^9/uL), median (range)	114 (4-647)	89 (19-505)	122 (7-342)
Overt myeloma*	(50.9%)28/55	45.8% (11/24)	(51.7%)15/29
Minimal residual diseases (MRD)**	(14.5%) 8/55	16.7% (4/24)	(17.24%) 5/29
No residual MM	(34.5%) 19/55	(37.5%)9/24	(24.13%) 7/29
MDS	0	18 cases (6RCUD, 2RARS, 5RCMD, 2RAEB1, 3 RAEB2)	0
MDS/MPN	0	1 (CMML+SM)	0
AML	0	2	0
MPN	0	3 (ET, CML, PMF)	9
% mutation	32.3% (18/55)	91.6%(22/24)	48.3%(14/29)
% mutation in patients with only cytopenia with no PCM or with MRD	33.3% (6/18)	59%(13/22)	42.9%(6/14)
% mutation detected in patients with myeloma MRD or no residual disease	33.3% (6/18)	(54.5%) 12/22	6/14 (42.9%)
The most frequent mutations	TP53x 5 (27.7%), TET2x4 (22.2%), DNMT3Ax3 (16.7%), and KRASx3 (16.7%) > 2 mutations x1 (5.6%)	RUNX1x4 (18.8%), TP53x3 (13.6%), KRASx3 (13.6%), SF3B1x2 (9%), and BCORx2 (9%) > 2 mutations x 5(22.2%)	TET2x5 (35.7%), NOTCH1x4 (28.5%), ASXL1x2 (14.2%), and TP53 x2 (14.2%) > 2 mutations (0%)

Note: *clonal plasma cells >=5%; **clonal plasma cells <5% detected by IHC and/or flow cytometry

Conclusions: Myeloid mutations are often identified in PCM patients with overt myeloid neoplasms, which support morphologic diagnosis of concomitant or sMNs. Close follow up is indicated for CP with myeloid mutations. Our study was limited to assess the clinical significance of myeloid mutations in PCM with CP given the small number of cases, short follow up period, and unknown status of PCM mutation profiles. Additional investigation with a larger cohort is indicated for further exploration.

1337 CD20-negative nodular lymphocyte-predominant Hodgkin lymphoma is enriched for variant patterns and shows aggressive clinical features

Joshua Menke[1], Michael Spinner[2], Bijayee Shrestha[3], Ranjana Advani[4], Yaso Natkunam[5], Dita Gratzinger[5]
[1]Millbrae, CA, [2]Stanford, Palo Alto, CA, [3]El Camino Hospital, Sunnyvale, CA, [4]Stanford Cancer Institute, Stanford, CA, [5]Stanford University Medical Center, Stanford, CA

Disclosures: Joshua Menke: None; Ranjana Advani: None; Yaso Natkunam: None; Dita Gratzinger: None

Background: Nodular lymphocyte-predominant Hodgkin lymphoma (NLPHL) is a low-grade B-cell lymphoma consisting of large neoplastic lymphocyte-predominant (LP) cells that express multiple B-cell markers, including CD20 in virtually all reported cases. CD20 positivity has been an inclusion criterion for the diagnosis of NLPHL in major studies and is a critical diagnostic feature in NLPHL that helps rule out differential diagnoses such as marginal zone lymphoma or classic Hodgkin lymphoma (cHL). We describe the clinicopathologic features of 10 NLPHL cases that either lack CD20 or show focal CD20 expression.

Design: Two consecutive cases of CD20-negative NLPHL were received in consultation at our institution over the course of 1 week. This prompted a retrospective search of our institutional pathology archive over a 20 year period that identified four additional cases. Another four cases were received prospectively in consultation over the following year. All slides and clinical records were reviewed when available. The diagnosis of NLPHL was confirmed by 2016 WHO criteria.

Results: Eight NLPHL cases showed absence of CD20 on LP cells, 1 case had equivocal CD20 expression, and 2 cases demonstrated focal CD20 expression. Interestingly, CD19 was either negative or subset in two CD20-negative cases that were tested. PAX5, CD79a, Bob.1, and Oct-2 were positive with varying intensities in all cases evaluated. Of note, the LP cells in 1 case expressed diffuse CD30 and focal CD30 in two other cases; all cases were negative for CD15 and EBER when evaluated. Five of ten cases (50%) showed variant patterns of NLPHL, including patterns D, E, and F described by Fan et al. Only 2 patients had documented rituximab administration prior to surgical sampling. The bone marrow biopsy from one patient showed neoplastic involvement and imaging from another patient showed involvement of the thoracolumbar spine. At follow up, 1 patient progressed to T-cell, histiocyte-rich large B-cell lymphoma, 1 patient failed CHOP, ICE, and DHAP therapies and was enrolled in hospice, and 3 patients achieved clinical remission after therapy.

Conclusions: NLPHL can completely lack or focally express CD20 immunohistochemical staining, despite the absence of rituximab administration. A small subset of these cases expresses CD30, necessitating a broad B-cell immunohistochemical panel to rule out cHL. CD20-negative NLPHL is enriched for variant patterns and can present with bone marrow involvement and other aggressive clinical features.

1338 Molecular Abnormalities in Chronic Myelomonocytic Leukemia: A Single-Institution Experience

Adam Miller[1], Jiehao Zhou[1]
[1]Indiana University School of Medicine, Indianapolis, IN

Disclosures: Adam Miller: None; Jiehao Zhou: None

Background: Chronic myelomonocytic leukemia (CMML) is a clonal stem cell disorder with overlapping features of myelodysplastic syndromes and myeloproliferative neoplasms. Biologic and clinical features are highly variable, probably due to diverse genetic abnormalities.

Design: Bone marrow biopsies with a diagnosis of CMML with associated next generation sequencing (NGS) data were queried from our department database. The NGS data included the mutation status of 54 genes frequently mutated in myeloid malignancies (TruSight Myeloid Sequencing Panel, Illumina). Mutations were classified into mechanistic categories and correlations with morphological, biologic, and clinical features were performed.

Results: 22 cases fulfilling the search criteria were identified. 77% of patients were male and the median age was 72 years (range: 47-90). Almost all of the cases (n=21, 95%) contained at least one mutated gene with the median number of mutations being 3. The median mutation allele frequency was 43.4%. Mutations were identified in genes involving splicing (n=15, 68%), signal transduction (n=14, 64%), DNA methylation (n=12, 55%), chromatin regulation (n=12, 55%), transcription (n=4, 18%), DNA damage response (n=3, 14%), & the cohesin complex (n=1, 5%). The most frequently mutated genes were *SRSF2* (59%), *TET2* (50%), *ASXL1* (50%), & *RAS* (41%). *RAS* mutations correlated with higher white blood cell (WBC) counts (p=.003) whereas mutations in *TET2* and *SRSF2* were associated with higher hemoglobin levels (p=.008 and p=.016, respectively). There were 13 cases of CMML-0, 4 cases of CMML-1, & 5 cases of CMML-2 with a median number of mutated genes of 3, 3.5, & 4, respectively. There was no statistically significant difference among CMML-0, CMML-1, & CMML-2 regarding the distribution of mutation mechanistic categories or allele frequencies in the most commonly mutated genes.

Conclusions: Myeloid NGS data at our institution show that gene mutations are common in CMML, comparable to previously published data. *RAS* mutations correlate with higher WBC counts while *TET2* and *SRSF2* mutations are predictive of higher hemoglobin levels.

Although there is a trend of increased mutation burden in higher grade CMML, no significant differences in terms of distribution or allele frequency of gene mutations are identified among CMML-0, CMML-1, and CMML-2. Further studies, particularly to include more cases and prognostic data are necessary to further elucidate the clinical significance of different mutations in CMML.

1339 p53 Protein Expression Predicts Cytogenetic and Molecular Abnormalities in Patients with Clinical Concern of Myelodysplastic Syndromes

Adam Miller[1], Jiehao Zhou[1]
[1]Indiana University School of Medicine, Indianapolis, IN

Disclosures: Adam Miller: None; Jiehao Zhou: None

Background: Myelodysplastic syndromes (MDS) are a group of clonal myeloid neoplasms characterized by cytopenias secondary to ineffective hematopoiesis and dysplasia. Cytogenetic abnormalities have been identified in a subset of MDS and indications for inclusion of next generation sequencing (NGS) testing are continually evolving. p53 mutations adversely affect MDS prognosis, but the role of p53 protein expression in MDS diagnosis has not been extensively investigated.

Design: Bone marrow biopsies performed for a clinical concern of MDS with associated cytogenetic studies and NGS data were queried from our department database. The NGS data included DNA sequencing of the coding region of 406 genes, selected introns of 31 genes, and RNA sequencing of 265 genes (FoundationOne Heme, Foundation Medicine). The clinical history, bone marrow morphology, immunophenotype, cytogenetic results, and NGS data were reviewed. Immunohistochemical staining for p53 was performed on bone marrow trephine biopsies and aspirate clot sections with positive staining defined as at least 1% strong nuclear staining of hematopoietic cells. Immunohistochemical results were correlated with cytogenetic and molecular findings.

Results: 58 cases fulfilling the search criteria were identified. 16 cases (27.6%) had abnormal cytogenetic results by karyotype or fluorescence in-situ hybridization. 49 cases (84.5%) had molecular abnormalities detected by NGS. Immunohistochemical staining for p53 was positive in 35 cases (60.3%). Immunohistochemistry for p53 had a sensitivity of 100% and a specificity of 56.1% for detecting cytogenetic abnormalities and a sensitivity of 67.4% and a specificity of 77.8% for detecting NGS abnormalities. Expression of p53 had a positive predictive value of 94.3% regarding NGS abnormalities and a negative predictive value of 100% regarding cytogenetic abnormalities.

Conclusions: Immunohistochemical staining for p53 demonstrates diagnostic utility in patients with clinical concern of myelodysplastic syndromes. Positive staining for p53 predicts molecular abnormalities whereas negative staining for p53 predicts normal cytogenetic results. As such, NGS testing should be performed in cases with positive p53 staining while the decision of whether or not to perform NGS testing should be left to the judgment of the pathologist in cases with negative p53 staining.

1340 Co-expression of MAL and PD-L2 by Immunohistochemistry Is Specific for Primary Mediastinal Large B-Cell Lymphoma

Prasuna Muppa[1], Linda Dao[2], Brooke McCann[2], Ellen Mcphail[2], Min Shi[2], Karen Rech[1]
[1]Rochester, MN, [2]Mayo Clinic, Rochester, MN

Disclosures: Prasuna Muppa: None; Linda Dao: None; Brooke McCann: None; Ellen Mcphail: None; Min Shi: None; Karen Rech: None

Background: Distinction of primary mediastinal large B-cell lymphoma (PMBCL) from systemic diffuse large B-cell lymphoma (DLBCL) is of increasing importance given the development of tailored therapeutic regimens for PMBCL. Gene expression studies have identified a characteristic profile for PMBCL, although no single marker has been shown to be entirely sensitive or specific. We performed immunohistochemistry (IHC) for 4 of the markers commonly expressed in PMBCL to determine if a practical algorithmic approach to classification could be identified.

Design: Tissue microarrays containing 42 PMBCL cases, 16 DLBCL cases occurring in the mediastinum, and 93 DLBCL cases involving other sites were evaluated. 8 additional cases of PMBCL were evaluated on whole tissue sections. Expression of MAL (clone E-1, Santa Cruz Biotechnology, Dallas, TX), PD-L2 (clone D7U8C, Cell Signaling Technology, Danvers, MA), CD23 (clone SP23, Roche Ventana Medical Systems, Tucson, AZ) and CD30 (clone JCM182, Leica Biosystems, Wetzlar, Germany) was assessed by IHC using optimized protocols. The stains were evaluated for both intensity and percentage of tumor cells staining.

Results: IHC results are summarized in the table. Expression of MAL, PD-L2, CD23 and CD30 was observed with higher frequency in PMBCL compared to DLBCL. Of the four markers, MAL and PD-L2 showed the best discrimination between PMBCL and DLBCL, and showed a similar level of sensitivity for PMBCL (58% and 56%). However, none of the markers alone was entirely specific for PMBCL. Co-expression of MAL and PD-L2 in the same tumor was 100% specific and 48% sensitive for PMBCL.

Immunohistochemistry Results			
	PMBCL n=50	**DLBCL, mediastinum n=16**	**DLBCL, other sites n=93**
MAL	29 (58%)	2 (12%)	1 (1%)
PD-L2	28 (56%)	1 (6%)	3 (3%)
CD23	24 (48%)	3 (19%)	4 (4%)
CD30	40 (80%)	10 (63%)	6 (6%)
MAL/PD-L2	24 (48%)	0 (0%)	0 (0%)

Conclusions: In routine clinical practice, IHC for MAL and PD-L2 is useful for classification of large B-cell lymphoma that involves the mediastinum. By combining these markers, about half of PMBCL cases can be confidently classified by IHC. At the current time, more complex molecular analysis may be required in the other cases. Future studies may be useful in identifying additional markers to include in an IHC algorithm that can accurately identify all cases of PMBCL.

1341 CAR T cells are effective in abrogating CD19dim B cell precursors

Kavitha Muralidharan[1], University Pennsylvania[1], Gerald Wertheim[2], Vijay Bhoj[1], Vinodh Pillai[3]
[1]Perelman School of Medicine at the University of Pennsylvania, Philadelphia, PA, [2]The Children's Hospital of Philadelphia, Philadelphia, PA, [3]The Children's Hospital of Philadelphia, Penn Valley, PA

Disclosures: Kavitha Muralidharan: None; University Pennsylvania: None; Gerald Wertheim: None; Vijay Bhoj: None; Vinodh Pillai: None

Background: Chimeric antigen receptor (CAR) T-cells targeting CD19 are effective in treating relapsed/refractory B lymphoblastic leukemia (B-ALL). They also abrogate normal B cells resulting in peripheral blood B cell aplasia. Maturing B cell precursors ('hematogones'), present in the marrow, are classified into three distinct developmental stages based on increasing expression of CD19 and other antigens. The stage at which CAR T-cells act has not been established in the pre-clinical or clinical setting. We determined the threshold of CD19 expression necessary for CAR T cell function using clinical flow cytometry data and in-vitro experiments.

Design: Hematogones in the bone marrow were evaluated by flow cytometry in 150 patients treated with CAR T-cell therapy at our institution. Bone marrow biopsies were performed at 0, 1, 3, 6, 9 and 12 months post-infusion. Hematogone stage was determined using CD45, CD19, CD20, CD10, CD22 and CD34 antigens.

K562, a leukemia cell line endogenously negative for CD19, was electroporated with increasing concentrations of mRNA encoding CD19. Quantibrite phycoerythrin beads were used to determine the CD19 antigen density on the cell. In parallel, healthy donor T-cells were transduced with a lentiviral vector encoding the FMC63 epitope-based CD19-targeted CAR to create CAR T-cells. CAR and non-transduced (NTD) T cells were used in functional assays against the electroporated K-562 cells. CD69 and CD137 expression on T-cells were used to determine T-cell activation.

Results: CAR T-cells abrogated all stages of CD19+ positive hematogones in the marrow, including early hematogones expressing low levels of CD19. Expanded populations of unusual CD19-negative CD22-positive B cell precursors were noted in many cases.

CD19 expression was consistently detectable by flow cytometry (using the J3-119 anti-CD19 clone) on K562 cells electroporated with 0.5ug of mRNA (2086 CD19 surface molecules) (p=.004). Using the FMC63 anti-CD19 clone, detection was noted at 0.5ug (p= 0.262) and highly significant at 2 ug (p=0.005). T-cell activation assessed by CD69 upregulation showed increased activity of CAR over NTD T-cells starting at 0.005ug (p=0.048). A similar result was achieved for CD137 expression starting at 0.1 ug of CD19 (p=0.003).

Figure 1 - 1341

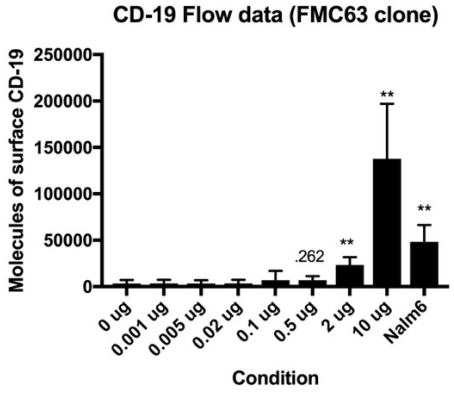

Figure 2 - 1341

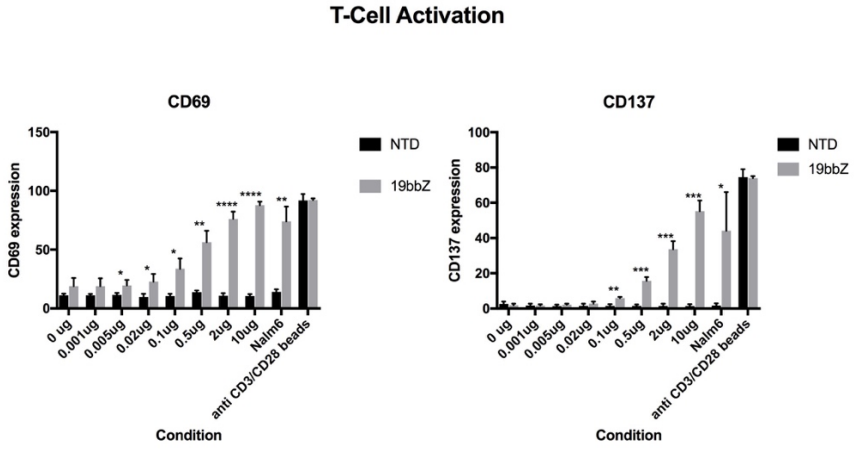

Conclusions: CAR T-cells function at the pre-pro B to pro B stage when CD19 is first expressed. RNA electroporation confirms CAR T-cells can detect low levels of CD19 expression, suggesting that CAR T cells are effective for treatment of CD19-dim B-ALL.<

1342 Deletion (20Q) and the Progression to Therapy-Related Myelodysplastic Syndrome in Plasma Cell Myeloma Patients Undergoing Total Therapy Treatment Regimens

Glenn Murray[1], Jeanette Ramos[2], Ginell Post[2], William Bellamy[2], Soumya Pandey[3]
[1]University of Arkansas, Little Rock, AR, [2]University of Arkansas for Medical Sciences, Little Rock, AR, [3]Little Rock, AR

Disclosures: Glenn Murray: None; Jeanette Ramos: None; Ginell Post: None; William Bellamy: None; Soumya Pandey: None

Background: Therapy-related myelodysplastic syndrome (t-MDS) commonly follows high-dose cytotoxic chemotherapy and autologous hematopoietic cell transplantation for non-myeloid neoplasms, like plasma cell myeloma (PCM). Deletion of the long arm of chromosome 20 is a common myeloid chromosomal aberration most often associated with a good prognosis in MDS. However, loss of 20q is not uncommonly seen in myeloma patients receiving a Total Therapy treatment regimen. Del(20q) appears early on in the cytogenetic evolution of myeloma, and we predict that its continued presence correlates with progression to overt t-MDS.

Design: MDS fluorescent in situ hybridization (FISH) and cytogenetic results were queried for del(20q) from our institutional image repository with an established diagnosis of PCM between 2007 and 2012. The MDS FISH probe set contained 5p15.2 (D5S23, D5S721), 5q31 (EGR1), 7cen (D7Z1), 7q31 (D7S486), 8cen (D8Z2), 13q14.3 (D13S319), 13q34 (LAMP1) and 20q12 (D20S108). Chromosome analyses were performed on trypsin-Giemsa banded metaphase cells of unstimulated aspirate cultures at the 400 band level resolution. Once identified, the cytogenetic/FISH landscape was documented throughout the course of each patient's PCM treatment.

Results: 47 of 760 patients undergoing melphalan-based stem cell transplant with MDS FISH/cytogenetic results had del(20q) (6.2%). Mean follow up was 71.4 months with del(20q) appearing at an average of 20.8 months after presentation. A total of 80.9% (n=38) of del(20q) patients progressed to t-MDS at an average of 19.8 months. Of the del(20q) patients who progressed to t-MDS, the most common unbalanced chromosomal abnormality was -13/del(13q) 42.1% (n=16). A complex karyotype was present in 39.5% (n=15) of del(20q) patients (*Table 1*). Two prognostic groups were identified based off whether del(20q) was present transiently or consistently (*Fig. 1*). Patients of the *Transient Group* had a mean progression to t-MDS of 32.5 months whereas the *Consistent Group* had a mean progression to t-MDS of 11.5 months (p= 0.02, d= 21.0) (*Fig. 2*).

		Male	Female	Mean Age at time of del(20q)	Presentation to development of del(20q)	Caucasian, n=44
Total Myeloma Patients	n=760					African American n=2
Total del(20q) Patients	n=47	n=37	n=10	64.7 Years	20.8 Months	Hispanic/Latino n=1
Progression to t-MDS	n=38					
Unbalanced MDS Cytogenetics		**With Complex Karyotype n=15**				
del(5q) or -5	n=8, (21.1)%	4 of 8, (50%)			**del(20q) to t-MDS**	
del(7q) or -7	n=10, (26.3%)	4 of 10, (40%)			**19.8 Months**	
del(9q)	n=1, (2.6%)	1 of 1, (100%)			**Consistent**	**11.5 Months**
del(11q)	n=6, (15.8%)	4 of 6, (67%)			**Transient**	**32.5 Months**
del(13q) or -13	n=16, (42.1%)	5 of 16, (31%)				
i(17)	n=1, (2.6%)	1 of 1, (100%)				
Complex Karyotype without other MDS-Defining Aberrations	n=3, (6.4%)				**First Cytogenetic Aberrancy**	
					del(20q)	n=32
Balanced Cytogenetics					-Y	n=32
t(1;3)(p36.3;q21.2)	n=1, (2.6%)	1 of 1, (100%)			Complex	n=y
inv(3)(q21.3q26.2)	n=1, (2.6%)	0 of 1, (0%)			Other	n=5

Figure 1 - 1342

Figure 2 - 1342

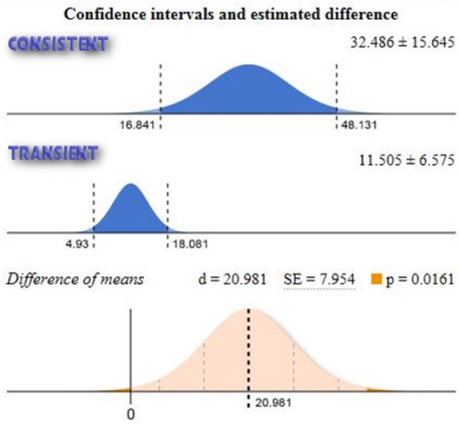

Conclusions: Deletion of 20q in myeloma patients is an early chromosomal aberration that most often appears in the consolidation or maintenance phases of the Total Therapy treatment regimens. Consistent presence of del(20q) in these patients was correlated with a quicker progression to t-MDS. Routine monitoring for the persistent presence of del(20q) may be informative for clinicians in risk stratifying myeloma patients for developing t-MDS.

1343 Correlating TP53 Genetic Derangements with Aberrant p53 Protein Expression in Mantle Cell Lymphoma

Damodaran Narayanan[1], David Yang[2], William Rehrauer[3], Molly Accola[4], Vanessa Horner[2], Les Henderson[2]
[1]University of Wisconsin Hospital and Clinics, Madison, WI, [2]University of Wisconsin, Madison, WI, [3]University of Wisconsin School of Medicine and Public Health, Madison, WI, [4]University of Wisconsin Hospital, Madison, WI

Disclosures: Damodaran Narayanan: None; David Yang: None; William Rehrauer: None; Molly Accola: None; Vanessa Horner: None; Les Henderson: None

Background: Mantle cell lymphoma (MCL) with *TP53* gene derangements, i.e. pathogenic *TP53* mutations (mut*TP53*) or loss of *TP53* (del*TP53*), is resistant to standard intensive therapy. mut*TP53* results in p53 overexpression which is an independent poor prognostic marker in MCL. Therefore, determining p53 expression (p53) by immunohistochemistry (IHC) has the potential to serve as a

surrogate to predict the clinical course in MCL. Moreover, the full interplay between mut*TP53*, del*TP53*, and p53 has not been examined in MCL. We aimed to characterize the relationship between p53 IHC expression and *TP53* derangements, and thereby, evaluate the clinical utility of assessing p53 IHC expression in MCL.

Design: p53 IHC intensity (0-3+) was scored in 200 lymphocytes per core of a tissue microarray containing 46 evaluable MCL cases represented in triplicate cores. The IHC intensity was multiplied by the number of positive cells and averaged between cores to obtain an IHC expression score, which was classified as low or high. Next Generation Sequencing with 100% coverage of coding regions was used to analyze mut*TP53*, and del*TP53* was determined using fluorescence *in-situ*hybridization.

Results: In all 26 cases without *TP53* derangements (i.e. neither mut*TP53* nor del*TP53*), p53 was low. In contrast, all 11 high p53 cases had some *TP53* aberration, including biallelic *TP53* derangement (i.e. concurrent mut*TP53* in one allele and del*TP53* in the other allele) in 7 cases, and monoallelic *TP53* derangement (i.e. either mut*TP53* alone or del*TP53* alone) in 4 cases.

Among the 11 cases with monoallelic *TP53* derangement, 7 had low p53 and 4 had high p53. Two (UW15 and UW26) of these 4 high p53 cases had mut*TP53* and mutant allele fractions >60%, suggestive of a loss of heterozygosity (LOH).

Biallelic *TP53* derangement was present in 9 cases, of which 7 had high p53. These results support the notion that high p53 is associated with biallelic *TP53* derangement or LOH. Interestingly, 2 cases with biallelic *TP53* derangement had low p53. These 2 low p53 cases harbored truncating non-sense (M003) and frameshift (M016) mutations, which disrupt p53 expression. All other mut*TP53* were identified as mis-sense mutations.

Relationship between p53 IHC expression and *TP53* derangements in MCL patients

IHC category (p53 IHC expression score)	Total number of cases	Cases without *TP53* derangements	Cases with monoallelic *TP53* derangement	Cases with biallelic *TP53* derangement
Low (0-100)	35	26 (74.3%)	7 (20%)	2 (5.7%)
High (>100)	11	0	4 (36.4%)	7 (63.6%)

Figure 1 - 1343

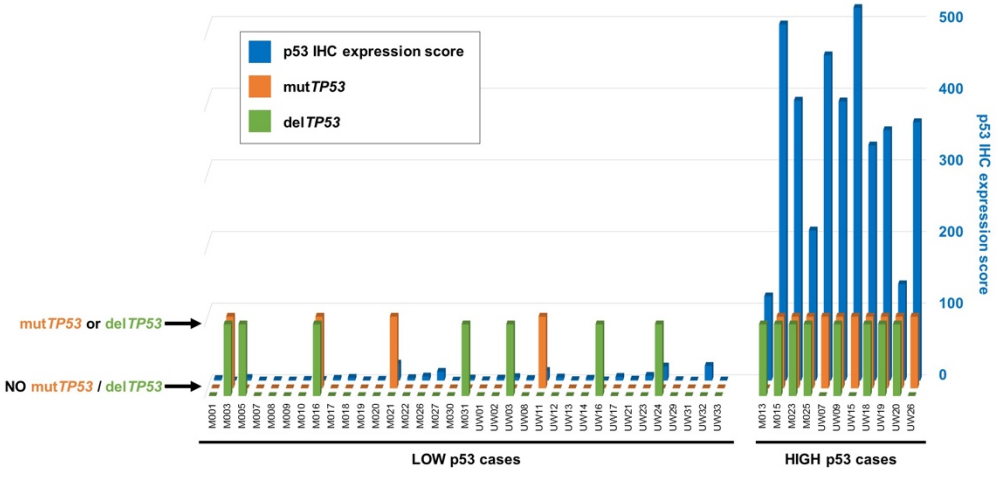

Relationship between p53 IHC expression and *TP53* derangements in MCL patients.
Columns represent p53 IHC expression score (blue) and presence or absence of mut*TP53* (orange) and del*TP53* (green).

Conclusions: Almost all high p53 cases displayed either biallelic *TP53* derangement or LOH. In contrast, only a few of the low p53 cases exhibited *TP53* derangements. Thus, quantification of p53 levels by IHC is a good predictor for mut*TP53*and/or del*TP53*, and can be an efficient discriminator in risk stratification of MCL patients.

1344 Clinicopathologic Features of Extranodal Marginal Zone (MALT) Lymphomas of the Central Nervous System Including Parenchymal Based Cases

Laila Nomani[1], Claudiu Cotta[1], Eric Hsi[1], James Cook[1]
[1]*Cleveland Clinic, Cleveland, OH*

Disclosures: Laila Nomani: None; Claudiu Cotta: None; Eric Hsi: *Primary Investigator*, Abbvie; *Primary Investigator*, Eli Lilly; *Advisory Board Member*, Seattle Genetics; *Advisory Board Member*, Celgene; James Cook: None

Background: Small B-cell neoplasms presenting in the central nervous system (CNS) are rare. In the prior literature, the most frequently reported cases are extranodal marginal zone (MALT) lymphomas involving the dura. Following diagnosis of an unusual index case, we have reviewed CNS MALT lymphomas at our institution in an effort to further characterize these uncommon tumors.

Design: The institutional pathology database from 2004-2018 was searched for CNS lymphomas, including meningeal lesions and excluding intraocular lymphomas. Available routine and immunohistochemistry (IHC) slides were reviewed for cases diagnosed as small B cell neoplasms and all cases were classified using 2016 WHO criteria. Where not previously performed, kappa and lambda IHC and paraffin section interphase fluorescence in situ hybridization for a *MALT1*translocation were performed when sufficient tissue was available.

Results: Of 194 cases of CNS lymphoma, 10 cases of MALT lymphoma were identified. Each of five cases involving the dura and one case arising in the choroid plexus of the lateral ventricle showed a largely diffuse lymphoid mass lesion composed predominantly of small lymphocytes. Of these cases, 3 were clinically suspected to be meningiomas prior to biopsy. Four cases arising in brain parenchyma showed a striking perivascular growth pattern without a lymphoid mass lesion, although one case contained a dominant mass of Congo Red negative proteinaceous material. Of these, two cases were clinically suspected to be gliomas prior to biopsy. The clinicopathologic features of parenchymal and non-parenchymal MALTs are summarized below. At median follow-up of 29 months, two patients with parenchymal lesions died with disease at 38 and 61 months. One patient with a dural lesion died on post-op day #1.

	Parenchymal (n=4)	non-Parenchymal (n=6)
Age (median, yrs)	63.75	71.5
Gender	M/F 1/3	M/F 5/1
Autoimmune history?	0/4 (0%)	0/6 (0%)
CD5	0/3 (0%) pos ; 1 n/a	0/4 (0%) pos; 2 n/a
CD10	0/1 (0%) pos; 3 n/a	0/5 (0%) pos; 1 n/a
Clonal plasma cells	3/4 (75%) pos	0/6 (0%) pos
MALT1 FISH	1/3 (33%) pos; 1 n/a	0/3 (0%) pos; 3 n/a
MYD88 L265P	0/2 (0%) pos; 2 n/a	6 n/a

Conclusions: Extranodal MALT lymphomas arising in the CNS include dural based as well as parenchymal based tumors; this latter subset has been incompletely described in the prior literature with only rare single patient case reports. While the number of cases examined to date is small, the parenchymal cases show striking morphologic similarities including perivascular growth pattern and abundant plasmacytoid/plasmacytic cells. SNP microarray studies are ongoing to further characterize these CNS MALT lymphomas. This study provides further insight into the spectrum of clinicopathologic findings in primary CNS MALT lymphomas.

1345 CD200 Expression in Diffuse Large B-cell Lymphoma-Type Richter Syndrome

Laila Nomani[1], Juraj Bodo[1], Lisa Durkin[1], Eric Hsi[1]
[1]*Cleveland Clinic, Cleveland, OH*

Disclosures: Laila Nomani: None; Juraj Bodo: None; Lisa Durkin: None; Eric Hsi: *Primary Investigator*, Abbvie; *Primary Investigator*, Eli Lilly; *Advisory Board Member*, Seattle Genetics; *Advisory Board Member*, Celgene

Background: Richter syndrome (RS) is the development of an aggressive lymphoma, commonly diffuse large B-cell lymphoma (DLBCL) histology, in patients with a previous or concomitant diagnosis of chronic lymphocytic leukemia (CLL). Immunophenotypic differences between the CLL and DLBCL-type RS are common, such as loss of CD5. CD200 is a type 1a membrane protein, related to the B7 family of costimulatory receptors. Previous studies have reported near uniform expression (100%) of CD200 in CLL by immunohistochemistry (IHC) as well as by flow cytometry. Its expression in DLBCL-type RS is unknown. We hypothesized that CD200 might be expressed in cases of DLBCL-type RS and be useful in distinguishing RS-DLBCL from *de novo* CD5-positive DLBCL.

Design: Cases of DLBCL-type RS and *de novo* CD5-positive DLBCL (defined according to 2016 WHO criteria) were retrieved from the departmental archives (1998-2018). CD200 expression was studied by immunohistochemistry (goat polyclonal, #AF2724; R&D Systems, Minneapolis, MN, 1:500 dilution) using an automated immunostainer (Ventana, Tucson AZ). Cases were scored positive if ≥20% of the lymphoma cells expressed CD200. Grading intensity was as follows: weak/1+ was light/pale tan, moderate/2+ was light brown, and strong/3+ was dark brown. Percentage of tumor cells was rounded to the nearest 10% and H scores were calculated. CD200 expression was correlated with CD5 expression in DLBCL-type RS cases.

Results: 14 cases of DLBCL-type RS and 5 cases of *de novo* CD5-positive DLBCL were evaluated for expression of CD200. Immunohistochemical findings are summarized in Table 1. Six of 14 (42%) cases of DLBCL-RS expressed CD200, 5 of which expressed CD5 in membranous pattern. Cases negative for CD200 were also negative for CD5 by IHC. Two out of five (40%) *de novo* CD5-positive DLBCL cases showed membranous CD200 expression in the neoplastic cells. The H scores for CD200-positive cases ranged from 70 to 300 (mean 200) in DLBCL-RS and from 80 to 300 (mean 190) in *de novo* CD5-positive DLBCL.

Case No	Diagnosis	Specimen source	CD20	CD5	CD200	CD 200 %/ Intensity	H score
1	DLBCL-RS	BM	+	-	-	0/NA	N/A
2	DLBCL-RS	LN	+	-	-	0/NA	N/A
3	DLBCL-RS	ST	+	+	+	100/3	300
4	DLBCL-RS	BM	+	+	+	100/3	300
5	DLBCL-RS	BM	+	wk	+	50/3	150
6	DLBCL-RS	Spleen	+	-	-	0/NA	N/A
7	DLBCL-RS	LN	-	-	-	0/NA	N/A
8	DLBCL-RS	LN	+	-	-	0/NA	N/A
9	DLBCL-RS	BM	+	-	-	0/NA	N/A
10	DLBCL-RS	BM	+	-	-	0/NA	N/A
11	DLBCL-RS	BM	+	+	+	90/2	180
12	DLBCL-RS	BM	+	-	-	0/NA	N/A
13	DLBCL-RS	BM	+	+	+	100/2	200
14	DLBCL-RS	LN	+	-	+	70/1	70
15	CD5+ DLBCL	LN	+	+	+	80/1	80
16	CD5+ DLBCL	LN	+	+	-	0/NA	N/A
17	CD5+ DLBCL	LN	+	+	+	100/3	300
18	CD5+ DLBCL	LN	+	+	-	0/NA	N/A
19	CD5+ DLBCL	BM	+	+	-	0/NA	N/A

Conclusions: CD200 is expressed in 42% of DLBCL-type RS and tracks closely with CD5 expression(83% concordance). However, CD200 is also expressed in 40% of *de novo* CD5-positive DLBCLs and is therefore not useful in identifying cases of DLBCL-type RS.

1346 Molecular Profiling Reveals Hypoxia-related Biomarkers and Therapeutic Targets in Breast Implant-associated Anaplastic Large Cell Lymphoma

Naoki Oishi[1], Surendra Dasari[1], Hailey Jacobs[1], Sergei Syrbu[2], Jennifer Chapman[3], Francisco Vega[4], Jagmohan Sidhu[5], Mark Clemens[6], L. Jeffrey Medeiros[6], Roberto Miranda[6], Andrew Feldman[1]
[1]Mayo Clinic, Rochester, MN, [2]University of Iowa, Iowa City, IA, [3]University of Miami, Miller School of Medicine, North Miami, FL, [4]University of Miami/Sylvester Cancer Center, Miami, FL, [5]UHS Hospitals, Vestal, NY, [6]The University of Texas MD Anderson Cancer Center, Houston, TX

Disclosures: Naoki Oishi: None; Surendra Dasari: None; Hailey Jacobs: None; Sergei Syrbu: None; Jennifer Chapman: None; Francisco Vega: None; Jagmohan Sidhu: None; Mark Clemens: None; L. Jeffrey Medeiros: None; Roberto Miranda: None; Andrew Feldman: None

Background: Breast implant-associated anaplastic large cell lymphoma (BIA ALCL) is a new provisional entity in the WHO classification that arises in association with breast implants. BIA ALCLs demonstrate STAT3 activation and consistently lack *ALK*, *DUSP22*, and *TP63* rearrangements (so-called “triple-negative” genetic subtype of ALCL). However, the overall molecular characteristics of BIA-ALCL are poorly understood.

Design: We performed RNA sequencing on FFPE tissue from 11 BIA and 24 non-BIA triple-negative ALCLs. Gene expression profiles were compared using gene set enrichment analysis. Immunohistochemistry (IHC) for carbonic anhydrase 9 (CA9) was performed in 17 BIA ALCLs, 11 ALK+ ALCLs, 23 systemic ALK- ALCLs, and 14 primary cutaneous ALCLs and scored as percent positive tumor cells.

Results: Hallmark gene sets positively associated with BIA ALCL included HYPOXIA (normalized enrichment score [NES], 2.727; false discovery ratio [FDR], 0.000) and TNFA_SIGNALING_VIA_NFKB (NES, 2.5303; FDR, 0.000). Overexpressed genes included *VEGFA* (RPKM, mean±SD: 13.2±6.5 vs. 5.1±3.7; p<0.001, t-test), *VEGFB* (13.6±2.9 vs. 8.9±3.3; p=0.002), *SLC2A3* encoding GLUT3 (68.6±36.2 vs. 28.9±16.7; p<0.001), and, notably, *CA9* (16.5±20.2 vs. 0.4±0.7; p=0.002), a hypoxia-associated biomarker and therapeutic target in renal cell carcinoma (RCC). By IHC, CA9 was expressed in BIA ALCL cells but not in admixed inflammatory cells and was mostly negative in non-BIA ALCLs (percent positive staining, mean±SD: BIA, 91±13%; ALK+, 2±6%; ALK-, 5±11%; cutaneous, 3±5%; p<0.0001, Kruskal-Wallis test; see Figures 1,2).

Figure 1 - 1346

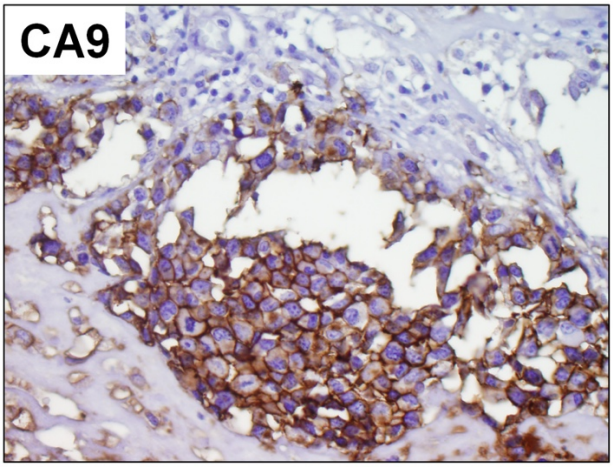

Figure 2 - 1346

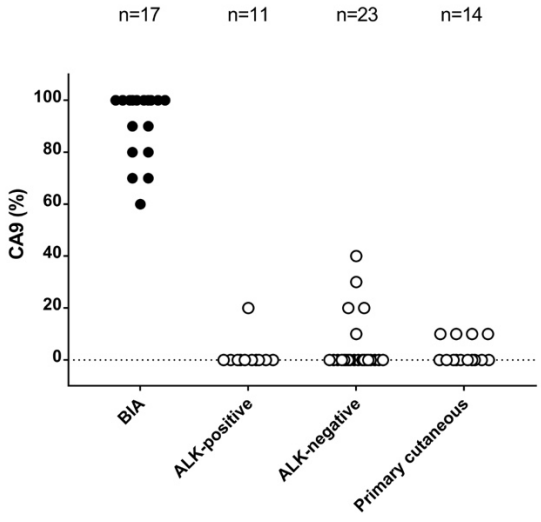

Conclusions: Molecular profiling of BIA ALCL demonstrated activation of the hypoxia signaling pathway, likely attributable to the unique microenvironment in which these tumors arise. *CA9*, a hypoxia-associated transcriptional target of HIF1alpha and STAT3, was specifically expressed in BIA ALCLs at the RNA and protein levels. Soluble CA9 is already being utilized as a biomarker in RCC, and clinical trials of CA9 inhibitors are underway. CA9 and other hypoxia signaling proteins merit further investigation as biomarkers and therapeutic targets in BIA ALCL.

1347 Prevalence and Clinical Implications of Splicing Factor Gene Mutation in Patients with Primary Myelofibrosis

Chi Young Ok[1], Zhining Chen[1], Sanam Loghavi[1], Rashmi Kanagal-Shamanna[2], Zhuang Zuo[1], C. Cameron Yin[1], Mark Routbort[1], Keyur Patel[1], Rajyalakshmi Luthra[1], L. Jeffrey Medeiros[1], Sa Wang[1]
[1]The University of Texas MD Anderson Cancer Center, Houston, TX, [2]The University of Texas MD Anderson Cancer Center, Bellaire, TX

Disclosures Chi Young Ok: None; Zhining Chen: None; Sanam Loghavi: None; Rashmi Kanagal-Shamanna: None; Zhuang Zuo: None; C. Cameron Yin: None; Mark Routbort: None; Keyur Patel: None; Rajyalakshmi Luthra: None; L. Jeffrey Medeiros: None; Sa Wang: None

Background: Mutations in the splicing factor genes *SF3B1, SRSF2, U2AF1* and *ZRSR2* are common in myelodysplastic syndromes (MDS). Recent pre-clinical studies have shown that splicing inhibitors may have therapeutic potential in MDS. Splicing factor gene mutations can be found in a subset of patients with primary myelofibrosis (PMF) and the clinical and pathological features of this patient subset has not been well studied.

Design: We searched the database of our laboratory from to identify patients with PMF who underwent next-generation sequencing-based sequencing using an 81-gene panel. Clinical and laboratory data were collected from electronic medical record.

Results: The study group included 75 patients with PMF, 48 men and 27 women, with the median age of 66 years (range, 35 to 86); 15 (20%) patients at time of initial diagnosis and 60 (80%) patients referred to our institution a median of 501 days (range, 31 to 6749) after initial diagnosis. 34 (45%) harbored splicing factor gene mutations: *SF3B1* (n=10), *SRSF2* (n=13), *U2AF1* (n=11), or *ZRSR2* (n=3). Three patients had mutations in ≥2 splicing factor genes. Most *U2AF1*mutations involved codons 156 to 159 (10/11).

Patients with non-SF3B1 mutations (n=24) had the highest median age (72 years), followed by SF3B1 mutations (n=10, 66 years) and patients without splicing factor mutations (n=41, 60 years) (p<0.01). Patients with SF3B1 mutations more commonly had anemia, dyserythropoiesis and ring sideroblasts (>5%) (table). There were no differences in gender, mean corpuscular volume, serum LDH level,

myeloid/erythroid ratio in bone marrow, or percentage of patients with advanced myelofibrosis (MF-2 or 3) among the 3 groups. Co-mutation in *ASXL1* was more frequent in patients with non-SF3B1 mutations than in other subgroups (p<0.01). With a median follow-up of 8.5 months, 1 patient died due to complications after stem cell transplant.

	SF3B1	non-SF3B1	no SF	p value
Age (years)	66	72	60	<0.01
Hemoglobin (g/dL)	8.9	9.4	11.8	<0.01
Dyserythropoiesis	80%	47%	17%	<0.01
Ring sideroblasts	80%	19%	8%	<0.01
ASXL1 mutation	20%	75%	29%	<0.01

Conclusions: Mutations in splicing factor genes are common in patients with PMF. *U2AF1* mutations involving codons 156 to 159 are significantly enriched. PMF patients with *SF3B1* mutations more commonly have significant anemia, dyserythropoiesis, and ring sideroblasts. PMF patients with splicing factor mutations other than SF3B1 were significantly older and frequently had co-mutation in *ASXL1.*

1348 Pre-B Acute Lymphoblastic Leukemia in Adolescents and Young Adults: Demographic and Cytogenetic Analysis at a Single Institution

Luke Olson[1], Hana Aviv[1]
[1]Rutgers Robert Wood Johnson Medical School, New Brunswick, NJ

Disclosures: Luke Olson: None

Background: Philadelphia (Ph)-like acute lymphoblastic leukemia (ALL) is an emerging subtype of ALL that has been consistently associated with a high-risk disease course in young children. However, data regarding the incidence of Ph-like ALL in older children and young adults are limited. Here we seek to better characterize the clinicopathologic and cytogenetic features of this patient population at our institution.

Design: A retrospective review of our institution's cytogenetic database was performed to identify all new and recurrent cases of pre-B ALL diagnosed between January 1, 2016 and September 20, 2018. Clinical parameters (including patient ethnicity), laboratory values and bone marrow specimen data were uncovered through review of the electronic medical record. Patients over 10 years of age at disease diagnosis that were born between 1980 and 2006 were selected for further analysis. Cytogenetic abnormalities were categorized as low risk (hyperdiploidy, t(12;21)), intermediate risk (all other abnormalities including normal cytogenetics), and high risk (Ph chromosome, Ph-like abnormality, hypodiploidy).

Results: A total of 88 cases of initial diagnosis or recurrent disease were identified, including 30 Hispanic individuals (34.1%). Twenty-five patients met our age criteria for continued analysis. Of these individuals, 14 were Hispanic (56%). These Hispanic patients were overwhelmingly male (78.6%). Five of the 25 patients had a white blood cell count (WBC) over 50 x 10^9/L at diagnosis. All of these patients were Hispanic, 4 were male and 4 had high-risk cytogenetic abnormalities (including 3 with Ph-like alterations). Cytogenetic analysis of the 25 patients revealed 4 patients within the low-risk category (16%), 12 within the intermediate risk category (48%) and 9 within the high risk category (36%). Of Hispanic patients, 7 (7/14, 50%) had high risk cytogenetics compared to 2 non-Hispanic patients (2/11, 22%). Ph-like abnormalities were seen in 6 patients (24%), with *CRLF2* abnormalities in 5 cases and *PDGFR-β* alteration in one case), including 4 Hispanic males, one non-Hispanic male and one Hispanic female.

Conclusions: Our findings show a high frequency of Ph-like abnormalities in our adolescent and young adult population. The occurrence of these abnormalities was strongly associated with Hispanic ethnicity as well as high-risk clinical parameters such as male sex and elevated initial WBC count.

1349 Survey of ERG Expression in Normal Bone Marrow and Myeloid Neoplasms

Nicholas Olson[1], Deborah Ornstein[2], Konstantinos Linos[3]
[1]University of Michigan, Ann Arbor, MI, [2]Dartmouth Hitchcock Medical Center, Lebanon, NH, [3]Dartmouth-Hitchcock Medical Center, Lebanon, NH

Disclosures: Nicholas Olson: None; Deborah Ornstein: None; Konstantinos Linos: None

Background: Translocations involving *ERG* have been identified in prostatic adenocarcinoma, but have also been detected in rare cases of acute myeloid leukemia (AML). *ERG* plays critical roles in the hematopoietic stem cell differentiation and regulates self-renewal. The immunohistochemical (IHC) stain for ERG protein is a useful diagnostic marker for vascular tumors, prostate adenocarcinoma, and leukemia cutis among others. We incidentally noted strong ERG expression in the granulocytic population during routine evaluation of bone

marrow specimens for the presence of metastatic prostatic adenocarcinoma. As there is minimal information in the medical literature about ERG expression in normal bone marrow cells or within myeloid neoplasms, we undertook the current study.

Design: We searched the Dartmouth-Hitchcock Medical Center electronic archive for trephine bone marrow biopsies performed over the previous year in which IHC for myeloperoxidase (MPO) was used to assess the granulocytic populations. We performed IHC staining for ERG on these cases and compared the results with the results obtained from MPO IHC performed previously. We scored correlation between ERG and MPO expression on a scale of 0 – 3+ as follows: zero (no correlation), 1+ (0-25%), 2+ (25-75%), and 3+ (>75%).

Results: We identified 28 bone marrow biopsy specimens that met the inclusion criteria (N = 6 normal, N = 12 AML, N = 6 myeloproliferative neoplasms (MPN) and N = 4 myelodysplastic (MDS)/MPN) (Table). Strong nuclear ERG staining was present within the granulocytes and precursors with 3+ concordance in 26/28 (93%) cases in both normal bone marrows (Figure 1) and in those with myeloid neoplasms (Figure 2). Fifty percent of AML cases demonstrated more staining in the leukemic cells for ERG than for MPO. In 5 of 6 (83%) MPN, there was 3+ concordance between ERG and MPO expression. All four biopsies with MDS/MPN showed strong nuclear ERG staining in granulocytes, precursors and monocytes in near 100% concordance with MPO.

Case	Age	Diagnosis	Cytogenetics	Concordance with MPO staining
1	55 F	Normal	Normal	3+
2	69 M	Normal	46,XY,del(5)(q13q33)[2]/46,XY[18]	3+
3	69 F	Normal	Not performed	3+
4	55 M	Normal	Normal	3+
5	14 M	Normal	Normal	3+
6	72 F	Normal	Normal	3+
7	78 F	AML	46,XY,-7,+12,del(12)(q15q24.3)	3+
8	63 M	AML	Normal	3+
9	59 F	AML	Normal	3+
10	71 F	AML	Failed	3+
11	68 M	AML	Normal	3+
12	59 M	AML	Normal	3+
13	67 M	AML	Complex	3+
14	56 F	AML	Normal	3+
15	64 M	AML	Complex	2+
16	64 M	AML	Normal	3+
17	15 F	AML	Complex	3+
18	65 M	AML	Normal	3+
19	47 M	CML	46,XY,t(9;22)(q34;q11.2)	3+
20	73 M	PV	Normal	3+
21	67 F	PMF	46,XX,del(7)(q22)	3+
22	88 M	PMF	45,X,-Y	3+
23	60 M	PMF	49,XY,+12,+18,+19	3+
24	64 F	PMF	Normal	2+
25	88 F	CMML-I	Normal	3+
26	75 M	CMML-I	Normal	3+
27	75 M	CMML-II	Normal	3+
28	56 F	Atypical CML	Normal	3+

Figure 1 - 1349

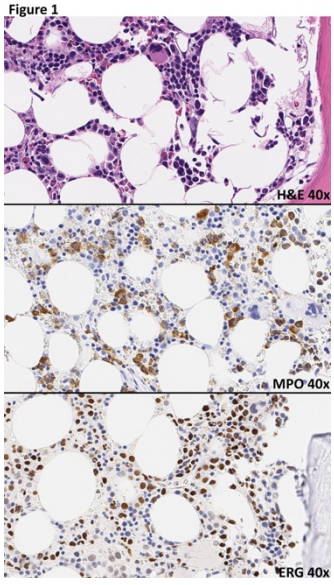

Figure 2 - 1349

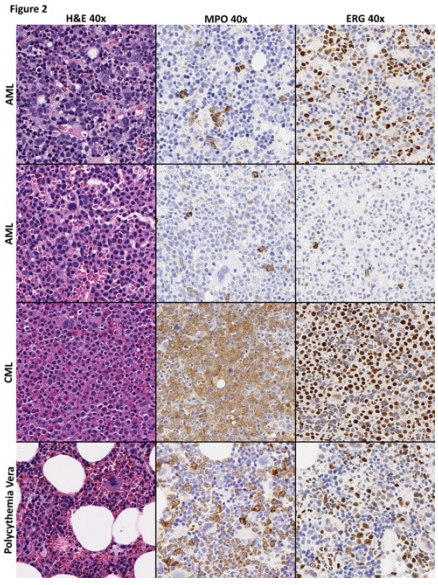

Conclusions: In summary, we demonstrated concordance between ERG and MPO expression by IHC staining in normal bone marrows, MPN, AML, and MDS/MPN. Additionally, ERG had the advantage of being a nuclear stain with considerably less background staining than MPO. We conclude that IHC for ERG has the potential to offer pathologists a potentially superior staining alternative to MPO for identification of myeloid cell populations in normal and disease states.

1350 Analysis of Bone Marrow Morphologic Features in Patients with Myeloproliferative Neoplasms following Ruxolitinib Therapy

Nicholas Olson[1], Sarah Choi[1]
[1]University of Michigan, Ann Arbor, MI

Disclosures: Nicholas Olson: None; Sarah Choi: None

Background: Myeloproliferative neoplasms (MPNs) are characterized by initial hypercellularity with accompanying peripheral blood cytoses, followed in later stages by changes in stromal composition including fibrosis and osteosclerosis. Genetic alterations which activate the JAK/STAT signaling pathway are detected in the majority of MPNs. Recent therapies, such as ruxolitinib, have sought to target and block this pathway. Ruxolitinib has been reported to improve symptoms and reduce spleen size in MPN patients, but studies examining the effects on bone marrow morphology (BM) have as of yet been limited.

Design: A cohort of 20 patients who had received ruxolitinib therapy for a diagnosis of MPN was retrospectively identified under an IRB approved protocol. Bone marrow morphologic features (including cellularity, fibrosis, and erythroid and myeloid components) and CBC parameters were collected pre and post-therapy. Pre-treatment parameters were compared to post-treatment time points (3, 6, 9, 12, 18, 24, 30, 36, 44 months). Statistical analysis was performed using ANOVA.

Results: Of a total of 35 post-treatment bone marrow biopsies, 11 patients had at least 2 post-treatment biopsies and 4 patients had 3 biopsies. When we analyzed the kinetics of bone marrow cellularity, following ruxolitinib, cellularity appeared to decrease steadily reaching a nadir at approximately 9 months followed by a return to pretreatment levels at 12 months (p=0.0010). This trend was observed even when accounting for discontinuation of therapy. On the other hand, bone marrow fibrosis and erythroid and myeloid precursors percentages did not show any statistically different changes over the same time course. Interestingly in the CBC, the hemoglobin concentration (but not platelet count or white blood cell count) showed a similar profile and time course which paralleled cellularity changes (p=0.0044).

Conclusions: Patients who received ruxolitinib therapy showed transient decreases in bone marrow cellularity and hemoglobin concentration without significant changes in other parameters, including fibrosis and other CBC parameters. The reason for this finding warrants further investigation, as it may indicate either a resistance to therapy that develops over time and/or it may potentially allude to other underlying physiologic or pathologic changes that may be affected by inhibition of JAK/STAT signaling.

1351 Comparative Evaluation of Flow Cytometry (FC) and Morphology for Detecting Malignant Cells in Cerebrospinal Fluid (CSF) from Patients with Known Hematologic Neoplasms

Horatiu Olteanu, Mayo Clinic, Rochester, MN

Disclosures: Horatiu Olteanu: None

Background: The National Comprehensive Network (NCCN) guidelines indicate routine evaluation of CSF in the staging and surveillance of patients with hematologic malignancies that have a high risk for CNS involvement. The guidelines recommend for FC immunophenotyping to be performed in addition to morphologic review of CSF specimens, as the two modalities combined improve detection of neoplastic cells. However, it is less clear what the optimal criteria (such as total nucleated cell [TNC] count) are for clinically appropriate use of FC in CSF specimens, and what incremental benefit CSF FC for hematologic malignancies provides over morphologic assessment alone. To explore this question, we undertook a pilot project whereby FC was performed in each case irrespective of morphology status, in this patient category.

Design: 570 CSFs from 163 consecutive patients were selected. Diagnoses included AML (54), B-ALL (31), Burkitt lymphoma (3), CLL/SLL (1), DLBCL (51), extranodal NK/T-cell lymphoma (3), mantle cell lymphoma (1), plasma cell myeloma (5), and T-ALL (14). For each case, cytology review of Wright-Giemsa stained cytospin slides and analysis of 8-color FC data was performed retrospectively in a blinded fashion.

Results: 149/570 (26%) and 144/570 (25%) cases showed neoplastic cells by morphology and FC, respectively. 138/149 (93%) (+) cases by morphology were also (+) by FC. All 144 (+) CSFs by FC were also (+) by morphology, except for 4 AML cases (3%; with 0.11-0.26% blasts by FC). When comparing (+) vs. (-) FC cases, there was no significant difference in the mean (±SD) TNC count/uL: 43±210 vs. 10±46 (p=0.139), or in the number of cells recovered for FC analysis: 4801±5327 vs. 4635±5792 (p=0.905).

Conclusions: To our knowledge, this is the largest cohort of patients with prior hematologic neoplasms that underwent a comparative FC and morphologic assessment for CSF involvement by malignant cells. FC was (+) in 25% of cases, a rate higher than reported in the literature (<10%) and that underscores the sensitivity of FC in detecting malignant cells in CSF, irrespective of the TNC count. We show a high correlation between morphology and FC in both (+) and (-) cases, with only 4/570 cases (1%) demonstrating blasts by FC in the absence of any morphologic evidence of disease. Our results support a judicious approach whereby FC evaluation is guided by morphologic triage in the vast majority of cases. The clinical utility of minimal residual disease detection in CSF by FC warrants further investigation.

1352 Quantitative Analysis of a Multiplexed Immunofluorescence Panel for Ki67, MYC and CD20 in Diffuse Large B Cell Lymphoma

Ming Liang Oon[1], Shuangyi Fan[2], Michal Hoppe[3], Phuong Mai Hoang[3], Anand D. Jeyasekharan[3], Siok-Bian Ng[3]
[1]National University Hospital, Singapore, [2]Yong Loo Lin School of Medicine, National University of Singapore, [3]National University of Singapore

Disclosures: Ming Liang Oon: None; Shuangyi Fan: None; Siok-Bian Ng: None

Background: Quantitative techniques in immunohistochemistry (IHC) and immunofluorescence (IF) using automated software to perform digital image analysis provide objective and accurate quantification of protein expression. This has been studied in epithelial cancers but remains relatively unexplored in lymphoma specimens. The aim of this study is to demonstrate the feasibility of applying an automated, quantitative analysis of a multiplexed IF panel in the study of the expression of Ki67 and MYC in diffuse large B cell lymphoma (DLBCL) specimens, and to compare this with conventional scoring by pathologists.

Design: Multiplexed IF staining for CD20/Ki67/MYC was applied to FFPE sections from DLBCL (n=30). Image acquisition and automated analysis of the stained samples were performed with Vectra 2 multispectral automated microscope and inForm 2.2 image analysis software. The same images for MYC and Ki67 were scored independently by two pathologists. Correlation of MYC and Ki67 expression between the two methods were performed for 27 and 26 cases, respectively.

Results: There was good correlation between pathologist and inForm scoring for both markers with r= 0.913 and r = 0.786 for MYC and Ki67, respectively. A variance analysis of mean MYC and Ki67 expression revealed that an average of 5 and 3 fields, respectively per case, were required to arrive at consistent scoring (Figure 1). The automated method was able to further quantify the co-localized expression of Ki67 and MYC in CD20-positive tumor cells, which is not feasible with conventional IHC. The results showed that at single-cell resolution, within a given tumor, most MYC-positive cells were Ki67 positive (Figure 2). This phenomenon was noted in almost all cases studied. However, there was wide variability in the co-expression of MYC in Ki67-positive cells, ranging from 80% to 0%, confirming that there are mechanisms other than MYC activation that drives cellular proliferation in DLBCL.

Figure 1 - 1352

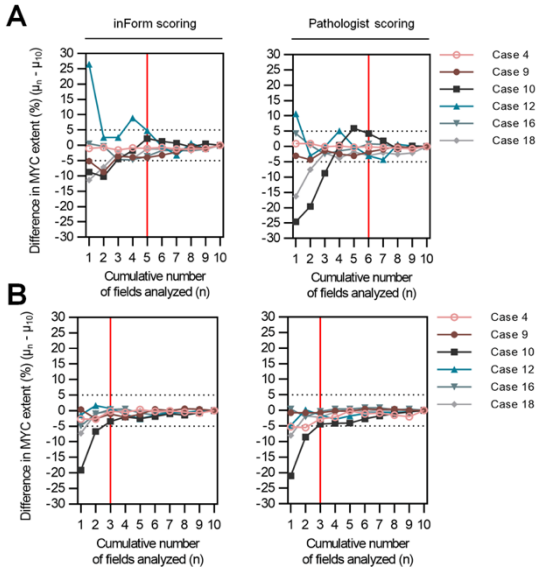

Figure 2 - 1352

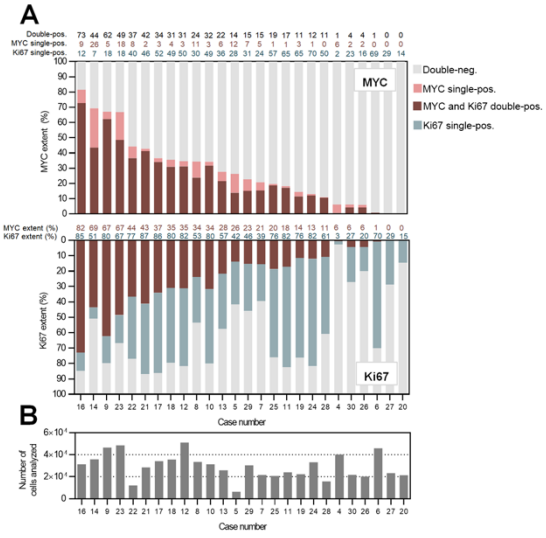

Conclusions: We demonstrate that it is feasible to apply CD20/KI67/MYC multiplex IF in DLBCL. The scoring of Ki67 and MYC expression using inForm software is comparable with conventional scoring by pathologists. Importantly, the study highlights the advantage of the automated multiplex IF platform in allowing precise quantification of multiple colocalized signals in single cells, yielding novel parameters, eg. percentage of MYC in Ki67-positive cells, which can be tested for clinical relevance in larger data sets.

1353 Genomic alterations in patients with mosaic loss of the Y chromosome in bone marrow cells

Madhu Ouseph[1], Valentina Nardi[2], David Steensma[3], Scott Lovitch[4], Robert Hasserjian[2], Paola Dal Cin[4], Olga Weinberg[5]
[1]Brigham and Women's Hospital, Harvard Medical School, Dedham, MA, [2]Massachusetts General Hospital, Boston, MA, [3]Dana-Farber Cancer Institute, Boston, MA, [4]Brigham and Women's Hospital, Boston, MA, [5]Children's Hospital Boston, Boston, MA

Disclosures: Madhu Ouseph: None; Valentina Nardi: None; David Steensma: None; Scott Lovitch: None; Robert Hasserjian: None; Paola Dal Cin: None; Olga Weinberg: None

Background: Loss of the Y chromosome (-Y) is one of the most common somatic genomic alterations in hematopoietic cells in men and recent studies suggest a likely role of -Y in oncogenesis. However, due to the high prevalence of -Y in the healthy older population, differentiating isolated -Y associated with clonal hematologic processes from aging-associated mosaicism can be difficult in the absence of definitive morphological features of disease. Various studies have proposed different cut offs of involved metaphases for considering –Y as a disease-associated clonal population. In this study we evaluated patients with isolated -Y for hematological neoplasia-associated genomic alterations to assess the frequency with which -Y is associated with other clonal variants.

Design: We searched the database at Cytogenetic laboratory for patients from Brigham and Women's Hospital and Massachusetts General Hospital with isolated -Y identified on bone marrow karyotype and reviewed clinical records. We excluded patients with recently diagnosed lymphoid malignancies and those who were receiving chemotherapy. We performed next generation sequencing (NGS) molecular analysis on cytogenetic cell pellets for) for genes associated with hematological neoplasms.

Results: We identified 62 patients with a median age of 75 years (range 46-90) with -Y as isolated cytogenetic abnormality. The percentage of –Y metaphases was 0-24% in 10 patients (16%), 25-49 in 18 (29%), 50-74 in 7 (11%) and 75-100 in 27 (44%). The percentage of -Y was significantly higher in older patients (p = 0.011). A threshold of ≥ 75% -Y was significantly associated with a higher likelihood of MDS (p = 0.04), while ≤ 25% -Y was associated with a normal morphology (p = 0.011). Among those patients who did not yet have diagnostic features of MDS, ≥ 75% -Y was associated with a higher incidence of subsequent MDS diagnosis (p = 0.024, median follow up of 13.5 months). A higher -Y percentage (≥ 75%) was associated with greater likelihood of having a somatic mutation associated with myeloid neoplasm (p=0.0005) and a higher number of myeloid mutations (p = 0.0062 and Table 1).

	[%]-Y			
	0-24	25-49	50-74	75-100
Age (yrs)				
25-49	0	1	0	0
50-74	7	7	3	9
75-100	3	10	4	18
Pathologic diagnosis				
No dysplasia	3	10	3	9
Minimal dysplasia, not diagnostic of MDS	4	4	1	0
MDS/t-MDS	2	4	2	18
Aplastic anemia	1	0	1	0
Somatic mutations	10	18	7	27
Number of patients with any somatic mutation	5 (50%)	3 (16.7%)	4 (57.1%)	20 (74.07%)
Mean number of somatic mutations per patient	1.1	0.22	1	1.78
Number patients with most frequent mutations				
TET2	1	1	2	9
SF3B1	1	0	0	8
JAK2	0	0	1	3
U2AF1	0	0	0	3
SH2B3	0	0	0	2
STAG2	0	0	0	2
ZRSR2	1	0	0	2
ASXL1	1	1	1	2
EZH2	0	0	0	2
CBL	0	0	0	2

Conclusions: Our findings indicate that ≥ 75% -Y in bone marrow is associated with a high frequency of molecular alterations in genes commonly seen in myeloid neoplasia and greater incidence of morphologic features diagnostic of MDS. These observations highlight the importance of NGS evaluation of patients with high -Y percentage.

1354 Differential Prognostic Impact of Myeloid Sarcoma in Patients with Acute Myeloid Leukemia at Presentation and Relapse

Anna Owczarczyk[1], Sarah Choi[1]
[1]*University of Michigan, Ann Arbor, MI*

Disclosures: Anna Owczarczyk: None; Sarah Choi: None

Background: Myeloid sarcoma (MS), a rare extramedullary tumor that is considered a subtype of acute myeloid leukemia (AML) according to the World Health Organization (WHO), may develop *de novo*, concurrently, or after AML, myelodysplastic syndrome (MDS), myeloproliferative disorder (MPN) or MDS/MPN. Additionally, MS may be the first evidence of AML, or precede it by years. Lastly, MS can represent the initial stage of relapse in a treated AML patient. Given the rarity of MS, much of the current knowledge is based on few retrospective studies and case reports. In this study, we aimed to expand upon these observations by evaluating clinical, cytogenetic and molecular features, and survival outcomes of myeloid sarcoma patients at presentation and relapse.

Design: A cohort of 40 patients with a diagnosis of myeloid sarcoma (2007-2018) was identified through a retrospective search of clinical/pathology databases through an IRB-approved protocol at our institution. A control group of *de novo* (20 cases) and relapsed AML (19 cases) within the same time period was used for comparison. Survival analysis was performed using GraphPad Prism 7 software, and statistical analysis was performed using the Gehan-Breslow-Wilcoxon test (limit of significance; $p < 0.05$).

Results: Most MS cases represented relapses of prior AML (50%) or transformations from MDS or MDS/MPN (25%). Top sites of involvement by MS included soft tissue and skin (combined ~40%). The presence of myeloid sarcoma at the time of diagnosis had no impact on overall survival of patient with *de novo* AML. However, a significant difference in survival was seen in relapsed AML presenting

as MS, which was dependent on the presence of concurrent bone marrow (BM) involvement. Isolated MS relapse showed improved survival compared to cases which had overt concomitant BM relapse (p = 0.0135) and to cases which had non-MS relapse (p = 0.0436).

Conclusions: The findings suggest that isolated myeloid sarcoma relapse may not necessarily portend a poor prognosis, in contrast to cases with overt BM relapse, which show significantly worse survival similar to non-MS AML relapse. Assessment of BM involvement in patients who present with MS relapse may therefore be an important step in accurate prognostication. Additional studies examining the relative contribution of other factors, including genetic and molecular information, on outcomes of patients with myeloid sarcoma relapse are warranted.

1355 Expression of SMARCB1/INI1 is Decreased in Chronic Myeloid Leukemia and B Lymphoblastic Leukemia/ Lymphoma with BCR-ABL1 Rearrangements

Ozgur Ozkayar[1], Ridas Juskevicius[2]
[1]Merkez/Corum, Turkey, [2]Vanderbilt University Medical Center, Nashville, TN

Disclosures: Ozgur Ozkayar: None; Ridas Juskevicius: None

Background: *SMARCB1/INI1* is a tumor suppressor (TS) encoding one of the subunits of highly conserved SWI/SNF chromatin remodeling complex with critical roles in controlling cell self-renewal and differentiation. INI1 is normally expressed in all nucleated cells. In mice, loss of single copy of *Smarcb1* leads to cancer. Inactivation of *SMARCB1/INI1* is a driver event in malignant rhabdoid tumors. Chronic myeloid leukemia (CML) and a subset of B-lymphoblastic leukemias (B-ALL) have t(9;22)(q34.1;q11.2) known as Philadelphia (Ph) chromosome involving *BCR* at the same locus as *SMARCB1/INI1*. Deletions of 22q11 including *SMARCB1/INI1* region on derivative 9 are frequent in CML and may result in haploinsufficiency of this TS gene contributing to outcome. This study's main aim is to assess expression of INI1 in bone marrow (BM) samples of CML and Ph+ B-ALL as compared to Ph- control BM samples.

Design: 13 CML, 11 B-ALL (5 Ph+) and 12 uninvolved BM biopsies were included in this study. IHC was performed using INI1 antibody (clone MRQ-27) validated for clinical use. Tonsil tissue was used for comparison. Image analysis was performed on the whole slide images using QuPath software platform after manual annotation of areas of interest and calibration of negative, weak (1+), moderate (2+) and strong (3+) staining thresholds. For precise comparison of the nuclear staining we used H-score where intensity of expression (0, 1+, 2+, 3+) with precise cell-by-cell total in each level was computed. Furthermore, to account for between-runs and within-run staining variation we calculated and compared tumor/control (T/C) H-score ratios.

Results: INI1 expression, as expected, was present in most nucleated cells in all Ph- cases. The overall INI1 staining of uninvolved control BM tissue was significantly weaker than tonsil control tissue (mean H-score 126 vs 178, p<0.001, t-Test, two-tail). When we compared all Ph+ and Ph- BM samples the mean H-score was significantly lower in Ph+ BMs (106 vs 156) which was also true using T/C H-score ratios (Figures 1 & 2, ** indicates p<0.01). Furthermore, the INI1 mean H-score was significantly lower in CML cases as compared to BM controls (99 vs 126, p=0.03).

Figure 1 - 1355

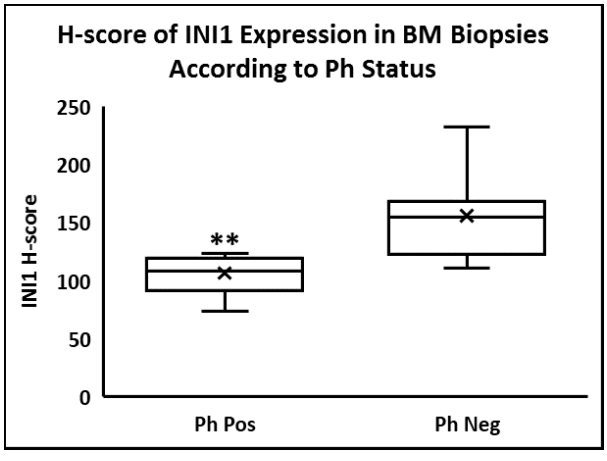

Figure 2 - 1355

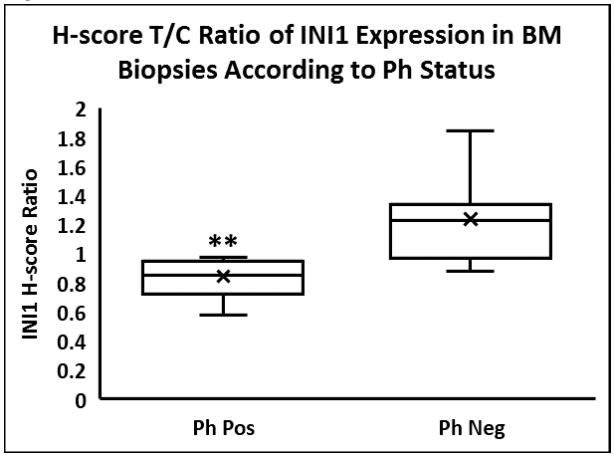

Conclusions: Expression of INI1 in CML and Ph+ B-ALL is decreased as compared to the Ph- control samples. This finding supports a possibility of *SMARCB1/INI1* haploinsufficiency in neoplasms with t(9;22), possibly due to one copy deletion. Further studies are needed to investigate clinical and diagnostic significance of this finding.

1356 Pathogenic RUNX1 Variants Frequently Co-Occur with Mutations in Genes Regulating Chromatin or RNA Splicing in a Large Cohort of Myeloid Neoplasms

Lincoln Pac[1], Adam Clayton[2], Kristin Karner[3], Jay Patel[1]
[1]University of Utah/ARUP Laboratories, Salt Lake City, UT, [2]ARUP Laboratories, Salt Lake City, UT, [3]University of Utah, Salt Lake City, UT

Disclosures: Lincoln Pac: None; Adam Clayton: None; Kristin Karner: None; Jay Patel: None

Background: *RUNX1* mutations in acute myeloid leukemia (AML) define a new provisional entity in the 2016 WHO classification and are associated with a worse prognosis. We hypothesize that variant allele fraction (VAF) data derived from NGS studies may provide insights into the clonal architecture of *RUNX1*-mutated myeloid neoplasms.

Design: This study was approved by our Institutional Review Board. Diagnostic peripheral blood or bone marrow samples collected 2014-2018 from *RUNX1*-mutated patients (n=708) were analyzed with targeted sequencing of a panel of 58 genes known to be mutated in myeloid neoplasms. Genomic DNA was extracted from samples by the Puregene method (Qiagen), followed by library preparation and enrichment for regions of interest by solution capture (SureSelect, Agilent). Massively parallel sequencing was performed on Illumina platforms. Genetic variants were identified by FreeBayes, LoFreq, and Scalpel (single nucleotide variants and small insertions/deletions), and Pindel and Manta (larger insertions/deletions) algorithms. Variants detected were subjected to a rigorous manual curation process.

Results: Of 708 patients with at least one pathogenic *RUNX1* variant, 3.2% (23/708) had *RUNX1* as the sole mutated gene and 96.8% had 1-14 concurrent pathogenic mutations in other genes. The median patient age was 69 years (range <1-102 years) with a male to female ratio of 2.5. A majority of cases (83%, 591/708) had a reported diagnosis of myeloid neoplasm (AML, MDS, MPN, or MDS/MPN) with 50% reported to have AML. 851 total pathogenic *RUNX1* mutations were identified, since 7.5% (53/708) of samples contained 2 or more *RUNX1* variants. Variants with very high VAFs (>90%, n=9) occurred more commonly in *RUNX1* than other genes analyzed (Figure 1). The most common co-mutations (occurring in ?50 patients, Table 1) were in genes involving chromatin regulation or RNA splicing (ASXL1, SRSF2, BCOR, STAG2, EZH2, SF3B1, U2AF1, PHF6) and DNA methylation (TET2, DNMT3A, IDH1/2). Co-mutations in genes defining other WHO diagnoses (NPM1, CEBPA) were infrequent or sub-clonal (VAF <10%).

Genes	Number of mutated patients (%)	Median variant allele fraction (%)
Chromatin-Spliceosome		
RUNX1	708 (100)	30.1
ASXL1	332 (46.9)	23.8
SRSF2	243 (34.3)	39.4
BCOR	141 (19.9)	33.0
STAG2	116 (16.4)	39.6
EZH2	79 (11.2)	47.1
SF3B1	74 (10.5)	41.0
U2AF1	74 (10.5)	36.0
PHF6	52 (7.3)	34.2
DNA Methylation		
TET2	223 (31.5)	38.3
DNMT3A	132 (18.6)	40.9
IDH2	76 (10.7)	37.8
IDH1	50 (7.1)	27.3
Cell Signaling		
FLT3	110 (15.5)	1.8
NRAS	92 (13.0)	24.4

Figure 1 - 1356

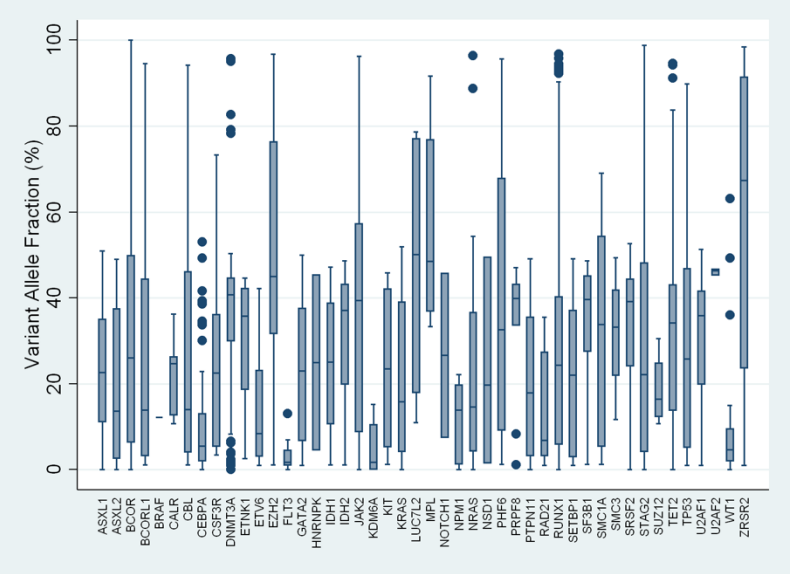

Conclusions: These data suggest pathogenic *RUNX1* variants predominately co-mutate with genes involved in chromatin regulation or RNA splicing (chromatin-spliceosome), and segregate from mutations in *NPM1* and *CEBPA*. *RUNX1* mutations rarely occur as a sole variant with a high VAF, suggesting monoallelic *RUNX1* mutations with loss of heterozygosity are infrequent drivers in myeloid neoplasms.

1357 Clinicopathologic and Genetic Characterization of non-AML NPM1-Mutated Myeloid Neoplasms

Sanjay Patel[1], Caleb Ho[2], Sam Sadigh[3], Adam Bagg[4], Julia Geyer[5], Mina Xu[6], Emily Mason[7], Elizabeth Morgan[1], David Steensma[8], Eric Winer[8], Robert Hasserjian[9], Olga Weinberg[10]
[1]Brigham and Women's Hospital, Boston, MA, [2]Memorial Sloan Kettering Cancer Center, New York, NY, [3]Hospital of the University of Pennsylvania, Philadelphia, PA, [4]University of Pennsylvania, Philadelphia, PA, [5]Weill Cornell Medicine, New York, NY, [6]New Haven, CT, [7]Vanderbilt University Medical Center, Nashville, TN, [8]Dana-Farber Cancer Institute, Boston, MA, [9]Massachusetts General Hospital, Boston, MA, [10]Children's Hospital Boston, Boston, MA

Disclosures: Sanjay Patel: None; Caleb Ho: None; Sam Sadigh: None; Adam Bagg: None; Julia Geyer: None; Mina Xu: None; Emily Mason: None; Elizabeth Morgan: None; David Steensma: None; Eric Winer: None; Robert Hasserjian: None; Olga Weinberg: None

Background: Nucleophosmin gene (*NPM1*) mutations are classically associated with de novo acute myeloid leukemia (AML), but are rarely encountered in non-AML myeloid neoplasms with <20% marrow or blood blasts. Whether or not *NPM1*mutations should be considered AML-defining remains to be determined. This study aimed to characterize the significance of *NPM1* mutations in a series of myeloid neoplasms with <20% marrow blasts.

Design: The pathology records from seven major academic medical institutions were queried for cases of *NPM1*-mutated myeloid neoplasms with <20% bone marrow and blood blasts at diagnosis. NGS data were evaluated in conjunction with clinicopathologic variables to identify any markers predictive of progression to AML and/or shorter overall survival (OS).

Results: 40 cases were identified, including CMML (9), MDS (23), t-MDS (5) and MDS/MPN-unclassifiable (3). Patients presented at a median age of 63, with WBC of 3.5 K/uL and 10% marrow blasts; 87% of cases had at least 5% marrow blasts and 32/37 (86%) had a normal karyotype. The median somatic mutation burden at diagnosis was 2. Twenty patients progressed to AML (median 5.2 mo); no specific factors were identified that correlated with progression to AML, including patient age, WBC, blast percentage, mutation burden, *NPM1* variant allele fraction, or co-occurrence of common mutations (p>0.05 for all). When compared to a control group of de novo *NPM1* mutated AML cases (n=109), the non-AML cases showed significantly more frequent mutations in spliceosome pathway genes (p=0.02), but lower rates of DNA methylation pathway (p=0.008) and *FLT3*-ITD mutations (p<0.0001). Multivariable analysis performed on the non-AML cases together with a subset of AML cases enriched for HMA therapy (n=62) revealed older age (p=0.002), abnormal karyotype (p=0.005), and higher mutational load (p=0.04) as independent predictors of shorter OS, while treatment with induction chemotherapy (p=0.048) and SCT (p=0.003) correlated with longer OS. Bone marrow blast percentage did not independently impact outcome in this analysis.

Conclusions: *NPM1*-mutated myeloid neoplasms with <20% blasts at diagnosis are rare and present a diagnostic and management dilemma. We find that the vast majority of these cases have excess (>5%) bone marrow blasts and a normal karyotype, and that a large

subset (50%) progress rapidly to AML. Our findings raise the possibility that many of these cases may represent early AML rather than MDS or MDS/MPN entities, as they are currently classified.

1358 Correlation of high NPM1 mutant allele burden at diagnosis with minimal residual disease in de novo AML

Sanjay Patel[1], Geraldine Pinkus[1], Lauren Ritterhouse[2], Jeremy Segal[3], Tamara Restrepo[4], Marian Harris[5], Paola Dal Cin[1], Robert Hasserjian[6], Olga Weinberg[5]
[1]Brigham and Women's Hospital, Boston, MA, [2]University of Chicago Medical Center, Chicago, IL, [3]University of Chicago, Riverside, IL, [4]Boston Children's Hospital, Boston, MA, [5]Children's Hospital Boston, Boston, MA, [6]Massachusetts General Hospital, Boston, MA

Disclosures: Sanjay Patel: None; Geraldine Pinkus: None; Lauren Ritterhouse: None; Jeremy Segal: None; Tamara Restrepo: None; Marian Harris: None; Paola Dal Cin: None; Robert Hasserjian: None; Olga Weinberg: None

Background: Acute myeloid leukemia (AML) with a mutated nucleophosmin (*NPM1*) gene is typically associated with a favorable outcome, although the presence of minimal residual disease (MRD) following induction chemotherapy has been shown to portend a poor prognosis. We recently found that high *NPM1* variant allele fraction (VAF) at diagnosis is associated with significantly shorter survival (Patel et al. *Blood*. 2018). In this study, we examined a subset of these patients for MRD by next-generation sequencing (NGS) and mutant protein expression by immunohistochemistry (IHC).

Design: An NGS assay designed to detect low-levels of mutated *NPM1* gene sequence (sensitivity <0.2%) using high read depth and molecular barcodes as error correction was performed on DNA extracted from cytogenetic cell pellets corresponding to the morphologic first remission (CR1) biopsy timepoint. Only patients who achieved CR1 according to standard criteria were included. Bouin- and B plus-fixed paraffin embedded morphologic CR1 bone marrow tissue was stained using an NPM1 mutant protein-specific antibody for these same cases. Staining was scored visually to identify positive cases (?1 cells) and quantify cells to a maximum of 200.

Results: DNA samples from 45 patients were evaluated, including 12 cases of AML with high *NPM1* VAF (>0.43) at the initial diagnosis. A total of 35 (78%) showed molecular MRD in the CR1 sample *(NPM1* VAF range 0-0.084, median 0.0002). The *NPM1* VAF in the CR1 samples correlated significantly with the VAF detected at diagnosis (r = 0.38, p=0.01). For 22 cases with concurrent IHC data, mutant NPM1-positive cells were identified in 14/16 (88%) cases that showed MRD by molecular testing. The number of positive cells counted (range: 4-200) correlated positively with the *NPM1* MRD VAF (r = 0.85, p<0.0001). Stratification at the median MRD VAF value (>0.0002) revealed statistically significantly shorter overall (p=0.01) and event-free survival (p=0.01) in the group with higher *NPM1* MRD at CR1.

Conclusions: *NPM1* VAF at diagnosis correlates positively with the VAF in paired CR1 biopsy samples. Additionally, NPM1 IHC and molecular MRD results correlate significantly. These findings suggest that the *NPM1* VAF at diagnosis and IHC for mutant NPM1 protein in the CR1 biopsy may both be useful and cost-effective adjuncts for high-sensitivity assays to detect molecular MRD, which are not available in all practice settings.

1359 CTLA-4, a targetable immune checkpoint, is Enriched in Classic Hodgkin Lymphoma and Identifies a T-cell Population Distinct from PD-1

Sanjay Patel[1], Mikel Lipschitz[2], Jason Weirather[2], Margaret Shipp[2], Scott Rodig[1]
[1]Brigham and Women's Hospital, Boston, MA, [2]Dana-Farber Cancer Institute, Boston, MA

Disclosures: Sanjay Patel: None; Mikel Lipschitz: None; Jason Weirather: None; Margaret Shipp: *Grant or Research Support*, Bristol-Myers Squibb; *Grant or Research Support*, Merck; *Grant or Research Support*, Bayer; *Advisory Board Member*, BMS
Scott Rodig: *Grant or Research Support*, Bristol Myers Squibb; *Grant or Research Support*, Merck; *Grant or Research Support*, KITE pharmaceuticals; *Grant or Research Support*, Affimed Inc.

Background: Classic Hodgkin lymphoma (cHL) is a tumor comprised of rare atypical germinal center-derived B-cells (Reed-Sternberg [R-S] cells) embedded within an ineffective inflammatory milieu. Recent work has revealed that the cHL microenvironment is compartmentalized into “niches” rich in PD-L1-positive R-S cells and tumor-associated macrophages (TAMs), which associate with PD1+ T-cells to suppress anti-tumor immunity via PD-L1/PD-1 signaling. The focus of this study was to profile the expression and distribution of CTLA4+ T-cells, an additional targetable immune checkpoint, within the cHL microenvironment.

Design: Multiparametric immunofluorescence (MIF) staining was performed on 14 formalin-fixed paraffin-embedded (FFPE) diagnostic cHL excisional biopsy specimens and 3 reactive tonsillar tissues using a panel of six primary antibody/fluorophore pairs (PAX5/Opal 650, CD4/Opal 620, CD8/Opal 540, CTLA4/Opal 520, FOXP3/Opal 570, and PD1/Opal 690). Regions of interest were captured with Mantra Quantitative Pathology Workstation (PerkinElmer) and annotated using InForm image analysis software (PerkinElmer). Resulting data outputs were parsed using custom R algorithms to acquire counts (cells/mm^2) and percentages of cell types of interest.

Results: Patients presented at a median age of 34.5 years (range 14-68). cHL subtypes included nodular sclerosis (10) and mixed cellularity (4), including 2 EBV-positive cases. MIF analysis revealed that cHL cases were specifically enriched for CTLA4-positive cells, including both CD4+CTLA4+ (17.5% vs. 1%, p=0.0003) and CD8+CTLA4+ (2% vs. 0.1%, p=0.008) compared to tonsillar interfollicular regions. CTLA4+ positive cells were most commonly PD-1- (24% vs. 6%, p=0.004). Cell-contact analysis revealed high percentages of CTLA4+ (34 +/- 5%) and PD-1+ (13 +/- 3.5%) cells in contact with R-S cells. No significant quantitative differences were observed between cHL and reactive tonsillar tissues, with regard to other cell types analyzed.

Conclusions: In this initial cohort, we find that the tumor microenvironment of cHL is enriched for CTLA4+CD4+ T-cells, that CTLA4+ T-cells are a largely distinct population from PD-1+ T-cells, and that CTLA4+ T-cells are frequently in contact with R-S cells. These findings suggest the possibility that cHL patients are rational candidates for CTLA4-blockade immunotherapy.

1360 Program Death Ligands 1 and 2, and Galectin9/TIM3 Expression in Post-Transplant Lymphoproliferative Disorders

Nisha Patel[1], Juraj Bodo[1], Lisa Durkin[1], Eric Hsi[1]
[1]Cleveland Clinic, Cleveland, OH

Disclosures: Nisha Patel: None; Juraj Bodo: None; Lisa Durkin: None; Eric Hsi: *Primary Investigator*, Abbvie; *Primary Investigator*, Eli Lilly; *Advisory Board Member*, Seattle Genetics; *Advisory Board Member*, Celgene

Background: Impaired immune surveillance and Epstein-Barr virus (EBV) play major roles in post-transplant lymphoproliferative disorders (PTLD). Data regarding expression of program death ligands 1 and 2 (PD-L1/2) in PTLD is limited and an alternative pathway of immune evasion, the T-cell mucin-domain containing protein-3 (TIM3)/Galectin9 has yet to be investigated. Understanding immune checkpoint expression will help elucidate disease biology and has potential therapeutic implications.

Design: Twenty-eight PTLD cases from 27 patients were collected over an 11 year period. PD-L1/2 immunohistochemistry (IHC) was manually scored based on percent membranous staining on tumor cells (positive >5%). TIM3 and Galectin9 IHC were scored based on an intensity score (0-3; 1=weak, 2=moderate, 3=strong) multiplied by a percent of cells score (0-4; 0<5%, 1= 5-24%, 2=25-49%, 3=50-74%, 4=75%). TIM3 and Galectin9 were interpreted in tumor and tumor-infiltrating cells.

Results: The cohort consisted of solid organ (n=26) and stem cell (n=1) transplant recipients. PTLD subtypes included monomorphic (n=24), polymorphic (n=3) and Classic Hodgkin-Lymphoma (n=1). Monomorphic lymphomas were divided into DLBCL (n=20, GCB (n=8), non-GC (n=9), and unknown cell-of-origin (n=3)), Peripheral T-cell Lymphoma (n=1), Burkitt lymphoma (n=2), and plasma cell myeloma (n=1). Of total cases, 54% (15/28) were EBV+.

Overall, PD-L1 was detected in 50% (14/28) and PD-L2 in 18% (5/28) of PTLDs. 54% (n=15) of PTLDs express PD-L1 alone (66%, n=10), PD-L2 alone (7%, n=1), or both (27%, n=4). Within monomorphic PTLDs, EBV+ cases correlated with PD-L1/2 expression (85% vs 25% in EBV-, p= 0.012, Fisher Exact).

Overall, TIM3 was seen primarily in tumor infiltrating cells. Galectin9 also stained predominantly microenvironment cells, with only two DLBCL cases appearing positive in tumor cells. Focusing further analysis on microenvironment, TIM3/Galectin9 expression in tumor infiltrating cells correlated with one another (P=0.022, Spearman rank order). No significant difference in TIM3 or Galectin9 was seen based on EBV status.

Conclusions: Over half of PTLDs had PD-L1/2 tumor expression, correlating with EBV status. Galectin9/TIM3 was primarily expressed in tumor infiltrating cells and correlated with one another. This suggests that these pathways might be active and a potential therapeutic target.

1361 Myc and Bcl2 double expression does not impact on the prognosis of pediatric diffuse large B-cell lymphoma and high-grade B-cell lymphoma, NOS: a multicenter Italian study

Marco Pizzi[1], Alberto Bellan[1], Marta Pillon[1], Elisa Carraro[1], Davide Massano[2], Lara Mussolin[1], Federica Lovisa[1], Emanuele D'Amore[3], Massimo Rugge[4]
[1]University of Padova, Padova, Italy, [2]Padova University Hospital, Padova, Italy, [3]Ospedale S. Bortolo, Vicenza, Italy, [4]Padova, Italy

Disclosures: Marco Pizzi: None; Elisa Carraro: None

Background: Aggressive peripheral B-cell lymphomas are among the most common malignancies of the pediatric age. While much is known on Burkitt lymphoma, few studies have as yet addressed the clinic-pathological features of pediatric diffuse large B-cell lymphomas (DLBLCs) and high-grade B-cell lymphomas (HGBLs). Little is also known on the prevalence and impact of *MYC* and *BCL2* gene and

protein status in these cases. The present study thus aimed: (i) to characterize the clinic-pathological features of a nation-wide cohort of pediatric DLBCLs and HGBLs; (ii) to evaluate the prevalence and prognostic impact of *MYC/BCL2* gene and protein status; (iii) to identify possible histological features correlating with prognosis.

Design: Clinically-annotated cases of DLBLC or HGBL were retrieved from the archives of the Italian Pediatric Hematology and Oncology Association (AIEOP). Overall, 49 cases had sufficient biopsy material for further histological and phenotypic characterization (immunohistochemistry for CD10, Bcl6, MUM1, Myc, Bcl2 and CD30; *in situ* hybridization for EBER). FISH for *MYC*, *BCL2* and *BCL6* rearrangements was also performed in all cases.

Results: The study population included 20 males and 19 females, with a mean age at diagnosis of 11.7 ± 5.1 years. The majority of cases arose in immunocompetent patiens (41/49 [83.7%]), while an underlying immunodeficiency was documented in 8/49 (16.3%) cases. Histologically, most tumours were classified as DLBLC, NOS (32/49 [65.3%]) and HGBL, NOS (8/49 [16.3%]). Most DLBCL, NOS disclosed a germinal center phenotype and 11/32 (34.4%) cases showed Myc and Bcl2 concurrent positivity. Myc/Bcl2 protein status and/or other histological parameters did not correlate with patients' prognosis. Instead, the adverse clinical events were associated with an immunodeficiency status (Figure 1). Notably, immunodeficiency-related cases disclosed more frequent anaplastic morphology, CD30 positivity, non-GCB phenotype and EBER positivity ($p<0.05$). By FISH analysis, *MYC* translocations were restricted to HGBL, NOS cases, while *BCL2* and *BCL6* translocations were rare in both DLBCL and HGBL, NOS. No cases with concurrent *MYC* and *BCL2* translocations were documented.

Figure 1 - 1361

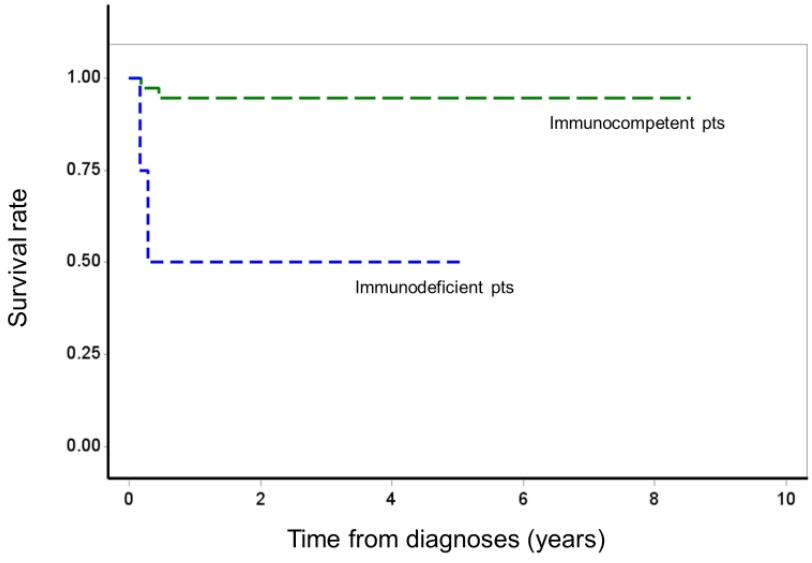

Conclusions: Myc and Bcl2 double expression is documented in a significant proportion of pediatric DLBCLs and HGBLs NOS. Unlike adult cases, the Myc/Bcl2 status is not associated with adverse prognosis. Immunodeficiency-related lymphomas carry a worse prognosis and may be identified by specific histological features.

1362 Presence of NPM1 Mutation May Alleviate the Negative Prognostic Significance of AML with Myelodysplasia-Related Changes

Maryam Pourabdollah[1], Gina Jiang[2], Eshetu Atenafu[3], Hong Chang[1]
[1]Toronto, ON, [2]University Health Network, Markham, ON, [3]University Health Network, Toronto, ON

Disclosures: Maryam Pourabdollah: None; Gina Jiang: None; Eshetu Atenafu: None; Hong Chang: None

Background: Acute myeloid leukemia with myelodysplasia-related changes (AML-MRC) is diagnosed when a patient has any one or more of the following: (1) a well-documented history of myelodysplastic syndromes (MDS) or myelodysplastic/myeloproliferative neoplasm (MDS/MPN), (2) MDS-related cytogenetic abnormality, (3) dysplasia in >50% of cells in at least two lineages (multilineage dysplasia). Generally, patients with AML-MRC have poor prognosis, however, they are still a group with heterogenous outcome. The prognostic significance of the *NPM1* mutation in patients within AML-MRC is unclear.

Design: Our retrospective study included 154 adult AML patients diagnosed with AML-MRC at our institution. We investigated the prognostic significance of relevant clinical and laboratory parameters including multilineage dysplasia, myelodysplasia-related cytogenetic

changes, previous MDS history, *NPM1* mutation, *FLT3*-ITD, age (>60 years), high WBC count (>30 x 10^9 per litre), and stem cell transplantation. Furthermore, 105 adult AML not otherwise specified (AML-NOS) with normal karyotype and wild-type *NPM1* were used as a control group.

Results: The *NPM1* mutation was detected in 14% of patients and *FLT3*-ITD was detected in 12%. 37% of patients had previous MDS history, 31% had MDS-related cytogenetic changes, and 32% had multilineage dysplasia. 23% of patients received stem cell transplantation. On univariate analysis, absence of MDS-related cytogenetic changes, multilineage dysplasia, *NPM1* mutation and stem cell transplantation were associated with longer EFS (P = 0.038, P = 0.004, P = 0.015, P < 0.0001, respectively) and OS (P = 0.045, P = 0.001, P = 0.015, P < 0.0001, respectively). Multivariate analysis confirms *NPM1* mutation and stem cell transplantation were independent predictors for longer EFS (P = 0.047, P < 0.001, respectively) and OS (P = 0.012, P = 0.0001, respectively). AML-MRC patients with mutated *NPM1* had similar outcome to the normal karyotype AML-NOS control group. However, AML-MRC patients with wild-type *NPM1* were associated with shorter EFS and OS (P = 0.003, P < 0.0001, respectively) when compared to the control group.

Conclusions: Presence of *NPM1* mutation confers a favorable outcome and supersedes the originally poor prognosis of AML-MRC. AML-MRC patients with mutated *NPM1* have comparable outcomes to AML-NOS patients with normal karyotype and wild-type *NPM1*.

1363 The Effects of Hypomethylating Agents on Mutational Profiles in Patients with Myelodysplastic Syndromes

Jihui Qiu[1], Priya Velu[2], Jason Rosenbaum[3], Daria Babushok[2], Adam Bagg[2]
[1]Jefferson Health New Jersey, Cherry Hill, NJ, [2]University of Pennsylvania, Philadelphia, PA, [3]UPenn, Center for Personalized Diagnostics, Philadelphia, PA

Disclosures: Jihui Qiu: None; Priya Velu: None; Jason Rosenbaum: None; Daria Babushok: None; Adam Bagg: None

Background: Myelodysplastic syndromes (MDS) are a heterogeneous group of hematologic neoplasms associated with cytopenias and risk of progressing to acute leukemia. Hypomethylating agents (HMA) are used to treat MDS patients. The correlation between mutational profiles including variant allelic fractions (VAFs) and response to HMAs is not well studied.

Design: A retrospective laboratory database search over a 40-month period was performed. Clinical Next-Generation Sequencing (NGS) data including VAFs, cytogenetic data and hematologic (hemoglobin, absolute neutrophil count, platelets, bone marrow (BM) blast counts) data were collected. Hematologic responses were gauged by standard criteria, and mutation and cytogenetic responses reflected a > 50% decrease in VAFs and abnormal metaphases, respectively. The total percentage of BM myeloid and erythroid (M+E) cells was also recorded as a metric that might affect VAFs.

Results: Of 108 patients with MDS on HMA, 22 had NGS data available on both pre- and post-treatment BMs. A total of 44 mutations were identified in 15 genes before HMA and 45 mutations in 16 genes after HMA (p=0.669). There was no statistically significant change in the percentage of M+E cells following HMA (p=0.38). The most frequently mutated genes were *TP53*, *ASXL1*, *DNMT3A*, *U2AF1*, *SF3B1* and *TET2*. Four of the 22 patients showed decreased VAFs, with all 4 (100%) accompanied by hematologic and cytogenetic responses. Nine of the remaining 18 (50%) without VAF decreases had hematologic but not cytogenetic responses; this reflects a significant difference in response to HMA treatment between patients with and without decreased VAFs (P = 0.02). Three of the 4 patients with decreased VAFs had *TP53* mutations that dropped from 46% to 8%, 28% to 0%, and 78% to 24%, respectively. All 3 had a complex karyotype before HMA; the number of abnormal metaphases decreased substantially in all three, with the proportion of metaphases with putative loss of *TP53* dropping from 70% to 5%, 77% to 0%, and 81% to 5%, respectively. The fourth responder had three mutations (*SETBP1*, *U2AF1* and *ASXL1*).

Conclusions: In this study, only 18% of patients displayed significantly decreased VAFs in response to HMA therapy. However, these responses correlated with hematologic and cytogenetic responses. Notably, patients with loss of *TP53* (due to mutations and/or del17p) appear to be especially sensitive to HMA treatment, suggesting that pre-therapy predictive testing may be helpful in guiding treatment.

1364 Pleckstrin-2 is a Novel Diagnostic Marker in JAK2V617F Positive Myeloproliferative Neoplasms

Nina Rahimi[1], Xu Han[2], Juehua Gao[3], Peng Ji[1]
[1]Chicago, IL, [2]Northwestern University Feinberg School of Medicine, Chicago, IL, [3]Northwestern Memorial Hospital, Chicago, IL

Disclosures: Nina Rahimi: None; Xu Han: None; Juehua Gao: None; Peng Ji: None

Background: JAK2V617F mutation is the leading cause of the Philadelphia chromosome negative (PhN) myeloproliferative neoplasms (MPNs). Patients with PhN MPNs are characterized by a distinct gene expression profile with upregulation of JAK-STAT downstream genes, regardless of the JAK2 mutational status. We recently discovered that Pleckstrin-2 (Plek2) is a novel downstream effector of the JAK2-STAT5 pathway and is overexpressed in JAK2V617F positive MPN patients. We discovered that knockout of Plek2 significantly ameliorated the MPN phenotypes in JAK2V617F knock-in mice including reticulocytosis, thrombocytosis, neutrophilia, and splenomegaly.

Loss of Plek2 reverted the widespread vascular occlusions and lethality of JAK2V617F knock-in mice. These studies highlight the significance of Plek2 in the pathogenesis of PhN MPNs. So far, there are no specific markers in the diagnosis of PhN MPNs.

Design: To explore the possibility of using Plek2 as a maker for the diagnosis of PhN MPNs, we performed immunohistochemical (IHC) stains and flow cytometric analysis of Plek2 in bone marrow biopsies (BMBx) and peripheral blood (PB), respectively, from patients with PhN MPNs. A database search identified a cohort of 25 MPN BMBxs diagnosed between 2010 and 2018 with molecular/genetic confirmation including mutations in JAK2, CALR, and MPL, as well as triple negative patients. PB samples were collected over a period of 6 months in 2017-2018 from patients who have tested JAK2V617F positive from oncology clinic. Antibodies for IHC stains and flow cytometric analysis of Plek2 is purchased from Abcam (ab121131). The flow cytometric data were analyzed using Kaluza software.

Results: We found that Plek2 is overexpressed in a pan-myeloid pattern in JAK2V617F positive PhN MPNs with varying degrees, compared to control bone marrow (lymphoma staging negative samples) that were all negative. Bone marrow core biopsies from CALR or MPL positive patients showed weaker staining compared to those with JAK2V617F positivity. Flow cytometric findings are consistent with the immunostain results, in that all patients with JAK2V617F positive MPNs showed significant upregulation of Plek2 in PB mononuclear cells (Figure 1).

Figure 1 - 1364

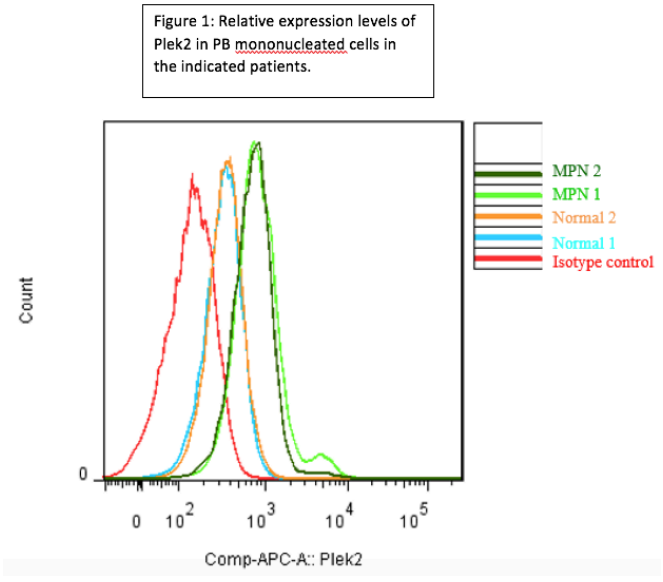

Conclusions: Our study suggests that Plek2 is a useful marker to test PhN MPNs as an ancillary study in addition to molecular testing.

1365 An Integrative Approach Reveals Genetic Complexity and Epigenetic Perturbation in Acute Promyelocytic Leukemia

Nina Rahimi[1], Yanming Zhang[2], Ester Wasserman[2], David Dittmann[3], Amir Behdad[4], Qing Chen[4], Yi-Hua Chen[3], Juehua Gao[3]
[1]Chicago, IL, [2]Memorial Sloan Kettering Cancer Center, New York, NY, [3]Northwestern Memorial Hospital, Chicago, IL, [4]Northwestern University Feinberg School of Medicine, Chicago, IL

Disclosures: Nina Rahimi: None; Yanming Zhang: None; Ester Wasserman: None; David Dittmann: None; Amir Behdad: None; Qing Chen: None; Yi-Hua Chen: None; Juehua Gao: None

Background: Acute promyelocytic leukemia (APL) is a distinct type of acute myeloid leukemia defined by t(15;17), *PML-RARA*; previous studies have shown that other cooperative mutations are required for the development of APL. In this study, we took an integrative approach to study the genetic complexity in a series of newly diagnosed APL cases.

Design: A database search identified 20 APL cases (14 females, 6 males, median age 48) with cytogenetic/FISH or molecular confirmation. We performed next generation sequencing targeting common myeloid genes and CytoScan HD microarray on these samples. To explore the epigenetic modulation in APL, we analyzed the histone methylation by performing immunohistochemistry for EZH2 and H3K27me on the 12 APL cases with available bone marrow particle clots.

Results: We identified somatic mutations in 12/20 cases (60%). 7/20 cases harbored 3 or more mutations (35%), 2/20 had 2 mutations (10%), and 3/20 had 1 mutation (15%). The most common mutations were *FLT3* (35%), *WT1* (30%) and *RAS* (15%). Additionally, we

identified mutations in several epigenetic modifiers including *TET2* (5%), *EZH2* (5%) and *DNMT3A* (5%), co-occurring with either *FLT3* or *WT1* mutations. Cytoscan SNP microarray analysis revealed that 12/20 cases had chromosome gains, loss or copy neutral-loss of heterozygosity (CN-LOH), including 3 cases with 11p CN-LOH which includes the *WT1* gene. One case had both *WT1* mutation and 11p CN-LOH. All cases except one demonstrated high EZH2 nuclear expression in blasts. 8/12 cases demonstrated a global reduction, but with focal perinuclear accumulation of H3K27me. Among these 8 cases, 6 had either *WT1* mutations, 11p aberrations or a *TET2* mutation.

Conclusions: Our study demonstrated that APL is a genetically heterogenous disease and harbors many co-occurring mutations commonly associated with other myeloid leukemias. *WT1* aberrations including somatic mutation and 11p CN LOH, could be a potential recurrent abnormality in APL. A significant number of APL cases had global reduction but focal accumulation of H3K27me, which is more common in cases with *WT1* aberration, indicating a generally more accessible chromatin status and perturbation of constitutive heterochromatin formation. Our studies raise the possibility of targeting the polycomb repressive complex, PRC2/EZH2, mediated epigenetic pathway in APL particularly in refractory or relapsed cases.

1366 Phenotypic Shift in Blasts in Post-Treatment Acute Myeloid Leukemia and its Effect on Clinical Course

Al Amri Raniah[1], Fei Fei[2], Frida Rosenblum[2], Deniz Peker[2]
[1]The University of Alabama at Birmingham, Birmingham, AL, [2]University of Alabama at Birmingham, Birmingham, AL

Disclosures: Al Amri Raniah: None; Fei Fei: None; Frida Rosenblum: None

Background: Acute myeloid leukemia (AML) is the most common acute leukemia in the adult population. Due to the heterogeneity of the disease and complex biology, clinical management of these patients remains a challenge. Clonal evolution during the course of AML is not uncommon. Here we investigated phenotypic shift in post-treatment AML cases and correlated with the molecular findings and clinical outcome.

Design: A retrospective study was designed and post-treatment adult AML cases between 2013-2017 with phenotypic change detected by flow cytometry during the disease course were identified. The collected parameters included age, sex, initial and post-shift phenotype, blast count, cytogenetics and FISH results, mutation status, and survival. GraphPad Prism program was used for statistical analysis.

Results: A total of 39 cases with karyotyping results and/or mutation status were included in the study. The median age was 62 years (ranging 27 to 75 years). Male:female ratio was 1.3. Chromosome studies (karyotyping and/or FISH) were available in all patients and mutation analysis was performed on 18 cases. The most common antigen shift was observed in CD34 (n=22); 15 cases had loss/reduced and 7 had gain/increased expression of CD34. 40% of cases with reduced/lost CD34 showed clonal evolution while gain of CD34 was not associated with any clonal evolution with or without change in other antigen expression. Shift in CD117 expression was the second most common in all cases (n=11); 9 with loss/reduced and 2 with gained expression. 44% of cases with loss/reduced CD117 showed clonal evolution. There was no statistical significance for any of the markers analyzed. Phenotypic shift also did not correlate with the overall survival (Figure 1).

AGE	SEX	DISEASE STATUS AND BLAST COUNT AT PHENOTYPIC SHIFT	PHENOTYPE CHANGE BEFORE	PHENOTYPE CHANGE AFTER	TREATMENT AND FOLLOW UP MARROW STATUS	INITIAL KARYOTYPE	KARYOTYPE AFTER SHIFT	INITIAL FISH	FISH AFTER SHIFT	INITIAL MUTATIONS	MUTATIONS AFTER SHIFT	OVERALL SURVIVAL (months)	SURVIVAL FOLLOWING SHIFT (months)	CURRENT STATUS
29	M	s/p induction 12%	CD13+ CD7+ CD15+ HLA-DR+	CD13- CD7+/- CD15- HLA-DR+/-	Re-induction, CR	47, XY,+8[20]	NA	Trisomy 8	NA	None	NA	4	9	0
62	F	persistent AML 11%	CD34- CD123+	CD34+ CD123-	no treatment/NA (patient died shortly)	46,XX[19]	NA	normal	normal	FLT3 ITD DNMT3A NPM1	NA	5	4	1
71	M	CR 1%	CD117+ CD56- HLA-DR+	CD117- CD56+/- HLA-DR -/dim	Azacytadine/MRD	46,XY[20]	46,XY[20]	normal	normal	IDH1 SRSF2 NPM1	IDH1 SRSF2	14	7	0
46	F	s/p initial induction 2%	CD34- CD123+	CD34+ CD123-/dim	No treatment/CR	47,XX,+21[18]/ 46,XX[4]	46,XX[20]	three copies of AML1 gene	normal	NPM1 NRAS ETV6	ETV6	6	4	0
35	M	s/p initial induction 8%	CD56- HLA-DR+ CD123- CD117+ CD64-	CD56het HLA-DR- CD123dim CD117- CD64+	no treatment/CR	46,XY[20]	46,XY[20]	normal	normal	FLT3 p.D835Y NPM1 DNMT3A	NA	6	5	0
69	F	s/p initial induction 3%	CD15-	CD15+	no treatment/CR	46,XX, t(8;21)(q22;q22)[20]	46,XX[20]	RUNX1T1/RUNX1 rearrangement	normal	NRAS DNMT3A	NA	6	5	0
63	M	persistent AML 27%	CD34+ CD38- CD33 dim HLA-DR-	CD34- CD38+ CD33+ HLA-DR +/-	no treatment/patient died	46,XY[20]	47,XY,+X,[10]/ 46,XY[10]	normal	normal	SETBP1 ASXL1 GATA2	SETBP1 ASXL1 PTPN11 NF1 ZRSR2	48	3	1
45	F	persistent AML 59%	HLA-DR+	HLA-DR-	re-induction/CR	46,XX,der(16)t(11;16)(q13.1;p13.3)[20]	46,XX[20]	three copies of MLL gene	normal	NPM1 DNMT3A FLT3 ITD	NPM1 DNMT3A IDH1 NF1	24	9	0
79	M	persistent AML 95%	CD34+	CD34-	re-induction/persistent AML	46,XY[20]	47,XY,+8[3]/46,XY[17]	normal	trisomy 8	SRSF2 NRAS ASXL1 STAG2 TET2	SRSF2 NRAS ASXL1 STAG2 TET2 C	9	7	1

65	M	CR 9%	HLA-DR+ CD123+ CD34-	HLA-DR- CD123- CD34+	no treatment/MRD	46,XY[20]	45,XY,add(7)(p13),dic(9;12)(p12;p11.1)[3]/46,XY,t(12;17)(q24.3;q21)[3]/46,XY,inv(3)(p25q12)[3]/47,XY,+8[2]/46,XY[11]	normal	normal	IDH1 FLT3 ITD STAG2	IDH1 FLT3 ITD STAG2	8	1	1
62	M	CR 7%	CD38+ CD13+	CD38- CD13+	Anti-CD33/NA	46,XY,del(1)(q21),dic(5;12)(q11.2;p13),+6,add(6)(q27),del(7)(q22),der(11)t(1;11)(p13;p15),-13,-15,+2mar[cp20]	44~48,XY,dic(5;12)(q11.2;p13),+6,add(6)(p23),add(6)(q27),del(7)(q22),der(11)t(1;11)(p13;p15),-13,-15,+1~3mar[cp15]	del 5q31, del 7q31	del of the TP53 gene at 17p13.1	none	NA	15	14	0
75	F	s/p induction 10%	CD34- CD7-	CD34+ CD7+	no treatment/CR	46,XX[16]	46,XX[20]	normal	normal	NPM1	NA	55	36	1
58	M	relapsed AML 73%	CD117 -/+ CD13 het	CD117+ CD13+	re- induction/CR	46,XY,i(17)(q10)[3]/46,XY[27]	NA	Three copies of the RARA gene at 17q21	normal	SRSF2	SRSF2	18	15	1
61	M	CR 1%	CD34- CD13- HLA-DR-	CD34+ CD13+ HLA-DR+	no treatment/CR	46,XY[20]	46,XY[20]	normal	normal	IDH2 NPM1 NRAS	none	22	21	0
76	F	s/p induction 75%	CD7 +/- CD13 het CD33 het CD123-	CD7- CD13+ CD33+ CD123+	re- induction/CR	46,XX[20]	46,XX[20]	normal	normal	NPM1 FLT3	NPM1 GATA2	15	7	1
64	F	refractory AML 5%	CD34- CD117-	CD34+ CD117+	anti-FLT3/CR	51,XX,+3,+8,+9,+10,+13[6]/53,XX,+8,+10,+13,+13,+15,+19,+21[cp13]/46,XX[1].	46,XX[20]	trisomy 8 three copies of 20q12 region	normal	FLT3 ITD	FLT3 ITD RUNX1 DNMT3A	19	18	1
65	F	s/p induction 2%	CD34+HLA- DR+ CD13+	CD34- HLA-DR -/+ CD13 het	no treatment/CR	46,XX[20]	46,XX[20]	normal	normal	PTPN11 U2AF1 WT1	PTPN11 U2AF1 WT1	12	12	0
65	F	s/p induction 43%	CD13 het CD56-	CD13+ CD56+	re- induction/MRD	46,XX[20]	45,XX,-7[3]/46,XX[18]	normal	del 7q31	KRAS ABL1 NF1 PTEN	NA	25	22	0
70	M	refractory AML 56%	CD34+ CD38+	CD34- CD38 bright	Azacytadine/MRD	46,XY[10]	46,XY[20]	normal	normal	NPM1	NA	9	3	1
58	M	s/p induction 7%	CD34+ CD117+	CD34 bright CD117 dim	no treatment/relapsed AML	47,XY,+13[17]/46,XY[3]	NA	four copies of D5523 region at 5p15.2 and four copies of 7q	NA	IDH2 BCOR	IDH2 IDH1	1	0	1
42	F	CR 36%	CD34 dim CD13 het CD123+	CD34+ CD13+ CD123 het	azacytadine and sorefinib/CR	46,XY[20]	NA	normal	normal	NA	NA	144	3	1
43	F	CR 1%	CD34+ CD117+ CD15+ CD64+ CD14 het	CD34 +/- CD117 -/+ CD15- CD64 dim CD14-	no treatment/relapsed	46,XX[20]	46,XX,t(1;11)(q21:p11.2),t(3;15)(q27;q22)[8]/46,XX	normal	normal	NA	NA	12	5	1
41	F	persistent AML 48%	CD34+ CD13+ CD64 het	CD34 +/- CD13- CD64-	clofarabine and cytarabine/refractory	46,XX[20]	46,XX,t(8;17)(q22;p13)[3]/46,XX[12]	normal	three copies of the AML1 gene	NA	NA	51	39	0
61	M	CR 19%	CD34+ CD117+	CD34- CD117 het	NA/relapsed	46,XY[20]	46,XY,t(1;4)(p36.1;q31.1)[6]/46,XY[9]	normal	normal	NA	NA	8	4	1
64	M	CR 1%	CD64- CD7-	CD64+ CD7+	azacytabine/relapsed	46,XY[20]	46,XY[20]	normal	rearrang ement of MLL gene at 11q23	NA	NA	6	3	1
71	M	s/p induction 12%	CD34+ CD38 dim	CD34 -/+ CD38+	consolidation/CR	47,XY,+8[11]/46,XY[4]	46,XY[20]	67% of the cells have three copies of the ETO gene at 8q22	normal	NA	NA	45	2	0
41	M	s/p induction 1%	CD34+	CD34-	consolidation/CR	46,XY[20]	46,XY[20]	normal	normal	NA	NA	1	1	1
29	M	s/p induction 28%	CD34+ CD117	CD34- CD117 het	re- induction/CR	46,XY,t(2;20)(p21;q11.2)[15]	46,XY[16]	normal	normal	NA	NA	48	46	0
27	M	s/p induction 4%	CD64+	CD64-	no treatment/CR	46,XY[20]	46,XY[20]	normal	normal	NA	NA	50	48	0
72	M	CR 7%	CD34+ CD117+ CD15+	CD34- CD117 -/+ CD15-	FLAG/CR	46,XY[20]	NA	normal	normal	NA	NA	17	17	1
65	M	s/p induction 24%	CD13+	CD13 dim	re- induction/CR	46,XY[20]	46,XY[20]	normal	normal	NA	NA	48	47	0
69	M	CR 6%	CD34+ CD117+ CD64-	CD34- CD117- CD64+	azacytabine/CR	46,XY[20]	46,XY[20]	normal	normal	NA	NA	5	4	1
59	M	persistent AML 56%	CD19+	CD19-	salvage/persistent	46,XY[20]	46,XY[20]	normal	normal	NA	NA	4	3	1
68	F	s/p induction 2%	CD117+ CD13+ HLA-DR+	CD117- CD13 het HLA-DR dim	no treatment/CR	48,XX,del(5)(q22q31),-7,+8,+11,inv(17)(p11.1p12),+22[15]	45,XX,del(3)(p13),del(5)(q22q31),-7,inv(17)(p11.1p12)[cp12]	del 5q, del 7q, trisomy 8	del 5q31, del 7q, trisomy 8	NA	NA	32	18	1
64	M	CR 35%	CD34+ CD64-	CD34- CD64+	no treatment/relapsed	46,XY,del(7)(q21.3)[14]	46,XY,del(7)(q22.1)[15]	del 7q	normal	NA	NA	5	4	1
33	F	persistent AML 23%	CD64+ CD13+	CD64 dim/- CD13-	no treatment/persistent	46,XX[20]	46,XX,t(9;11)(p22;q23)[3]/45,idem,dic(X;7)(p11.2;p12)[5]/46,XX[12]	normal	rearrang ement of MLL	NA	NA	17	5	1
46	M	CR 3%	CD34+ CD64-	CD34- CD64 dim	no treatment/CR	46,XY[20]	NA	normal	NA	NA	NA	12	2	1
39	F	persistent AML 37%	CD34+ CD19+	CD34 het CD19-	FLAG/persistent	46,XX,t(4;11)(q21;q23)[15]	46,XX[20]	rearrang ement of MLL	normal	NA	NA	19	5	1

Figure 1 - 1366

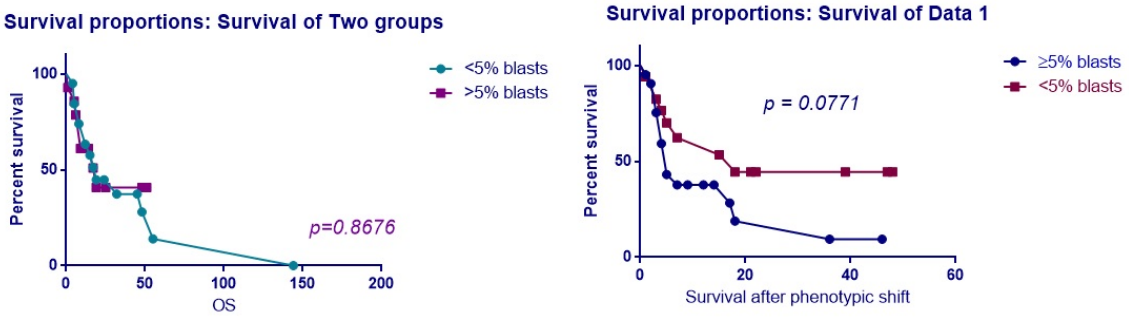

Conclusions: Phenotypic shift may occur in AML cases uncommonly following treatment with chemotherapy or stem cell transplant. Our preliminary results suggest that the phenotypic changes are likely related to treatment and are not a good predictor of the disease course. Larger scale studies are warranted to further investigate phenotypic alterations in AML.

1367 Genetic abnormalities and follow-up of patients with isolated 20q- without myeloid neoplasms

Aishwarya Ravindran[1], Rong He[1], Majd Jawad[2], Rhett Ketterling[1], Dong Chen[1], Jennifer Oliveira[1], Phuong Nguyen[1], David Viswanatha[1], Kaaren Reichard[1], James Hoyer[1], Ronald Go[1], Min Shi[1]
[1]Mayo Clinic, Rochester, MN, [2]UMMS-Baystate, Holyoke, MA

Disclosures: Aishwarya Ravindran: None; Rong He: None; Majd Jawad: None; Rhett Ketterling: None; Dong Chen: None; Jennifer Oliveira: None; Phuong Nguyen: None; David Viswanatha: None; Kaaren Reichard: None; James Hoyer: None; Ronald Go: None; Min Shi: None

Background: Myelodysplastic syndromes (MDS) are a heterogeneous group of clonal hematopoietic stem cell diseases characterized by cytopenia(s), ineffective hematopoiesis, dysplasia in one or more hematopoietic lineages and distinct cytogenetic abnormalities. The presence of isolated 20q- is not considered defining cytogenetic evidence for MDS in the absence of dysplasia by the 2016 WHO criteria. In this study, we aim to analyze the molecular and cytogenetic abnormalities and follow-up of patients with isolated 20q-.

Design: We reviewed bone marrow (BM) pathology reports of patients from 01/2005 to 12/2015 with isolated 20q- ($\geq$2 of 20 metaphases) and without morphologic features of myeloid neoplasms (MNs). Cases with Next-Generation Sequencing (NGS) targeting 35 genes commonly associated with MNs performed on the initial and subsequent available archived bone marrow aspirate pellets were included in this study series.

Results: Eleven patients met the inclusion criteria. At the time of 20q- detection, the median age was 65 years (range: 44-75), 64% were male. The median hemoglobin (Hb), absolute neutrophil count (ANC) and platelet count (Plt) were 11.1 g/dL (range: 9.3-14.5), 2.6 x 10^9/L (range: 1.1-4.3) and 189 x 10^9/L (range: 79-274), respectively. The indications for bone marrow biopsies were follow-up of multiple myeloma (patient 5-10), non-Hodgkin lymphoma (patient 1, 2, 11), and persistent/progressive cytopenias (patient 3, 4). NGS revealed pathogenic/likely pathogenic mutations in 7 patients, and 6 of them progressed to a myeloid neoplasm at a median duration of 47.1 months (range: 1.9-78.4; patient 1-6, table 1). At time of progression, all 6 patients had developed new mutations and/or increase of variant allele frequency (VAF) in pre-existing mutations; and two of them (patient 1, 5) gained complex cytogenetic abnormalities. There was no significant difference in percentage of 20q- of total metaphases (p=.73), Hb (p=.16), ANC (p=.59), Plt (p=.28) between the initial 20q- detection and time of progression in these 6 patients.

Table 1

Patient	At initial 20q- detection				At progression of myeloid neoplasm/ follow-up					
	Age/Sex	% 20q-	Gene mutations: variant allele frequency	Bone marrow morphology	Myeloid neoplasm progressed	Gene mutations: variant allele frequency	% 20q-	Bone marrow morphology	Time to progression (months)	Time to final follow-up (months)
1	75/M	50	*TP53*: 5.2%	Occasional large megakaryocytes	Acute myeloid leukemia, likely therapy-related	*TP53*: 10.1%	10	80% blasts and occasional hypogranular neutrophils.	32.8	33.5
2	70/M	15	*CBL*: 25.3% *SF3B1*: 25.3%	Normal	Chronic myeloid neoplasm, not further classified	*CBL*: 32% *SF3B1*: 37% *EZH2*: 28%	60	Hyperlobate and hyperchromatic megakaryocytes with focal clusters.	40.2	99.0
3	70/M	10	*ASXL1*: 12.8% *IDH1*: 32.2% *SRSF2*: 29.1%	Rare small monolobate megakaryocytes	MDS with excess blasts-1	*ASXL1*: 11% *IDH1*: 35% *SRSF2*: 31%	5	Trilineage dysplasia with 8% blasts	1.9	88.0
4	73/F	10	*PHF6*: 10% *TET2*: 44.8% *TET2*: 42.7%	Rare hypogranular neutrophils; rare hypolobate/bilobate megakaryocytes	MDS w/multilineage dysplasia	*PHF6*: 16% *TET2*: 49.1% *WT-1*: 6%	85	Dyserythropoiesis, dysgranulopoiesis and small megakaryocytes.	53.9	54.3
5	58/M	40	None	Normal	MDS with excess blasts-1	*DNMT3A*: 10.7%	0	Mild erythroid and megakaryocytic dysplasia with 7% blasts	78.4	85.4
6	65/F	15	None	Occasional atypical megakaryocytes with large and hyperlobate nuclei	MDS, unclassified	*IDH2*: 12.1%	20	Large megakaryocytes with dark and condensed chromatin	60.1	68.8
7	70/M	6.7	*ASXL1*: 5.6% *ASXL1*: 6.7%	Normal	No progression	*ASXL1*: 24.6%	15	Normal	Not applicable	82.7
8	61/F	45	None	Normal	No progression	None	40	Normal	Not applicable	108.5
9	65/F	30	None	Normal	No progression	None	55	Normal	Not applicable	21.9
10	62/M	50	None	Normal	No progression	None	95	Large hyperlobated, hyperchromatic megakaryocytes with coarse chromatin and occasional clusters	Not applicable	63.9
11	44/M	10	None	Normal	No progression	None	15	Normal	Not applicable	124.0

Conclusions: Based on our study, among patients with isolated 20q- and no MN at initial diagnosis, the acquisition of additional mutations, increase in mutational VAFs, and gain of complex cytogenetic abnormalities may be associated with subsequent development of MNs.

1368 Mutational Landscape of Epstein-Barr Virus-Positive MALT Lymphomas

Bryan Rea[1], Yen-Chun Liu[1], Lorinda Soma[2], Chris Bacon[3], Michael Bayerl[4], Molly Smith[5], Steven Swerdlow[1], Sarah Gibson[6]
[1]University of Pittsburgh School of Medicine, Pittsburgh, PA, [2]University of Washington Medical Center, Seattle, WA, [3]Newcastle University, Newcastle upon Tyne, United Kingdom, [4]Penn State Hershey Medical Center, Hershey, PA, [5]University of Kentucky College of Dentistry, Lexington, KY, [6]University of Pittsburgh School of Medicine, Scottsdale, AZ

Disclosures: Bryan Rea: None; Yen-Chun Liu: None; Lorinda Soma: None; Chris Bacon: None; Michael Bayerl: None; Molly Smith: None; Steven Swerdlow: None; Sarah Gibson: None

Background: Epstein-Barr virus (EBV)-positive MALT lymphomas were initially described in the post-transplant setting, with a predilection for subcutaneous/soft tissue sites and IgA restriction. More recently EBV+ MALT lymphomas have been described in other immunodeficiency settings. However, little is known about the mutational landscape of these lymphomas in comparison to EBV- MALT lymphomas.

Design: 8 EBV+ MALT lymphomas were identified. The mutational landscape of 6/8 was assessed using next-generation sequencing mutation analysis with a custom probe panel comprising 4099 target coding regions within 220 genes recurrently mutated in B-cell lymphomas. Non-synonymous variants and insertions/deletions with an allele frequency greater than or equal to 10% were recorded except those with an allele frequency of 40-60% that may represent germline variants.

Results: The 8 patients had a median age of 34 years (4 males, 4 females). 6/8 cases occurred post-transplant (PTx), 1 case occurred in the setting of primary immunodeficiency (PI), and 1 case was age-related. 6/8 EBV+ MALT lymphomas were sequenced and showed a median of 1 variant per case. Disease-associated mutations in *BRAF* and *TNFAIP3* were seen in 1/6 cases each, and no recurrent mutations were identified.

Clinicopathologic and Genomic Features of 8 EBV+ MALT Lymphomas

	1	2	3	4	5	6	7	8
Age (years)/ Gender	24/F	44/M	12/M	71/F	16/M	63/M	67/F	10/F
Immunodeficiency	PTx	PTx	PTx	PTx	PI	PTx	Age	PTx
Site of biopsy	SC tissue	SC tissue	Orbit	SC tissue	Parotid	Parotid	Breast	Lip
Heavy chain	IgA	IgA	IgA	IgA	IgM	IgA	IgA	IgG
No. of variants	0	1	0	2	1	7	NA	NA
Variants	None	*IRF8*p.Q401Rfs*52	None	*BRAF* p.G469A *NSD2*p.E1050K	*TNFAIP3*p.R183*	*APC2* p.R2098C *BRD4*p.R1237H *CREBBP*p.R1702L *PLCB4*p.R621H *SMARCA4*p.V1016M *TENM4*p.R1300Q *UBR5*p.R472Q	NA	NA
Treatment	Excision, ROI	ROI, antiviral, rituximab	ROI, antiviral	Antiviral, rituximab	Rituximab	Excision	Excision	CTx, rituximab
Status at last follow-up (years)	ANED (10)	DNED (3.4)	ANED (16)	ANED (8.8)	DNED (3)	ANED (5.5)	ANED (0.5)	AWD (0.9)

PTx, post-transplant; PI, primary immunodeficiency; SC, subcutaneous; ROI, reduction of immunosuppression; CTx, chemotherapy; ANED, alive with no evidence of disease; DNED, died with no evidence of disease; AWD, alive with disease

Conclusions: EBV+ MALT lymphomas have a low mutational burden similar to EBV- MALT lymphomas. Although recurrent mutations were not seen in this limited cohort, disease-associated mutations in *TNFAIP3*, common in MALT lymphomas, and *BRAF*, common in nodal marginal zone lymphomas, were identified in 1 case each.

1369 Co-occurrence of Driver Mutations in Myeloid Neoplasm

Aida Richardson[1], Thomas White[1], Kristin Karner[2], Jay Patel[1]
[1]University of Utah/ARUP Laboratories, Salt Lake City, UT, [2]University of Utah, Salt Lake City, UT

Disclosures: Aida Richardson: None; Thomas White: None; Kristin Karner: None; Jay Patel: None

Background: While thought to be mutually exclusive, rare cases with co-occurring driver mutations in myeloproliferative neoplasms have been identified. Due to limited data, it is difficult to determine their incidence or true clinical relevance.

Design: In this study we describe those patients who had co-existing driver mutations at any point during the course of their disease. We retrospectively analyzed a total of 1111 patients using a next generation sequencing myeloid panel of 57 genes.

Results: We identified 22 patients (1.98%) with co-occurring driver mutations of which 16 patients were diagnosed with myeloproliferative neoplasm (MPN), 4 patients with acute myeloid leukemia (AML), and 2 patients with myelodysplastic syndrome (MDS).

JAK2 was the most common co-occurring driver mutation, seen in 17 patients (1.53%) and included JAK2+MPL (10 patients) followed by JAK2 + CALR (3 patients), JAK2 + CSR3R (3 patients), and JAK2 + BCR/ABL minor (1 patient). Out of 17 patients, 10 patients diagnosed with MPN, 4 patients had AML and 2 patients had MDS.

CALR was the second most common co-occurring driver mutation, seen in remaining 5 patients (0.45%), and included either CALR + MPL (3 patients) or CALR + CSF3R (2 patients). All 5 patients had diagnosis of MPN.

The frequency of other known important non-driver but clonal mutation associated with myeloid neoplasm within 22 patients was as follows: ASXL1 (9 patients), DNMT3A (6 patients), SRSF2 (4 patients), TET2 (4 patients), EZH2 (4 patients), SF3B1 (4 patients) and IDH2 (2 patients). Notably, all 3 patients with CALR + MPL co-occurrence had ASXL1 with a variant allele fraction ranging from 22.5 to 36.1%.

Conclusions: Although the incidence of the co-existing driver mutation is low, it is important to be aware of their existence for making the correct diagnosis and consideration for appropriate management. The clinical relevance of the coexistent driver mutations awaits further investigation.

1370 Molecular profile is useful to predict clinical outcome in myeloproliferative neoplasm, unclassifiable: Bone marrow pathology group study

Heesun Rogers[1], Julia Geyer[2], Beenu Thakral[3], Sa Wang[3], Geoffrey Wool[4], K. David Li[5], Adam Davis[6], Carlos Bueso-Ramos[3], Daniel Arber[4], Tracy George[7], Adam Bagg[8], Robert Hasserjian[9], Attilio Orazi[10], Eric Hsi[1]
[1]Cleveland Clinic, Cleveland, OH, [2]Weill Cornell Medicine, New York, NY, [3]The University of Texas MD Anderson Cancer Center, Houston, TX, [4]University of Chicago, Chicago, IL, [5]University of Utah/ARUP Laboratories, Salt Lake City, UT,[6]Hospital of the University of Pennsylvania, Philadelphia, PA, [7]University of Utah, Salt Lake City, UT, [8]University of Pennsylvania, Philadelphia, PA, [9]Massachusetts General Hospital, Boston, MA, [10]Weill Cornell Medical College/NYP, New York, NY

Disclosures: Heesun Rogers: None; Julia Geyer: None; Beenu Thakral: None; Sa Wang: None; Geoffrey Wool: None; K. David Li: None; Adam Davis: None; Carlos Bueso-Ramos: None; Daniel Arber: None; Tracy George: None; Adam Bagg: None; Robert Hasserjian: None; Attilio Orazi: None; Eric Hsi: *Grant or Research Support*, Abbvie; *Grant or Research Support*, Eli Lilly; *Advisory Board Member*, Seattle Genetics; *Advisory Board Member*, Celgene

Background: Myeloproliferative neoplasm (MPN), unclassifiable (-U) includes cases with early or advanced stage MPNs and cases with features obscured by coexisting disorders. MPN-U has highly variable clinicopathologic features. Its clinicopathologic features and *JAK2/MPL/CALR* mutation status have been reported in only a few studies. This is the first study evaluating genetic features and clinical outcomes in a large cohort of well characterized MPN-U patients.

Design: This multicenter study evaluated clinicopathologic features, *JAK2/MPL/CALR* mutation status, next generation sequencing (NGS) and clinical outcomes in MPN-U patients. WHO 2016 criteria were applied following re-review of the patients.

Results: 76 MPN-U patients (median age 64 years) had median WBC 11.1 x10^3/uL, Hb 13.0 g/dL and platelet 388 x10^3/uL. Patients often presented with splenomegaly (66%), leukocytosis (44%), thrombocytosis (36%) and venous thrombosis (20%). The hypercellular marrow showed megakaryocytic proliferation in 77% of the patients with atypical morphology in 38%. 19% had an abnormal karyotype. The MPN-U was subcategorized as early stage (49), advanced stage (23) or coexisting disorders (4). Patients in advanced stage had lower Hb, and more frequent leukoerythroblastosis and abnormal karyotype than those in early stage (all $p<0.05$).

47% expired during the median follow-up of 29 months (mo). The median overall survival (OS) was 48 mo, with shorter OS in advanced stage than early stage disease (29 vs 113 mo, logrank p=0.001). 64% of patients progressed to aggressive neoplasms including 5 who

progressed to acute myeloid leukemia. Patients who progressed to aggressive neoplasms had shorter OS than those without progression (30 mo vs not reached, logrank p=0.007).

JAK2, MPL and *CALR* mutations were noted in 64%, 6% and 4%, respectively. NGS (n=24) detected one or more mutations in 83% (median 1.5, range 1-5), most frequently in *ASXL1*, *U2AF1, SRSF2* and *TET2* genes. Patients with *JAK2* mutation had longer OS (113 vs 30 mo, logrank p=0.005) and patients with *ASXL1* and/or *SRSF2* mutation had shorter OS (18 vs 54 mo, logrank p=0.015) compared to patients without those mutations. Presence of abnormal karyotype was not associated with clinical outcome. *JAK2* and *ASXL1* and/or *SRSF2* mutations remained significant in multivariate analysis.

Conclusions: This study demonstrated MPN-U has heterogeneous clinicopathologic features and clinical outcomes. Molecular genetic studies provide important prognostic information in MPN-U patients.

1371 Quantitative Tumor-Specific BCL2 Expression Incorporating Intensity & Proportion Better Predicts Prognosis in DLBCL

Jin Roh[1], So-Woon Kim[2], Min Jeong Song[3], Eun-mi Son[4], Chan-Sik Park[3]
[1]Ajou University School of Medicine, Suwon-si, Korea, Republic of South Korea, [2]Asan Medical Center, Songpa-gu, Korea, Republic of South Korea, [3]Seoul, Korea, Republic of South Korea, [4]Asan Medical Center, Seoul, Korea, Republic of South Korea

Disclosures: Jin Roh: None; So-Woon Kim: None; Min Jeong Song: None; Eun-mi Son: None; Chan-Sik Park: None

Background: The BCL2 overexpression has been reported to be associated with poor prognosis in diffuse large B-cell lymphoma (DLBCL). However, the criteria for BCL2 positivity by immunohistochemistry (IHC) are highly variable between studies. In addition, the conventional method evaluates only the proportion of BCL2 expressing cells regardless of its intensity. In this study, we used automated quantitative analysis (AQUA) score which integrates both intensity and proportion of BCL2 expression.

Design: We analyzed 322 patients with primary DLBCL who were treated with R-CHOP (rituximab, cyclophosphamide, doxorubicin, vincristine, and prednisone). Tumor-specific AQUA scoring for BCL2 using multiplex immunofluorescence was performed. The prognostic significance of BCL2 expression was analyzed using the univariate and multivariate analysis. To confirm the significance of BCL2 intensity in the practical field, the H-score and conventional method (50% cutoff) were compared in the single chromogenic IHC using quantitative image analysis.

Results: A survival analysis for the training set (N = 211) revealed that high BCL2 AQUA score (N = 83, 39.3%) is significantly associated with poor prognosis independent of the cell of origin, the international prognostic index, and the MYC expression (p = 0.032). The poor prognostic impact of the BCL2 expression was confirmed in the validation set (N = 111). In single chromogenic IHC, high BCL2 expression showed significantly shorter overall survival in the H-scoring system (p = 0.0003) but not in the conventional method (p = 0.22). Overall, the tumor-specific AQUA scoring system showed the best performance in predicting prognosis (AUROC = 0.66 (AQUA), 0.63 (H-score), and 0.54 (50% cutoff)).

Conclusions: We showed the independent poor prognostic impact of the BCL2 expression using reproducible and quantitative scoring system. Unlike the conventional method, this new analyzing method incorporating both intensity and proportion better predicts the prognostic impact of BCL2 in DLBCL.

1372 Advances in TEMPI Syndrome: Molecular Genetic Characterization of a Novel Disease

Flavia Rosado[1], Danijela Lekovic[2], Jeffrey Gagan[1], James Malter[1], Roberto Rodriguez[3], Casey O'Connell[4], Wilfried Schroyens[5], David Sykes[6]
[1]University of Texas Southwestern, Dallas, TX, [2]Clinic for Hematology, Belgrade, Serbia, [3]Kaiser Permanent, Los Angeles, CA, [4]Keck School of Medicine of University of Southern California, Los Angeles, CA, [5]Universitair Ziekenhuis Antwerpen, Edegem, Belgium, [6]Massachusetts General Hospital, Boston, MA

Disclosures: Flavia Rosado: None; Danijela Lekovic: None; David Sykes: None

Background: TEMPI syndrome (telangiectasias, elevated erythropoietin level and erythrocytosis, monoclonal gammopathy, perinephric fluid collections and intrapulmonary shunting) is a paraneoplastic syndrome first described in 2011, and recently included in the 2017 WHO Classification of Hematopoietic Tumors. The syndrome clinically mimics polycythemia vera, and is likely under recognized. While the pathogenesis of TEMPI is not yet understood, patients have responded to myeloma-type regimens. To our knowledge, there are no previous studies attempting to identify genetic abnormalities in this disease.

Design: This study is the first that aims to characterize the genetics of TEMPI syndrome. To date, we have tested bone marrow samples from 4 TEMPI patients. Paraffin embedded bone marrow clot preparation and fresh samples were utilized. We performed next generation sequencing using a custom panel of DNA probes covering 1,385 known cancer-related genes, to include genes typically mutated in

myeloproliferative neoplasms. In 3 patients, plasma cells were isolated by flow cytometry cell sorting to perform whole exome and RNA sequencing.

Results: The clinical and known genetic findings of all the 15 known TEMPI patients are shown in the table. Ages ranged from 35 to 65 years (median 49), male:female ratio 3:4. The majority of cases showed MGUS levels of clonal plasma cells (<10% in 8 of 15 cases). However, in one case, up 30% clonal plasma cells were identified. We found no molecular genetic abnormalities associated with TEMPI in the samples tested.

Figure 1 - 1372

Table: Summary of Clinical and Genetic Findings of All Known TEMPI patients

	Telangiectasias	Erythrocytosis	Highest EPO (mU/ml)	M-spike (g/dL)	Perinephric collection	Intrapulmonary shunting	% of Clonal Plasma Cells	Genetics
1	Yes	Yes	>5000	0.7 IgG kappa	Yes	Yes	<10%	Normal
2	Yes	Yes	>5000	NR	Yes	Yes	<10%	Normal
3	Yes	Yes	4262	0.7 IgG kappa	NR	Yes	NR	Normal
4	Yes	No*	444	2.3 IgG kappa	Yes	NA	30%	Normal
5	Yes	Yes	>5000	IgG kappa	Yes	NR	<10%	
6	NR	Yes	>500	NA	Yes	NR	<10%	
7	Yes	Yes	NA	IgG	NR	Yes	<10%	
8	NR	Yes	NA	NA	Yes	NR	<10%	
9	Yes	Yes	8000	IgG kappa	NR	Yes	NR	
10	Yes	Yes	100	3.6 IgG lambda	Yes	NR	15%	
11	Yes	Yes	134	1.4 IgA lambda	Yes	No	10%	
12	Yes	Yes	78	0.2 IgG kappa	Yes	Yes	<10%	
13	Yes	No*	8144	1.8 IgG kappa	Yes	Yes	<10%	
14	Yes	No *	5000	0.8 IgG kappa	Yes	Yes	NR	
15	Yes	Yes	>5000	2.3 IgG kappa	No	Yes	10%	

NA= not available/ not applicable ; NR = not reported
** phlebotomized*

Conclusions: The preliminary results of this ongoing study indicates that there are no molecular abnormalities associated with TEMPI syndrome. We conclude that when polycythemia vera is clinically suspected due to unexplained erythrocytosis, a negative molecular workup should trigger additional testing with plasma cell clonality studies to rule out TEMPI syndrome.

1373 Isolated Monoclonal B-Cell Lymphocytosis (MBL) in the Bone Marrow (BM): Revisiting the Criteria for Chronic Lymphocytic Leukemia/Small Lymphocytic Lymphoma (CLL/SLL)

Christopher Ryder[1], Kirsten Boughan[1], Erika Moore[1]
[1]University Hospitals Cleveland Medical Center, Cleveland, OH

Disclosures: Christopher Ryder: None; Kirsten Boughan: None; Erika Moore: None

Background: MBL is a clonal B-cell expansion in the peripheral blood (PB) of <5x10^9/L without extramedullary (EM) disease, often with a CLL/SLL phenotype. Extent of BM involvement is not currently part of the diagnostic criteria for MBL or CLL/SLL, but CLL-type MBLs in BM can be seen in patients (pts) lacking PB lymphocytosis. Data is limited on the outcome of such cases. We assessed the clinicopathologic characteristics of isolated BM CLL-type MBL in pts not meeting criteria for CLL/SLL.

Design: BMs from 2006-2018 with CLL-type MBL but <5x10E9/L PB monoclonal B-cells & no EM disease were evaluated for: % BM involvement (by morphology & immunohistochemistry (IHC)), PB counts, flow cytometric (FC) & cytogenetic findings (CG), lymphadenopathy (LAD), splenomegaly (SM), & therapy (tx).

Results: A total of 21 cases were identified; 9/21 had additional hematopoietic neoplasms. Extent of MBL in the BM was classified as <5% (n=10), 5-9% (n=3), 10-19% (n=3), 20-49% (n=1) or >50% (n=4), (Fig 1). 18/21 had obvious lymphoid infiltrates; 3/21 were seen by IHC. Mean MBC count by FC was 11% (range: 0.2-67%). Mean PB absolute lymphocyte count (ALC) was 1.8x10E9/L (range: 0.5-5.0x10E9/L). 76% had anemia & 43% had thrombocytopenia. 8 CLL-related CG were found in 6 cases (trisomy 12 (n=5); deletion 13q14 (n=3)). No pts had LAD or SM by physical exam. By imaging, 4/18 had LAD (all <1.5 cm) & 3/18 had SM but with other probable etiologies. 3 pts had CLL-tx after BM due to cytopenias (3/3 had >50% in BM & +CG) & 1 years later for EM progression; 6 pts had tx for other neoplasms (2 with CLL-effective tx). No pt ever met PB criteria for CLL/SLL; only 2/21 ever had ALC>5 but with FC MBC of <5x10E9/L. One pt had lymph node biopsy 3 years later with CLL & large cell transformation.

Figure 1 - 1373

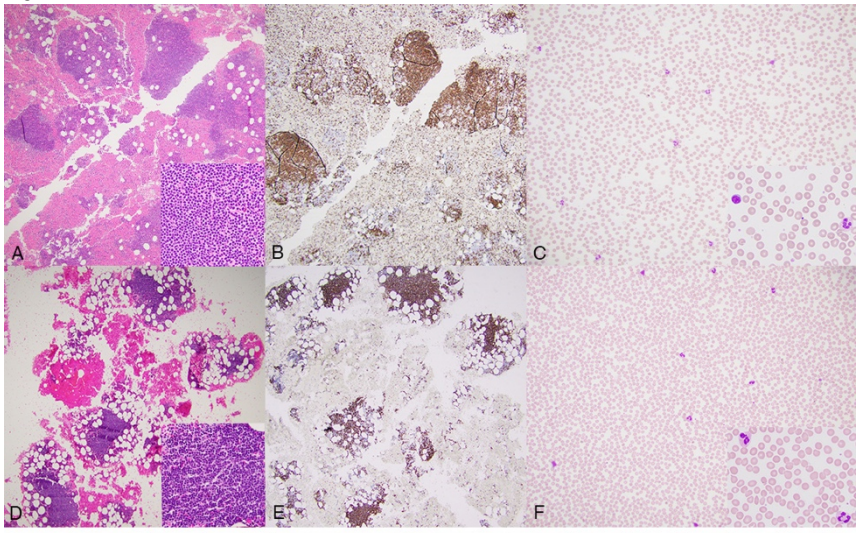

Figure 1: Two BM CLL-type MBL cases with >50% involvement by H&E of BM clot section, 40x, 400x (A&D) & by CD20 IHC, 40x (B&E) but without lymphocytosis on PB smear, 200x,1000x (C&F).

Conclusions: Isolated BM CLL-type MBL represents a diagnostic gray area & this study highlights the range of clinical outcomes. In all 3 cases where tx was initiated quickly due to cytopenias pts had >50% in BM & +CG but not PB ALC of ≥5x10E9/L or LAD >1.4 cm, suggesting that not all pts with clinically significant disease will meet criteria for CLL/SLL. The results also show that concurrent disease may complicate CLL diagnosis, as the disease course or tx may result in leukopenia, thereby precluding PB absolute lymphocytosis. Though larger studies are needed, degree of BM involvement & CG may help predict disease progression & perhaps re-evaluation of criteria for CLL/SLL to include such cases of "BM MBL" with extensive involvement are warranted.

1374 Clinicopathologic and prognostic significance of survivin gene mutation and protein expression in T/NK-cell lymphoma

Hyang Joo Ryu[1], Sun Och Yoon[2]
[1]Yonsei University College of Medicine, Seoul, Korea, Republic of South Korea, [2]Seoul, Korea, Republic of South Korea

Disclosures: Hyang Joo Ryu: None; Sun Och Yoon: None

Background: Survivin, a member of the inhibitor of apoptosis gene family, is known to be upregulated in a variety of human cancers and is an important target for cancer therapeutics. We aimed to evaluate the survivin gene (BIRC5) mutation and protein expression in T/NK-cell lymphoma patients.

Design: We performed targeted sequencing and immunohistochemistry with image analysis (GenASIs HiPath program) using FFPE samples.

Results: Of 46 T/NK-cell lymphomas, BIRC5 mutation was detected in 20 (43%) cases, in which 3 missense variants and 1 frameshift variant were observed. Of 131 T/NK-cell lymphomas, survivin overexpression was shown in 51 (33.1%) when using a cutoff of mean value (>22.9%). There was no association between the genetic alteration and protein expression (p=0.332). Survivin overexpression tended to be more frequent in T lymphoblastic lymphoma than in mature T/NK-cell lymphoma (80.0% vs. 37.3%, p=0.075), but there was no association between BIRC5 mutation or survivin overexpression and other clinicopathological variables. In Kaplan-Meier survival analysis, BIRC5 mutation or survivin overexpression was not associated with patients' overall survival (OS). However, BIRC5 mutation showed a tendency of worse OS among the younger patients (p=0.054) and among the patients with gastrointestinal T/NK-cell lymphoma (p=0.086). In addition, survivin overexpression was significantly associated with reduced OS among the patients with stage III-IV (p=0.009), among those with peripheral T-cell lymphoma, not otherwise specified (p=0.024), and among those with EBV-positive tumor (p=0.045).

Conclusions: Our results suggest that survivin may be implicated in pathogenesis of T/NK-cell lymphoma and its role needs to be further investigated.

1375 Homogeneously Staining Region (hsr) on Chromosome 11 Is Highly Specific for KMT2A Amplification in Acute Myeloid Leukemia (AML) and Myelodysplastic syndromes (MDS)

Ali Sakhdari[1], Zhenya Tang[2], Carlos Bueso-Ramos[2], Guilin Tang[2], L. Jeffrey Medeiros[2], Yang Huh[1]
[1]Houston, TX, [2]The University of Texas MD Anderson Cancer Center, Houston, TX

Disclosures: Ali Sakhdari: None; Zhenya Tang: None; Carlos Bueso-Ramos: None; Guilin Tang: None; L. Jeffrey Medeiros: None; Yang Huh: None

Background: AML and MDS are of the most common myeloid neoplasms and affect mainly older patients. Overexpression of certain oncogenes plays an indispensable role in tumorgenesis of these neoplasms. Rearrangement and amplification of *KMT2A* located at band 11q23 is a well-characterized genetic driver in a subset of AML/MDS cases with poor prognosis. At the chromosomal level, an amplification of genetic material can result from formation of extra-chromosomal double minutes or intra-chromosomal homogeneously staining regions (hsr). The presence of hsr in certain chromosomes can be correlated with amplification of specific oncogene, such as hsr(8)(q24) and *MYC*. The presence of hsr(11)(q23) has been shown to likely be related to *KMT2A* amplification in small number of cases previously. In this study, we correlated hsr(11) with *KMT2A* in a large cohort of AML/MDS patients.

Design: We searched our database to identify AML/MDS patients with hsr(11) detected by conventional cytogenetic analysis. The presence of *KMT2A* amplification was evaluated by targeted fluorescent in situ hybridization (FISH). We compared the chromosomal analysis with a control group of 18 AML/MDS patients with hsr other than the hsr(11)(q23).

Results: We identified 36 patients with hsr(11)(q23), 18 men and 18 women with a median age of 68 years (range, 28-89). Using the current WHO criteria, 26 (72%) had AML (8 therapy-related) and 10 (28%) had MDS (2 therapy-related). The median BM blasts was 39% (range, 30-80) and 13% (range, 3-15) in AML and MDS patients, respectively. All patients showed a complex karyotype including 12 cases with monosomy 17. FISH analysis was available for 34 patients which showed *KMT2A* amplification in all of these patients. Among the control cases, FISH analysis for *KMT2A* was available in 11 cases which showed no *KMT2A* amplification in any of the cases (p=0.0001, Fisher's exact test, two-tailed). Mutational analysis was performed in 32 patients with hsr(11)(q23). The most common mutated gene was *TP53* (n=29, 91%), followed by *DNMT3A* (n=4, 13%), *NF1* (n=4, 13%), and *TET2* (n=3, 9%). One *FLT3*-TKD mutation was detected in 29 cases with *FLT3* assessment. 30 (83%) patients died over a median follow-up of 7.4 months (range, 0.4-33.4).

Conclusions: The presence of hsr(11)(q23) is significantly associated with *KMT2A* amplification, while no amplification detected in non-11(q23) hsr. Cases with hsr(11)(q23) and *KMT2A* amplification are enriched for *TP53* mutations and are associated with a very poor clinical outcome.

1376 Enhancer of Zeste Homolog 2 (EZH2) Expression in Mantle Cell Lymphoma Correlates with Ki-67 Proliferation Rate, but Does Not Correlate with Trimethylation of Histone H3 at Lysine 27

Ali Sakhdari[1], Ken H. Young[2], Roberto Miranda[2], L. Jeffrey Medeiros[2], Chi Young Ok[2]
[1]Houston, TX, [2]The University of Texas MD Anderson Cancer Center, Houston, TX

Disclosures: Ali Sakhdari: None; Ken H. Young: None; Roberto Miranda: None; L. Jeffrey Medeiros: None; Chi Young Ok: None

Background: Mantle cell lymphoma (MCL) is an aggressive B-cell lymphoma. MCL is not curative and virtually all patients will have recurrent or relapsed diseases. Polycomb group proteins (PcG) are regulators of gene silencing and thier dysregulation has been associated with various types of cancer. The polycomb repressive complex 2 (PRC2) is a key component of PcG, and enhancer of zeste homolog 2 (EZH2) has the catalytic activity of the PRC2. The PRC2 induces trimethylation of histone H3 at lysine 27 (H3K27me3), leading to gene repression. Recently, a promising result was shown in patients with *EZH2*-mutated lymphoma who were treated with an EZH2 inhibitor (Lancet Oncol. 2018). However, there are limited data available regarding expression of PRC2 and its association of H3K27me3 in MCL.

Design: We identified a total of 63 MCL patients with available fixed, paraffin-embedded tissue blocks. A tissue microarray was constructed from these blocks. Immunohistochemical studies for Ki-67, EZH2 and H3K27me3 were performed. Expression of each marker was evaluated semi-quantitatively with 10% increments.

Results: Our cohort includes 51 men and 12 women with a median age of 61 years at diagnosis (range: 41 to 83 years). Specimens were obtained from lymph node (n=25), spleen (n=10), Waldeyer's ring (n=8) and other extranodal tissues (n=20). These included 34 with classic morphology and 29 aggressive variants (blastoid and pleomorphic). In all patients, the median Ki-67 proliferation rate, EZH2 expression and H3K27me3 expression was 30% (range: 0-100%), 30% (range: 0-100%) and 90% (range: 0-100%), respectively. Ki-67 proliferation rate and EZH2 expression showed a strong correlation ($p<0.01$, Pearson $r=0.8944$). Expression of EZH2 and H3K27me3 were not correlated. Ki-67 proliferation rate is significantly different between classic variant (median: 15%) and aggressive variant (median: 60%) ($p<0.01$). Expression of EZH2 showed a similar pattern between classic and aggressive variants (median: 15% and 60%, respectively, $p<0.01$). However, expression of H3K27me3 was similarly high in both classic and aggressive groups (median: 90% and 100%, respectively, $p=0.13$).

Conclusions: Our data show expression of EZH2 in MCL is correlated with Ki-67 proliferation rate and that EZH2 is higher in morphologically aggressive variants. However, EZH2 expression is not correlated with H3K27me3. These data suggest that EZH2 is a potential therapeutic target in patients with mantle cell lymphoma , particularly in aggressive morphologic variants.

1377 Acute Myeloid Leukemia (AML) with Sole del(11q) Is Associated with Cytopenia, Dysplasia and a Poor Outcome

Ali Sakhdari[1], Kirill Lyapichev[1], L. Jeffrey Medeiros[2], Guilin Tang[2]
[1]Houston, TX, [2]The University of Texas MD Anderson Cancer Center, Houston, TX

Disclosures: Ali Sakhdari: None; Kirill Lyapichev: None; L. Jeffrey Medeiros: None; Guilin Tang: None

Background: del(11q) has been classified as a “very good” cytogenetic abnormality in the Revised International Prognostic Score System for myelodysplastic syndromes (MDS). On the other hand, del(11q) has been defined as being “sufficient” evidence for AML with myelodysplasia-related changes (AML-MRC), a subgroup in the World Health Organization (WHO) classification in which patients generally have a poor prognosis and a low remission rate. Nevertheless, del(11q) as a sole abnormality in AML has not been well studied.

Design: We searched our institutional database over 15 years to identify patients with AML and del(11q) as a sole abnormality. Patients with *KMT2A* rearrangement were excluded from the study. Clinical information, pathological findings and laboratory data were collected.

Results: We identified 18 AML patients with del(11q) as a sole abnormality. There were 15 men and 3 women with a median age of 66 years (range, 32-85). 9 patients had no history (group A) and 9 had a history of a myeloid neoplasm (MN) (group B): MDS (all with del11q, n=4,), CMML (n=2), MPN (n=2), and AML (n=1), the latter 5 acquired del(11q) during transformation or relapse. At the time of AML/del(11q) diagnosis, 17 patients had anemia (median: 9 ; range: 7-14.2 g/dL); 17 had thrombocytopenia (median: 66 ; range: 18-700 $x10^9$/dL); and the leukocyte counts were variable (median: 8.5 ; range: 2.1-120 $x10^9$/dL). The median blast counts were 55% (range, 21-90) in BM and 30% (range, 0-79) in PB. Multilineage dysplasia was detected in 4/7 patients in group A and 6/9 in group B. All 9 patients in group A received AML-based chemotherapies; 5 achieved complete remission (CR), and 4 were refractory for therapy. In group B, 4 patients were treated with AML-based regimens, 2 achieved CR and 2 were refractory to therapy, the other 5 patients either deceased soon after transformation or lost follow-up. At the last follow-up, 12 patients (5 from group A and 7 from group B) died with a median survival of 9.4 months (18.6 months for group A and 3.9 months for group B, respectively, p=0.04).

Conclusions: AML with sole del(11q) is very rare (<0.5%), and about half of the patients are transformed from MDS or other myeloid neoplasms. Patients with AML/del(11q) almost always have anemia and thrombocytopenia, often have multilineage dysplasia, and have a general poor outcome, especially for the patients who had a prior history of a myeloid neoplasm. Our findings endorse the inclusion of AML with del(11q) in the WHO subgroup of AML-MRC.

1378 Gaucher disease and associated plasma cell myeloma: A diagnostic challenge

Sandra Sanchez[1], Robert Ali[2], Neal Weinreb[3], Nicole Osorio[4], Daniel Cassidy[5], Kyle White[6], Jennifer Chapman[7], Francisco Vega[1], Offiong Ikpatt[8]
[1]University of Miami/Sylvester Cancer Center, Miami, FL, [2]University of Miami, Miller School of Medicine, Miami, FL, [3]University of Miami, Miller School of Medicine, Boca Raton, FL, [4]University of Miami, Davie, FL, [5]Miami, FL, [6]Lake Worth, FL,[7]University of Miami, Miller School of Medicine, North Miami, FL, [8]UMH, Miramar, FL

Disclosures: Sandra Sanchez: None; Robert Ali: None; Neal Weinreb: *Advisory Board Member*, Genzyme, a Sanofi Company; *Primary Investigator*, Shire HGT; *Advisory Board Member*, Pfizer Corporation; Nicole Osorio: None; Daniel Cassidy: None; Kyle White: None; Jennifer Chapman: None; Francisco Vega: None; Offiong Ikpatt: None

Background: Gaucher disease (GD) patients have an increased risk of cancer, including plasma cell neoplasm. The clinical manifestations of both GD and plasma cell myeloma overlap as both may present with anemia and lytic bone lesions.

In this study, we describe the clinical features, laboratory parameters and molecular features of 9 patients with GD who developed an M-spike during follow-up.

Design: We reviewed the medical records of 62 GD patients seen at an academic hospital. We identified 9 patients that had an M-spike demonstrated by SPEP. GBA1 mutations, presence of anemia, renal and bone lesions were annotated.

Results: The features of Gaucher Disease patients with and without M-spikes are shown in Table 1.

	Gaucher Disease with no M-spike (n=53)	Gaucher Disease with an M-spike (n=9)
Mean age (y) ±SD	59 ±19	72 ± 5
Gender (M:F)	9:2	7:2
Race	Jewish: 48 (91%) Hispanics:5 (9.4%)	Jewish: 5 (55.5%) Hispanic: 2 (22.2%) Caucasian: 2 (22.2%)
Anemia (Hb <10g/dl)	9 (17%)	4 (44.4%)
Lytic bone lesions	17 (32.1%)	4 (44.4%)
Renal dysfunction*	15 (28.3%)	4 (44.4%)
Frequency with N370S/N370S mutation	31 (58.5%)	6 (66.6%)

* Renal dysfunction is not usually part of the clinical spectrum of GD but associated with other co-morbidities.

In cases with an M-spike, abnormal free light chain ratio was seen in 4 patients. M-spike was less than 3mg/dl in all. All had IgG isotype.

Clonal plasma cells over 10% was seen in the 3 patients that had a bone marrow biopsy. Karyotype and myeloma specific FISH were normal in 2. One showed del13.

Conclusions: We expand the landscape of GD with secondary plasma cell neoplasm.

The overlap of symptoms between the 2 diseases make classification of plasma cell neoplasm a challenge as the cause of associated anemia, or lytic lesion may be ascribed to either of the disease.

Type of GD mutations cannot predict patients that develop an M-spike.

Patients with GD should be monitored for plasma cell neoplasm.

1379 GATA-1 Down- Regulation is Associated with Fibrotic Progression of Myeloproliferative Neoplasms

Valentina Fabiola Sangiorgio[1], Anna Nam[2], Zhengming Chen[3], Attilio Orazi[4], Wayne Tam[5]
[1]Istituto Europeo di Oncologia, Milan, Italy, [2]New York, NY, [3]Weill Cornell Medicine, New York, NY, [4]Weill Cornell Medical College/NYP, New York, NY, [5]Weill Cornell Medical College, New York, NY

Disclosures: Valentina Fabiola Sangiorgio: None; Anna Nam: None; Zhengming Chen: None; Wayne Tam: None

Background: Globin transcription factor 1 (GATA1) is a transcription factor essential for effective hematopoiesis. It is normally expressed in erythroid precursors and megakaryocytes and required for their proper maturation. GATA1-deficient mice experience anemia and thrombocytopenia. There are two isoforms of GATA1, derived for alternative splicing, GATA1 and GATA1-s. GATA1 (413 aa) is the full-length protein; GATA1-s (330 aa) is the truncated isoform devoid of the N-terminal activation domain, of which the activity is controversial. In hematologic malignancies, GATA1 expression is reduced in idiopathic myelofibrosis, in which its downregulation impairs megakaryocytic maturation. In the present study we seek to investigate the role of GATA1 in *BCR-ABL* negative myeloproliferative neoplasms (MPNs) and their progression by a comprehensive immunohistochemical evaluation of GATA1 expression in these neoplasms.

Design: We selected a cohort of 64 cases of *BCR-ABL* negative MPNs: 16 essential thrombocythemia (ET), 9 polycythemia vera (PV), 6 pre-primary myelofibrosis (pre-PMF), 6 post-ET myelofibrosis (post-ET MF), 14 post-PV myelofibrosis (post-PV MF) and 13 overt primary myelofibrosis (PMF). We performed immunohistochemistry using two clones of rabbit monoclonal antibodies: EPR17362 (Abcam) which reacts to both GATA1 and GATA1-s and D52H6 (Cell Signaling) which recognizes GATA1 only. For each case, the number of all the megakaryocytes present in the core biopsy was evaluated and the percentage of GATA1 “positive”, “weakly positive” or “negative” megakaryocytes was reported (Figure 1; red arrows indicate GATA1 negative megakaryocytes). Student's t-test was used to compare GATA-1 relative expression between the positive group and the combined weakly positive/negative group.

Results: We observed a significant reduction in GATA1 expression in pre-PMF compared to ET/PV ($p < 0.05$). No difference was observed between PV and ET. There was a significant decrease in GATA1 expression from ET and PV to post-ET MF and post-PV MF, respectively ($p < 0.05$). The decrease was more prominent for full-length GATA1 compared to total GATA1, suggesting that the loss is preferential for the long form of GATA1. There is also a trend for a reduction of GATA1 from pre-PMF to PMF ($p = 0.1$).

Figure 1 - 1379

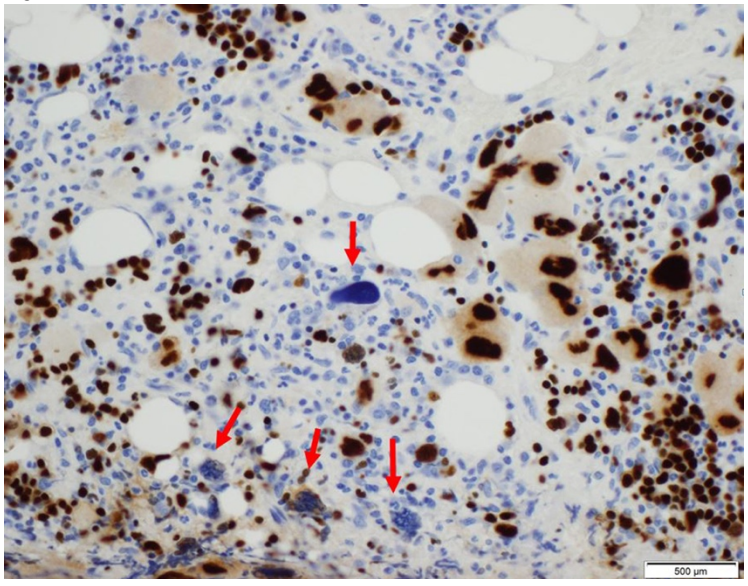

Conclusions: Our results support a role of GATA-1 down-regulation in the fibrotic progression of MPNs. Immunohistochemical evaluation of GATA1 may also be helpful in the clinically relevant differential diagnosis between ET and pre-PMF.

1380 Methotrexate-associated Lymphoproliferative Disorders of T-cell Phenotype: Clinicopathological Analysis of 28 Cases

Akira Satou[1], Tetsuya Tabata[2], Hiroaki Miyoshi[3], Kei Kohno[4], Yasuharu Sato[5], Tadashi Yoshino[6], Koichi Ohshima[7], Taishi Takahara[1], Toyonori Tsuzuki[8], Shigeo Nakamura[9]

[1]Aichi Medical University Hospital, Nagakute, Japan, [2]Okayama University Graduate School of Medicine, Okayama, Japan, [3]Kurume University, School of Medicine, Kurume, Japan, [4]Nagoya University Hospital, Nagoya, Japan, [5]Okayama University Graduate School of Medicine, Dentistry and Pharmaceutical Sciences, Okayama, Japan, [6]Okayama University Medical School, Okayama, Japan, [7]Kurume University, Kurume, Japan, [8]Toyonori Tsuzuki, Nagoya, Japan, [9]Nagoya University Hospital, Nagoya-shi, Japan

Disclosures: Akira Satou: None; Tetsuya Tabata: None; Hiroaki Miyoshi: None; Kei Kohno: None; Yasuharu Sato: None; Tadashi Yoshino: None; Koichi Ohshima: None; Taishi Takahara: None; Toyonori Tsuzuki: None; Shigeo Nakamura: None

Background: Methotrexate (MTX)-associated lymphoproliferative disorders (LPD) is categorized as other immunodeficiency-associated LPD in the WHO classification. MTX-associated LPD are mainly B-cell LPD or Hodgkin lymphoma, while T-cell LPD is rare. Only a small number of MTX-associated T-LPD (MTX T-LPD) with detailed description has been reported so far, and clinicopathological characteristics of MTX T-LPD still remain unknown.

Design: A total of 28 cases of MTX T-LPD were retrospectively analyzed. Furthermore, to characterize MTX T-LPD, we have compared the clinicopathologic characteristics of MTX T-LPD and 33 cases of MTX B-LPD consist of 14 monomorphic and 19 polymorphic type. Patients diagnosed as EBV-positive mucocutaneous ulcer were excluded from the MTX B-LPD group. All patients enrolled were treated with MTX for RA at the onset of MTX LPD.

Results: The clinical features of MTX T-LPD cases are summarized in Table. The 15 men and 13 women had a median age of 69.5 years (range, 56-85). 21 patients (78%) showed stage III/IV disease, 15 (54%) had B symptom, and none of them had bulky masses. Histologically and immunohistochemically, MTX T-cell LPD were divided into three main types: AITL (n=19), PTCL-NOS (n=6), and $CD8^+$ cytotoxic T-cell lymphoma (CTL) (n=3). Among the 28 cases, only one case of $CD8^+$ CTL expressed EBER on tumor cells. Tumor cells of the other 27 cases were negative for EBER, but scattered EBV-infected B-cells were detected in 23 cases (85%), implying the reactivation of EBV caused by immunodeficient status of the patients. After the diagnosis of MTX T-LPD, MTX was immediately withdrawn in 26 cases. 20 (77%) of the 26 cases showed spontaneous regression (SR).

Compared with MTX B-LPD, patients with MTX T-LPD showed significantly higher ratio of males ($p=0.035$) and presence of B-symptom ($p=0.036$) and lower ratio of EBV positivity of tumor cells ($p < 0.001$). Although MTX T-LPD group tended to show SR more frequently ($p=0.061$), patients with MTX T-LPD tended to show worse disease-specific survival compared with MTX B-LPD ($p=0.079$, Figure).

Variable	MTX T-LPD (n=28)	MTX B-LPD (n=33)	*P*
Sex (M/F)	16/12	10/23	0.035
Age (median[range])	70 (56-85)	68 (47-82)	0.27
PS > 1	7/28 (25%)	11/30 (37%)	0.34
Stage III/IV	21/27 (78%)	26/33 (79%)	0.92
B symptom	15/28 (54%)	9/33 (27%)	0.036
Bulky mass	0/28 (0%)	1/31 (1.7%)	-
Extranodal site > 1	7/27 (26%)	9/33 (27%)	0.91
LDH > normal	15/28 (54%)	24/32 (75%)	0.083
IPI HI/H	16/26 (62%)	20/29 (69%)	0.56
EBER	1/28 (3.6%)	20/33 (61%)	< 0.001
SR	20/26 (77%)	17/32 (53%)	0.061

Figure 1 - 1380

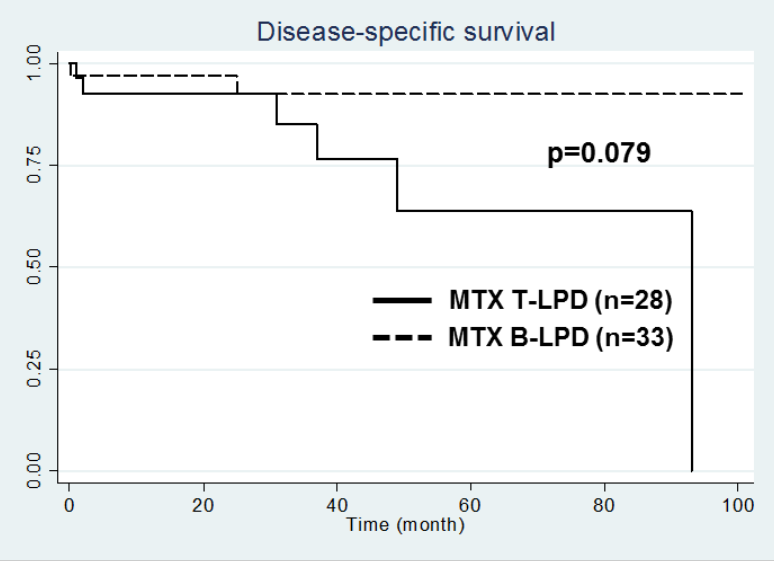

Conclusions: We have highlighted that majority of MTX T-LPD show AITL pattern based on histological and immunohistochemical findings. EBV positivity of the MTX T-LPD was significantly lower compared with MTX B-LPD, suggesting the different pathogenesis of the two. Although MTX T-LPD patients frequently show SR after MTX cessation, MTX T-LPD might have worse prognosis compared with MTX B-LPD.

1381 Stratification of Anaplastic Large Cell Lymphoma by Routine Diagnostic Immunohistochemistry

Akira Satou[1], Naoki Oishi[2], Andrew Feldman[2]
[1]Aichi Medical University Hospital, Nagakute, Japan, [2]Mayo Clinic, Rochester, MN

Disclosures: Akira Satou: None; Naoki Oishi: None; Andrew Feldman: None

Background: Anaplastic large cell lymphomas (ALCLs) comprise a group of T-cell lymphomas unified by common pathologic features. While ALCLs classically express cytotoxic markers and show loss of pan-T-cell antigens, variations in phenotype occur. The significance of these variations on the diagnosis and classification of ALCL remain unclear. Here, we analyzed ALCL phenotype agnostically in a large case series and examined results in the context of genetic classification into ALK, DUSP22, TP63, and triple-negative (TN) subtypes.

Design: We first analyzed immunohistochemistry (IHC) results from consultative pathology reports in a discovery set of 565 ALCLs using unsupervised hierarchical clustering and principal component analysis (PCA), agnostic to ALK status and clinical presentation. We then confirmed findings in an independent validation set of 102 ALCLs that were re-reviewed for diagnostic accuracy and stain interpretation, and on which genetic subtyping by FISH was performed.

Results: Unsupervised clustering and PCA in the discovery set showed similar findings. Top principal components (PCs) mainly reflected contributions of T-cell antigens (PC1: CD2>CD3>CD43) and cytotoxic markers (PC2: TIA1>GrzB>EMA). These patterns were confirmed in the validation set. Patterns were similar in systemic ALK- ALCL and primary cutaneous ALCL, but differed markedly among genetic subtypes (Figure 1). ALK cases were PC1-/PC2+ while DUSP22 cases were PC1+/PC2-. Notably, TN ALCLs were heterogeneous and stratified into 2 main groups predominantly based on PC2. Too few TP63 cases were available for analysis.

Figure 1 - 1381

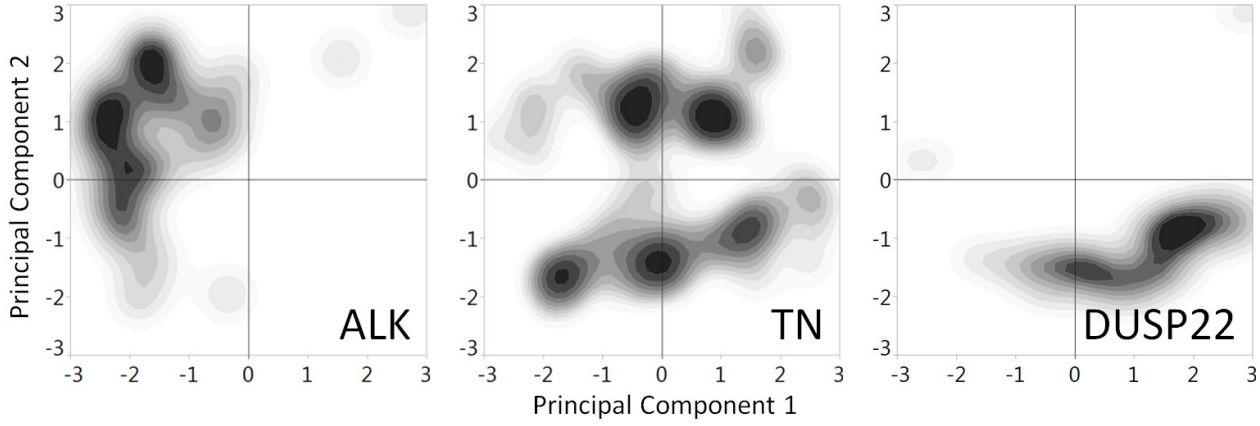

Conclusions: Analysis of routine IHC results in a large series of ALCLs demonstrated reproducible patterns of phenotypic variation that strongly associated with genetic subtype but not clinical presentation. Even without results of ALK IHC, ALK+ ALCL and DUSP22 ALCL each showed characteristic phenotypes that differed strikingly from one another. TN ALCLs showed phenotypic heterogeneity, with at least 2 distinct groups including a subset lacking cytotoxic markers. Thus, phenotypic variation in ALCL is non-random, and routine IHC stratifies ALCLs into subgroups with unique molecular features not fully reflected by the current WHO classification. These results highlight the need for comprehensive molecular classification of ALCL.

1382 Distinctive Immunophenotype of Acute Myeloid Leukemia with IDH Mutations

Adam Seegmiller[1], Emily Mason[1], Aaron Shaver[1]
[1]Vanderbilt University Medical Center, Nashville, TN

Disclosures: Adam Seegmiller: None; Emily Mason: None; Aaron Shaver: None

Background: Identification of isocitrate dehydrogenase (IDH) mutations in acute myeloid leukemia (AML) has become increasingly important with the recent approval of targeted IDH inhibitor therapies. However, because of long turn-around times for molecular testing, mutation status is often unknown at the time of therapy initiation. In this study, we show that IDH-mutated AML (IDH-AML) has a distinctive immunophenotype by multiparameter flow cytometry (MFC) and that this immunophenotype can be used to identify IDH-AML with high sensitivity and specificity.

Design: All cases of de novo AML with complete immunophenotype by MFC and full genotype using a 37-gene next generation sequencing panel from December 2014 to July 2018 were included. Myeloblasts were identified by MFC using standard gating. The mean fluorescence intensity (MFI) was determined for CD2, CD4, CD11b, CD13, CD14, CD15, CD16, CD19, CD33, CD34, CD38, CD45, CD56, CD64, CD117, and HLA-DR. The lineage and MFIs of IDH-AML myeloblasts were compared with those of other AMLs. A classification algorithm was created using the MFI ranges for each marker on cases in each of the three IDH mutation categories (IDH1 R132, IDH2 R140, and IDH2 R172). Cases were classified as potentially IDH positive if the myeloblast MFI for each marker fell within at least one of these sets of ranges.

Results: Of 180 AML cases, 37 (21%) carried mutations at IDH1 R132 (N=14), IDH2 R140 (N=17), or IDH2 R172 (N=6). Of these, 28 (72%) showed myeloid, 9 (23%) showed myelomonocytic, and 2 (5%) showed monocytic differentiation. Compared with other AMLs, myeloblasts in IDH-AML showed lower expression of CD7 (P=0.01), CD13 (P=0.01), CD34 (P=0.0001), CD45 (P<0.0001), and HLA-DR (P=0.0007). Excluding cases with solely monocytic differentiation, a classification algorithm based on these results correctly identified all IDH-AML cases. In addition, it correctly identified the specific gene and mutation site in 29 of 37 cases (78%), and correctly called 100 of 120 (83%) other AMLs negative for IDH mutations.

Conclusions: These results show that AMLs with IDH mutations have a distinctive immunophenotype when compared to other AMLs. Using immunophenotype alone, IDH-AML can be correctly identified with high sensitivity (100%) and specificity (87%) in acute myeloid and myelomonocytic leukemias. If these results are borne out in prospective studies, this approach may lead to more rapid identification of IDH-AML cases, potentially allowing earlier inclusion of mutation-directed therapies.

1383 Distinctive Genotype-Immunophenotype Correlations in Acute Myeloid Leukemia

Adam Seegmiller[1], Emily Mason[1], Aaron Shaver[1]
[1]*Vanderbilt University Medical Center, Nashville, TN*

Disclosures: Adam Seegmiller: None; Emily Mason: None; Aaron Shaver: None

Background: Recent developments in sequencing of acute myeloid leukemia (AML) have allowed organization of cases into genotypic categories that have prognostic significance. Because deep sequencing is not universally available and has long turn-around times, it may be helpful to have other methods for assigning cases to these categories. Using multiparametric flow cytometry (MFC), we evaluated the immunophenotype of myeloblasts and monocytic elements in AML to determine if certain genotypic categories are associated with distinct immunophenotypes.

Design: A total of 180 de novo AMLs with a complete immunophenotype by MFC, karyotype, and a full genotype using a 37-gene next generation sequencing panel were analyzed. Each case was assigned a genotypic category using the criteria of Papaemmanuil *et al.* (*N Engl J Med.*, 2016;374:2209). Myeloblasts and/or monocytic elements were identified by MFC using standard gating, and mean fluorescence intensity (MFI) was determined for CD2, CD4, CD11b, CD13, CD14, CD15, CD16, CD19, CD33, CD34, CD38, CD45, CD56, CD64, CD117, and HLA-DR. Cases were categorized as positive or negative (above or below an empiric cut-off) for markers expected to be negative, or as high or low expressers (above or below median MFI) for markers expected to be positive. Cases were analyzed to determine if the observed pattern of expression in each of the 13 genotypic categories differed significantly from that of all AMLs.

Results: Blast lineage (myeloid, myelomonocytic, and monocytic) was not evenly distributed across genotypic categories (P<0.0001); some categories showed mostly myeloid and others showed mostly monocytic differentiation. Significantly distinctive myeloblast phenotypes were observed for AML in the following categories: CEBPA ($CD7^{POS}$, $CD13^{LO}$, $CD38^{HI}$, $CD64^{POS}$, $HLA\text{-}DR^{HI}$) (P<0.0001), NPM1 ($CD34^{LO}$, $CD117^{LO}$, $HLA\text{-}DR^{LO}$) (P<0.0001), t(15;17) ($CD2^{POS}$, $CD14^{POS}$, $CD34^{LO}$, $CD64^{POS}$) (P<0.0001), and t(8;21) ($CD15^{HI}$, $CD19^{POS}$, $CD34^{HI}$, $CD38^{HI}$, $CD56^{POS}$, $CD117^{HI}$, $HLA\text{-}DR^{HI}$) (P<0.0001). Distinctive monocytic phenotypes were seen for MLL fusions ($CD11b^{LO}$, $CD14^{LO}$, $CD56^{POS}$, $CD117^{POS}$) (P=0.0005) and TP53 ($CD13^{HI}$, $CD34^{POS}$) (P=0.02). All together, distinctive phenotypes were seen for 6 of 13 categories, representing 83 of 180 cases (46%).

Conclusions: AML cases in some genotypic categories exhibit unique and distinctive patterns of cell surface marker expression. These patterns could potentially help predict categorization based on genotype at the time of diagnosis before molecular data is available.

1384 Hodgkin Lymphoma Following Diffuse Large B-Cell Lymphoma: A Clinical and Pathologic Review

Shenon Sethi[1], Ira Miller[2]
[1]*Rush University Medical Center, Chicago, IL,* [2]*Chicago, IL*

Disclosures: Shenon Sethi: None

Background: The development of Hodgkin lymphoma (HL) following diffuse large B-cell lymphoma (DLBCL) has been previously reported. Evaluation of rare patients with both HL and DLBCL have shown that the Hodgkin/Reed-Sternberg cells and the DLBCL cells are often clonally related, as evidenced by identical VDJ rearrangements of the Ig heavy chain locus and shared somatic mutations within the VDJ region. Herein, we review the clinical and pathologic characteristics of HL in patients with history of DLBCL.

Design: A comprehensive analysis of the Rush database was performed. Between November 1992 and August 2018, 1745 adult patients with new untreated DLBCL and 451 patients with new untreated HL were identified. Grey zone lymphomas, composite lymphomas and cases that were difficult to classify, B-cell lymphoma, unclassifiable, with features intermediate between DLBCL and classic HL (CHL) were excluded. Patients were included when HL followed the diagnosis of DLBCL. For the purpose of comparison, patients that developed DLBCL following the diagnosis of HL were also included.

Results: In 8 cases the diagnosis of DLBCL preceded the diagnosis of HL (rate of transformation = 0.46 %; median interval 41.5 months) and 8 cases had HL that subsequently developed DLBCL (rate of transformation = 1.77%; median interval 52 months). In the group with HL as the first diagnosis, most were males (M: F=5:3) and all the cases were that of CHL with nodular sclerosis as the most common subtype. Of the cases that were tested, majority of them (85.7%; 6/7) had activated B-cell (ABC) immunophenotype. At least some level of CD30 expression was seen in all (100%; 6/6) cases of DLBCL that followed. CD30 expression was also seen in 75% (6/8) of DLBCLs following HL. Involvement of spleen (12.5%; 1/8) or bone marrow (37.5%, 3/8) was occasionally present. Mediastinal location and anaplastic morphology were seen in 12.5% (1/8) and 25% (2/8), respectively. Epstein-Barr virus (EBV) in situ hybridization or human immunodeficiency virus (HIV) was positive in 2 of 5 cases tested. Other hematologic malignancies were seen in 62.5% (5/8) of cases. In contrast, none of the cases that had DLBCL following HL had such history.

	HL to DLBCL	DLBCL to HL
Median age at first diagnosis (years)	53.5	52.5
Male:Female	7:1	5:3
Median follow up (months)	26	22
EBV in situ hybridization in DLBCL	1/6	1/4
Subtype of HL:		
CHL	6/8	8/8
NLPHL	2/8	0/8
Positive HIV serology	0/4	1/5
Other hematologic disorder:		
Marginal zone lymphoma	0/8	2/8
AITL/PTCL	0/8	1/8
Plasma cell neoplasm	0/8	1/8
Primary myelofibrosis	0/8	1/8
CD30 positivity in DLBCL	6/8	6/6
Mediastinal location of DLBCL	0/8	1/8
Anaplastic morphology in DLBCL	0/8	2/8
Cell of origin		
Germinal center	3/8	1/8
ABC	4/8	6/8
Unknown	1/8	1/8
Median Interval between two diagnoses (months)	52	41.5
Abnormal genetics:		
Bcl-2 rearrangement	1/8	0/8
c-Myc rearrangement	1/8	0/8
Abnormal karyotype	0/8	2/8
Bone marrow involvement by DLBCL	1/8	3/8
Spleen involvement by DLBCL	2/8	1/8

AITL: Angioimunoblastic T-cell lymphoma; PTCL: Periheral T-cell lymphoma; CHL: classical Hodgkin lymphoma; NLPHL: Nodular lymphocyte predominant Hodgkin lymphoma

Conclusions: The development of HL following DLBCL was extremely rare (0.46%) with slightly higher incidence in males. All HLs that developed were CHL and almost all the DLBCLs that preceded were ABC type. Other hematologic malignancies were commonly associated whereas mediastinal location, EBV or HIV status were not.

1385 Next-Generation Sequencing of Peripheral Blood in Routine Evaluation of the Cytopenic Patient Enhances Bone Marrow Biopsy Diagnostic Yield

Vignesh Shanmugam[1], Annette Kim[1], Aric Parnes[1], Elizabeth Morgan[1]
[1]Brigham and Women's Hospital, Boston, MA

Disclosures: Vignesh Shanmugam: None; Annette Kim: None; Aric Parnes: None; Elizabeth Morgan: None

Background: Many institutions are incorporating next-generation sequencing (NGS) to assist in the evaluation of patients with possible hematologic malignancy. In the evaluation of cytopenias, routine mutational profiling of peripheral blood could serve as a minimally invasive screening tool to triage patients for bone marrow biopsy. Here we describe the clinical utility of NGS testing and its impact on hematology practice in a large cohort of cytopenic patients.

Design: After IRB approval, we identified all patients presenting with cytopenias to the Adult Hematology Clinic over two 3-year time periods: (1) before (2011-2013, n=1142) and (2) after (2015-2017, n=1491) the introduction of routine NGS testing. In the latter group, 244 (16%) patients underwent testing of peripheral blood using a custom 95-gene, amplicon-based sequencing panel surveying genes recurrently mutated in hematologic (predominantly myeloid) malignancies. Relevant clinical and laboratory data was abstracted from the electronic medical record.

Results: Bone marrow biopsy rates were comparable between both groups (pre-NGS: 6.4%; post-NGS: 5.6%). Both groups who underwent bone marrow biopsy testing were comparable in terms of age, gender, number, and severity of cytopenias (**Table 1**). Notably, compared to the pre-NGS group, the post-NGS group demonstrated a higher rate of hematologic malignancy on subsequent bone marrow biopsy (pre-NGS: 26%, post-NGS: 43%, P<0.05) (**Figure 1**). Of the 95 patients in the post-NGS era who underwent bone marrow biopsy, 56 (59%) had preceding NGS testing of peripheral blood with detection of pathogenic somatic mutation(s) in 26 (47%). In the post-NGS era, patients who underwent NGS testing were more likely to have a bone marrow biopsy diagnostic of a hematologic malignancy (28/56, 50%), compared to those who did not (13/39, 30%). Among patients who underwent NGS testing, presence/absence of a pathogenic somatic mutation was predictive of the presence/absence of a hematologic malignancy on bone marrow biopsy (+LR: 2.92, -LR: 0.39), particularly a myeloid neoplasm (+LR: 3.13, -LR: 0.16).

Table 1: Characteristics of patients who underwent bone marrow biopsy before (2011-2013) and after (2015-2017) introduction of routine NGS testing

	Before	After	P-value
N	73	95	
Sex (M/F)	37/36	53/42	0.5124
Age (median, range)	64 (20-85)	65 (28-88)	0.3711
Hemoglobin (g/dL) (median, range)	11.0 (6.0-16.0)	11.2 (6.4-15.8)	0.9260
Mean corpuscular volume (fL) (median, range)	92.0 (67-115)	92.4 (35.3-114.7)	0.0321
White blood cells (x 103/µL) (median, range)	5.4 (0.9-27.6)	5.15 (0.8-29.3)	0.4020
Absolute neutrophil count (x103/µL) (median, range)	2.90 (0.1-20.4)	3.09 (0.1-19.6)	0.6037
Platelets (x 103/µL) (median, range)	155 (7-562)	166 (23-486)	0.8524
Abnormal CBC finding at initial visit			
Anemia (%)	54 (74%)	74 (78%)	0.5470
Leukopenia (%)	22 (30%)	28 (29%)	0.8882
Thrombocytopenia (%)	34 (47%)	43 (36%)	0.1516
Number of cytopenias			
1	42 (57%)	55 (58%)	0.8969
2	24 (33%)	30 (32%)	0.8912
3	7 (10%)	10 (10%)	1.0000
Severe cytopenias (absoluteneutrophil count <1.8 x 103/µL, hemoglobin <10.0 g/dL, platelet count <100 x103/µL)	42 (58%)	63 (66%)	0.2897

Figure 1 - 1385

Figure 1: Flow diagram showing patient selection and bone marrow biopsy diagnoses before and after implementation of routine NGS testing

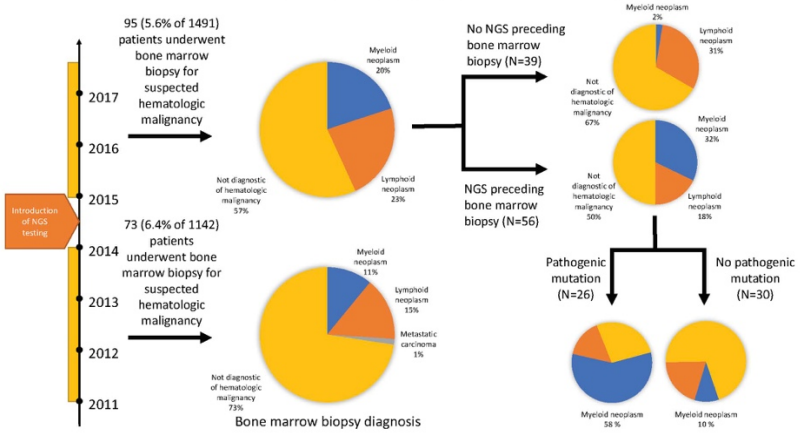

Conclusions: Pre-screening of peripheral blood of cytopenic patients with NGS increased the diagnostic yield of bone marrow biopsies likely by providing additional diagnostic information (i.e. altering pre-biopsy probability of underlying hematologic malignancy) to hematologists. Therefore, these findings support the use of routine mutational profiling of peripheral blood to inform the diagnostic work-up of cytopenias.

1386 Gene Landscape Identified in Philadelphia Chromosome Negative (Ph-) Adult B-lymphoblastic Leukemia and a Debating Role of CRLF2 Rearrangements in Clinical Outcome – a Single Institutional Experience

Rohit Sharma[1], Yun Seongseok[2], David Gajzer[3], Ling Zhang[4]
[1]Moffitt Cancer Center, Tampa, FL, [2]H. Lee Moffitt Cancer Center & Research Institute, Tampa, FL, [3]University of Miami/Jackson Memorial Hospital, Miami, FL, [4]Tampa, FL

Disclosures: Rohit Sharma: None; David Gajzer: None; Ling Zhang: None

Background: Approximately 20% of Philadelphia chromosome negative (Ph-) adult B-lymphoblastic leukemia (B-ALL) harbor gene rearrangements involving cytokine receptor gene *CRLF2* and other ABL-like genes. Patients with such abnormalities benefit from targeted tyrosine kinase therapy. Use of *CRLF2* translocation as a negative predictor of prognosis has been controversial. We present preliminary results of mutation profiling in adult Ph- B-ALL on the prognostic impact of *CRLF2* rearrangements.

Design: The bone marrow or peripheral blood from 36 patients with Ph- B-ALL managed at our institution between March 2014 and April 2017 were submitted for next generation sequencing (NGS) FoundationOne®Heme assay. Statistical analysis of test results included relevant clinical information and correlated mutation profiling. Patients were sub-grouped based on presence or absence of *CRLF2* rearrangements. Overall survival (OS) was assessed with the Kaplan-Meier method and log-rank tests.

Results: NGS identified mutation or gene alteration of *CDKN2A* most frequently (n=17, 47%) followed by *CRLF2* (n=10, 28%), *IKZF1* (n=6, 17%), *KRAS* (n=10, 28%), *NRAS* (n=7, 19%), *JAK2* (n=6, 17%), *PTPN11* (n=5, 14%), *FLT3* (n=4, 11%), and *NF1* (n=2, 6%). The median age was 49 (35-79) years with a male to female ratio of 1.7. The median bone marrow blast count was 61% (25-100) of total cellularity, with 19 patients having blast counts >85%. A total of 26 patients were treated with hyperCVAD and 10 patients received other induction regimens as the first line therapy. Median OS was 13.9 months (3.125-101.84). No statistically significant difference in OS was identified between patients with *CRLF2* rearrangements (*IgH-CRLF2*, n=9; *P2RY8-CRLF2*, n=1) and those without (median OS 58 vs. 107 months, HR 1.02, 95% CI 0.31-3.38, p=0.95), with exclusion of allogeneic stem cell transplant recipients (10) from analysis also not revealing any significant difference in OS (median OS 102 vs. 107 months, HR 1.275, 95% CI 0.35-4.66, p=0.68). *IKZF1* and *CDKN2A* mutations did not have prognostic impact on OS. OS in patients with >3 gene alterations (n=13) was similar to those with ?3 mutations (p=0.73).

Conclusions: Our results of frequent *CDKN2A* and *CRLF2* gene alterations in adult B-ALL are in line with previous studies, yet *CRLF2* rearrangements did not result in a statistically significant difference in OS. Larger study cohorts are indicated to further validate the prognostic roles of key gene alterations in Ph- B-ALL patients.

1387 CD8 Expression in Anaplastic Large Cell Lymphoma Identifies a Subgroup with Advanced Stage, Non-common Morphology, Unique Phenotype, and Poorer Outcome

Jing Shen[1], Shaoying Li[1], C. Cameron Yin[1], Sa Wang[1], Pei Lin[1], Jeff Jorgensen[1], Guilin Tang[1], Shimin Hu[1], L. Jeffrey Medeiros[1], Jie Xu[2]
[1]The University of Texas MD Anderson Cancer Center, Houston, TX, [2]Houston, TX

Disclosures: Shaoying Li: None; C. Cameron Yin: None; Sa Wang: None; Pei Lin: None; Guilin Tang: None; Shimin Hu: None; L. Jeffrey Medeiros: None; Jie Xu: None

Background: Anaplastic large cell lymphoma (ALCL) is a T-cell neoplasm characterized by uniformly strong CD30 expression and often CD4 expression with loss of other T-cell markers such as CD3, CD5, and CD7. A small subset of cases of ALCL has been reported to express CD8, but little is known about the cliniopathologic and prognostic features of CD8+ ALCL.

Design: Among the 222 cases of ALCL diagnosed in our institution from 2007-2017, CD8 expression was assessed in 46 cases by flow cytometry immunophenotypic analysis. The clinicopathologic and immunophenotypic features and outcome were compared between CD8+ and CD8-negative ALCL using Fisher's exact test. Overall survival (OS) was analyzed using the Kaplan-Meier method and compared using the log-rank test.

Results: Twelve of 46 (26%) cases were positive for CD8. Compared to patients with CD8-negative ALCL, patients with CD8+ ALCL more often had stage IV disease (90% vs. 47%, p = 0.03) and absolute lymphocytosis (33% vs. 0%, p = 0.04). Patients with CD8+ ALCL also more frequently had anemia (100% vs. 61%) and extra-nodal involvement (90% vs. 56%), but these differences did not reach statistical significance (p = 0.07 and p = 0.07, respectively). Morphologically, CD8+ ALCL more often showed non-common morphology (usually

small-cell and/or lymphohistiocytic variant) (50% vs. 3%, p = 0.001). CD8+ ALCL was more often positive for CD3 (73% vs. 29%, p = 0.02) and CD7 (91% vs. 38%, p = 0.004), but less frequently positive for CD25 (33% vs. 86%, p = 0.02). There was no significant difference in the expression of CD2, CD4, CD5, CD30, CD52, CD56, TCR A/B, TCR G/D, ALK, cytotoxic markers, and proliferation index by Ki67. Patients with CD8+ ALCL received induction treatment similar to patients with CD8-negative ALCL. OS of patients with CD8+ ALCL was significantly shorter than CD8-negative group (median survival, 14.6 months vs. undefined, p = 0.03).

Conclusions: CD8 expression in ALCL was associated with stage IV disease, absolute lymphocytosis, small-cell and/or lymphohistiocytic morphology, retained expression of CD3 and CD7, loss of CD25, and poorer outcome.

1388 Prevalence and Spectrum of T-cell Lymphoproliferative Disorders in Patients with Hypereosinophilia

Min Shi[1], Karen Rech[2], Gregory Otteson[1], Pedro Horna[1], Animesh Pardanani[1], Dong Chen[1], Dragan Jevremovic[1]
[1]Mayo Clinic, Rochester, MN, [2]Rochester, MN

Disclosures: Min Shi: None; Karen Rech: None; Gregory Otteson: None; Pedro Horna: None; Animesh Pardanani: None; Dong Chen: None; Dragan Jevremovic: None

Background: Eosinophilia is associated with non-neoplastic and neoplastic conditions where peripheral blood absolute eosinophil count (AEC) is more than 0.5 X 10 (9)/L. When persistently elevated AEC ≥ 1.5 X 10 (9)/L, it is defined as hypereosinophilia (HE). Primary HE is a clonal myeloid neoplasm where eosinophils can be a part of the neoplastic clone. Secondary HE is reactive eosinophilic hyperplasia largely in response to antigens/allergens. Occasionally, the eosinophilic hyperplasia is driven by clonal T-cells such as in lymphocytic variant of hypereosinophilia syndrome (LV-HES) or other T-cell lymphoproliferative disorders (TLPDs). In this study, we investigated the prevalence and spectrum of TLPDs in patients with HE.

Design: From 2014 to 2016, flow cytometry was performed on peripheral blood (PB) and bone marrow (BM) specimens with the indication of “eosinophilia”. The patients with HE were included in this cohort. Medical records and pathologic reports including BM and tissue biopsy findings, karyotype, FISH for CHIC2, PDGFRA and FIP1L1, and TCR gene rearrangement, were reviewed.

Results: 124 patients with HE were identified, with median age at 63 years (14-92), and male-to-female ratio of 1:1. The median AEC and absolute lymphocyte count (ALC) was 3.5 X 10 (9)/L (1.5-36.7) and 1.9 X 10 (9)/L (0.2-17), respectively. Flow cytometry demonstrated discrete populations of T-cells in 15/124 cases (12%), which were all CD4-positive. Molecular studies concordantly identified clonal TCR gene rearrangement in these cases. There was no significant difference in AEC or ALC between the groups with and without abnormal T-cell populations. Out of the 15 cases, 10 were diagnosed as LV-HES and 5 as T-cell lymphoma (3 peripheral T-cell lymphoma NOS, 2 cutaneous T-cell lymphoma). The 10 LV-HES cases revealed minimal cytological atypia on PB or BM slides, and 7 of 10 LV-HES cases had sCD3 loss, consistent with the common LV-HES phenotype (CD3-CD4+CD8-). In contrast, all 5 T-cell lymphoma cases displayed overt cytological atypia and only 1 showed loss of sCD3. All available cytogenetic and FISH studies were normal.

Conclusions: 12% of patients with HE had abnormal T-cell populations that were initially detected by flow cytometry. Further studies showed HE cases had a spectrum of TLPDs from indolent LV-HES (8%) to aggressive T-cell lymphoma (4%). These findings underscore the importance of flow cytometry as a screen tool to identify TLPDs in patients with HE.

1389 Distinct Clinicopathologic Features of Chronic Lymphocytic Leukemia/Small Lymphocytic Lymphoma (CLL/SLL) Based on MYD88 Mutations at Hotspot versus Non-Hotspot Codons

Wen Shuai[1], Pei Lin[1], Mark Routbort[1], Keyur Patel[1], Shimin Hu[1], Beenu Thakral[1], Boris Zhong[2], L. Jeffrey Medeiros[1], Wei Wang[1]
[1]The University of Texas MD Anderson Cancer Center, Houston, TX, [2]Kansas City University of Medicine and Biosciences, Kansas City, MO

Disclosures: Wen Shuai: None; Pei Lin: None; Mark Routbort: None; Keyur Patel: None; Shimin Hu: None; Beenu Thakral: None; Boris Zhong: None; L. Jeffrey Medeiros: None; Wei Wang: None

Background: A small subset of CLL/SLL carries *MYD88* mutations. The clinicopathologic features of *MYD88* mutations in CLL/SLL are not well established.

Design: *MYD88* mutations were assessed using NGS-based 29-gene panel. The clinical data, morphologic and immunophenotypic results as well as FISH studies were reviewed.

Results: Thirty-one CLL/SLL cases were identified to carry *MYD88* mutations. Based on mutation sites, these cases were: L265P (n=19, 61%), V217F (n=6, 19%), and one case each of M232T, Y180C, S219C, A6fs, N291S/T294B, and F252I/M232T. For comparison, we divided these cases into two groups: group A with *MYD88* L265P mutation (n=19, 61%) and group B with mutations in other sites (n=12,

39%). The median age at diagnosis was 46 years (range, 23-73) for group A and 63 years (range, 51-79) for group B. Paraproteins were detected in 4 cases: 3 were in group A including one with IgM Kappa (1,720 mg/dL), one with IgG kappa (2,678 mg/dL) and one with two paraproteins (IgG 1,402 mg/dL, IgM 243 mg/dL); 1 case was in group B with IgM Kappa (173 mg/dL). Of note, lymphoplasmacytic lymphoma was ruled out in all cases.

Morphologically, majority of cases (87%) showed lymphoid infiltrate with nodular and interstitial patterns on bone marrow biopsy. Abnormalities detected by FISH studies included loss of D13S319 (RB locus), trisomy 12, *TP53* deletion and *ATM* deletion (Table 1). All (18/18) patients in group A and 70% (7/10) patients in group B showed mutated *IGHV*. Other concurrent mutations by NGS analysis included: *TP53* mutations (4/31, 13%), *ATM* mutations (5/31, 16%), *SF3B1* mutation (1/31, in group A), and *NOTCH1* mutation (1/31, in group B). No *CXCR4* mutation was detected. Of note, 52% (16/31) cases had an atypical immunoprofile including moderate to bright CD20, partial FMC-7, absence of CD23 or CD43. All cases showed CD5 expression. For ZAP-70, 18% (3/17) in group A and 73% (8/11) CLL/SLL in group B had ZAP-70 expression.

Table 1 Clinicopathologic Features of CLL/SLL with *MYD88* Mutations

MYD88 mutation	A 61% (n = 19)	B 39% (n = 12)	*P*	Total (n = 31)
Age @ dx	46 (23-73)	63 (51-79)	0.031	53 (23-79)
M:F	2.8:1 (14:5)	1:2 in V217F, all M in others	NS	2.4:1 (22:9)
Serum paraprotein +	16% (3/19)	8% (1/12)	NS	13% (4/31)
D13S319 deletion by FISH	58% (11/19)	55% (6/11)	NS	57% (17/30)
Trisomy 12 by FISH	5% (1/19)	9% (1/11)	NS	7% (2/30)
TP53 deletion by FISH	16% (3/19)	0 (0/11)	NS	10% (3/30)
ATM deletion by FISH	5% (1/19)	18% (2/11)	NS	10% (3/30)
Mutated *IGHV*	100% (18/18)	70% (7/10)	0.037	89% (25/28)
TP53 mutation by NGS	16% (3/19)	8% (1/12)	NS	13% (4/31)
ATM mutation by NGS	5% (1/19)	33% (4/12)	0.039	16% (5/31)
ZAP-70 +	18% (3/17)	73% (8/11)	0.004	39% (11/28)

A, *MYD88* L265P mutation; B, Other *MYD88* mutation variants; dx, diagnosis; NS, not significant.

Conclusions: CLL/SLL cases with *MYD88* L265P hotspot mutation are different from cases with other mutation variants (Table 1), showing significantly younger age at presentation, higher percentage of mutated *IGHV*, less positivity in ZAP-70, and less *ATM* mutations by NGS. The different clinicopathologic features associated with different *MYD88* mutations may be due to the heterogeneous activities among different *MYD88* mutations. It may be helpful to separate *MYD88* L265P from other variants in future studies of CLL/SLL with *MYD88* mutations.

1390 MDMX is Overexpressed in Anaplastic Large Cell Lymphoma (ALCL), ALK+ and ALK-, and Contributes to the Growth and the Survival of ALCL Cells

Vaios Sinatkas[1], Dimitra Vyrla[2], Aristides Eliopoulos[3], L. Jeffrey Medeiros[4], George Z. Rassidakis[5], Elias Drakos[2]
[1]Karlstad, Sweden, [2]University of Crete, Heraklion, Greece, [3]Laboratory of Molecular and Cellular Biology, Medical School, National and Kapodistrian University of Athens, Athens, Greece, [4]The University of Texas MD Anderson Cancer Center, Houston, TX, [5]The University of Texas MD Anderson Cancer Center, Karolinska Institutet, Stockholm, Sweden

Disclosures: Vaios Sinatkas: None; Dimitra Vyrla: None; L. Jeffrey Medeiros: None; George Z. Rassidakis: None; Elias Drakos: None

Background: *p53*, the most frequently mutated tumor suppressor gene in human cancer, is rarely mutated in anaplastic lymphoma kinase (ALK)-positive and ALK-negative anaplastic large cell lymphoma (ALCL) tumors. We have shown previously that activation of p53 by nutlin-3a, a MDM2 specific inhibitor, results in p53-mediated cell cycle arrest and apoptosis of ALCL cells harboring potentially functional p53. MDMX (also known as MDM4) is a negative regulator of the p53 pathway. However, the expression levels and the biologic significance of MDMX in ALK+ ALCL and ALK- ALCL is unknown.

Design: Using immunohistochemical methods and tissue microarrays, we assessed for total MDMX protein expression in 30 ALK+ and 18 ALK- ALCL tumors. Also, we used two ALK+ ALCL cell lines, SUP-M2 harboring wild-type (*wt*) *p53* and Karpas 299 with mutated *(mt) p53* and two ALK- ALCL cell lines, Mac1 and Mac2A, harboring *wt p53.* After treatment with XI-006, a MDMX-specific inhibitor, in order to activate the p53 signaling pathway, we investigated the growth and cell death of ALCL cells by MTS, colony formation assay, trypan blue negative stain and Annexin V staining.

Results: MDMX immunoreactivity was primarily nuclear. MDMX protein was strongly expressed in all 32 (100%) ALK+ ALCL and 16 of 18 (85%) ALK- ALCL tumors. The average percentage of MDMX+ neoplastic cells in each tumor was 96% (range 75-100%) in ALK+ ALCL and 93% (range 70-100%) in ALK- ALCL.Treatment with XI-006 induced a dose dependent cytotoxicity specifically in wt-p53 ALCL cells. A dose of 1μM XI-006 inhibited completely the formation of colonies and after 24 hours resulted in up to 90% inhibition of cell growth and induction of up to 65% apoptotic cell death in *wt-p53* ALK+ ALCL and ALK- ALCL cell lines, while no significant biologic activity against *mt-53* ALCL cells was observed. Also, combined treatment of ALCL cells harboring potentially functional p53 with nutlin-3a and XI-006 resulted in enhanced cytotoxicity.

Conclusions: MDMX is overexpressed in both ALK+ and ALK- ALCL tumors. Inhibition of MDMX induces apoptotic cell death and inhibits the growth of ALCL cells, through activation of the p53 pathway. Reactivation of p53 signaling, by targeting MDMX may provide a new therapeutic approach for patients with ALK+ and ALK- ALCL.

1391 Newly Mutated Genes During Myelodysplastic Syndrome Progression or Acute Myeloid Leukemia Relapse

Jinming Song[1], Hailing Zhang[2], Xiaohui Zhang[2], Mohammad Hussaini[3]
[1]Moffitt Cancer Center, Tampa, FL, [2]Tampa, FL, [3]H. Lee Moffitt Cancer Center, Tampa, FL

Disclosures: Jinming Song: None; Mohammad Hussaini: None

Background: Myelodysplastic syndrome (MDS) is a clonal hematopoietic disorder that could progress from low grade to high grade, and eventually to acute myeloid leukemia (AML) if untreated. In addition to cytogenetic studies, gene mutation profiling, especially by large panel NextGen sequencing, has played a more and more important roles in the diagnosis and in the stratification of patients with MDS or AML. Patients are more and more frequently followed by NextGen sequencing in their treatment course, aiming to understand the disease status and with the hope to predict patient outcomes.

Design: To understand the association of gene mutations with MDS progression and AML relapse, we analyzed our in-house NextGen sequencing database with ~3500 patients to search for the patients with MDS or AML, and with new gene mutations developed in follow-up NextGen tests, and then correlate the gene mutations with disease status or progression.

Results: There were ~1003 patients with MDS or AML and at least one or more follow up NextGen testes. Of these, 54 patients were found to have new genes mutated in the follow up tests, including 9 patients occurred at AML relapse (16.7%), 18 patients during MDS progression (33.3%), and 27 patients with persistent MDS or AML (50%). For the patients with new mutations at AML relapse, the newly mutated genes include ASXL1 (33%), IDH2 (22%), BCOR (11%), BCORL1 (11%), NPM1 (11%), PTPN11 (11%), SF3B1 (11%), STAG2

(11%), and WT1 (11%) with a decreasing frequency. Most of these patients (44%) had good cytogenetics, while 33% and 22% of the patients had intermediate and poor cytogenetics. For patients with new genes mutated during MDS progression, the new genes mutated include RUNX1 (16.7%), BCOR (16.7%), TP53 (11.1%), ASXL1 (11.1%), FLT3(11.1%), IDH2 (11.1%), IHD1 (11.1%), DNMT3A (11.1%), EZH2 (11.1%), SRSF2 (11.1%), TET2 (11.1%), CBL (11.1%), GATA2 (11.1%), KDM6A (11.1%), ABL1 (11.1%), BCORL1 (11.1%), CEBPA (11.1%), GATA1 (11.1%), GNAS (11.1%), JAK2 (11.1%), NRAS (11.1%), PDGFRA (11.1%), PTPN11 (11.1%), SF3B1 (11.1%), STAG2 (11.1%), and U2AF1 (11.1%), with a decreasing frequency. Most of these patients (56%) had poor cytogenetics, while 28% and 17% of the patients had good and intermediate cytogenetics.

Conclusions: These results will help us to understand the mutational evolution in MDS and AML patients, and facilitate our understanding of the association of new gene mutations with MDS progression or AML relapse.

1392 Importance of monitoring clonal dynamics of IDH2 mutations in Acute Myeloid Leukemia

Jinming Song[1], Sallman David[2], Eric Padron[2], Rohit Sharma[1], Mohammad Hussaini[2]
[1]Moffitt Cancer Center, Tampa, FL, [2]H. Lee Moffitt Cancer Center, Tampa, FL

Disclosures: Rohit Sharma: None; Mohammad Hussaini: None

Background: Recenlty, molecular profiling has become part and parcel of the diagnostic work up of AML, especially due to the advent of targetable mutations such as *FLT3*, *IDH2*, and *IDH1* which now have FDA approved therapies. *IDH2*mutations occur in 10-20% of AML and usually involve R140 and R172. In late 2017, FDA granted approval to Enasidenib for the treatment of IDH2 mutated, relapsed/refractory AML. In this study, we explored the clonal dynamics of *IDH2*mutations to understand how this may affect personalized medicine care of these *IDH2*-mutated AML patients.

Design: In-house next generation sequencing (NGS) database with ~3500 patients was searched for serially tested AML patients with IDH2 mutation in one test but absent in another. Mutation status was correlated with disease status (negative, minimal, positive, persistent, or relapse).

Results: There were 1003 patients with MDS or AML and ≥1 follow up NGS tests. Filtering for >1 NGS test, AML, and *IDH2* mutation in ≥1 test resulted in 130 NGS assays from 38 patients with AML with *IDH2* mutations. Range of serial assays was 2-8 (average = 3.4/patient). The most common diagnoses were AML with MDS related changes (n=7), M1 (n=9), M2 (n=10). One case of T/myeloid leukemia was included. 91 tests detected one or more mutations with an average of 2.6 mutations per case. The remaining tests were negative, in many cases expectedly due to treated disease resulting in mutational clearance. Concurrent *IDH1* mutation was seen in 2 patients. Commonly co-occurring mutations included *DNMT3A*, *RUNX1*, *SRSF2*, *NPM1*, and *ASXL1*.

7 patients (25%) who were *IDH2*-negative acquired the *IDH2* mutation at relapse and 1 acquired it during disease progression (4%). 8 patients (21%) with *IDH2*-positive AML lost *IDH2* despite the presence of persistent AML and 4 patients lost the *IDH2* mutation at the time of AML relapse (11%). One CMML-2 patient acquired an *IDH2* mutation shortly prior to AML transformation. In one case, an *IDH2* mutation was found in the negative marrow of a patient who had concurrent late AML relapse as leukemia cutis. 2 patients (5%) showed persistent *IDH2* mutations though the marrow had become negative for AML.

Conclusions: Our results show the markedly dynamic landscape of AML genomics with *IDH2* mutations often being acquired or lost the course of treatment, disease progression, and disease relapse. These findings underscore the importance of serial testing of AML patients to monitor clonal evolution and tailor targeted therapy accordingly.

1393 Epstein-Barr virus (EBV) incidental expression in bone marrow cells, a study of 230 consecutive bone marrow biopsy samples

Sami Souccar[1], Daniel Farrell[2], Sherif Rezk[3], Lawrence Weiss[4], Ali Nael[5], Xiaohui Zhao[2]
[1]Irvine, CA, [2]University of California, Irvine, Orange, CA, [3]Orange, CA, [4]City of Hope National Medical Center, Pasadena, CA, [5]Children Hospital of Orange County, University of California Irvine, Orange, CA

Disclosures: Sami Souccar: None; Daniel Farrell: None; Ali Nael: None

Background: Scattered Epstein-Barr virus (EBV)-positive lymphocytes can be detected in the lymph node of healthy individuals and they usually indicate latently infected cells with no neoplastic association. The incidence of EBV detection in bone marrow samples has not been studied and remains largely unknown. The lack of knowledge regarding the true incidence of encountering bystander latent EBV-positive cells in the bone marrow may potentially lead to a diagnostic dilemma when assessing a staging bone marrow for a patient with an EBV-positive B or T/NK-cell lymphoma. The aim of our study is to investigate the rate of detection of EBV expression in bone marrow samples and correlate any positive findings with various clinical parameters and follow-up data.

Design: We retrospectively analyzed sequential bone marrow biopsies for EBV expression by in situ hybridization. We searched bone marrow biopsies from 2013 and early 2014 that were performed for any indication that included clot sections. Inclusion criteria included the presence of a clot biopsy section to avoid possible RNA degradation due to the decalcification process on the core sections. Any marrow biopsies from pregnant women and pediatric patients younger than 18 years of age were excluded from the case selection due to an Institutional Review Board requirement. These cases represented an ethnically-diverse population. Approximately 54% of the patients were immunocompetent, while 46% of the patients were immunocompromised, including 5 patients with HIV infection (3% of total patients).

Results: Out of 230 consecutive bone marrow biopsies performed, we found 5 cases (2.17%) with scattered EBV-positive cells. One patient was immunocompetent and 4 patients were immunocompromised, including 3 patients with HIV infection. By IHC, the EBV positive cases showed scattered T cells in all cellular areas containing EBV positive cells, whereas only 3 of the 5 cases showed scattered B cells in the same region. Our data shows that the EBV-positive cells likely represent latently infected T cell.

Case	Age, Sex, Ethnicity	BMB Diagnosis	History	Immune Status	Follow Up	EBER	PAX-5	CD3
1	68 M Korean	Slightly hypercellular marrow with active trilineage hematopoiesis. No evidence of lymphoma	Recently diagnosed EBV-negative Diffuse large B-cell lymphoma in maxillary sinus	Preserved	5 year follow-up available. Currently alive and in remission.	Rare cells positive	Scattered cells positive	Scattered cells positive
2	48 M Caucasian	Normocellular marrow with active trilineage hematopoiesis and marked erythroid hyperplasia	HIV infection, on HAART therapy, history of ITP	HIV Positive	5 year follow-up available. Currently alive with no development of any hematopoietic/ EBV-related disorders.	Rare cells positive	Scattered cells positive	Scattered cells positive
3	54 M Caucasian	Moderately hypocellular marrow with active trilineage hematopoiesis, left-shifted myeloid hyperplasia, and megakaryocytic hyperplasia	Recently diagnosed acute myeloid leukemia (AML) status post induction chemotherapy	Day 14 status post induction chemotherapy	Only 3 month follow-up data available. Negative for residual AML or any other hematopoietic/ EBV-related disorder in that time period.	1 cell positive	Negative	Scattered cells positive
4	47 M Hispanic	High normocellular marrow with active trilineage hematopoiesis, negative for lymphoma involvement, with scattered EBV cells of undetermined significance. Flow cytometry and IHC showed no evidence of lymphoma	HIV infection, on HAART therapy, Kaposi sarcoma, recently diagnosed plasmablastic lymphoma	HIV Positive	5 year follow-up available. Currently alive and in remission for both plasmablastic lymphoma and Kaposi sarcoma. Negative for any hematopoietic/ EBV-related disorder in that time period.	Scattered cells positive (average 4-5/HPF)	Scattered cells positive	Scattered cells positive
5	24 M Hispanic	Mildly hypocellular marrow with mild myeloid and megakaryoid hyperplasia and erythroid hypoplasia	HIV infection, on HAART therapy, Kaposi sarcoma	HIV Positive	Only 5 month follow-up data available. Negative for any hematopoietic/ EBV-related disorder in that time period.	Rare cells positive	Negative	Scattered cells positive

Figure 1 - 1393

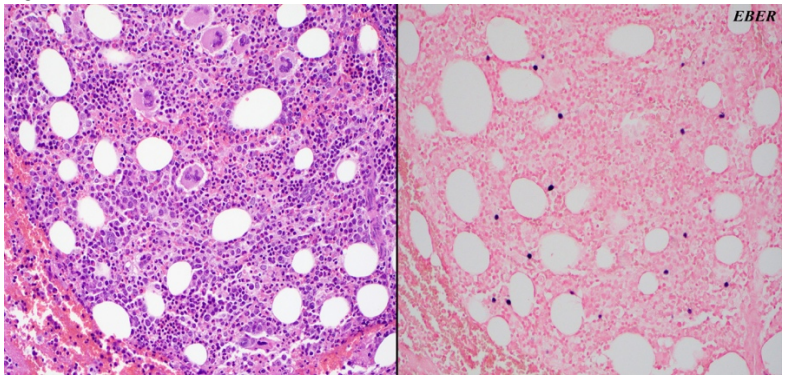

Figure 2 - 1393

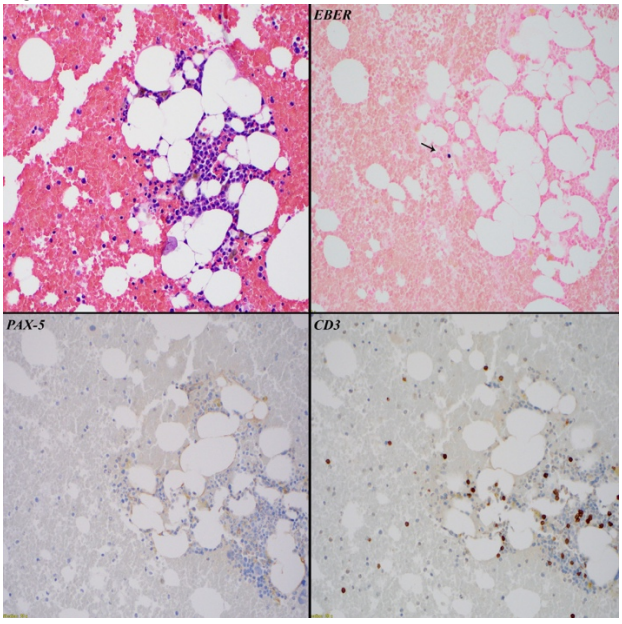

Conclusions: The rate of detection of EBV-positive cells in the bone marrow appears to be slightly higher in immunodeficient individuals than in immunocompetent patients. Although it is a small sample size, but the detection of EBV positivity in 3 out of 5 total HIV-positive patients in our study may represent truly increased incidence of EBV detection in patients with HIV infection, similar to that observed in other sites.

1394 Novel Multi-Parameter Flow Cytometry Approaches and Data Analysis Tools for the Evaluation and Detection of Leukemia Stem Cells

Kritika Srinivasan[1], Anurag Bhaskar[1], Jason Alexandre[1], Aidan Winters[1], Emily Zhang[1], Yelena Akker[1], Cynthia Liu[1], Arnaldo Arbini[2], Pratip Chattopadhyay[1], Christopher Park[3]
[1]NYU Langone Health, New York, NY, [2]NYULMC, New York, NY, [3]NYU School of Medicine, New York, NY

Disclosures: Kritika Srinivasan: None; Anurag Bhaskar: None; Jason Alexandre: None; Aidan Winters: None; Emily Zhang: None; Yelena Akker: None; Cynthia Liu: None; Arnaldo Arbini: None; Pratip Chattopadhyay: None; Christopher Park: None

Background: AML is driven by leukemia stem cells (LSCs), a subset of blasts that are therapy resistant and mediate relapse. Despite their importance, clinical flow cytometry (cFC) panels are not designed to detect LSCs, especially in minimal residual disease (MRD) settings. Multiplexed antibody panels may increase sensitivity/specificity of MRD detection by detecting subtle antigenic differences across phenotypically heterogenous blasts.

Design: Three 23+ color antibody panels were designed to detect AML LSCs. Panels contain a shared core of markers currently used in cFC, along with experimentally defined LSC markers (Table 1). To develop these panels, we used Colorwheel, a new automated software for rapid panel design (cutting development time from >1 year to <2 weeks). We visualized data using a novel tool, Phenoscan, which generates simple summaries of high parameter data (by performing hierarchical clustering, plotting clusters around a central point, and overlaying a density gradient for cell frequency). Finally, with a rapid computing platform, CytoBrute, we precisely defined combinatorial expression of all markers for populations of interest.

Results: Our new approach faithfully identified major bone marrow hematopoietic cell populations in normal and AML samples. We found that blasts from diagnostic AML samples exhibit unique phenotypes compared to relapsed AML, and that phenotypic heterogeneity among blasts varied between diagnosis and recurrence. Panels 1 and 2 identify two unique blast populations that were differentially modulated between new and recurrent AMLs (Figure 1, panel 2); the first population increased, the second was completely lost. Notably, some cell types modulated with recurrence were also observed in patients with CLL or non-malignant pancytopenia, while others were unique to AML. We could rapidly characterize interesting cells by reporting expression of all markers (Figure 2). CytoBrute took this data and reported the frequency of cells defined by each combination of panel markers. For example, panel 3 identified a unique population of cells, increasing upon recurrence, that is - CD45+CD38+CD19+CD90+CD164+CD47+CD109+CD312+CD49d+CD43+CD200+CD166+CD32+.

AML PANEL 1	AML PANEL 2	AML PANEL 3
CD34	CD34	CD34
CD117	CD117	CD117
HLA-DR	HLA-DR	HLA-DR
CD45	CD45	CD45
CD38	CD38	CD38
CD19	CD19	CD19
CD45RA	CD45RA	CD45RA
CD90	CD90	CD90
CD123	CD123	CD123
CD164	CD164	CD164
CD47	CD47	CD47
CD97	CD97	CD97
CD99	CD99	CD99
TIM3 (CD366)	TIM3 (CD366)	TIM3 (CD366)
CD25	CD9	CD109
CD36	CD126	CD166
CD44	CD18	CD200
CD70 (CD27 ligand)	CD26	CD32
CD96	CD49f	CD43
CD98	CD55	CD49d
CLL-1 (CLEC12A/CD371)	CD58	EMR2
CXCR2 (CD182)	CD69	IL18ra
GPR56 (ADGRG1)	CD74	folate receptor B (FOLR2)
IL1RAP	tmTNFa	

Figure 1 - 1394

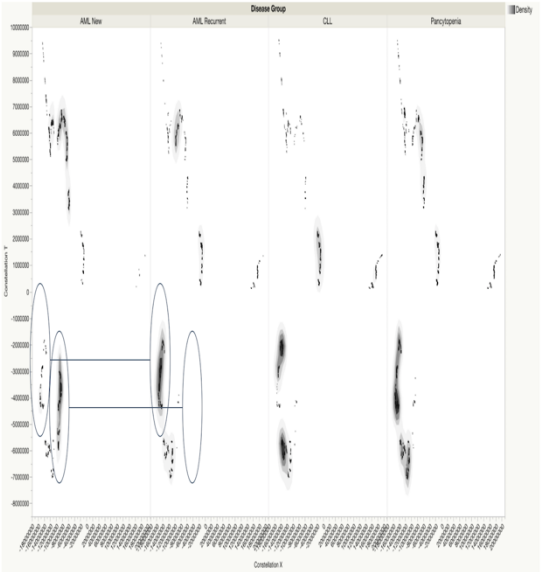

Figure 2 - 1394

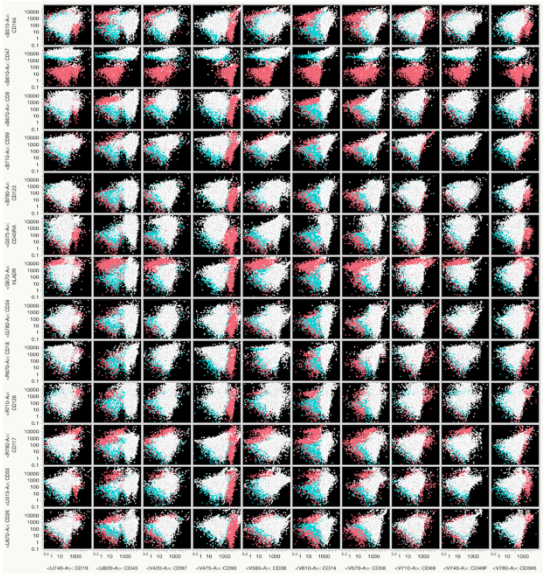

Conclusions: Applying multiple new technologies, we can identify specific and heterogenous immunophenotypes for blasts at AML diagnosis and relapse. Preliminary data indicate we can sensitively detect LSCs in MRD. These tools provide a modern pipeline to evaluate AML biology with great depth and ease.

1395 Clinicopathologic evaluation of aggressive variants of mantle cell lymphoma

Lukas Streich[1], Girish Venkataraman[2], Shanxiang Zhang[3], Yi-Hua Chen[4], Qing Chen[5], Juehua Gao[4], Kristy Wolniak[6], Amir Behdad[5]
[1]Northwestern University, Chicago, IL, [2]University of Chicago Medical Center, Chicago, IL, [3]Indiana University School of Medicine, Indianapolis, IN, [4]Northwestern Memorial Hospital, Chicago, IL, [5]Northwestern University Feinberg School of Medicine, Chicago, IL, [6]Northwestern University, Evanston, IL

Disclosures: Lukas Streich: None; Girish Venkataraman: None; Shanxiang Zhang: None; Yi-Hua Chen: None; Qing Chen: None; Juehua Gao: None; Amir Behdad: None

Background: The current WHO classification recognizes two aggressive variants of mantle cell lymphoma (MCL): blastoid (B-MCL) and pleomorphic (P-MCL). These comprise ~20% of MCLs and are associated with poor clinical outcomes. Our study examines the clinical and pathologic features of these variants.

Design: A total of 19 cases of B-MCL and P-MCL were identified from three institutions between 2001 and 2018. The cases were reviewed by three pathologists; 15 of 19 cases met inclusion criteria (8 B-MCL, 7 P-MCL). Immunohistochemical stains (IHC) for p53, SOX-11 and PD-L1 were performed in 12 cases.

Results: Our cohort included 13 males and 2 females with a median age of 61 years. Three cases showed P-MCL in a background of conventional MCL. Two of 15 (13%) cases were cyclin D1 negative but SOX-11 positive. SOX-11 was negative in 3 of 13 cases (23%) including 2 P-MCLs progressed from leukemic, non-nodal MCL. CD5 was negative in 1 case and weak in 3. CD23 was negative in all cases, and CD10 was positive in 1 of 13 (7%). The mean proliferative index (Ki-67) was 75%. PD-L1 was negative in tumor cells in all cases, and 10 of 12 (83%) of cases showed frequent PD-L1 positive macrophages. P53 was expressed in >80% of tumor cells in 5 of 12 (41%) cases, weakly expressed in 1 case, and negative in 6 cases (50%). All cases with overexpression of P53 also demonstrated a high proliferative index (>90%).

7 of 12 (58%) carried a prior diagnosis of conventional MCL, and 66% of the patients were alive at a median follow up of 4.8 months. The mean serum LDH at diagnosis was 591 U/L, and 10 of 11 (91%) of the patients had bone marrow involvement at diagnosis. The most common chemotherapeutic regimen was rituximab plus Hyper-CVAD, CHOP, or bendamustine; 4 of 11 (36%) of patients underwent or planned to have autologous stem cell transplant.

Conclusions: P-MCL and B-MCL often demonstrate an atypical immunophenotype including CD5-, CD10+, cyclinD1- and SOX11-. Thus, BCL-1 and SOX11 staining should be considered in all B-cell lymphomas with high-grade morphology. More than half of our cases represent transformation of previously diagnosed conventional MCL including leukemic, non-nodal MCL. P53 is highly expressed in aggressive variants of MCL and associated with very high proliferative index. Underlying *TP53* mutation may account for aggressive transformation of MCL. PD-L1 is negative in tumor cells but highly expressed in tumor-infiltrating macrophages, suggesting a role for immunotherapy in patients with this disease.

1396 Correlation of EZH2 Expression with Ki-67 Proliferation Index in Non-Hodgkin B Cell Lymphoma and Benign Lymph Nodes

Qigang Sun[1], Jianmin Ding[1], Songlin Zhang[1], Robert Brown[2], Xiaohong Iris Wang[3]
[1]The University of Texas Health Science Center at Houston, Houston, TX, [2]UTHealth, McGovern Medical School, Houston, TX, [3]Bellaire, TX

Disclosures: Qigang Sun: None; Jianmin Ding: None; Songlin Zhang: None; Robert Brown: None; Xiaohong Iris Wang: None

Background: EZH2, Enhancer of Zeste Homologue 2, is an important enzymatic subunit of the epigenetic regulator polycomb repressive complex 2 and functions as a methytransferase that targets at the lysine 27 of histone H3 and controls gene silencing through posttranslational modification. EZH2 is frequently overexpressed in various malignancies and functions as an oncogenic protein for tumor cell proliferation, metastasis, and survival. EZH2 is highly expressed in germinal center B cells. Somatic mutations of Y641 and A677 residues within the catalytic SET domain of EZH2 were reported in diffuse large B-cell lymphoma (DLBCL) and follicular lymphoma (FL). Targeted therapy against EZH2 has been used for treatment of DLBCL. The goal of this study is to evaluate correlation between EZH2 expression and Ki-67 proliferation index in a variety of 31 non-Hodgkin B cell lymphoma and 6 benign lymph nodes cases.

Design: Tissue microarray (TMA) was manually made with 2.0 mm tissue cores from the paraffin embedded tissue blocks. Immunostains for EZH2 and Ki-67 were performed using Ventana automated stainer. Three higher power images (400X) were photographed on each core, and the mirror images were taken for EZH2 and Ki-67 at the matched areas for each core. ImageJ software was used for computer assistant digital image analysis, and Pearson Correlation Coefficient was used for statistical analysis.

Results: The study cases included 17 DLBCL, 10 FL, one case each for small lymphocytic lymphoma, mantle cell lymphoma, MALT lymphoma, high grade B cell lymphoma, and 6 benign/reactive lymph nodes. Total 220 matched images (110 images each) for EZH2 and

Ki-67 were photographed and analyzed with ImageJ digital analysis software. There was strong positive correlation between EZH2 expression and Ki-67 proliferation index with R value of 0.8748. The R value between EZH2 and Ki-67 was 0.8518 in DLBCL and FL and 0.945 in benign lymph nodes.

Conclusions: EZH2 expression is significantly correlated with Ki-67 proliferation index in both non-Hodgkin lymphoma and benign lymph nodes using the matched images and computer assistant digital image analysis. EZH2 overexpression is often seen in high grade lymphoma with high tumor proliferation, and the targeted therapy to EZH2 may provide an effective treatment for the high grade non-Hodgkin B cell lymphoma with high Ki-67 proliferation index.

1397 Evaluation of FOXP3+ and FOXP3+/CD25+ T Regulatory Cells in Various Lymphoma Entities Using Tissue Microarray

Qigang Sun[1], Tatiana Belousova[1], Jianmin Ding[1], Songlin Zhang[1], Xiaohong Iris Wang[2]
[1]The University of Texas Health Science Center at Houston, Houston, TX, [2]Bellaire, TX

Disclosures: Qigang Sun: None; Tatiana Belousova: None; Jianmin Ding: None; Songlin Zhang: None; Xiaohong Iris Wang: None

Background: Studies have shown that high FOXP3+ T regulatory cells (Tregs) are associated with better survival in diffuse large B cell lymphoma (DLBCL), follicular lymphoma (FL) and classic Hodgkin lymphoma (CHL). FOXP3 was identified as a marker of Tregs. However, FOXP3 is not Treg-sepcific and CD25 is expressed in most Tregs. There is no well-established FOXP3/CD25 immunohistochemical double staining for Tregs evaluation. The goals of our current study were to study the correlation between FOXP+ and FOXP3+/CD25+ cells, and to evaluate the expression of FOXP3+ and FOXP3+/CD25+ lymphocytes in various lymphoma entities.

Design: Duplicate tissue microarray (TMA) was manually built with 2.0 mm punch cores using the excision lymphoma tissue and some benign nodes as controls. FOXP3/CD25 double stain antibody cocktail and Biocare double stain detection kit were used. ImageJ digital analysis software was used for FOXP3 count, and manual count was performed for FOXP3+/CD25+ lymphocytes because some lymphoma cells are CD25 positive. T-test for 2 independent mean and Pearson correlation coefficient were used for statistical analysis.

Results: Seventy six cases were used for the TMA including 18 DLBCL, 11 FL, 18 CHL, 10 various T cell lymphoma, 5 nodular lymphocyte predominant Hodgkin lymphoma (NLPHL), 8 other type B cell lymphoma, and 6 benign nodes. FOXP3+/CD25+ double positive cells were moderately positively correlated with FOXP3+ cells (R=0.669). DLBCL, various T cell lymphoma and NLPHL had significant lower FOXP3+ (p=0.003, 0.0004, and 0.006) and FOXP3+/CD25+ cells (p=0.0001, 0.00004 and 0.001) than the benign nodes. CHL and FL lymphomas had no significant differences of FOXP3+ and FOXP3+/CD25+ cells compared to the benign nodes. DLBCL, T cell lymphoma and NLPHL had significant lower FOXP3+ and FOXP3+/CD25+ T lymphocytes than CHL and FL.

Conclusions: FOXP3+ cells only have moderate correlation with FOXP3+/CD25+ double positive cells, so FOXP3 stain alone can't represent FOXP3/CD25 double stained Tregs. There are significant variations of FOXP3+ and FOXP3+/CD25+ cell count among different types of lymphomas. DLBCL, T cell lymphoma and NLPHL have significantly lower Tregs than CHL and FL, which may have prognostic value and therapeutic application for lymphoma treatment.

1398 HDAC6 inhibition exerts anti-neoplastic effects in combination with autophagy suppression in diffuse large B-cell lymphoma

Chenbo Sun, Fudan University Shanghai Cancer Center, Shanghai, China

Disclosures: Chenbo Sun: None

Background: Diffuse large B-cell lymphoma (DLBCL) is the major common non-Hodgkin's lymphoma in China. HDAC6 plays a major role in the progression of DLBCL and ACY-1215 is a selective HDAC6 inhibitor that could reduce HDAC6 expression.

Design: In the study, we profiled downstream genes that altered after HDAC6 overexpression/knockdown with NanoString nCounter assay. Then we found that autophagy related genes varied mostly. We then used lentivirus transfection, qPCR, western blot, CCK-8 assays to explore the regulating mechanism between HDAC6 and autophagy.

Results: In our study, we found ACY-1215 as a novel anti-neoplastic HDAC6 inhibitor which retarded DLBCL survival. After validation in DLBCL tissues, we found that knockdown of BECN1, a key autophagy regulator, suppressed DLBCL cell lines proliferation, and inhibited nude mice tumor growth. In addition, the combination use of HDAC6 inhibitor ACY-1215 and autophagy inhibitor Chloroquine showed synergetic effect both in vitro and in vivo. Mechanistically, Rel A/p65 was found to increase BECN1 expression by promoting its transcription level, and its nuclear translocalization could be activated by HDAC6. Furthermore, the expression of BECN1 was positively correlated with HDAC6 and DLBCL patients with high expression of BECN1 had a worse overall survival.

Conclusions: Our results demonstrated that the combination strategy of ACY-1215 and Chloroquine may be a potent targeting therapy in DLBCL treatment.

1399 Molecular Subtyping of Diffuse Large B-Cell Lymphoma Using a Novel qRT-PCR Assay

Robert Ta[1], Christopher Santini[2], Patricia Gou[3], Greg Lee[3], Cathal O'Brien[3], Yu Tai[4], Marcel Fontecha[5], Cliona Grant[3], Larry Bacon[3], Stephen Finn[6], Elisabeth Vandenberghe[3], Fiona Quinn[3], Rajiv Dua[5], Richard Flavin[3]
[1]Beth Israel Deaconess Medical Center, Boston, MA, [2]Roche Molecular Systems, Pleasanton, CA, [3]St. James's Hospital, Dublin, Ireland, [4]Pleasanton, CA, [5]Roche Molecular Diagnostics, Pleasanton, CA, [6]University of Dublin, Trinity College, Dublin, Ireland

Disclosures: Robert Ta: None; Christopher Santini: *Employee*, Roche Molecular Systems, Inc.; Patricia Gou: None; Greg Lee: None; Cathal O'Brien: None; Yu Tai: *Employee*, Roche Molecular Systems, Inc.; Marcel Fontecha: *Employee*, Roche Molecular Systems, Inc.; Cliona Grant: None; Larry Bacon: None; Stephen Finn: None; Elisabeth Vandenberghe: None; Fiona Quinn: None; Rajiv Dua: *Employee*, Roche Molecular Systems, Inc.; Richard Flavin: None

Background: Diffuse large B-cell lymphoma (DLBCL) is the most common form of Non-Hodgkin's lymphoma accounting for approximately 30-40% of all cases. Gene expression profiling has identified two major molecular subtypes of DLBCL based on cell of origin (COO): Activated B-Cell (ABC) and Germinal Center B-Cell (GCB). Patients with the ABC subtype have significantly reduced median overall survival compared with those with GCB. Currently, DLBCL subtyping is performed by immunohistochemistry (IHC) from formalin-fixed, paraffin-embedded (FFPE) tissue in the routine clinical setting. The aim of this study was to evaluate a novel Roche 14-gene signature qRT-PCR assay for COO classification in DLBCL.

Design: Sixty Hans-classified DLBCL samples were selected retrospectively. FFPE tissue blocks were deparaffinized following standard protocols and RNA was extracted as per High Pure FFPE RNA Isolation Kit (Roche Molecular Systems, Inc). COO-classification was performed using the Roche qRT-PCR assay, Nanostring Lymphoma Subtyping Testing (LST) and by RMS G100 microarray gene expression profiling. A DLBCL COO score was generated via the qRT-PCR testing platform in order to classify DLBCL cases as GCB, ABC, or unclassified. The various subtyping platforms were then correlated with progression-free survival and overall survival.

Results: Hans classification identified 36 GCB and 24 Non-GCB DLBCL cases. qRT-PCR identified 35 GCB, 21 ABC, and 3 unclassified cases. Microarray results had an overall concordance of 88.1%, 88.3% and 86.7% to qRT-PCR, Hans classification, and Nanostring LST, respectively. Comparatively, qRT-PCR and Nanostring both had a 92.9% concordance when considering GCB and ABC samples only. The progression-free survival and overall survival of GCB and ABC subtypes were not significantly different across the testing platforms.

Method Concordance vs Microarray	**qRT-PCR (N=59)**	**IHC (N=60)**	**Lymph 2Cx (Nanostring) (N=60)**
ABC concordance	94.7%	90.5%	88.9%
GCB concordance	91.9%	87.2%	94.7%
Concordance within ABC and GCB subsets	92.9%	88.3%	92.9%
Overall Concordance	88.1%	88.3%	86.7%

Figure 1 - 1399

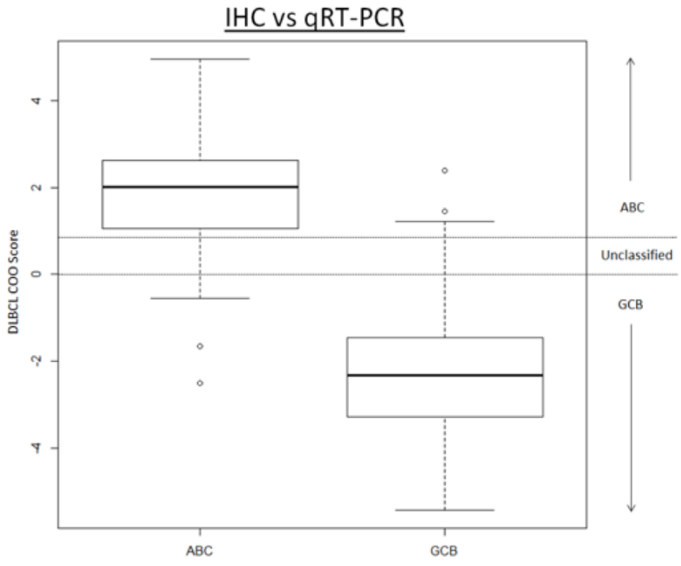

Conclusions: qRT-PCR based COO classification for DLBCL was shown to correlate with microarray based classification and had comparable concordance to IHC and Lymph 2Cx (NanoString). We propose that this new RNA based technique utilizing qRT-PCR could be incorporated into routine diagnostics for discriminating ABC from GCB DLBCL on formalin fixed paraffin embedded tissue.

1400 Loss of 5-Hydroxymethylcytosine (5-hmC) Expression is Near-Universal in B-Cell Lymphomas

Kevin Tanager[1], Brian Chiu[1], Sonali Smith[2], Peter Riedell[1], Justin Kline[1], Girish Venkataraman[3]
[1]University of Chicago, Chicago, IL, [2]University of Chicago Medicine, Chicago, IL, [3]University of Chicago Medical Center, Chicago, IL

Disclosures: Kevin Tanager: None; Brian Chiu: None; Sonali Smith: None; Peter Riedell: *Speaker*, Kite/Gilead; *Consultant*, Kite/Gilead; *Speaker*, Bayer; *Consultant*, Bayer; Justin Kline: None; Girish Venkataraman: None

Background: Epigenetic pathways related to gene expression, including DNA methylation, have been demonstrated to be dysregulated in human cancers. Loss of expression of 5-hydroxymethylcytosine (5-hmC) via immunohistochemistry has been reported in several solid tumor types, including melanomas, which has been useful in identifying progressed cases. One recent study in TET1-deficient mutant mice demonstrated development of B-cell lymphomas, also with loss of 5-hmC by IHC. While T-cell lymphomas frequently demonstrate loss of 5-hmC, data on B-cell lymphomas are sparse.

Design: Tissue microarrays of paraffin-embedded tissues from the Hoogland Lymphoma Biobank including B-cell lymphomas (44 diffuse large B-cell lymphomas (DLBCL), 32 low-grade B-cell lymphomas including 15 follicular lymphomas, 8 CLL/SLL, 4 marginal zone lymphomas, 2 mantle cell lymphomas, and 3 others; and 45 Hodgkin lymphomas (HL) including classical (CHL) and nodular-lymphocyte predominant) were selected and stained for 5-hmC antibody (Polyclonal 1:1000, Active Motif). Normal tonsils (n = 5) were also stained to assess expression pattern in normal lymphoid tissues. Cellular compartment with loss of expression were assessed in all tissues examined.

Results: In normal tonsils, naïve/mantle zone B-cells, paracortical T-cells and follicular dendritic cells showed retained expression of 5-hmC, while germinal center B-cells and to a lesser extent marginal zone B cells showed loss of expression. Among lymphoma cases, the majority of high-grade B-cell lymphomas, low-grade B-cell lymphomas, and Hodgkin lymphomas showed loss of 5-hmC in all neoplastic cells (95%, 94%, and 93% of cases, respectively). In a few cases of DLBCL transformation from a low-grade lymphoma, some of the residual low-grade component showed retained 5-hmC. Additionally, in some HL cases, some of the non-neoplastic background milieu cells also demonstrated loss of 5-hmC expression. Representative micrographs of these 5-hmC staining patterns in DLBCL (including a rare focally 5-hmC positive case), CLL, HL, and normal tonsil control are displayed in Figure 1.

Figure 1 - 1400

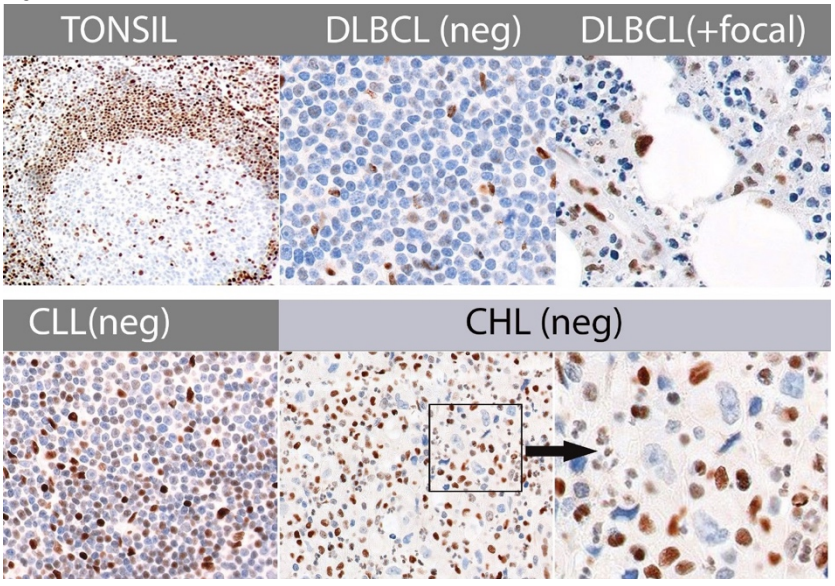

Conclusions: When assessing lymphoid aggregates with concern for malignancy, loss of 5-hmC staining may help identify a malignant lymphoid process. This finding may be useful in small biopsy specimens without adequate material for flow cytometry and/or molecular studies. The loss of 5-hmC in background cells of lymphoma is also intriguing and deserves further investigation.

1401 PICALM-MLLT10 Fusion Commonly Presents with Extramedullary Acute Leukemia and Often with a Mixed Phenotype (MPAL)

Hammad Tashkandi[1], Wenbin Xiao[1], Mikhail Roshal[1], Yanming Zhang[1], Maria Arcila[1], Ryma Benayed[1], Filiz Sen[1], Caleb Ho[1], Jeeyeon Baik[1], Janine Pichardo[1], Jacob L. Glass[1], Mark Geyer[1], Ahmet Dogan[1], Kseniya Petrova-Drus[1]
[1]Memorial Sloan Kettering Cancer Center, New York, NY

Disclosures: Hammad Tashkandi: None; Wenbin Xiao: None; Yanming Zhang: None; Maria Arcila: *Speaker*, archer; Ryma Benayed: None; Filiz Sen: None; Jeeyeon Baik: None; Mark Geyer: *Speaker*, Dava Oncology; Ahmet Dogan: *Advisory Board Member*, Roche/Genentech; *Advisory Board Member*, Corvus Pharmaceuticals; *Speaker*, Physicians' Education Resource; *Advisory Board Member*, Seattle Genetics; *Advisory Board Member*, Pharmacyclics; Kseniya Petrova-Drus: None

Background: The *PICALM-MLLT10* fusion (formerly *CALM-AF10*) results from the rare recurrent chromosomal translocation t(10;11)(p12;q14) previously described in less than 100 cases of predominantly pediatric T-lymphoblastic leukemia/lymphoma (T-ALL), rarely in acute myeloid leukemia (AML), and biphenotypic acute leukemias. Given its rarity and preponderance of older cases, complete immunophenotypic, molecular, and clinical characterization of this subset of acute leukemias (AL) is lacking in the literature. Here we report 13 cases and describe their clinicopathologic features and molecular profiling.

Design: A search of our pathology archives from 1995 to 2018 identified 13 patients with AL harboring the t(10;11) (p12;q14); *PICALM-MLLT10* fusion out of >2400 cases. Conventional cytogenetics in 10/13 (77%) or an NGS-based RNA-fusion assay in 7/13 (54%) were used to detect this event. Molecular profiling (MSK-IMPACT) was performed in 6/13 patients. Where available, clinical information, immunophenotypic, and cytogenetic data were reviewed.

Results: Eleven (11/13, 85%) were male and the median age was 32 years (range 15-58). Based on the WHO 2017 criteria, blast lineage assignment was most commonly MPAL in 5/13 (38%) (including 3 T/My, 1 B/My, and 1 T/B), 2/13 (15%) were T-ALL, 1/13 (8%) AML, and 4 cases with incomplete immunophenotyping (AL, ongoing work-up). Lineage assignment was unclear in 1 case despite complete information and ETP-ALL vs. M0 AML was favored. At presentation, 11/13 (85%) had extramedullary involvement (EM, mostly CNS and mediastinum), and 3/13 (23%) had either no or minimal bone marrow involvement. Recurrent pathogenic alterations were detected in the following genes: *PHF6* (3/6 50%), *PTEN* (3/6 50%), *TP53* (2/6 33%), *ETV6* (2/6 33%), *CREBBP* (2/6 33%), and *CDKN2Ap16INK4A / CDKN2Ap14ARF* (2/6 33%). The overall survival (OS) was poor and 8/13 (62%) died with a median OS of 15 months (range 2.4-42.6). In total, 6/13 (46%) received HSCT, however 5/6 (83%) patients relapsed and died with a median follow-up of 14 months (range 2-40). Five patients are alive with a median follow-up of 10 months (range 4-14.4).

Table 1

Case	Sex	Age at Dx	Cytogenetics/ Fusion detection	Lineage	EM	BM	Status, OS (months)
1	M	32	t(10;11)(p12;q14); *PICALM-MLLT10*	AML	Mediastinum	Yes	Died, 32.7
2	F	42	t(10;11)(p12;q14); *PICALM-MLLT10*	MPAL T/My	Skin and CNS	No	Alive, 14.4
3	M	37	45,XY,add(1)(p?22),der(3)t(1;3)(p22;q21),-9,t(10;11)(p12;q14), del(12)(p11.2),add(14)(q32),i(17)(q10), der(18)t(9;18)(q13;q23)[cp18]; PICALM-MLLT10	MPAL T/My	Paraspinal soft tissue and CNS	Yes	Died, 42.6
4	M	25	NA; *PICALM-MLLT10*	T-ALL	LN and CNS	Minimal	Alive, 11.5
5	M	18	t(10;11)(p12;q14), +4, +8	MPAL T/My	LN	Yes	Died, 27.3
6	M	55	t(10;11)(p12;q14)	AL	NA	Yes	Died, 5
7	M	15	t(10;11)(p12;q14),+19	T-ALL	NA	Yes	Died, 24
8	F	19	t(10;11)(p12;q14)	AL	Mediastinum	Yes	Died, 2.4
9	M	46	der(10)t(10;11)(p12;q14)ins(11)(q23)	AL	CNS	Yes	Died, 5.6
10	M	22	t(10;11)(p12;q14)	AL	Skin	Yes	Died, 2.9
11	M	31	Normal karyotype; *PICALM-MLLT10*	MPAL (T/B)	LN	Yes	Alive, 8.2
12	M	58	NA; *PICALM-MLLT10*	MPAL (B/ My)	Mediastinum	Minimal	Alive, 4
13	M	35	del(4)(q21q31),-5,t(10;11)(p12;q14),-17,add(17)(p11.2),+1~3mar ; *PICALM-MLLT10*	T-ALL vs AML vs MPAL	Mediastinum	Yes	Alive, 10

Dx=diagnosis, AL= acute leukemia, NA=not available, EM= extramedullary involvement, BM=bone marrow involvement

Figure 1 - 1401

Recurrent alterations (figure 1)

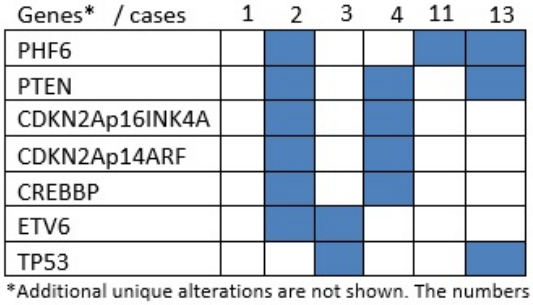

*Additional unique alterations are not shown. The numbers correspond to Table 1.

Conclusions: AL with *PICALM-MLLT10* fusion have a male predominance, younger age for adults, frequent EM involvement, and poor OS. AL harboring this fusion also show frequent MPAL phenotype associated with T-lineage differentiation and PHF6 and PTEN mutations. Therefore, the *PICALM-MLLT10* fusion may genetically define a subset of MPAL with unique biology and clinicopathologic features.

1402 Upregulation of the MYD88-Toll-like receptor-B-Cell Receptor (My-T-BCR) Supercomplex and mTOR Signalling Axis in Primary Testicular Diffuse Large B-cell Lymphoma

Jeffrey Tompkins[1], Ariz Akhter[2], Kiril Trpkov[2], Asli Yilmaz[3], Meer-Shabani Taher-Rad[4], Carolyn Owen[2], Douglas Stewart[2], Adnan Mansoor[2]

[1]University of Calgary, Edmonton, AB, [2]University of Calgary, Calgary, AB, [3]Calgary Laboratory Services, Calgary, AB, [4]University of Calgary/Calgary Laboratory Services, Calgary, AB

Disclosures: Jeffrey Tompkins: None; Ariz Akhter: None; Kiril Trpkov: None; Asli Yilmaz: None; Adnan Mansoor: None

Background: Diffuse large B-cell lymphoma (DLBCL) shows a high degree of clinical and biological heterogeneity. Primary testicular DLBCL (PTL) is an extranodal variant of DLBCL with inferior outcomes relative to its nodal counterpart. PTLs mostly are of activated B-cell

(ABC) sub-type and have been shown to have high frequency of mutations in genes linked with B-cell receptor and Toll-like receptor signalling pathways. Recent studies indicate that NF-kB activation is a key oncological event in nodal DLBLC and is regulated by members of these pathways (particularly MyD88, TLR9 and BCR, which form the so called My-T-BCR supercomplex) in conjunction with the mTOR pathway (*Nature-2018*). The involvement of these pathways in PTL has not previously been assessed, and if active, may represent potential therapeutic targets.

Design: Twelve PTLs and thirty-four nodal DLBCLs, all of ABC sub-type were assessed. RNA from formalin fixed paraffin embedded diagnostic tissue were subject to expression evaluation utilizing nCounter analysis System by Nanostring technologies. We employed a 154 gene custom panel covering major ontological pathways in lymphoma; while cell of origin was determined by Lymph2CXpanel. Principle component analysis and hierarchical clustering were performed, with significant differential expression defined as genes having minimum of 2.5-fold change with $p<0.001$ by multiple t-test and false discovery (q value) rate of <0.001.

Results: Fifty six genes were upregulated in PTL relative to nodal ABC-DLBCL (Figure 1). These included genes involved in proximal B-cell receptor signalling (CD79b, BTK, SYK, LYN, BLNK, MYD88), the BCL10-MALT1-CARD11 signalosome, toll-like receptors (TLR2, TLR3, TLR5 and TLR9) and members of the mTOR pathway (AKT, PI3K, mTOR and RICTOR), all of which are known to converge and activate NF-kB.

Figure 1 - 1402

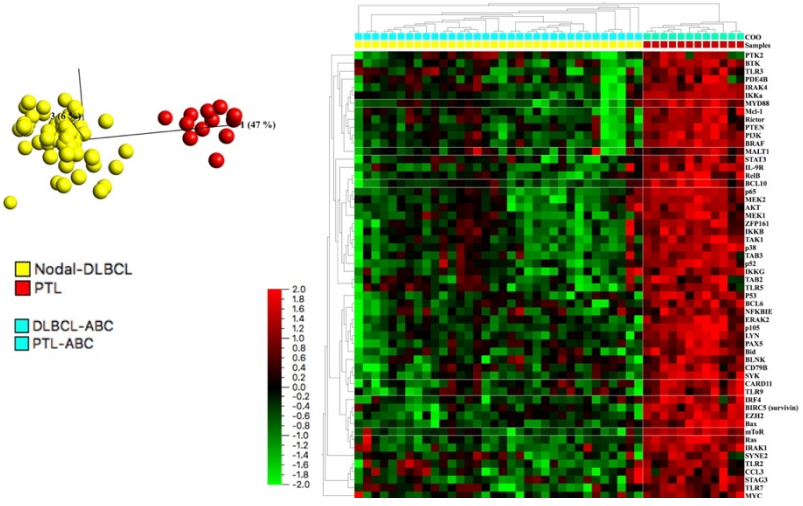

Conclusions: Differential gene expression involving the B-cell receptor, toll-like receptor, NF-kB and mTOR pathways exists between PTL and nodal ABC-DLBCL and may contribute to differences in clinical and biological behavior. Given the overexpression of the B-cell receptor and mTOR pathways, inhibitors targeting members of these pathways (i.e. BTK and mTOR) may warrant further study in PTL.

1403 Flow Cytometric Evaluation of Eosinopoiesis in Patients with Hypereosinophillic Syndrome and Systemic Mastocytosis

Christopher Trindade[1], Xiaoping Sun[2], Dragan Maric[3], Christopher Hourigan[4], Dean Metcalfe[5], Amy Klion[6], Irina Maric[3]
[1]NIH/NCI/CCR/LP, Bethesda, MD, [2]CC/NIH, Bethesda, MD, [3]National Institutes of Health, Bethesda, MD, [4]National Heart, Lung, and Blood Institute, Bethesda, MD, [5]National Institute of Allergy and Infectious Diseases, Bethesda, MD,[6]NIAID/NIH, Bethesda, MD

Disclosures: Christopher Trindade: None; Xiaoping Sun: None; Dragan Maric: None; Christopher Hourigan: None; Dean Metcalfe: None; Amy Klion: None; Irina Maric: None

Background: Assessment of flow cytometric immunophenotypic maturational patterns of bone marrow precursors is used daily in clinical laboratories for diagnosis of numerous hematopoietic diseases. Maturational patterns of almost all hematopoietic lineages have been well described, with the exception of eosinophilic precursors. We have developed a novel flow cytometric antibody panel that identifies normal patterns of eosinophilic maturation. Then, we used this panel to investigate eosinophilic maturation in two rare hematopoietic disorders with eosinophilia: hypereosinophilic syndrome (HES) and systemic mastocytosis (SM).

Design: Multiparameter flow cytometric analysis of bone marrow aspirates was performed in 15 normal donors, 20 patients with HES and 15 patients with SM, using numerous candidate markers. Elucidation of immunophenotypic patterns of eosinophil maturation was first performed in normal marrows and maturational stages confirmed morphologically using flow cytometric sorting. Then, patterns of eosinopoiesis were assessed in marrow aspirates and peripheral blood samples from SM and HES patients.

Results: Siglec-8, CD11b, CD9, CCR3, CD49d and CD49f displayed the highest statistically significant differences in mean fluorescence intensities between different stages of eosinophil maturation. The expression of most of these markers increased during maturation, while CD49d expression decreased. Anti-EMR1 antibody was used for eosinophil lineage verification. All stages were CD34 negative. Peripheral blood eosinophils had mature immunophenotypic pattern. Comparison between bone marrow and peripheral blood eosinophils is shown in Figure 1. Eosinophilic precursors from HES and SM patients displayed similar general immunophenotypic maturational patterns, but expression levels of several antigens significantly differed from normal. Siglec 8 expression was significantly lower in both HES and SM eosinophils, while CCR3 and CD9 expression significantly increased on maturing eosinophils in SM. CD69 expression was mostly restricted to mature eosinophils in the marrow and peripheral blood.

Figure 1 - 1403

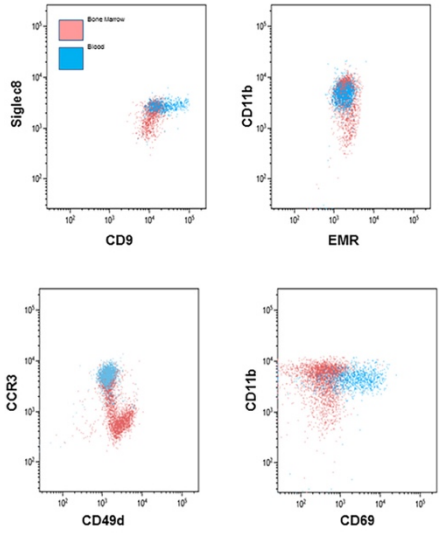

Conclusions: We developed the first in human flow cytometric panel to study eosinopoiesis in normal marrows. This novel panel was then used to identify changes in eosinophilic maturational patterns in two rare hematopoietic disorders: hypereosinophilic syndrome and systemic mastocytosis. Our study paves the way for routine flow cytometric analysis of eosinophils in multiple hematopoietic malignancies.

1404 The Tumor Suppressor SAMHD1 is a Novel Downstream Target of NPM-ALK Oncoprotein and MYC in Anaplastic Large Cell Lymphoma (ALCL)

Nikolaos Tsesmetzis[1], Nikolas Harold[1], Pedro Farrajota Neves da Silva[1], Daniela Kas Hanna[1], Ioanna Xagoraris[2], L. Jeffrey Medeiros[2], Elias Drakos[3], Vasiliki Leventaki[4], George Z. Rassidakis[5]
[1]Karolinska Institutet, Stockholm, Sweden, [2]The University of Texas MD Anderson Cancer Center, Houston, TX, [3]University of Crete, Heraklion, Greece, [4]St. Jude Children's Research Hospital, Memphis, TN, [5]The University of Texas MD Anderson Cancer Center, Karolinska Institutet, Stockholm, Sweden

Disclosures: Nikolaos Tsesmetzis: None; Nikolas Harold: None; Pedro Farrajota Neves da Silva: None; Daniela Kas Hanna: None; Ioanna Xagoraris: None; L. Jeffrey Medeiros: None; Elias Drakos: None; Vasiliki Leventaki: None; George Z. Rassidakis: None

Background: ALK+ anaplastic large cell lymphoma (ALCL) frequently carries the t(2;5) resulting in overexpression of NPM-ALK oncogenic kinase, which activates multiple oncogenic pathways. The SAM domain and HD domain 1 (SAMHD1) protein is a deoxynucleoside triphosphate (dNTP) triphosphohydrolase, which is capable of depleting intracellular dNTPs. Mutations of SAMHD1 gene have been identified in several tumors including T-prolymphocytic leukemia. Thus, SAMHD1 may play a role in lymphomagenesis as a tumour suppressor. However, the role of SAMHD1 in ALCL pathogenesis is unknown.

Design: The study group included 46 adult patients with ALK+ (n=26) and ALK- (n=20) ALCL with tumor tissues available for immunohistochemical analysis performed on tissue microarrays as well as reactive lymph node and tonsil's tissues. Also, a cohort of 30 pediatric ALK+ ALCL with available RNA sequencing data (RNAseq) was included in the study. The in vitro system included 5 ALK+ and 2 ALK- ALCL cell lines as well as Ba/F3 paternal and stably transfected clones. A variety of molecular biology techniques including transient transfections, Western blots, pharmacologic studies, flow cytometry as well as double immunostainings (i.e. SAMHD1/CD68) were performed.

Results: SAMHD1 protein was strongly expressed in reactive T-cells and histiocytes (CD68+) in all reactive lymphoid tissues with strong staining intensity (3+). In ALCL tumors, SAMHD1 was positive in 14 of 20 (70%) ALK- and 11 of 26 (42%) of ALK+ ALCL with moderate

intensity (2+). SAMHD1 was differentially expressed among ALCL cell lines and correlated with MYC mRNA and protein levels. SAMHD1 was substantially downregulated in Ba/F3 cells stably transfected with NPM-ALK plasmid as compared to paternal or control stable Ba/F3 clones. In the cohort of 30 pediatric ALK+ ALCLs patients, SAMHD1 mRNA levels inversely correlated with MYC-associated genes (signature). Inhibition of MYC activity by JQ-1 or MYC gene silencing with specific siRNA resulted in increased SAMHD1 protein level in ALCL cell lines. Inversely, transient transfection with a MYC overexpressing plasmid resulted in decreased levels of SAMHD1. Accordingly, in silico analysis revealed potential binding sites for MYC on the SAMHD1 gene promoter. Treatment of ALK+ ALCL cells with viral VPX protein, successfully depleted SAMHD1.

Conclusions: SAMHD1 is downregulated by NPM-ALK in ALK+ ALCL and by MYC in both ALK+ and ALK- ALCL and might represent a novel tumor suppressor in lymphoma.

1405 Reduced Diversity of the T-Cell Receptor Gamma Repertoire in Monomorphic Compared to Polymorphic EBV-Positive Post-Transplant Lymphoproliferative Disorders

Karine Turcotte[1], Weiwei Zhang[1], Courtney Schweikart[1], Philip Bierman[1], Timothy Greiner[1]
[1]University of Nebraska Medical Center, Omaha, NE

Disclosures: Karine Turcotte: None; Weiwei Zhang: None; Courtney Schweikart: None; Philip Bierman: None; Timothy Greiner: None

Background: The analysis of the molecular diversity of T-cell populations by next generation sequencing (NGS) is useful to understand the biology of the tumor micro-environment. The aim of this study was to perform an analysis of the diversity of the T-cell Receptor Gamma (*TRG*) gene rearrangements in post-transplant lymphoproliferatve disorders (PTLD). We hypothesized that there is a difference in the T-cell repertoire between EBV-positive monomorphic (Mono) and polymorphic (Poly) PTLD and between PTLD and infectious mononucleosis (IM). We also hoped to identify EBV specific *TRG* sequences. To our knowledge, there has been no publication on the diversity of the *TRG* repertoire in PTLD.

Design: Pathology records were queried for PTLD cases that had frozen tissue or DNA available, and known EBV status. 14 cases of EBV-positive Mono-PTLD, 27 cases of EBV-positive Poly-PTLD, five cases of EBV negative Mono-PTLD and three cases of IM from 1989 to 2015 were selected for the study. We collected clinicopathologic data, reviewed the slides to confirm the diagnosis and confirmed the EBV status by either Southern blot, LMP1 stain and/or EBERs in situ hybridization. DNA was PCR amplified using the LymphoTrack TRG Assay-PGM kit (Invivoscribe, San Diego, CA). Samples were sequenced using the Ion Torrent Personal Genome Machine (Thermo Fisher Scientific). *TRG* sequence data were analyzed with LymphoTrack software (Invivoscribe). The mean number of total and unique *TRG* reads was determined for each group. A one-tailed T-test was used to assess the diversity of the *TRG* repertoire measured by the Shannon index.

Results: The mean total number of *TRG* reads was 258,039 for EBVpos Mono-PTLD, 320,084 for Poly-PTLD 325,754 for EBVneg Mono-PTLD and 299,125 for IM. The mean number of unique *TRG* reads was 26,985 for EBVpos Mono-PTLD, 34,299 for poly-PTLD, 32,634 for EBVneg Mono-PTLD and 52,779 for IM. The Shannon index of the TCR repertoire shows less diversity in Mono-PTLD than in Poly-PTLDs (One tailed T-test P = 0.01), less in Mono-PTLD than in IM (P=0.007), and less diversity in Poly-PTLD than in IM (P= 0.03). We identified two *TRG* rearrangement sequences that are seen in the EBV positive PTLD groups and IM but not seen in the 5 EBV-negative PTLD.

Conclusions: Our findings demonstrate that there is a more limited diversity of the T-cell repertoire in monomorphic PTLD compared to polymorphic PTLD or IM. We have also identified putative EBV specific *TRG* sequences that warrant further study and confirmation.

1406 Immune Escape of KMT2A-rearranged B-ALL Via Myeloid Lineage Switch After CD19 CAR-T Therapy

John Van Arnam[1], Eline Luning-Prak[2], Michele Paessler[3], Vinodh Pillai[4]
[1]Philadelphia, PA, [2]University of Pennsylvania, Philadelphia, PA, [3]The Children's Hospital of Philadelphia, Newtown, PA, [4]The Children's Hospital of Philadelphia, Penn Valley, PA

Disclosures: John Van Arnam: None; Eline Luning-Prak: None; Michele Paessler: None; Vinodh Pillai: None

Background: CD19-specific chimeric antigen receptor (CAR) T cells have revolutionized the treatment of relapsed or refractory B cell acute lymphoblastic leukemia (B-ALL). Rearrangement of the *KMT2A* gene carries a poor prognosis in B-ALL. The leukemia initiating event is thought to occur in a myeloid stem cell prior to lymphoid commitment. Lineage switch to acute myeloid leukemia (AML) has been reported in *KMT2A*-rearranged cases after chemotherapy and immunotherapy with resultant loss of CD19 expression permitting immune escape.

Design: The archives from 2002-2017 were reviewed for cases of *KMT2A*-mutated B-ALL. Of 633 patients identified with B-ALL, 49 had *KMT2A* rearrangement of which 13 were treated with CD19 CAR T therapy. Next generation sequencing analysis (MiSeq) was

performed on IgH regions using bone marrow aspirate smears. VDJ usage, clonal frequency, and CDR3 sequence was determined and compared between the original lymphoid leukemia and the myeloid relapse.

Results: Of the 36 patients with *KMT2A*-mutated B-ALL who did not receive cell based therapy or blinatumumab, only two patients underwent lineage switch, 1 and 22 week(s) after induction. Of the 13 patients with *KMT2A*-rearranged B-ALL who received CD19 CAR T-cell therapy, 4 underwent lineage switch to AML. A resultant AMLs had monocytic morphology and expressed myelomonocytic markers without B cell antigens. Time from CAR T therapy to diagnosis of lineage switch ranged from 3 to 32 weeks. Three of four patients undergoing CAR T induced lineage switch died of disease, with time from lineage switch to death ranging from 5 to 15 weeks; the fourth is alive with persistent marrow involvement. Of the 9 patients with CAR T treatment without lineage switch, only one relapse with identical immunophenotype was noted.

FISH studies and karyotypes showed identical *KMT2A*-rearrangments in both the lymphoid and myeloid lineages in all four patients. IgH sequencing showed identical clones by VDJ family usage and CDR3 sequence in both the lymphoid and myeloid leukemias.

Conclusions: This is the largest study characterizing *KMT2A*-rearranged B-ALL undergoing lineage switch after conventional chemotherapy and CAR T-cell therapy. There is an increase in AML lineage switch after CD19 CAR T-cell therapy associated with a dismal prognosis. The presence of identical IgH gene rearrangements in both the B-ALL and AML clones in all patients suggests a mechanism of reprogramming of the leukemic cell rather than the expansion of precursor myeloid population.

1407 MEF2B is Paradoxically Expressed in a Subset of Mantle Cell Lymphomas

Tayler van den Akker[1], Michael Markson[2], Abeer Salama[2], Shafinaz Hussein[3], Adolfo Firpo-Betancourt[4], Julie Teruya-Feldstein[5], Ali Saad[6], Matko Kalac[2], Siraj El Jamal[2]
[1]Mount Sinai, New York, NY, [2]Icahn School of Medicine at Mount Sinai, New York, NY, [3]Mount Sinai Hospital, New York, NY, [4]Mount Sinai Medical Center, New York, NY, [5]Mount Sinai Hospital Icahn School of Medicine, New York, NY,[6]Methodist/LeBonheur Health System, Memphis, TN

Disclosures: Tayler van den Akker: None; Michael Markson: None; Abeer Salama: None; Shafinaz Hussein: None; Adolfo Firpo-Betancourt: None; Julie Teruya-Feldstein: None; Ali Saad: None; Matko Kalac: None; Siraj El Jamal: None

Background: MEF2B is a member of the BCL6 gene transcriptional complex and its expression correlates to that of BCL6. In addition, MEF2B expression has been demonstrated in virtually all cases of follicular lymphoma and in most cases of GC-DLCBL. However, reports with limited data showed MEF2B expression in cases of mantle cell lymphomas (MCL). In this study, we describe a detailed comparative analysis of MEF2B expression in MCL via immunoblotting in cell lines, immunohistochemistry on patients' samples, and in an in-silico analysis of a representative NIH public dataset.

Design: We evaluated the expression of the MEF2B protein by immunoblotting in five MCL cell lines (Mino, Maver 1, Z-138, Jeko-1, and JVM2). The IHC expression of MEF2B was examined in formalin-fixed paraffin-embedded tissue from 19 cases of MCL using a modified H-score for a semiquantitative approach based on both the intensity and proportion of the staining cells. We used a cut-off value for positive cases (H=105) as proposed by a previous study. IHC staining for BCL1, SOX11, and BCL6 was performed in all cases to confirm the MCL diagnosis. Then, we analyzed the publicly available microarray dataset GSE16411 from the GEO database that contains MCL and CLL cases (known to be MEF2B-negative), comparing the differential expression of MEF2B in the MCL group to the CLL group using the GEO2R tool. Non-paired t-test used to asses for statistical significance.

Results: All patients' specimens were positive for SOX11 and BCL1, and negative for BCL6. MEF2B was positive (nuclear expression) in 42% (8/19) of the MCL cases (Fig. 1). Blastoid morphology was seen in 26% (5/19) of the cases. None of the blastoid MCL cases showed expression of MEF2B. In the MCL cell lines, MEF2B was expressed in all of the five cell lines, albeit at varying levels, with Z-138 and Mino expressing the highest levels of MEF2B (Fig. 2). Analysis of the GEO public dataset showed that MEF2B expression was statistically significant in the MCL group in comparison the CLL group (p-value <0.0001).

Figure 1 - 1407

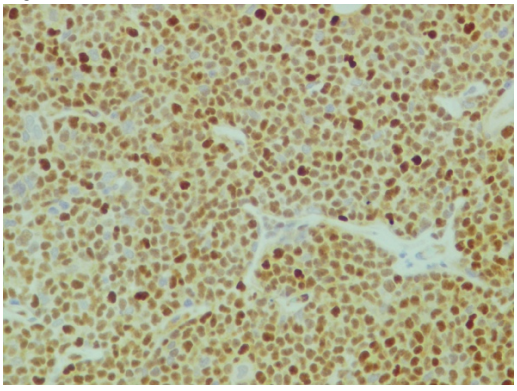

Figure 2 - 1407

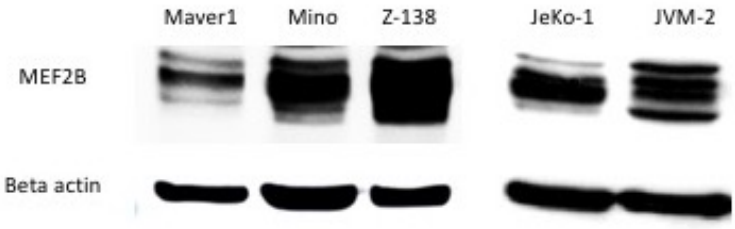

Conclusions: This study shows that MEF2B is paradoxically expressed in a sizable subset of MCL. Although MEF2B being closely related and having a mechanistic role in the BCL6 expression, its expression in MCL appears to be independent of its usual association with BCL6 expression. These findings suggest cautious utilization of MEF2B expression in the diagnostic workup of B-cell lymphomas and warrant further studying of the mechanism in which MEF2B acts in MCL.

1408 Pathologic Spectrum and Molecular Landscape of Myeloid Disorders (MD) Harboring SF3B1 Mutations

Elise Venable[1], Dong Chen[1], Phuong Nguyen[1], Jennifer Oliveira[1], James Hoyer[1], Kaaren Reichard[1], Aref Al-Kali[1], Kebede Begna[1], Hassan Alkhateeb[1], David Viswanatha[1], Rong He[1]
[1]Mayo Clinic, Rochester, MN

Disclosures: Elise Venable: None; Dong Chen: None; Phuong Nguyen: None; Jennifer Oliveira: None; James Hoyer: None; Kaaren Reichard: None; Aref Al-Kali: None; Kebede Begna: None; Hassan Alkhateeb: None; David Viswanatha: None; Rong He: None

Background: Somatic mutations in *SF3B1*, a gene encoding the splicing factor 3B subunit 1, are common findings in myelodysplastic syndrome (MDS) with ring sideroblasts (RS) and MDS/myeloproliferative neoplasm (MPN) with RS and thrombocytosis. Their distribution in other myeloid disorders (MD) has not been fully evaluated. Our study aim is to assess the pathologic spectrum and molecular landscape of MD harboring *SF3B1* mutations.

Design: Bone marrow (BM) cases performed during 2015-2017 with 35-gene next generation sequencing data were screened. Cases with pathogenic/likely pathogenic *SF3B1* mutations were recruited. Recorded data included patient demographics, CBCs, BM/peripheral blood morphology, mutation variant allele frequencies (VAF) and number. MD pathologic diagnoses were based on 2016 WHO criteria. Statistical analysis was done using the non-parametric Wilcoxon test.

Results: 75 patients (median age 73Y, range 35-89, 50 male) were identified. Diagnoses encompassed 4 (5%) clonal cytopenia of uncertain significance (CCUS), 38(51%) MDS [32 MDS-RS, 1 MDS with multilineage dysplasia (MDS-MLD), 4 MDS with excess blasts (MDS-EB), and 1 MDS with fibrosis (MDS-F)], 16(21%) MDS/MPN with 6(8%) RARS-T, 6(8%) MPN, 10(13%) acute myeloid leukemia (AML) [8 AML with myelodysplasia-related changes (AML-MRC), 2 de novo including 1 with inv(3)(q21;q26)], and 1 (1%) systemic mastocytosis (SM). Median VAF ranged from 31% to 43% in MDS-RS, MDS-EB, MDS-F, MDS/MPN, MPN and AML, significantly higher than in CCUS and SM (20%, p=0.007, and 5%, respectively). The most frequent *SF3B1* mutation was K700E (n=38, 51%) followed by K666R/T/N (n=15, 20%), most prevalent in MDS-RS. Other mutations spanned from E622 to D781 in the HEAT repeat regions. Concurrent mutations were mainly in epigenetic modifiers: *DNMT3A*, *TET2*, and *ASXL1* but not other spliceosome genes. Total number of gene mutations detected in ascending order (median): CCUS (1, p£0.05, all other), MDS-RS and MDS/MPN (2, p<0.01, AML and MPN), MDS-EB and AML (3) and MPN (4). RS ranged from 5% to 90% in MDS-RS, MDS-EB, MDS/MPN, and AML-MRC, but was absent in others.

Conclusions: *SF3B1* mutations occur in a wide spectrum of MD ranging from CCUS to AML. The mutational hotspots involve K700 and K666. VAFs and number of concurrent mutations were significantly lower in CCUS, and higher in AML and MPN. The prevalence of AML-MRC supports a strong association between *SF3B1* and secondary AML and suggests clonal evolution from preceding MDS in these cases.

1409 CD79a Expression is Significantly Associated with EBER Expression in Classical Hodgkin Lymphoma

Ashley Vogel[1], Jennifer Gregory[1], Dorothy Glaze[1], Jerald Gong[2], Guldeep Uppal[3]
[1]Thomas Jefferson University Hospital, Philadelphia, PA, [2]Thomas Jefferson University, Philadelphia, PA, [3]Thomas Jefferson University Hospital, Cherry Hill, NJ

Disclosures: Ashley Vogel: None; Jennifer Gregory: None; Dorothy Glaze: None; Jerald Gong: None; Guldeep Uppal: None

Background: Hodgkin and Reed-Sternberg (HRS) cells of Classical Hodgkin Lymphoma (CHL) are known to arise from germinal center B-lymphocytes. However, classical markers of the B-cell phenotype are expressed in a significant minority of cases. CD79a is one such pan-B-cell marker that is infrequently detected in CHL. Despite improvements in the understanding of the pathogenesis of CHL, the precise contribution of Epstein-Barr virus (EBV) remains largely unknown. We have observed a trend toward an increased likelihood of CD79a positivity in cases which were positive for Epstein-Barr encoded RNA (EBER). We present a series assessing the concurrent expression of EBER and CD79a in CHL.

Design: 49 cases of CHL between 2004-2018 were reviewed. 19 cases were EBER-positive: 11 nodular sclerosis, 6 mixed cellularity, 1 lymphocyte-rich, and 1 case not further specified. 30 cases were EBER-negative: 17 nodular sclerosis, 6 mixed cellularity, 1 lymphocyte-rich, and 6 cases not further specified. Marker status of CD79a and EBER were assessed by immunohistochemistry and in situ hybridization, respectively. The intensity and pattern of CD79a expression in HRS cells was graded descriptively: Negative; Variable Dim Positive; Dim Positive; or Moderate Positive.

Results: CD79a was consistently coexpressed with EBER in all but two EBER-positive cases (17/19; 89.5%): 3/19 Variable Dim Positive; 12/19 Dim Positive; 2/19 Moderate Positive. CD79a was expressed much less in EBER-negative cases (4/30; 13.3%). When positive, CD79a staining pattern was consistently dim and cytoplasmic. Interestingly, one case had only focal EBER-positivity, and it was only in this area that CD79a expression was observed.

	EBV POSITIVE	EBV NEGATIVE	
CD79a POSITIVE	17	4	
CD79a NEGATIVE	02	26	
	19	30	P value <0.001

Figure 1 - 1409

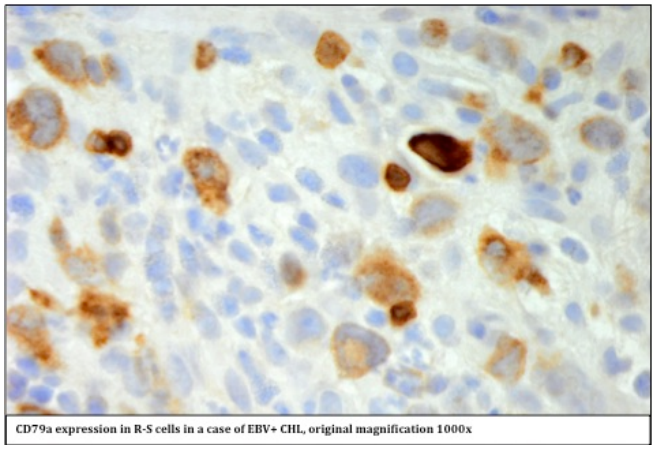

CD79a expression in R-S cells in a case of EBV+ CHL, original magnification 1000x

Figure 2 - 1409

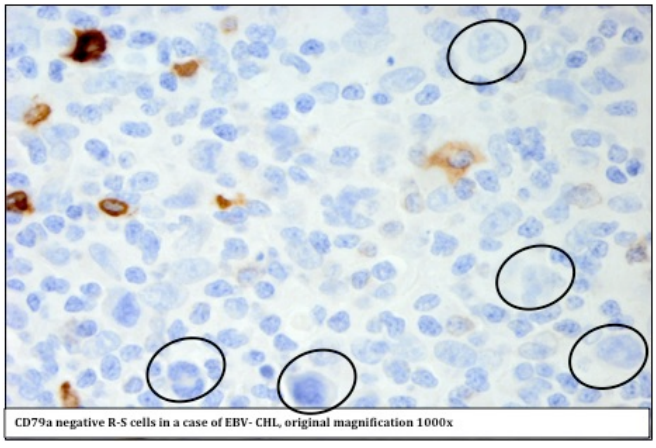

CD79a negative R-S cells in a case of EBV- CHL, original magnification 1000x

Conclusions: The relationship between EBER expression and B-cell marker status is understudied. Our study showed CD79a expression is consistently associated with EBV expression in HRS cells. It is possible that an interaction between B-cell receptor complex proteins and EBV viral proteins occurs at the level of the *sac* and/or *syk* family kinases, noted to be common to both pathways. The overall significance of our observations are not known, nor have similar findings been reported previously to our knowledge. The presence and pattern of CD79a positivity may serve as a supportive marker, of particular use in the differential diagnosis between gray zone lymphoma, or other EBV+ lymphoproliferative disorders. Future work to identify the role of EBV viral products and their influence on CD79a expression is required.

1410 PD-1 and PD-L1 Immunohistochemical Expression Patterns in Core Needle Biopsies of Reactive Lymph Nodes Versus Classic Hodgkin Lymphoma

Ashley Volaric[1], Alejandro A. Gru[1]
[1]*University of Virginia, Charlottesville, VA*

Disclosures: Ashley Volaric: None; Alejandro A. Gru: *Consultant*, Seattle Genetics; *Speaker*, Takeda

Background: Currently, it is becoming increasingly important to obtain detailed diagnostic and prognostic information on small-volume tissue biopsies, such as core needle biopsies. This is particularly crucial in the work-up and diagnosis of Classic Hodgkin Lymphoma (CHL), where small-volume lymph nodal biopsies often represent the frontline tissue source, and the differential involves a reactive process. Although it is difficult to make a diagnosis of lymphoma off core needle biopsy alone, pathologists are feeling more pressured to do so. Therefore, immunohistochemical markers would be helpful to differentiate CHL from a reactive lymph node (RLN) in this setting. Particularly, proliferation of activated immunoblasts can be seen which are potential mimickers of Hodgkin Lymphoma cells. The use of programmed cell death-1 (PD-1) and its ligand (PD-L1) immunohistochemical markers has primarily focused on the predictive therapeutic value in the work-up of CHL. However, in the present study, we evaluated lymph node core needle biopsies of CHL and RLN using PD-1 and PD-L1 to determine the diagnostic value of these markers in the small-volume setting.

Design: Core needle biopsies of 25 cases of confirmed CHL and 31 cases of RLN were evaluated by PD-1 (Abcam, NAT105) and PD-L1 (Abcam, SP142) immunohistochemistry. PD-1 and PD-L1 staining in inflammatory and neoplastic Hodgkin Lymphoma cells were classified as negative (<1%), 1-5%, 6-10%, 11-25%, 26-50% and >50%.

Results: Different PD-1 and PD-L1 expression patterns are observed in RLN and CHL (Figure 1). PD-1 expression is seen in 90% of RLN, and 60% of CHL. Whereas, all cases of RLN and CHL demonstrate PD-L1 expression. As such, PD-1 and PD-L1 co-expression is dictated by PD-1 and is observed in 90% of RLN and 60% of CHL. CHL cases show an overall greater expression of PD-L1 than RLN, with 40% of CHL having >50% PD-L1 expression compared to no cases observed for RLN (Figure 2). Conversely, CHL cases show an overall lower expression of PD-1, where 40% of CHL has no PD-1 expression compared to 10% of RLN (Figure 3).

Table 1.

	Classic Hodgkin Lymphoma	**Reactive Lymph Node**
PD-1 Expression		
<1%	40% (10/25)	10% (3/31)
1-5%	20% (5/25)	52% (16/31)
6-10%	20% (5/25)	29% (9/31)
11-25%	16% (4/25)	3% (1/31)
26-50%	4% (1/25)	6% (2/31)
>50%	0%	0%
PD-L1 Expression		
<1%	0%	0%
1-5%	0%	0%
6-10%	0%	23% (7/31)
11-25%	12% (3/25)	68% (21/31)
26-50%	48% (12/25)	10% (3/31)
>50%	40% (10/25)	0%
Overall PD-1 Expression	60% (15/25)	90% (28/31)
Overall PD-L1 Expression	100%	100%
PD-1/PD-L1 Co-Expression	60% (15/25)	90% (28/31)

Figure 1 - 1410

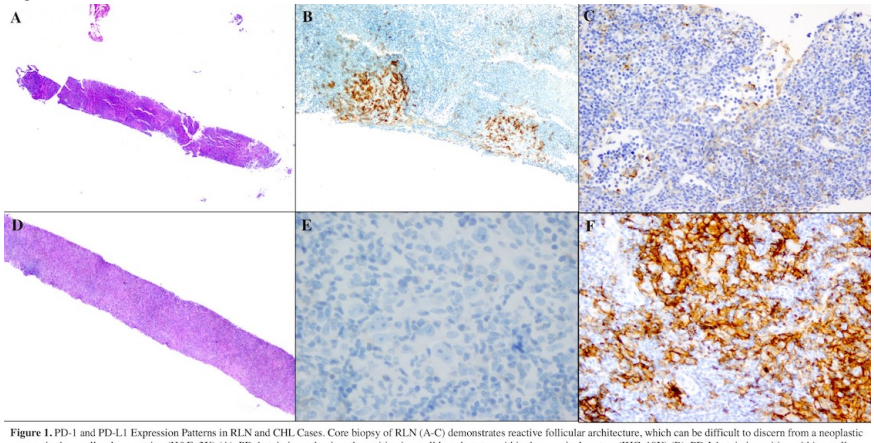

Figure 1. PD-1 and PD-L1 Expression Patterns in RLN and CHL Cases. Core biopsy of RLN (A-C) demonstrates reactive follicular architecture, which can be difficult to discern from a neoplastic process in the small-volume setting (H&E, 2X) (A). PD-1 stain is predominantly positive in small lymphocytes within the germinal centers (IHC, 10X) (B). PD-L1 stain is positive within small lymphocytes of the interfollicular areas (IHC, 20X) (C). Core biopsy of CHL (D-F) shows a slightly more diffuse pattern but is still difficult to discern from a reactive process in the small-volume setting (H&E, 2X) (D). PD-1 stain is negative within the neoplastic lymphocytes and Hodgkin Lymphoma cells (IHC, 40X) (E). PD-L1 stain, however, is strongly positive (>50%) within the neoplastic lymphocytic and Hodgkin Lymphoma cell population, highlighting the potential utility of this stain in discerning neoplastic CHL from RLN (IHC, 20X) (F).

Figure 2 - 1410

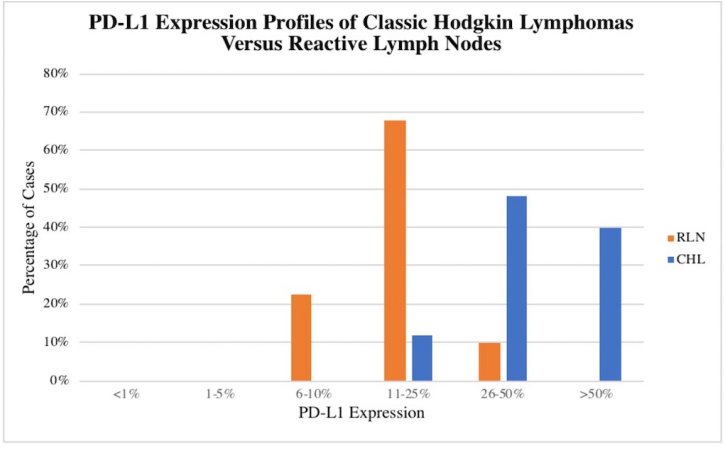

Conclusions: CHL cases demonstrate increased overall PD-L1 and decreased overall PD-1 and subsequent PD-1/PD-L1 co-expression compared to RLN cases on small-volume lymph node samples. Upfront PD-1 and PD-L1 immunohistochemistry on lymph node core needle biopsies could help differentiate CHL from a reactive process. Further correlation with fluorescent in situ hybridization (FISH) analysis for PD-L1 are ongoing in this current study.

1411 miR-181c Expression in GATA2 Deficiency Cells

Weixin Wang[1], Emily Barber[2], Layla Saleh[3], Meghan Corrigan-Cummins Nelson[4], Vollter Anastas[5], Stephenie Droll[6], Rui Chen[7], Nga Voong Hawk[8], Amy Hsu[9], Steven Holland[5], Katherine Calvo[5]
[1]Clinical Center/NIH, Bethesda, MD, [2]Encino, CA, [3]Mansoura University, Mansoura, Egypt, [4]Clinical Center/NIH, Graniteville, SC, [5]National Institutes of Health, Bethesda, MD, [6]Clinical Center/NIH, Chicago, IL, [7]Beijing TonRen Hospital, Capital Medical University, Beijing, China, [8]National Cancer Institute/NIH, Bethesda, MD, [9]NIAID/NIH, Bethesda, MD

Disclosures: Weixin Wang: None; Emily Barber: None; Layla Saleh: None; Meghan Corrigan-Cummins Nelson: None; Vollter Anastas: None; Stephenie Droll: None; Rui Chen: None; Amy Hsu: None; Katherine Calvo: None

Background: GATA2 is a transcription factor required for the survival of hematopoietic stem cells. Germline *GATA2* mutations result in haploinsufficiency, which is associated with cytopenias of several cell linages, including monocytes, B- and NK-cells; and susceptibility to opportunistic infections and strong propensity to develop hypocellular MDS/AML or CMML. MiRNAs (miRs) are short, non-coding RNAs that inhibit translation of messenger RNAs (mRNAs) by targeting the 3' untranslated region (3'UTR).

Design: MiRNA was profiled by microarray to assess differential miRNA expression in EBV-immortalized B cells from patients with GATA2 deficiency and controls. miRNA and gene expression were assessed by transient transfection in cell lines (SP53, K562, HEK293, HL60 and LY-8) and qRT-PCR. Cell death was measured by apoptosis ELISA and FACS sorting. GATA2 regulation of miR-181c was confirmed by transient transfection and RNA interference.

Results: miR-181c was significantly increased (> 2-fold; $p < 0.05$) in cell lines derived from patients with GATA2 deficiency in comparison to control derived cell lines, and was validated by qRT-PCR. Functional studies of miR181c showed potent induction of cell death by apoptosis in cell lines transfected with miR-181c. Predicted targets of miR-181c included MCL1 based on TargetScan analysis. qRT-PCR and western blot demonstrated that MCL1 expression was significantly decreased in GATA2 deficient cell lines in comparison to controls ($p<0.05$). In order to assess the relationship of miR-181c and MCL-1, transfection of miR-181c in multiple cell lines was performed resulting in significantly reduced MCL1 mRNA; and reduced cell survival. Luciferase reporter assays confirmed that miR-181c targets the MCL1 3'UTR. The relationship between GATA2 and miR-181c was elucidated by transient transfection of GATA2 and RNA interference assays which demonstrated marked decrease in miR-181c by GATA2 consistent with transcriptional repression of miR-181c; conversely GATA2 knock-down led to increased miR-181c expression.

Conclusions: These findings provide evidence that GATA2 represses miR-181c transcription, and GATA2 deficiency leads to increased miR-181c expression resulting in degradation of MCL1 and increased cell death. Increased miR-181c levels in GATA2 deficiency may play a role in the depletion of hematopoietic progenitors, cytopenias, immunodeficiency and the clinical phenotype that evolves in patients with germline mutations in GATA2.

1412 Pro-apoptotic protein BIM as a prognostic factor in Mantle cell lymphoma

Jeff Wang[1], Sam Katz[1], Elizabeth Morgan[2], David Yang[3], Xueliang Pan[4], Mina Xu[5]
[1]Yale University School of Medicine, New Haven, CT, [2]Brigham and Women's Hospital, Boston, MA, [3]University of Wisconsin, Madison, WI, [4]The Ohio State University, Columbus, OH, [5]New Haven, CT

Disclosures: Jeff Wang: None; Sam Katz: None; Elizabeth Morgan: None; David Yang: None; Xueliang Pan: None; Mina Xu: None

Background: Mantle cell lymphoma (MCL) is an aggressive B-cell lymphoma. Numerous studies have demonstrated many genetic aberrations in MCL in addition to the characteristic t(11:14). One such study reveals frequent biallelic deletions of BIM, a pro-apoptotic member of the BCL-2 family. Recent work by Katz et al. shows that *Bim* deletion coupled with cyclin D1 overexpression generates pathologic and molecular features of human MCL in mice. Since the regulation of apoptosis is crucial in MCL pathogenesis, we hypothesize that BIM expression may be associated with tumor cell survival.

Design: Diagnostic formalin-fixed, paraffin-embedded lymph node tissue specimens from 100 patients diagnosed with MCL between 1988 and 2009 were collected from three academic medical centers and stained with a validated commercial BIM IHC stain. BIM expression intensity was quantified and averaged by two independent pathologists. Additional data, including Ann Arbor staging, ECOG score, MIPI score, histologic variant, Ki-67 proliferation index, date of diagnosis, treatment modality, relapse, date of death, transplant status, and overall response rate, was obtained. Statistical analysis was conducted using SAS and Minitab software.

Results: The average patient age of our MCL cohort was 65.5 years old (range: 8-97) with a 2:1 male to female ratio. The inter-observer correlation of BIM expression was high (r=0.97). Patients were separated into low and high BIM-expressing categories with a cutoff of 80%. As expected for a pro-apoptotic tumor suppressor, patients with high BIM were less likely to have progressive disease and more likely to have a complete response (p=0.022). In addition, high BIM expressing MCL tumors revealed a trend toward increased overall survival with this trend persisting in sub-analysis of Ann Arbor Stages 3 and 4. No correlation between BIM expression, Ki-67 index, and MIPI score was observed.

Figure 1 - 1412

Overall Response Rate (ORR)	Low BIM IHC Expression (<80%)	High BIM IHC Expression (≥80%)
Complete Response	41.7% (15/36)	56.3% (18/32)
Partial Response	2.8% (1/36)	15.6% (5/32)
Stable Disease	2.8% (1/36)	6.3% (2/32)
Progressive Disease	52.8% (19/36)	21.9% (7/32)

p = 0.022

Figure 2 - 1412

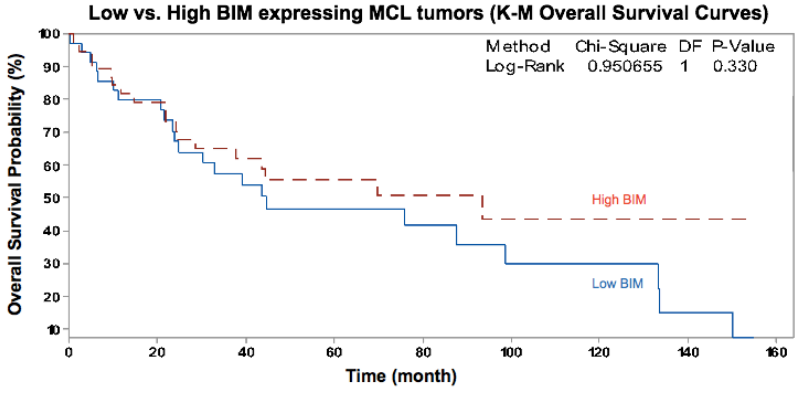

Conclusions: MCL patients with high BIM expressing tumors showed a better response to therapy and were less likely to have disease progression. These patients also demonstrated a trend toward longer overall survival, especially in advanced stages. The lack of correlation between BIM expression and Ki-67, MIPI score, and histologic variant suggests that BIM expression may be an independent

variable. While BIM is only one member of a complex family of apoptosis-regulating proteins, these findings may yield clinically relevant information for the prognosis and therapeutic susceptibility of MCL.

1413 CD138 Negative Plasmablastic Lymphoma: A Diagnostic Pitfall

YI Wang[1], Zenggang Pan[2], Ji Yuan[3], Mingyi Chen[4], Chen Zhao[5], Yanhua Wang[6], Yang Shi[6], Xiaojun Wu[7], Gang Zheng[7]
[1]Montefiore Medical Center, Stony Brook, NY, [2]Yale University School of Medicine, New Haven, CT, [3]University of Nebraska Medical Center, Omaha, NE, [4]University of Texas Southwestern Medical Center, Dallas, TX, [5]University of Iowa, Iowa City, IA, [6]Bronx, NY, [7]Johns Hopkins School of Medicine, Baltimore, MD

Disclosures: YI Wang: None; Zenggang Pan: None; Ji Yuan: None; Mingyi Chen: None; Chen Zhao: None; Yanhua Wang: None; Yang Shi: None; Xiaojun Wu: None

Background: Plasmablastic lymphoma (PBL) is a rare and aggressive type of large B lymphoma that is usually positive for CD138 and associated with immune-deficient state. However, rarely, they can be negative for CD138. CD138 negative PBL is often diagnostically very challenging and even misdiagnosed.

Design: We collected 21 cases of CD138 negative PBL from multiple institutes and 13 cases that were published since 1997.

Results: Our study showed that MUM1 is positive in 95.2% cases; CD45 is positive in 54.5% cases; restricted light chain expression in 91.3% cases while 14.3% cases lack kappa or lambda expression; CD20 is negative in 93.5% cases; PAX5 is positive in 9.1%, focally positive in 4.5% and negative in 86.4% cases; CD79a is positive in 19.2%, focally positive in 19.2% cases and negative in 61.5% cases; EBER is positive in 72.4% and HHV8 is negative in all cases. Most of the above cases are extra-oral cavity (85.1%), including lymph node (38.1%) and anus (7.4%). 65.3% patients are positive for HIV; 15.4% patients had kidney transplant while 28.6% patients have no definite history of immunodeficiency.

Conclusions: CD138 negative PBL is often a diagnostic challenge for both surgical pathologists as well as hematopathologists, because they are negative for CD3, CD20, CD138 and often negative for CD45. Sometimes they are diagnosed as undifferentiated malignant neoplasm. Here, we summarized the immunophenotypic features of CD138 negative PBL. They are positive for MUM1, Kappa or lambda light chain and negative for CD20, CD79a or Pax5. Compared to CD138 positive PBL, the majority CD138 negative PBL cases are found in extra oral cavity locations, providing more challenge to the diagnosis. We hope we can raise more awareness of the unusual features of CD138 negative PBL to prevent misdiagnosis.

1414 Cyclin D1 Expression in Prolymphocytic Transformation of Marginal Zone Lymphomas

Kyle White[1], Daniel Cassidy[2], Khaled Algashaamy[2], Oleksii Iakymenko[3], Sandra Sanchez[4], Offiong Ikpatt[5], Francisco Vega[4], Jennifer Chapman[6]
[1]Lake Worth, FL, [2]Miami, FL, [3]Jackson Memorial Hospital, Miami, FL, [4]University of Miami/Sylvester Cancer Center, Miami, FL, [5]UMH, Miramar, FL, [6]University of Miami, Miller School of Medicine, North Miami, FL

Disclosures: Kyle White: None; Daniel Cassidy: None; Khaled Algashaamy: None; Oleksii Iakymenko: None; Sandra Sanchez: None; Offiong Ikpatt: None; Francisco Vega: None; Jennifer Chapman: None

Background: Prolymphocytic transformation is a concept applied in CLL / SLL to describe a high percentage of prolymphocytes in peripheral blood (>55%). Prolymphocytic transformation is also been reported in mantle cell lymphoma (MCL) but only rarely in splenic or nodal marginal zone lymphoma (SMZL, NMZL). Among B-cell lymphomas, strong and uniform expression of cyclin D1 generally supports the diagnosis of MCL.

We encountered an index case of SMZL with prolymphocytic transformation defined by the presence of aggregates of prolymphocytes in tissue biopsy and increased prolymphocytes in peripheral blood (51%). The case was unusual because lymphoma cells expressed strong & diffuse cyclin D1 protein, mimicking MCL. Expression of cyclin D1 in SMZL is not reported. This case in conjunction with the fact that confirmatory FISH studies are not performed in the majority of MCL prompted us to investigate the expression of cyclin D1 in MZL.

Design: We retrospectively reviewed our cases of MZL with and without prolymphocytic transformation and performed cyclin D1 immunohistochemistry in all cases. Cyclin D1 positive MZL were further interrogated by cytogenetic and molecular analysis, including next generation sequencing (NGS).

Results: We identified 3 cases of MZL expressing strong and diffuse cyclin D1 including 2 SMZL and 1 NMZL, all of which had increased prolymphocytes in peripheral blood and / or tissue biopsies (Table 1 & Figure 1, 2). Despite diffuse cyclin D1 protein expression, all cases lacked the t(11;14)(q13;q32) as detected by several approaches in each case including NGS, FISH using both *CCND1* break apart probe and fusion probes for t(11;14)(q13;q32), and conventional karyotyping.

CASE	AGE	SEX	WBC/uL	% LYMPHOCYTES	% PROLYMPHOCYTES IN PERIPHERAL BLOOD OR PROLYMPHOCYTIC TRANFORMATION IDENTIFIED IN BIOPSY	CYTOGENETIC ABNORMALITIES / GENE MUTATIONS
1: SMZL	71	M	$9.4x10^3$	21.0	51%; TRANSFORMED IN BIOPSY	*NOTCH2*, *SRSF2*, *BCRA2*
2: SMZL	53	M	210 $x10^3$	94.0	88%	del7q, del13q, del17p, *TP53*
3: NMZL	81	F	$6.5 x10^3$	34.6	TRANSFORMED IN BIOPSY	*MAP3K14*

Figure 1 - 1414

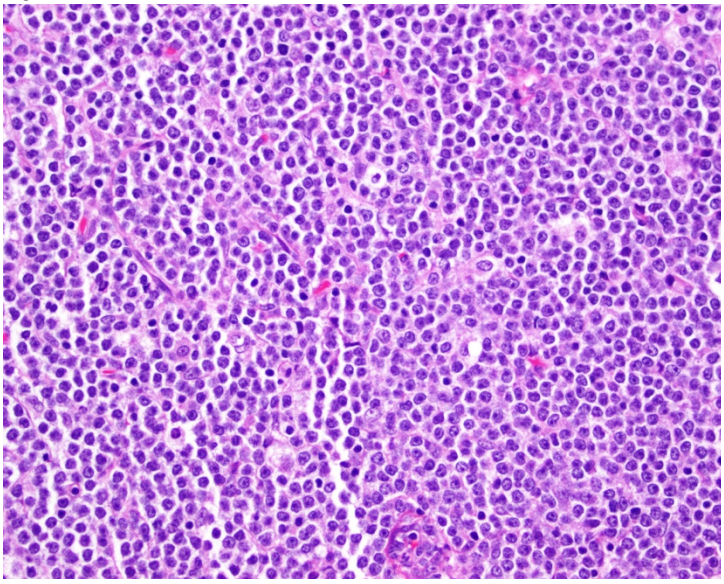

Figure 2 - 1414

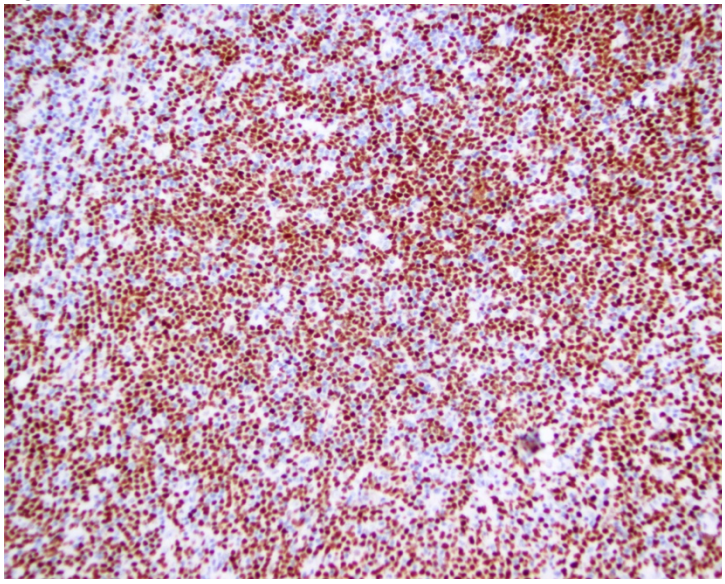

Conclusions: Cyclin D1 expression mimicking MCL is seen in a subset of SMZL and NMZL and in our cases appears to be associated with prolymphocytic transformation. These cases simulate prolymphocyitc variant MCL creating a previously unreported diagnostic pitfall. In our series, cyclin D1 expression was not seen in extranodal MZL nor in cases lacking prolymphocytic transformation. The association with prolymphocytic transformation is intriguing given the precedent of cyclin D1 expression in proliferation centers of CLL / SLL. Our findings suggest that the specificity of diffuse cyclin D1 expression in identifying MCL is not absolute, particularly among splenic or nodal lymphomas with prolymphocytes and raise the question of whether confirmatory FISH should be considered in leukemic, splenic MCL.

1415 A Subset of Extranodal NK/T-cell Lymphoma, Nasal Type Has Indolent Clinical Behavior Without Therapy

Adam Wilberger[1], Tawatchai Pongpruttipan[2], John Goodlad[3], Noa Lavi[4], Nidhi Aggarwal[5], Arivarasan Karunamurthy[5], Steven Swerdlow[1], Sarah Gibson[6]

[1]University of Pittsburgh School of Medicine, Pittsburgh, PA, [2]Siriraj Hospital, Mahidol University, Bangkok, Thailand, [3]NHS Greater Glasgow and Clyde/University of Glasgow, Glasgow, United Kingdom, [4]Rambam Medical Center, Haifa, Israel,[5]University of Pittsburgh Medical Center, Pittsburgh, PA, [6]University of Pittsburgh School of Medicine, Scottsdale, AZ

Disclosures: Adam Wilberger: None; Tawatchai Pongpruttipan: None; John Goodlad: None; Noa Lavi: None; Nidhi Aggarwal: None; Arivarasan Karunamurthy: None; Steven Swerdlow: None; Sarah Gibson: None

Background: Extranodal NK/T-cell lymphoma, nasal type (ENKTL) is an Epstein-Barr virus (EBV)-associated lymphoma that generally has an aggressive clinical course with poor long-term survival in a majority of cases. However, there are some patients with ENKTL that have a more protracted clinical course, including very rare reports of patients who survive for significant periods of time without treatment.

Design: 5 patients diagnosed with ENKTL who had a protracted clinical course prior to receiving anti-neoplastic therapy were identified, and the clinicopathologic features of these cases were reviewed.

Results: The 5 patients had a median age of 62 years (range 42-66), and included 4 males and 1 female. All patients initially presented with tumor limited to the nasal cavity. The patients all had a period of untreated disease ranging from 0.4-8 years (median 2.3). A diagnosis of ENKTL in the initial biopsy was made only in retrospect in 4/5 cases. Additional sites of disease outside of the nasal cavity occurred

during the clinical course of 3/5 patients, but 4/5 patients are alive with disease or with spontaneous partially regressed disease at last follow-up.

Clinicopathologic Features of 5 ENKTL with More Indolent Clinical Behavior					
	Patient 1	Patient 2	Patient 3	Patient 4	Patient 5
Age (years)/Gender	60/F	62/M	58/M	66/M	42/M
Initial site of disease	Nasal	Nasal	Nasal	Nasal	Nasal
Stage at initial presentation	IE	IE	IE	IE	IE
Initial diagnosis made retrospectively	Yes	Yes	No	Yes	Yes
PB EBV DNA at diagnosis (copies/mL)	<200	10,000	<1000	NA	NA
Cytology of neoplastic cells in initial biopsy	Small-medium, irregular cells	Small, slightly irregular cells	Medium, irregular cells	Small-medium, irregular cells	Small, slightly irregular cells
Admixed non-neoplastic inflammatory cells	Yes	Yes	Yes	Yes	Yes
Angioinvasion	No	No	No	No	No
Necrosis	Yes	No	No	No	No
Cell of origin	NK	NK	γδT	γδT	NK
Ki-67	NA	<5%	15%	<5%	NA
Secondary sites of disease (years from initial diagnosis)	Skin (2), arytenoid (2.4)	Skin (2.3)	NA	NA	Tonsil (7.4)
Cytology of neoplastic cells in last biopsy	Medium-large, irregular cells	Medium, irregular cells	NA	Small-medium, irregular cells	Medium-large, irregular cells
Time elapsed before treatment (years)	0.8	>2.3	0.4	NA	8
Anti-neoplastic therapy	Yes	Yes	Yes	No	Yes
Status, survival time (years)	DWD, 2.8	AWD, 3.5	AWPRD, 0.4	AWD, 5.4	AWD, 8

PB, peripheral blood; DWD, died with disease; AWD, alive with disease; AWPRD, alive with spontaneous partially regressed disease.

Conclusions: A subset of ENKTL has an indolent clinical course or an extended prodromal phase prior to more aggressive disease in the absence of any treatment. These cases may have minimal cytologic atypia (2/5), are associated with non-neoplastic inflammatory infiltrates (5/5), lack angioinvasion (5/5), and have low Ki-67 proliferative rates (3/3). The diagnosis is often missed because the biopsies closely resemble an inflammatory process. An EBER stain is particularly useful in identifying the neoplastic cells in such cases. Relapses frequently show more cytologic atypia. Further studies are warranted to determine the biologic mechanisms underlying this subset of ENKTL, to assess criteria that could identify these cases prospectively, and to determine which patients may not require aggressive therapies.

1416 TIM3 and Galectin-9 are Novel Therapeutic Targets for Mastocytosis

Margaret Williams[1], Tracy George[1], Sheryl Tripp[2], Michael Deininger[1], Jason Gotlib[3], Karin Hartmann[4]
[1]University of Utah, Salt Lake City, UT, [2]ARUP Laboratories, Salt Lake City, UT, [3]Stanford University, Stanford, CA, [4]University of Luebeck, Luebeck, Germany

Disclosures: Margaret Williams: None; Tracy George: *Consultant*, Blueprint Medicines; *Speaker*, Novartis; *Consultant*, Deciphera; Sheryl Tripp: None; Michael Deininger: *Consultant*, Pfizer Inc.; *Advisory Board Member*, Blueprint and Pfizer; *Grant or Research Support*, Pfizer; Karin Hartmann: None

Background: Immune checkpoint molecules have become important as immune checkpoint inhibitor therapy has advanced immunotherapies in cancer. We previously showed expression of PD-1 and PD-L1 in mastocytosis. New therapies have been developed that target additional checkpoint molecules, including the negative immune checkpoint molecule T-cell immunoglobulin mucin 3 (TIM3) and its ligand, galectin-9 (GAL9). Expression of inhibitory and stimulatory checkpoints in mastocytosis are important to understand as we develop different combinatorial treatment strategies. We aim to describe expression of TIM3 and its ligand in mastocytosis.

Design: We evaluated TIM3 (D5D5R, Cell Signaling Technology, Danvers, MA) and GAL9 (HPA047218, Atlas Antibodies, Bromma, Sweden) expression on the Benchmark, Ultra (Ventana Medical Systems, Tuscon, AZ) using antigen retrieval in 31 paraffin-embedded

tissues (bone marrow, skin, colon) from 29 patients, including 5 cutaneous mastocytosis (CM) and 26 systemic mastocytosis (SM): 17 indolent SM (ISM), 2 aggressive SM (ASM), and 7 SM with associated hematologic neoplasm (SM-AHN) diagnoses. Slides were scored on a 0-3 scale for stain intensity (0=none, 2= dim, 3= strong) and an overall percentage of both mast cells and tumor associated macrophages/monocytes with positive staining was given.

Results: TIM3 showed moderately intense cytoplasmic staining of mast cells in 93% of cases with an increased percentage of mast cells staining in SM (range 5-100%, median 90%, n=26) than in CM (range 0-75%, median 2.5%, n=4). TIM3 showed similar staining in ISM (range 5-100%, median 90%, n=17) and advanced SM including cases of ASM and SM-AHN (range 25-100%, median 90%, n=9). GAL9 showed moderate to strong intensity of dot-like cytoplasmic staining in mast cells in 86% of cases with an increased percentage of mast cells staining in SM (range 0-90%, median 50%, n=24) than in CM (range 0-90%, median 7.5%, n=4). GAL9 showed similar staining in ISM (range 0-90%, median 50%, n=15) and advanced SM (range 0-90%, median 50%, n=9). Both TIM3 and GAL9 showed strong staining within tumor infiltrating macrophages/monocytes in a subset of cells across all types of mastocytosis (range 5-100%, median 25%).

Conclusions: Staining of TIM3 and its ligand GAL9 is present in neoplastic mast cells with more staining in SM compared to CM. These results suggest a possible role for immune checkpoint inhibitor therapy in patients with mastocytosis.

1417 Loss of 18p is associated with genomic abrogation of the DNA damage response pathway in CLL

Waihay Wong[1], Christine Ryan[1], Michele Baltay[1], Neal Lindeman[2], Paola Dal Cin[1], Matthew Davids[3], Adrian Dubuc[1]
[1]Brigham and Women's Hospital, Boston, MA, [2]Brigham and Women's Hospital Pathology, Boston, MA, [3]Dana-Farber Cancer Institute, Boston, MA

Disclosures: Waihay Wong: None; Christine Ryan: None; Michele Baltay: None; Neal Lindeman: None; Paola Dal Cin: None; Matthew Davids: None; Adrian Dubuc: None

Background: Chronic lymphocytic leukemia (CLL) is a heterogenous disease characterized by recurrent genomic abnormalities. For example, del(13q14.3), trisomy 12, del(11q22.3), and del(17p13.1) are used as prognostic indicators to guide treatment decisions. While other recurrent genetic aberrations have been reported, their clinical utility remains uncertain due to the relative rarity of these events. Loss of 18p has been identified as a recurrent cytogenetic abnormality in CLL that is associated with predictors of poor outcome, including unmutated IGHV and del(17p)/TP53. However, larger cohort analyses are needed to clarify the clinical and biological significance of this finding.

Design: Our CLL cytogenetic database (n=3067) was queried for patients with structural aberrations resulting in loss of 18p. Targeted gene sequencing was performed on cases not previously characterized by molecular methods.

Results: 50 (1.6%) cases of CLL showed loss of 18p, representing the largest known cohort. Cytogenetic analysis identified three groups with distinct structural rearrangements leading to loss of 18p: (1) a single structural aberration resulting in concomitant loss of 17p and 18p, i.e. der(17;18)(q10;q10) (n = 21); (2) unbalanced structural rearrangements not involving loss of 17p, e.g. der(15;18)(q10;q10) (n = 14); (3) loss of 18p mediated by rearrangements with genomic material of unknown origin, i.e. add(18)(p11.2) (n = 15). Across all groups, we observed a strong enrichment for copy number loss of *TP53* and/or *ATM* in 35 (70%) and 10 (20%) patients, respectively. *TP53* loss occurred in patients with der(17;18) and add(18p) (groups 1 and 2). *ATM* loss, with concurrent gain of 2p, occurred mostly in patients in group 3. Molecular characterization identified biallelic inactivation of *TP53*/*ATM* in 36 (82%) of 44 patients with 18p loss. Furthermore, multiple subclonal mutations in *TP53*/*ATM* were present in 10 (23%) of 44 patients, suggesting convergent evolution towards *TP53*/*ATM* inactivation.

Conclusions: Loss of 18p is strongly associated with genomic markers of aggressive disease in CLL, including frequent biallelic inactivation of *TP53* and/or *ATM*. We describe three structural rearragements by which deletion of 18p arises, and hypothesize that selective pressures result in the convergence of del(18p) and abrogation of the DNA damage response pathway in this high-risk CLL subgroup.

1418 Next Generation Sequencing of Calreticulin Driven Myeloproliferative Neoplasms Underestimates Mutation Burden

Richard Wong[1], John Thorson[1], Sarah Murray[2], Shulei Sun[1]
[1]University of California, San Diego, La Jolla, CA, [2]University of California, San Diego, San Diego, CA

Disclosures: Richard Wong: None; John Thorson: None

Background: Next generation sequencing (NGS) is increasingly relied upon to assess hematologic malignancies for the presence of diagnostic and therapeutically relevant mutations. While a powerful tool NGS has inherent limitations, particularly in detecting insertions and deletions. In this report we highlight how a 52-base pair deletion in the calreticulin (*CALR*) gene, the detection of which has known clinical significance in myeloproliferative neoplasms (MPNs), may be inadequately assessed by NGS.

MPNs are characterized by overproduction of mature blood cells and variable marrow fibrosis. Driver mutations in *CALR* are second only to JAK2 mutations in their frequency in JAK2 pathway MPNs. The most commonly encountered *CALR* mutation is a 52 bp deletion in exon 9. Current laboratory methods for assessing *CALR* mutations include amplified fragment analysis using capillary electrophoresis (FCE), Sanger sequencing, and NGS. While FCE and Sanger methods provide direct quantitative, qualitative, and sequence (Sanger) information, data from NGS must be bioinformatically processed before mutations that have passed predetermined metrics are presented.

Design: NGS was performed on an Illumia MiSeq platform. BWA-MEM aligner, LoFreq (v2.1.3) variant caller, and Integrative Genomics Viewer (v2.4) were used for NGS data evaluation. Capillary electrophoresis was performed with an Applied Biosystems Genetic Analyzer.<

Results: In 17 patients with a MPN, a *CALR* 52 bp deletion was identified by FCE (figure 1). In subsequent NGS testing, the *CALR* mutation was present at a lower measured allele fraction (MAF) than expected. In one case the MAF fell below the 5% threshold filter and thus was not presented for review by the variant caller. Direct visualization of sequence reads revealed that a significant number containing the 52 bp deletion had been "soft clipped" by the software due to insufficient alignment to the reference sequence, resulting in a 4% to 29% reduction in the MAF of the deletion variant (figure 2).

Figure 1 - 1418

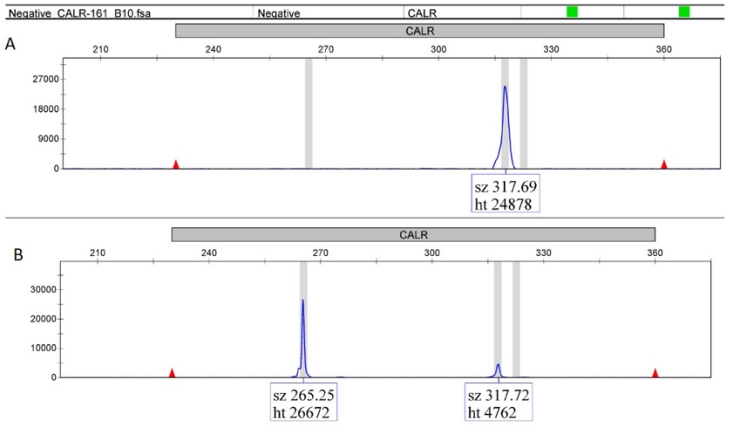

Figure 1. Amplified fragment analysis of *CALR* using capillary electrophoresis. (A) Normal patient sample with a wildtype fragment size of ~317 bases. (B) MPN patient sample with a fragment size of ~265 bases characteristic of a 52 base deletion.

Figure 2 - 1418

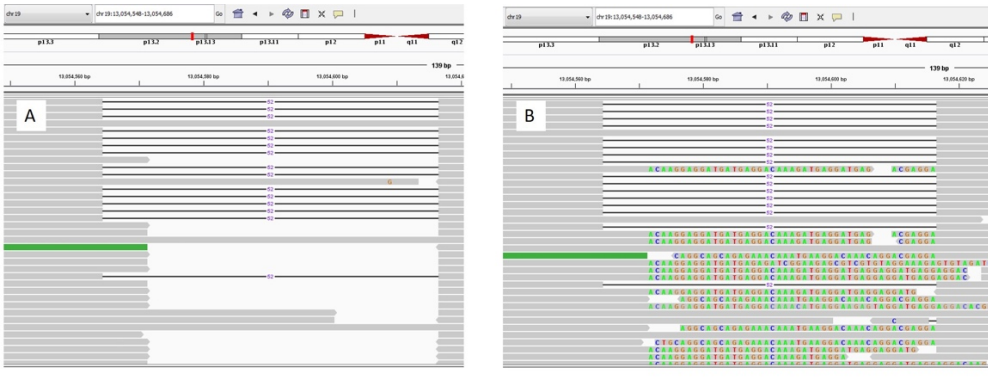

Figure 2. *CALR* sequence from NGS. (A) MPN patient with *CALR* 52 base deletion sequence reads denoted by –52—. Empty spaces represent uncalled bases. (B) Same data from (A) with "soft clipped" bases visualized.

Conclusions: NGS is a powerful tool in the clinical assessment of various pathologies. It is important for pathologists to be aware of limitations in these assays so they may anticipate pitfalls and discordant results from other testing methods. Here we highlight how *CALR* 52 bp mutation driven MPNs may be missed or disease burden underestimated by NGS. It is reasonable to assume pathologies driven by other deletion mutants in a similar size range may also be inadequately evaluated by NGS testing.

1419 Acute Myeloid Leukemia with t(8;16)(p11.2;p13.3)/KAT6A-CREBBP in Adult Patients

Wei Xie[1], Guilin Tang[1], Ting Zhou[2], Jie Xu[2], L. Jeffrey Medeiros[1], Shimin Hu[1]
[1]The University of Texas MD Anderson Cancer Center, Houston, TX, [2]Houston, TX

Disclosures: Wei Xie: None; Guilin Tang: None; Ting Zhou: None; Jie Xu: None; L. Jeffrey Medeiros: None; Shimin Hu: None

Background: Acute myeloid leukemia (AML) with t(8;16)(p11.2;p13.3)/*KAT6A-CREBBP* is an uncommon but distinct entity with a higher prevalence in the pediatric population. Previous studies suggested that AML with t(8;16) is associated with monocytic features, hemophagocytosis and poor outcome.

Design: Cytogenetic archives in our institution over the past 20 years were searched for t(8;16)(p11.2;p13.3) regardless of the pathological diagnoses. Clinical, morphological, immunophenotypic, molecular, genetic and follow-up data were analyzed.

Results: The study included 15 adult patients diagnosed with AML with t(8;16)(p11.2;p13.3). No cases of other types of myeloid or lymphoid neoplasm harboring this translocation were identified. There were 13 women and 2 men with a median age of 50 years (range: 19-62 years) at initial diagnosis. In all patients, t(8;16)(p11.2;p13.3) was detected at initial diagnosis. Ten of 15 patients had a history of various malignancies including: breast carcinoma (n=5), diffuse large B-cell lymphoma (n=3), marginal zone lymphoma (n=1) and liposarcoma (n=1). Four of these patients also had a history of autoimmune diseases (n=3) or acquired immune deficiency syndrome (n=1). The median interval from the diagnosis of the primary malignancy to the diagnosis of therapy-related AML (t-AML) was 18 months (range, 4-153 months). The blast count was high with a median of 74%, the blasts showed monocytic differentiation, and the neoplasm was classified as acute monoblastic leukemia (n=12) or acute myelomonocytic leukemia (n=3). Mild dysplasia was observed in 3 patients, and hemophagocytosis in 1 patient. T(8;16)(p11.2;p13.3) was observed as a sole chromosomal abnormality in 6 patients. After diagnosis of AML, all patients received chemotherapy and 5 underwent stem cell transplantation (SCT) (4 within 6 months after diagnosis). Twelve patients achieved complete remission. Eight patients, including 7/10 patients with t-AML and 1/5 with *do novo* AML, died at last follow-up with a median survival of 22 months.

Conclusions: T(8;16)(p11.2;p13.3) is exclusively associated with AML, predominantly in female patients with a history of cytotoxic therapy, and is associated with a high blast count, monoblastic morphology, and minimal dysplasia. The overall survival of this patient cohort is slightly better than that reported in the literature, which may be explained by the higher rate of complete remission, a lower incidence of hemophagocytosis, and a higher rate of utilization of SCT.

1420 Nanostring Platform Using Formalin-Fixed Paraffin-Embedded For Risk Prediction In Multiple Myeloma

Wei Xie[1], Roberto Ruiz-Cordero[2], Shimin Hu[1], L. Jeffrey Medeiros[1], Eric Fountain, Elisabet Manasanch[1], Pei Lin[1]
[1]The University of Texas MD Anderson Cancer Center, Houston, TX, [2]UCSF Pathology, San Francisco, CA

Disclosures: Wei Xie: None; Roberto Ruiz-Cordero: None; Shimin Hu: None; L. Jeffrey Medeiros: None

Background: Multiple myeloma (MM) is a heterogeneous disease with highly variable patient outcomes that depend on different risk factors. Gene expression profiling (GEP) using fresh bone marrow (BM) aspirates has been shown to be a powerful tool for risk stratification. However, fresh tissue is not universally available. GEP using Nanostring platform has been successfully applied on formalin-fixed paraffin-embedded (FFPE) tissue in lymphoma risk stratification. Here we explore the utility of Nanostring in myeloma risk prediction.

Design: We profiled myeloma cells with a custom NanoString panel using RNA derived from routinely processed FFPE BM clot specimens and compared the data with GEP-defined high and low risk groups by Affymatrix array using corresponding fresh samples of MM patients. A total of 70 genes were investigated by GEP and a previously published subset of 19 genes by NanoString. Gene counts were normalized prior to assessing significant differences between gene expression and risk groups, BM, cytogenetic, and clinical findings.

Results: Twenty-four patients with GEP-defined high and low risk myeloma (high risk: n=11, low risk: n=13) were included in the study. The cohort was male predominant (n=15) with a median age at diagnosis of 71 years (range: 61-89 years). Hierarchical clustering showed significant differences between high and low risk groups with high correlation of GEP data between fresh and FFPE tissue samples. Of note, differential expression of 10 genes was significantly associated with complex karyotype ($p<0.05$).

Conclusions: Gene expression profiling of a reduced number of genes quantified from FFPE specimens shows strong correlation with matched fresh tissue samples of MM patients. This small gene panel is useful for MM risk prediction and is associated with complex karyotype status. Further validation of these findings on larger cohorts could lead to potential implementation of FFPE tissue GEP of MM in routine clinical practice.

1421 Myelodysplastic Syndrome or Myelodysplastic/Myeloproliferative Neoplasm Followed by Acute Lymphoblastic Leukemia

Wei Xie[1], Sa Wang[1], Zhining Chen[1], Shaoying Li[1], Roberto Miranda[1], Shimin Hu[1], L. Jeffrey Medeiros[1], Guilin Tang[1]
[1]The University of Texas MD Anderson Cancer Center, Houston, TX

Disclosures: Wei Xie: None; Sa Wang: None; Shaoying Li: None; Roberto Miranda: None; Shimin Hu: None; L. Jeffrey Medeiros: None; Guilin Tang: None

Background: Approximately 30 patients with myelodysplastic syndrome (MDS) or myelodysplastic/ myeloproliferative neoplasm (MDS/MPN) followed by acute lymphoblastic leukemia (ALL) have been reported. However, most of these cases were case reports during 1980s to 1990s with very limited immunophenotyping and/or molecular cytogenetic workup. Whether ALL and MDS are clonally related or just a coincidence, and how does this clonality-association affect patient response to ALL-based chemotherapy, have not been explored.

Design: We searched our institutional database from 2008 to 2018 for patients with the diagnoses of ALL proceeded by MDS or MDS/MPN or were diagnosed synchronously. Cases with mixed phenotype acute leukemia or with recurrent rearrangements including *KMT2A, BCR-ABL1, PDGFRA/B, FGFR1 or JAK2* were excluded. Clinicopathologic and laboratory data were collected from the charts. Map-back FISH was performed on Wright-Giemsa stained bone marrow smears to elucidate the clonal relationship between the lymphoblasts and myeloid cells.

Results: The study cohort includes 5 patients: 4 had MDS or MDS/MPN preceding ALL (cases #1-4) and 1 had MDS and ALL diagnosed synchronously (case #5) (Table 1). All patients had co-existing MDS or MDS/MPN when ALL was detected initially. All cases demonstrated lymphoblasts markers (B- or T), 4 patients (except case #4) also had CD13 and/or CD33 (partial) expression. Four patients had an abnormal karyotype and map-back FISH showed: del20q (case #1) and -7 (case #2) detected in both lymphoblasts and myeloid/erythroid cells; i(9q) (case #4) detected only in lymphoblasts, and del(5q) (case #5) detected only in myeloid/erythroid cells. All patients were treated with ALL-based chemotherapy regimens; patients #3-5 responded and achieved a complete remission after the induction and patients #1 and #2 were refractory to therapy.

case	Age/sex	Preceding disease	Int+ (mon)	ALL type	Cytogenetic abnormalities	ALL and MDS clonally related?	Response to therapy	Outcome* (months)
1	66/M	MDS/MPN, NOS	33	B-ALL	Del(20q) [20]	Yes	Refractory	Died (2)
2	75/M	MDS	14	T-ALL	-7 [14/20]	Yes	Partial	Died (10)
3	72/M	MDS	28	B-ALL	Normal [20]	NA	CR	Alive (16)
4	58/M	CMML-1	3	B-ALL	Complex [10/20]	No	CR	Died (23)
5	82/F	No	0	B-ALL	Del(5q) [14/20]	No	CR	Died (7)

+from the diagnosis of MDS or MDS/MPN to onset of ALL; *from the onset of ALL to last follow-up

CR: Complete remission

Conclusions: ALL developing after MDS or MDS/MPN is very rare. In this study, we show that ALL and MDS are clonally related in 2 cases and these patients tend to be resistant to ALL-based chemotherapies. In the other 2 cases, ALL and MDS are not clonally related, it may be coincidental or possibly related to host susceptibility.

1422 Immunohistochemical Characterization of 5-Hydroxymethylcytosine Expression in Reactive Lymph Nodes and Follicular Lymphoma

Guangwu Xu[1], Karen Dresser[2], Benjamin Chen[1]
[1]UMass Memorial Medical Center, Worcester, MA, [2]UMass Memorial Health Care, Worcester, MA

Disclosures: Guangwu Xu: None; Karen Dresser: None; Benjamin Chen: *Grant or Research Support*, TESARO

Background: Genes affecting epigenetic pathways are frequently mutated in hematopoietic malignancies, such as acute myeloid leukaemia and some lymphomas. The genes encoding TET2, IDH1 and IDH2 are among the most commonly mutated genes, and result in reduced conversion of 5-methylcytosine into 5-hydroxymethylcytosine (5hmC) impairing demethylation of DNA and presumably serving as driver mutations in tumorgenesis. In fact, TET1/TET2 deficient mice are prone to development of B-cell lymphomas. The aim of this study was to characterize the immunohistochemical expression of 5hmC in benign, reactive lymph nodes (LNs) and compare this to the pattern found in follicular lymphoma (FL).

Design: Immunohistochemical staining with an anti-5hmC antibody was performed on 37 formalin-fixed paraffin-embedded specimens from patients with benign/reactive LNs (n=13), low grade (grade 1-2) FL (n=17), and high grade (grade 3A/3B) FL (n=7). 5hmC reactivity was scored for staining intensity (0-3+) and percentage of lymphocytes showing reactivity.

Results: Benign, reactive LN sections showed a distinct distribution of 5hmC staining, with the majority of cells in the interfollicular zones showing moderate to strong staining, whereas reactive germinal centers (GCs) were largely negative for 5hmC (<5% positive cells). We found that FL cases showed a similar distribution of 5hmC staining. Neoplastic follicles showed greater variability in size compared to reactive GCs; however 5hmC was negative in both neoplastic follicles and reactive GCs. The interfollicular zones, while diminished in FL due to expanded neoplastic follicles, showed retained 5hmC staining, similar to that seen in reactive LNs. Furthermore, significant differences in 5hmC distribution between low and high grade FL were not observed.

Conclusions: 5hmC expression in benign, reactive LNs is characterized by positive expression in interfollicular lymphocytes and negative expression in GCs. No significant differences in 5hmC distribution were seen between benign LNs and FL. Negative expression of 5hmC in both reactive GCs and neoplastic follicles is likely due to BCL6 upregulation, as recently described. Further examination of 5hmC expression in other lymphoma types, and correlation to other modifiers of epigenetic function, will be pursued.

1423 Chronic Lymphocytic Leukemia/Small Lymphocytic Lymphoma-Like Mantle Cell Lymphoma

Jie Xu[1], Sa Wang[2], Lifu Wang[3], Guilin Tang[2], Pei Lin[2], C. Cameron Yin[2], L. Jeffrey Medeiros[2], Shaoying Li[2]
[1]Houston, TX, [2]The University of Texas MD Anderson Cancer Center, Houston, TX, [3]Henan Provincial People's Hospital, Zhengzhou, China

Disclosures: Jie Xu: None; Sa Wang: None; Lifu Wang: None; Guilin Tang: None; Pei Lin: None; C. Cameron Yin: None; L. Jeffrey Medeiros: None; Shaoying Li: None

Background: Mantle cell lymphoma (MCL) is typically negative for CD23 and CD200, which is helpful for distinguishing MCL from chronic lymphocytic leukemia/small lymphocytic lymphoma (CLL/SLL). Some MCL may have atypical immunophenotype such as CD23+, but CD5+CD23+CD200+ MCL (designated as CLL-like for this study) is rare and the clinicopathologic features are unknown.

Design: Here we report 11 cases of CLL-like MCL. CD5, CD23 and CD200 expression were detected by flow cytometry. Clinicopathologic features were evaluated and overall survival (OS) was analyzed using the Kaplan-Meier method.

Results: There were 7 men and 4 women (M/F = 1.8:1) with a median age of 62 years (range 44-80). Six (55%) patients were older than 60 years. Six (55%) patients had leukocytosis and no patient had an elevated serum LDH level. All 11 patients had BM involvement and stage IV disease. Nine of 11 (82%) patients had leukemic non-nodal disease, whereas 2 (18%) patients had nodal involvement. The Mantle cell lymphoma International Index (MIPI) was intermediate in 8 (73%) patients and low in 3 (27%) patients. Pathologically, all 11 cases showed classic MCL morphology. By immunohistochemistry, all 11 cases were positive for cyclin D1 but none were positive for SOX11. Nine cases were tested for LEF1 and all were negative. Proliferation index by Ki67 stain was available in 6 cases and all were <30%. Fluorescence in situ hybridization and karyotype were tested in 9 cases and all showed *CCND1* rearrangement or t(11;14). Ten patients had treatment history available: 8 (80%) patients were observed initially and 2 (20%) patients received immunochemotherapy. After a median follow-up of 46.9 months (range 4-67), all patients were alive.

Conclusions: Patients with CLL-like MCL have leukemic non-nodal disease, low to intermediate MIPI, classic MCL morphology, lack of SOX11 expression, and a low Ki67 proliferation index. Most patients were observed initially with a good prognosis. The results of this study show that CD5+CD23+CD200+ MCL mimics CLL/SLL clinically and pathologically and may cause a diagnostic challenge.

1424 Loss of 5-Hydroxymethylcytosine is an Epigenetic Hallmark in Nodular Lymphocyte Predominant Hodgkin Lymphoma, a Novel Discovery

Shuo Amanda Xu[1], Deniz Peker[2], Qin Huang[1], Serhan Alkan[3]
[1]Cedars-Sinai Medical Center, Los Angeles, CA, [2]University of Alabama at Birmingham, Birmingham, AL, [3]Cedars-Sinai Medical Center, Beverly Hills, CA

Disclosures: Shuo Amanda Xu: None; Serhan Alkan: None

Background: DNA methylation at the C5 position of cytosine (5-methylcytosine, [5mC]) is a critical epigenetic event, and plays key roles in regulating gene expression in normal development and physiology. 5mC can be oxidized to 5-hydroxymethylcytosine (5hmC), a potential DNA demethylation intermediate, facilitated by TET family enzymes. Global loss of 5hmC has been described in non-hematological and hematological malignancies, including acute myeloid leukemia and T-cell lymphomas. The epigenetic characters of nodular lymphocyte predominant Hodgkin lymphoma (NLPHL) have not been previously studied. Here, we report that 5hmC is decreased in the neoplastic cells in NLPHL, which carries potential diagnostic and therapeutic importance.

Design: We retrospectively identified 21 NLPHL cases in our pathology archives at Cedars Sinai Medical Center. The hematoxylin-and-eosin and immunohistochemically stained slides for all the identified cases were reviewed by a hematopathologist. We established a 5hmC/CD20 double staining using the RevMab 5hmC(RM236) rabbit monoclonal antibody and Dako CD20(L26) mouse monoclonal antibody. 5hmC and CD20 were detected as nuclear red and membranous brown signals, respectively. The double stain was applied to all 21 NLPHL cases.

Results: In majority of the NLPHL cases, the neoplastic cells (CD20-positive) show complete loss of 5hmC staining (19/21). In 2 cases, the neoplastic cells show attenuated staining with 5hmc. In contrast, many of the background non-neoplastic small B-lymphocytes (CD20-positive) have retained strong staining with 5hmC.

Figure 1 - 1424

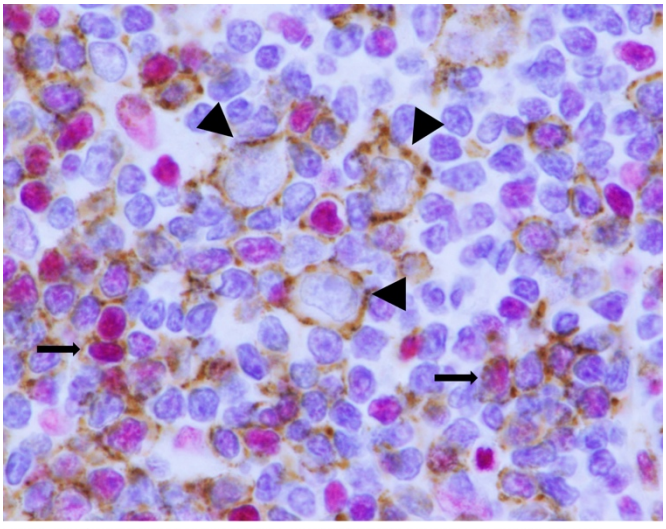

Figure1. 5hmC/CD20 double stain on nodular lymphocyte predominant Hodgkin lymphoma. The CD20-positive neoplastic LP cells (arrow head) have complete loss of 5hmC staining; whereas many background CD20-positive non-neoplastic small B-cells have retained bright 5hmC staining (arrow).

Conclusions: Here, we found that 5hmc is universally lost or diminished in the neoplastic cells in NLPHL, indicating that DNA methylation may play an important role in the molecular pathogenesis of NLPHL. In contrast, the small non-neoplastic B-cell in NLPHL have retained strong 5hmC staining, implying that the stain can be an useful adjunct to identify neoplastic cells in NLPHL. Moreover, our finding raises the possibility for new treatment strategies by targeting pathways that can reconstitute 5hmC levels in NLPHL.

1425 Regulatory mechanism of Fbw7-mediated LDHA ubiquitination on the regulation of glycolysis lactate production in the progression of diffuse large B-cell lymphoma

Su Yao, Guangdong General Hospital, Guangdong Academy of Medical Sciences, Guangzhou, China

Disclosures: Su Yao: None

Background: The ubiquitin-ligase Fbw7 targets several protooncogenes for ubiquitination and degradation and acts as a tumor suppressor in many human malignancies. Recently, we confirmed that Fbw7 regulates apoptosis in activated B-cell like diffuse large B-cell lymphoma by targeting Stat3 for ubiquitylation and degradation (J Exp Clin Cancer Res, 2017). However, the role of Fbw7 in the regulation of tumor metabolism in DLBCL is poorly understood.

Design: To comfirm that Fbw7 regulates tumor metabolism in DLBCL, we proform experiments of glycolysis. Using Mass spectrometry, we found Fbw7 interates with LDHA. And using protein coimmunoprecipitation and ubiquitination experiments to test if Fbw7 interacts with LDHA and targets it for ubiquitination degradation. Furthermore, it's reported that miR-223 targets Fbw7 in lots of cancer and we detect the regulation effect of miR-223 using its mork and inhibitor invitro and in vivo experiments. Morover, we detect the expression of Fbw7 and LDHA In clinical samples.

Results: We found that Fbw7 inhibits glycolytic lactate production in diffuse large B-cell lymphoma. Protein coimmunoprecipitation and ubiquitination experiments revealed that Fbw7 interacts with LDHA and targets it for ubiquitination degradation. Furthermore, we found upstream regulatory mechanism of Lactate-induced miR-223 inhibits the expression of Fbw7. In clinical samples, Fbw7 and LDHA expression was negatively correlated. Accordingly, we propose that Fbw7-mediated ubiquitination of LDHA regulates glycolytic lactic acid production in the progression of diffuse large B-cell lymphoma and its regulatory mechanism.

Conclusions: Our study will elucidate the new mechanism of Fbw7-mediated LDHA ubiquitination on the regulation of glycolysis lactate production in the progression of diffuse large B-cell lymphoma, which may offer a new approach for Fbw7-mediated tumor metabolism therapy.

1426 Endothelial C4d Deposition for the Differential Diagnosis between Kikuchi Disease and Necrotizing Lupus Lymphadenitis

Shan-Chi Yu[1], Kung-Chao Chang[2], Chih-Jung Chen[3], Hsuan Wang[4], Yueh Min Lin[5]
[1]Taipei, Taiwan, [2]National Cheng Kung University and Hospital, Tainan, Taiwan, [3]Changhua Christian Hospital, Changhua, Taiwan, [4]National Taiwan University Hospital, Hsinchu, Taiwan, [5]Changhua City, Taiwan

Disclosures: Shan-Chi Yu: None; Kung-Chao Chang: None; Chih-Jung Chen: None; Hsuan Wang: None; Yueh Min Lin: None

Background: Kikuchi disease is among the most common etiologies of neck lymphadenopathies in endemic countries. Diagnosing this self-limited disease prevents unnecessary tests and treatment. Characterized by necrosis and karyorrhexis, the histology of Kikuchi disease is indistinguishable from lupus necrotizing lymphadenitis. Serological test for systemic lupus erythematosus (SLE) is usually necessary after the pathological diagnosis of Kikuchi disease is made. While most SLE patients have antibody-mediated injuries due to autoantibodies, the pathogenesis of Kikuchi disease is T-cell-based. In this study, we use C4d, a complement split end product, as a marker of antibody-mediated classical pathway of complement activation. Based on the different immunopathogenesis between these two diseases, we hope to recognize SLE patients among Kikuchi-like lymph node biopsies.

Design: Lymph node biopsies from Kikuchi disease and SLE patients were collected from four hospitals. Immunohistochemistry for C4d was carried out by Ventana autostainer. The immunostains were semiquantitatively scored according to the intensity and number of positive vessels, and the vessels were evaluated separately by size and histological location.

Results: When biopsies were taken, the majority (13/15, 87%) of necrotizing lupus lymphadenitis lacked a past history of SLE. Clinically, both Kikuchi disease and necrotizing lupus lymphadenitis had a female predominance. SLE patients were slightly older in age (mean age, 32 vs. 25 years old, p=0.008). There was no significant difference in clinical presentation, including fever and extent of lymphadenopathy. Histologically, the presence of plasma cells was more commonly noted in necrotizing lupus lymphadenitis than Kikuchi disease (70% vs. 30%, p=0.001). No significant difference was noted in other histological features. Immunohistochemically, endothelial C4d deposition was more frequently seen in necrotizing lupus lymphadenitis than Kikuchi disease (necrotic area: 58%, 11/18 vs. 3%, 2/61, $p<10^{-6}$; viable trabecular and hilar vessels: 64%, 14/23 vs. 6%, 5/78, $p<10^{-7}$). No difference was found in the C4d deposition at germinal centers, and perinodal fat and vessels.

Results of C4d immunohistochemical stain

	Kikuchi disease	Necrotizing lupus lymphadenitis	p-value
Necrotic area			
Endothelial staining	3% (2/61)	58% (11/18)	$<10^{-6}$
Perivascular staining	8% (5/61)	42% (8/18)	0.002
Viable area			
Capillaries and venules	23% (18/78)	57% (13/23)	0.004
Trabecular and hilar vessels	6% (5/78)	64% (14/23)	$<10^{-7}$

Figure 1 - 1426

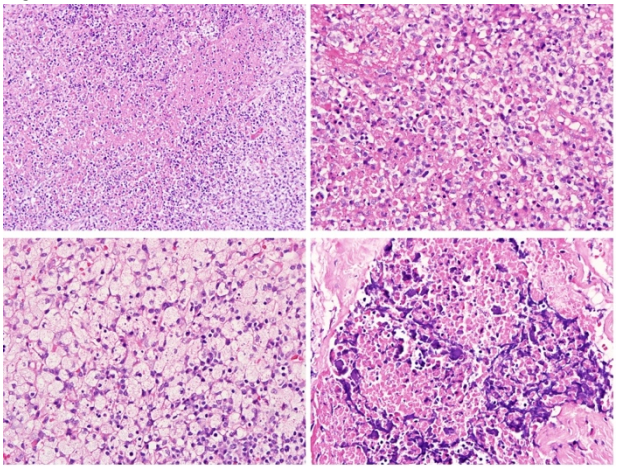

Histological features of necrotizing lupus lymphadenitis
(Left upper) Necrosis with abundant karyorrhexis
(Right upper) Crescent histiocytes
(Left lower) Xanthomatous stage
(Right lower) Hematoxylin bodies

Figure 2 - 1426

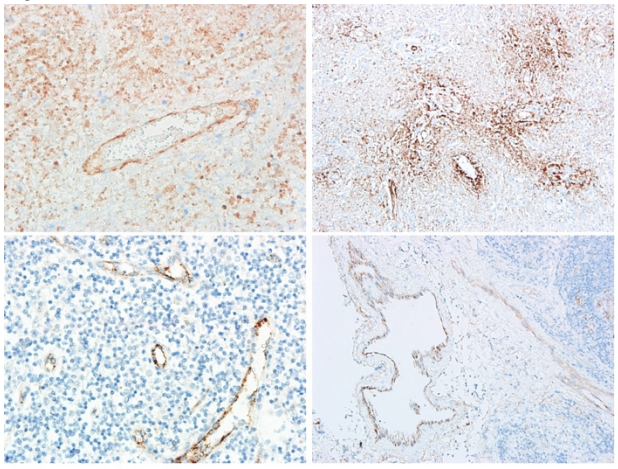

C4d immunohistochemistry
(Left upper) Endothelial staining in necrotic area
(Right upper) Perivascular staining in necrotic area
(Left lower) Endothelial staining of viable capillaries and venules
(Right lower) Endothelial staining of hilar and trabecular vessels

Conclusions: Kikuchi disease and necrotizing lupus lymphadenitis had similar clinical presentation and histology. Besides serological tests following a pathological diagnosis, C4d immunohistochemical stain is helpful to recognize SLE patients promptly in lymph node biopsies with Kikuchi-like features.

1427 Expressions of BCL2 and MIB1 in plasma cells of multiple myeloma and the correlation with genetic alterations

Yougen Zhan[1], Shafinaz Hussein[2], Julie Teruya-Feldstein[3]
[1]West Roxbury, MA, [2]Mount Sinai Hospital, New York, NY, [3]Mount Sinai Hospital Icahn School of Medicine, New York, NY

Disclosures: Yougen Zhan: None; Shafinaz Hussein: None; Julie Teruya-Feldstein: None

Background: Multiple myeloma (MM) is a disease of accumulation of neoplastic plasma cells. BCL2 is an anti-apoptotic protein that supports the survival of neoplastic cells and is thought to highly express in plasma cells. Venatoclax is now widely used to treat MM, so knowing BCL2 expression in MM is important. MIB1 expression is used as proliferation rate. It is known to be low in plasma cells, but a high level indicates an aggressive process.

Design: We randomly chose 40 patients who had over 20% plasma cells in marrow. We use IHC to examine BCL2 and MIB1 expression. The strength of BCL2 expression is estimated as no (0+), weak (1+) and strong expression (2+), comparing to the normal internal T cells. The percentage of plasma cells expressing BCL2 was estimated. The H scores of BCL2 were calculated as the strength of expression (H score = 0x percentage + 1x percentage + 2x percentage). The highest H score is 200 and the lowest is 0. The MIB1 expression is estimated as a percentage of cells that are MIB1 positive. The statistics was calculated as student's T test

Results: We found BCL2 is variably expressed in plasma cells of MM patients. 21 out of 40 (52.5%) patients show the highest expression with H score 200, and 17.5% of patients show H score less than 100 (7 out of 40). Among three common translocations, t(11;14) shows prominent BCL2 expression (13/14 patients with H score 200), which is significantly higher than those without any translocation (p=0.0017). T(14;16) translocation (n=2) had 200 in both H scores. T(4;14) (n=5) does not correlate with high BCL2 expression. Gain of 1q appears to associate with a poor prognosis. We have total of 5 patients with gain of 1q, but we did not find any statistic difference in BCl2 expression. Deletion 13 is the most common cytogenetic abnormality (17 out of 40) among patients, but BCL2 expression does not differ significantly from those without deletion (p=0.306). Furthermore, we found 47.5% of MM (19 out of 40) have over 10% proliferation rate in plasma cells. These cells show very high level of BCL2 expression (H score greater than 180), which is significantly higher than those with proliferation rate less than 10% (p=0.0009)

Conclusions: Our data demonstrate that BCL2 is variably expressed in plasma cells and t(11;14) correlates with the highest BCl2 expression. 47.5% plasma cells show over 10% proliferation rate which also had high BCL2 expression. Our data suggest BCL2 stain is needed to screen patients before venatoclax treatment.

1428 PD-1 Expression Is Upregulated in Diffuse Large B-Cell Lymphoma Transformed from Marginal Zone Lymphoma and Significantly Higher in Comparison with de novo Diffuse Large B-Cell Lymphoma

Shanxiang Zhang, Indiana University School of Medicine, Indianapolis, IN

Disclosures: Shanxiang Zhang: None

Background: Marginal zone lymphoma (MZL) is an indolent B-cell lymphoma, however approximately 10% of MZL may transform into diffuse large B-cell lymphoma (t-DLBCL), portending an accelerated clinical course and in general poor prognosis. Current standard chemotherapy for DLBCL leads to long-term remission in only 50-60% of DLBCL patients. Recently programmed death-1 (PD-1) blockade targeting the PD-1 immune checkpoint has shown great success in the treatment of advanced cancers including hematological malignancies. However, there has been no systemic report of PD-1 status in the t-DLBCLs associated with MZL, though PD-1 expression has been studied in MZL and DLBCL.

Design: Three tissue cases of DLBCLs in patients with prior history of MZL were retrieved and stained with antibodies against PD-1 (NAT105), PD-L1 (22C3), CD3, CD20, CD5, CD10, CD30, CD43, cyclin D1, BCL-6, MUM-1, Ki-67, p53, and c-MYC. In addition, tissue microarrays constructed from our archival cases of MZL and *de novo* DLBCL (d-DLBCL) diagnosed during 2000-2014 were stained for CD3, CD20 and PD-1. Patient's clinical history and treatment were obtained from our electronic medical system.

Results: Three patients (1 male, 2 female) were diagnosed with DLBCLs at the age of 61, 97 and 64 years old with a corresponding history of splenic MZL, MZL of mucosa-associated lymphoid tissue and splenic MZL, respectively. The internal from MZL to DLBCL is 3, 1 and 4 years, respectively. The three DLBCLs all show strong PD-1 expression in at least 10% of tumor cells while none of their corresponding MZLs showed any detectable PD-1 expression. In addition, marked upregulation of PD-L1, p53, c-MYC and Ki-67 was observed in one DLBCL while another one shows no changes other than higher Ki-67 expression. There is not enough tissue left for the third DLBCL. There is no strong PD-1 expression in the 86 MZLs with moderate PD-1 expression in 14 cases (16%). Three out of the 72 d-DLBCLs (4%) showed strong PD-1 expression in at least 10% of tumor cells. PD-1 expression is significantly higher in the three t-DLBCLs compared to d-DLBCLs (100% vs 4%, $p<0.001$).

Conclusions: PD-1 expression is upregulated in DLBCLs transformed from MZLs and significantly higher in comparison with d-DLBCLs, suggesting its potential mechanistic contribution in the DLBCL transformation from MZL. While this observation needs to be verified in a larger cohort, it nevertheless suggests worthwhile for us to explore PD-1/PD-L1 blockade in the treatment of patients with transformed DLBCLs.

1429 Ionized Calcium Binding Adaptor Molecule 1 (IBA1): A Novel, Highly Sensitive and Specific Marker for Acute Myeloid Leukemia with Monocytic Differentiation

Xiaoming Zhang[1], Amy Ziober[1], Li-Ping Wang[1], Paul Zhang[2], Adam Bagg[3]
[1]Hospital of the University of Pennsylvania, Philadelphia, PA, [2]Hospital of the University of Pennsylvania, Media, PA, [3]University of Pennsylvania, Philadelphia, PA

Disclosures: Xiaoming Zhang: None; Amy Ziober: None; Li-Ping Wang: None; Paul Zhang: None; Adam Bagg: None

Background: Despite the importance of genetics in the classification and prognosis of acute myeloid leukemia (AML), AML with monocytic differentiation (AMoL) is important to recognize and diagnose, given its clinical features (e.g. risk of CNS involvement) and often-adverse prognosis. Morphology, flow cytometry and cytochemistry are used to diagnose AMoL but require aspirates that may not always be available. Immunohistochemistry (IHC) can be valuable in such circumstances; however, IHC for AMoL is challenging due to a lack of highly sensitive and specific antibodies. IBA1, also known as allograft inflammatory factor 1, is a novel marker of microglia/macrophages that has not been used in hematopathology. We aimed to evaluate its utility in identifying cases of AMoL and compare it with CD14, CD68 and CD163.

Design: A total of 68 AML cases (49 AMoL, diagnosed based upon morphologic and immunophenotypic features, including AML, not otherwise specified and other WHO entities, and 19 AML without monocytic differentiation/nonMoAML) were studied (Table). IHC for IBA1 (rabbit, polyclonal), CD14 (EPR 3653), CD68 (KP1) and CD163 (10D6), was performed. Percentage blast expression for each was determined. ROC curve analysis was used to compare the performance of these markers and select the optimal cut-off values for positivity (Fig 1). Blast staining was considered positive based on these cut-offs.

Results: Comparison of the ROC curves for identification of AMoL showed a significantly greater AUC value using IBA1 as compared with CD14, CD68 and CD163 (0.93 vs 0.69, 0.73 and 0.75, $p<0.01$, Fig 1), indicating IBA1's superior overall performance in distinguishing AMoL from nonMoAML. IBA1 was expressed in 46 of 49 AMoLs and 3 of 19 nonMoAMLs (Table). Compared with the others, IBA1 was more sensitive for monocytic differentiation than CD14, CD68 and CD163 (94% vs 59%, 71%, and 55%). IBA1 also showed much more robust staining as compared with the others (Fig 2). Although CD163 was the most specific marker in our study it was not statistically superior to IBA1 ($p=0.318$). In addition, all 3 IBA1 positive nonMoAMLs also showed reactivity for at least one other monocytic marker by

IHC. Non-specific esterase cytochemistry will be performed and positivity in these 3 cases might determine if they could be reclassified as AMoL upon re-review.

		AML with monocytic differentiation (n=49)	AML without monocytic differentiation (n=19)
Immunohistochemical analysis			
	IBA1 expression	46/49 (93.9%)	3*/19 (15.8%)
	CD14 expression	29/49 (59.2%)	4**/19 (21.0%)
	CD68 expression	35/49 (71.4%)	6***/19 (31.6%)
	CD163 expression	27/49 (55.1%)	1/19 (5.3%)
Flow cytometry analysis			
	CD4 expression	25/42 (59.5%)	3/17 (17.6%)
	CD14 expression	22/42 (52.4%)	0/17 (0.0%)
	CD64 expression	40/42 (95.2%)	2/17 (11.8%)
WHO Classification			
	AML, not otherwise specified	14/49 (28.6%)	4/19 (21.0%)
	AML with myelodysplasia-related changes	14/49 (28.6%)	12/19 (63.2%)
	Therapy-related AML	2/49 (4.1%)	2/19 (10.5%)
	AML with mutated *NPM1*	13/49 (26.5%)	1/19 (5.3%)
	AML with t(9;11)(p21.3;q23.3);*MLLT3-KMT2A*	3/49 (6.1%)	0/19 (0.0%)
	AML with inv(16)(p13.1q22) or t(16;16)(p13.1;q22);*CBFB-MYH11*	3/49 (6.1%)	0/19 (0.0%)

* All 3 cases were also positive for CD14 and/or CD68;

** 3 of 4 cases were also positive for IBA1 and/or CD68;

*** 3 of 6 cases were also positive for IBA1 and/or CD14.

AML: acute myeloid leukemia.

Figure 1 - 1429

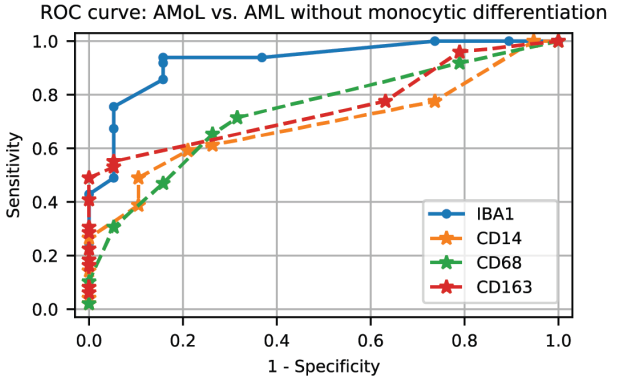

Marker	Area under the curve (AUC)			Optimal cut-off value	Sensitivity	Specificity
		95% CI	*p*-value*			
IBA1	0.927	0.837-0.976	NA	20%	93.9%	84.2%
CD14	0.691	0.567-0.798	< 0.0001	20%	59.2%	78.9%
CD68	0.735	0.614-0.835	0.0031	15%	71.4%	68.4%
CD163	0.754	0.635-0.850	0.0068	15%	55.1%	94.7%

*p-value for comparison of AUC: IBA1 vs other markers;
Statistical analysis was performed using MedCalc version 18.9.

Figure 2 - 1429

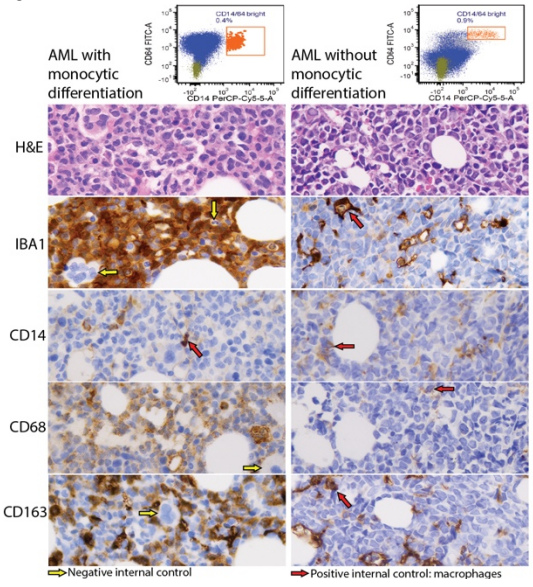

Conclusions: IBA1 is a novel, and highly sensitive and specific marker in distinguishing AMoL from other AML subtypes and could play a valuable role in diagnostic hematopathology.

1430 Evaluation of the Association for Molecular Pathology Recommended Core 34-Gene Panel for Next Generation Sequencing In Chronic Myeloid Neoplasms

Fang Zhao[1], David Bosler[2], James Cook[1]
[1]*Cleveland Clinic, Cleveland, OH,* [2]*Cleveland Clinic, Beachwood, OH*

Disclosures: Fang Zhao: None; David Bosler: None; James Cook: None

Background: Next generation sequencing (NGS) has become an increasingly important diagnostic tool to guide the management of patients with chronic myeloid neoplasms (CMNs). There is significant variability in the genes included on targeted NGS panels from different laboratories. Recently, the AMP CMN working group recommended a core 34-gene set as a minimum list for laboratories endeavoring to develop a pan-myeloid panel. This list was recommended based on literature review and its diagnostic yield is unknown. In this study we aim to assess the diagnostic yield of the core 34-gene NGS and to assess the impact of additional genes.

Design: Retrospective review was conducted among patients who underwent NGS testing at the Cleveland Clinic for known or suspected CMN between 6/2018 and 9/2018 using a 62-gene panel that includes all 34 AMP core genes and an additional 28 genes. All variants were classified using AMP/CAP/ASCO guidelines. Diagnostic yields were assessed for the total 62 genes and core 34 genes.

Results: 62 patients (35 males and 27 females) with a median (range) age 66 (22-90) years old were tested. As shown in table 1, the AMP 34 genes had a diagnostic yield of 82% to detect at least one variant with strong/potential clinical significance and 60% to detect >=2 strong/potential clinically significant variants. The expanded 62-gene panel had a diagnostic yield as of 84% and 65%, respectively. VUSs were identified in 34% using the AMP 34 genes vs. 48% using the expanded 62-gene panel. The diagnostic yield of the AMP 34 genes was highest in patients with MDS/MPN, with 100% showing >=1 variant with strong/potential clinical significance and 92% for >=2 strong/potential clinically significant variants. Overall, the median number of detectable variants with strong/potential clinical significance per case was similar between the AMP 34 genes and the 62-gene panel. Among the additional 28 genes, *CUX1*, *ETNK1*, and *SUZ12* were the most frequently mutated genes that were seen in 5, 3, and 2 cases, respectively.

	Diagnostic Yield				**Number of variants with strong/potential clinical significance per case** Median (Range)	
	>=1 variant(s) with strong/potential clinical significance		>=2 variants with strong/potential clinical significance			
Clinical/Pathological Diagnosis (n)	AMP 34-gene set	62-gene NGS panel	AMP 34-gene set	62-gene NGS panel	AMP 34-gene set	62-gene NGS panel
MDS (n=22)	77% (17)	77% (17)	68% (15)	73% (16)	2 (0-7)	2 (0-7)
MPN (n=25)	80% (20)	84% (21)	44% (11)	48% (12)	1 (0-5)	1 (0-5)
MDS/MPN (n=12)	100% (12)	100% (12)	92% (11)	92% (11)	4 (1-5)	4 (1-6)
SM (n=3)	67% (2)	67% (2)	0% (0)	33% (1)	1 (0-1)	1 (0-2)
Total (n=62)	**82% (51)**	**84% (52)**	**60% (37)**	**65% (40)**	**2 (0-7)**	**2 (0-7)**

Note: MDS, myelodysplastic syndrome; MPN, myeloproliferative neoplasm; MDS/MPN, myelodysplastic/myeloproliferative neoplasms; SM, systemic mastocytosis.

Conclusions: This study for the first time assesses the diagnostic yield of the AMP recommended core 34-gene set for patients with CMNs. Our results suggest that this core 34-gene set has a high diagnostic yield for CMNs, especially for MDS/MPN cases. The inclusion of additional genes beyond the core 34 genes slightly increased the yield for diagnosis, while also increasing the detection rate of VUS. These results will assist laboratories in designing an optimized NGS panel for CMNs.

1431 Body Fluid Blast Phase of Chronic Myeloid Leukemia

Ting Zhou[1], Yun Gong[2], Zimu Gong[3], Pei Lin[2], Aileen Hu[2], Wei Wang[2], L. Jeffrey Medeiros[2], Shimin Hu[2]
[1]Houston, TX, [2]The University of Texas MD Anderson Cancer Center, Houston, TX, [3]Chicago, IL

Disclosures: Ting Zhou: None; Yun Gong: None; Zimu Gong: None; Pei Lin: None; Aileen Hu: None; Wei Wang: None; L. Jeffrey Medeiros: None; Shimin Hu: None

Background: Blast phase (BP) of chronic myeloid leukemia (CML) is defined by the presence of $\geq$ 20% blasts in the bone marrow or peripheral blood (medullary BP) or by an extramedullary blast proliferation resulting in architectural effacement, namely, myeloid sarcoma or lymphoblastic lymphoma (tissue BP). Occasionally, blasts involve body fluid, particularly cerebrospinal fluid. In these scenarios, there is no architectural effacement or a threshold percentage of blasts to define BP, and it is often challenging to distinguish genuine leukemic involvement of body fluid from blood contamination. Here we report a series of CML patients diagnosed with BP involving body fluids but with no or minimal involvement of peripheral blood.

Design: Patients diagnosed with CML-BP involving body fluids over past 20 years were retrospectively reviewed. Those cases with $\geq$ 20% blasts in peripheral blood concurrently were not included.

Results: The study group included 15 patients: 11 men and 4 women, with a median age of 36 year (range, 20-72) at initial diagnosis of CML. The first body fluid BP developed a median of 20 months (range, 0.7-175) after initial diagnosis: 11 involving cerebrospinal fluid, 3 pleural fluid and 1 pericardial fluid. By immunophenotype, 8 patients developed myeloid BP, 6 lymphoid BP, and 1 T/myeloid BP. Five patients had concurrent medullary or tissue BP, 5 patients had isolated body fluid BP and also a previous history of medullary or tissue BP, and 5 patients never developed medullary or tissue BP during the study disease course. The median blast count in the body fluid specimens was 80% (range, 21-99), and the concurrent median blast count in the peripheral blood was 0% (range, 0-4). After diagnosis of body fluid BP, 14/15 patients received tyrosine kinase inhibitor therapy, 13/15 received chemotherapy with or without radiation, and 7 received stem cell transplant. After a median follow-up of 13 months (range, 2-39), 10/15 patients died. Of the 8 patients who did not received stem cell transplant, 5 did not achieve complete cytogenetic remission, and 6 died a median of 10 months after diagnosis of body fluid BP.

Conclusions: Blast phase of CML involving body fluids tends to occur in male patients who are significantly younger than patients with medullary or tissue BP. As a rare type of presentation of CML-BP, body fluid BP can occur as an isolated presentation, or concurrently or sequentially with medullary or tissue BP. The overall survival of these patients is very poor.

1432 Significance of idic(X)(q13) in Myeloid Neoplasms

Ting Zhou[1], Guilin Tang[2], Sanam Loghavi[2], Habibe Kurt[3], Carlos Bueso-Ramos[2], L. Jeffrey Medeiros[2], Shimin Hu[2]
[1]Houston, TX, [2]The University of Texas MD Anderson Cancer Center, Houston, TX, [3]Alpert Medical School of Brown University, Providence, RI

Disclosures: Ting Zhou: None; Guilin Tang: None; Sanam Loghavi: None; Habibe Kurt: None; Carlos Bueso-Ramos: None; L. Jeffrey Medeiros: None; Shimin Hu: None

Background: In the current WHO classification, idic(X)(q13) is considered as presumptive evidence of a myelodysplastic syndrome (MDS) in the absence of morphologic dysplasia in the setting of cytopenia, and also considered as a MDS-related cytogenetic abnormality in the classification of acute myeloid leukemia (AML) with myelodysplasia-related changes. We investigated the disease distribution, pathological features and prognostic impact of idic(X)(q13) in myeloid neoplasms.

Design: Patients with hematologic malignancies and idic(X)(q13) diagnosed over past 20 years were reviewed retrospectively. Clinicopathological, genetic and follow-up data were analyzed.

Results: The study group included 20 patients with myeloid neoplasms and idic(X)(q13). No cases of lymphoid neoplasms with idic(X)(q13) were identified. All patients were women, with a median age of 73 years (range, 26-85) at initial diagnosis: 7 patients had MDS (including 2 therapy-related), 6 AML, 4 myeloproliferative neoplasms (MPN), and 3 MDS/MPN. Of 13 patients in whom the emerging time of idic(X)(q13) was known, 10 had idic(X)(q13) at initial diagnosis, and the other 3 had idic(X)(q13) 6, 27 and 49 months after initial diagnosis, respectively. In 6/13 patients, idic(X)(q13) was the sole chromosomal alteration at initial emergence. However, additional chromosomal changes were acquired during the disease course in 16/20 patients, including extra copies of idic(X)(q13) in 9 patients. Of 16 non-MPN cases, 14 had adequate bone marrow cellularity for morphological evaluation, and 12 showed a variable degree of and often mild dysplasia. Four of 20 patients developed >15% ring sideroblasts during the disease course. Eighteen patients received standard therapies, including 3 also receiving stem cell transplant. The treatment in the other 2 patients was unknown. At last follow-up, 12 patients died. The median survival was 36.7 months from initial diagnosis and 23.8 months from emergence of idic(X)(q13).

Conclusions: idic(X)(q13) is a rare but recurrent rearrangement exclusively seen in female patients with myeloid neoplasms, frequently *de novo* MDS and AML, but also MPN and MDS/MPN. Although it is the sole change at initial emergence in less than half of patients,

additional chromosomal alterations are usually acquired during the disease course, most commonly, extra copies of idic(X)(q13). Dysplasia, usually mild, is commonly seen. Ring sideroblasts are observed in a small subset of patients. The overall prognosis of these patients is poor.

1433 A Modified Risk Stratification for Pediatric Acute Myeloid Leukemias with Complex Karyotypes

Ting Zhou[1], Kevin Fisher[1], Michele Redell[2], Andrea Marcogliese[3], M. Tarek Elghetany[4], Dolores Lopez-Terrada[5], Jyotinder Punia[6], Choladda Curry[1]
[1]Houston, TX, [2]Texas Children's Cancer Center, Houston, TX, [3]Texas Children's Hospital and Baylor College of Medicine, Houston, TX, [4]Texas Children's Hospital, Houston, TX, [5]Texas Children's Hospital/Baylor, Houston, TX, [6]Katy, TX

Disclosures: Ting Zhou: None; Michele Redell: None; M. Tarek Elghetany: None; Jyotinder Punia: None; Choladda Curry: None

Background: Complex karyotype in acute myeloid leukemia (AML) is considered an adverse prognostic factor. However, this is a highly heterogeneous category and current management seldom takes into consideration the specific kind of aberrations detected in this group. Additionally, the prognostic value of clonal heterogeneity remains unclear. Here, we examined pediatric AML cases and analyzed the prognostic significance of the individual components of complex karyotypes, clonal heterogeneity, and clonal cytogenetic evolution.

Design: We retrospectively obtained clinicopathological and cytogenetic data from a series of 200 newly diagnosed *de novo* pediatric AML cases from 2000-2016 at our institution. Survival analysis was performed using the Kaplan-Meier method. Complex karyotype is defined as >=3 chromosome abnormalities, clonal heterogeneity as >=2 cytogenetically abnormal clones and clonal cytogenetic evolution as acquisition of new chromosomal aberrations.

Results: Cytogenetic data were available in 170 patients with an age ranging from 9 days to 18 years and a M:F ratio of 1.2:1. Chromosomal aberrations were detected in 138 patients (81.2%) at initial diagnosis and complex karyotype was found in 42 patients **(Table 1).**

Based on the specific chromosomal aberrations comprising the complex karyotype, we established a 3-tier risk stratification model for complex karyotype (**Figure 1**): High risk: 3-way or 4-way complex translocation, complete or partial loss involving >=2 chromosomes (monosomy 7, 5q-, *etc.*), and complex karyotype not otherwise specified; Intermediate risk: trisomy karyotype, t(8;21) including complex translocation, t(15;17); Low risk: *KMT2A* rearrangements and sex chromosomal abnormalities.

In contrast to findings in adult AML, clonal heterogeneity at diagnosis does not impact complete remission rate, relapse or overall survival in this study. However, clonal heterogeneity acquired at relapse is associated with a shorter survival time after relapse (median survival = 129 versus 390 days, p=0.13). Cytogenetic clonal evolution during the disease course did not influence the outcomes (p=0.81).

Table 1. Demographic, clinical and cytogenetic characteristics of pediatric AML patients.

Male sex – no. (%)	92 (54)
Age (years) at diagnosis, median (range)	8 (0.1-18)
Follow-up (days), median (range)	832 (4-5647)
Overall survival (days), median	1950
Concomitant myeloid sarcoma	19 (9.5)
Cytogenetic profile – no. (%)	
Non-Complex chromosomal abnormalities	115 (67.6)
t(15;17)	9 (5.3)
t(8;21)	14 (8.2)
inv(16)/t(16;16)	9 (5.3)
Normal	35 (20.6)
t(9;11)	6 (3.5)
t(6;9)	1 (0.6)
MLL rearrangement excluding t(9;11)	18 (10.6)
Other	23 (13.5)
Complex chromosomal abnormalities	42 (24.7)
Sex chromosomal abnormalities	4 (2.4)
MLL rearrangement	8 (4.7)
Trisomy	3 (1.7)
Balanced t(8;21)	3 (1.7)
Complex variants of t(8;21)	3 (1.7)
t(15;17)	1 (0.6)
3-way or 4-way complex translocations	4 (2.4)
Monosomy/deletion	9 (5.3)
Other	7 (4.1)
Constitutional trisomy 21 (Down syndrome)	13 (7.6)

Figure 1 - 1433

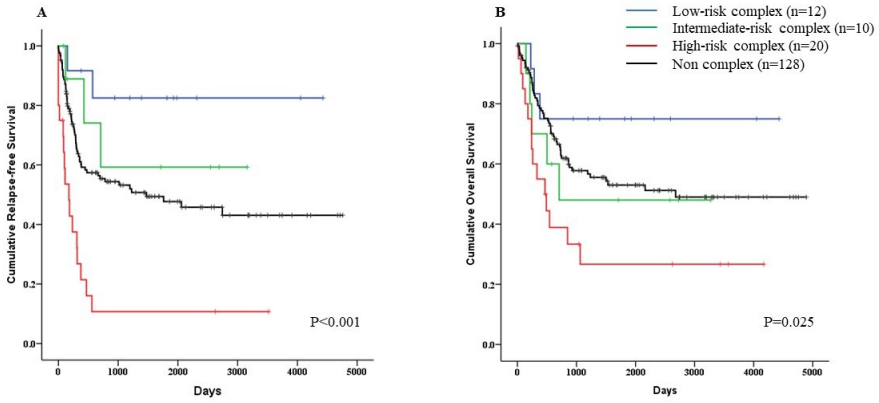

Figure 1. Cumulative relapse-free (A) and overall survival (B) of different cytogenetic groups of pediatric AML patients. The 5-year cumulative probabilities of relapse from initial diagnosis of AML for low-, intermediate-, and high-risk subgroups are 89%, 41%, and 17% (p<0.001), respectively; the corresponding 5-year overall survival rates are 27%, 48%, and 75%, respectively (p=0.025). Of note, the 5-year relapse and survival rates of the intermediate group are comparable to those of patients with non-complex karyotype (52% relapse and 53% overall survival).

Conclusions: This is one of the largest single institutional cohorts of pediatric AML. Complex karyotype in pediatric AML can be stratified into 3 cytogenetic groups based on the specific aberrations. Patients with complex karyotypes having t(8;21) and t(15;17) do worse than those with *KMT2A* rearrangements. Clonal heterogeneity at relapse is associated with a shorter survival after relapse.

1434 Children's CAEBV diseases presenting initially with HLH: A clinicopathological analysis of 11 cases

Jin Zhu[1], Yu Li[1]
[1]*Chongqing, China*

Disclosures: Yu Li: None

Background: Chronic active Epstein-Barr virus (CAEBV) disease is a progressive lymphoproliferative disorder associated with active EBV infection. Hemophagocytic lymphohistiocytosis (HLH) is a potentially fatal disease primarily of children. In some reports, patients with CAEBV were prone to accompany HLH. Here we reported our experience on 11 cases of children's CAEBV disease presenting initially with HLH.

Design: 11 Children with CAEBV diseases presenting initially with HLH from Children's Hospital of Chongqing Medical University were retrospectively analyzed by HE stain for morphology, IHC for phenotype, EBER in situ hybridization for EBV status and gene arrangement, coupled with clinical data study and follow-up.

Results: The patients included 6 male and 5 female ranging in age from 1 to 14 years (median age: 6.5 years). All cases met diagnosis of HLH when hospitalization. Anemia or/and thrombocytopenia could be found in 7 cases. All children had B symptom, lymphadenopathy, hepatosplenomegaly and hemophagocytosis in bone marrow, with either elevated EBV antibody titers or increased serum EBV DNA levels. The course of the diseases before diagnosis ranged from 3 months to 24 months. Morphologically, 8/11 cases showed different degree of architecture effacement. Necrosis could be observed in 6 cases. 8/11 cases showed obvious atypia. 10/11 cases were CAEBV T/NK-LPD including different grade : A3(5 cases), A2 (3 cases) and A1 (2 cases). 1 case was CAEBV B-LPD with grade A2-3. EBER was positive in all cases. TCR rearrangement was found in 6/8 cases. 5/11 cases were alive, including CAEBV T/NK-LPD grade A3 (2 cases) , grade A1(2 cases), and 1 case was CAEBV B-LPD grade A2-3. One patient with CAEBV T/NK-LPD grade A3 treated by Chinese herbs is still alive with recurrent fever. Another grade A3 patient received supportive treatment alive with mild symptoms. 6 cases received IVIG and corticoid steroid as immunoregulatory treatment and 2 cases received VP16 chemotherapy. 6 children including T/NK-LPD grade A2 (3 cases) and grade A3 (3 cases) died of serious complications, the shortest survival was 1 month. The longest survival (60 months) was in CAEBV T/NK-LPD grade A3 case without any treatment which died finally.

Case No.	Sex/Age	Course of disease (month)	Clinical symptoms	Blood test	EBV detected in blood	Follow-up(month)
1	M/7y	3	Fever, Lymphadenopathy, Hepatosplenomegaly, hemophagocytic lymphohistiocytosis	WBC 2.67×10^9/L, PLT 30×10^9/L, RBC 2.47×10^{12}/L, HG 88g/L, AST 463U/L, ALT 424U/L	EBV-CV-IgG	60, Dead
2	M/4y	4	Fever, Lymphadenopathy, hemophagocytic lymphohistiocytosis	WBC 2.68×10^9/L, PLT 69×10^9/L, RBC 1.67×10^{12}/L, HG 68g/L, CRP 38mg	EBV-CV-IgG	1, Dead
3	M/14y	3	Fever, Lymphadenopathy, Hepatosplenomegaly, hemophagocytic lymphohistiocytosis	WBC 2.9×10^9/L, PLT 22×10^9/L, RBC 3.02×10^{12}/L, HG 100g/L, ALT 59.5U/L	EBV-CV-IgG EBV PCR 2.99×10^6copies/ml	1, Dead
4	F/11y	3	Fever, Lymphadenopathy, Hepatosplenomegaly, hemophagocytic lymphohistiocytosis	WBC 0.2×10^9/L, PLT 22×10^9/L, RBC 3.09×10^{12}/L, HG 86g/L, CRP 55mg, AST 589U/L, ALT 109.2U/L	EBV PCR 2.67×10^3copies/ml	1, Dead
5	F/5y	3	Fever, Lymphadenopathy, hemophagocytic lymphohistiocytosis	WBC 2.27×10^9/L, PLT 151×10^9/L, RBC 3.25×10^{12}/L, HG 91g/L, CRP 91mg, AST 206U/L, ALT 123U/L	EBV PCR 1.89×10^5copies/ml	22, Alleviation
6	M/8y	9	Fever, Lymphadenopathy, Hepatosplenomegaly, hemophagocytic lymphohistiocytosis	WBC 0.82×10^9/L, PLT 61×10^9/L, RBC 3.66×10^{12}/L, HG 87g/L, CRP 41mg	EBV-CV-IgG	3, Dead
7	F/1y	12	Fever, Lymphadenopathy, Hepatosplenomegaly, hemophagocytic lymphohistiocytosis	WBC 5.5×10^9/L, PLT 79×10^9/L, RBC 3.2×10^{12}/L, HG 76g/L	EBV-CV-IgG	11, Alleviation
8	F/6y	3	Fever, Lymphadenopathy, Hepatosplenomegaly, hemophagocytic lymphohistiocytosis	WBC 6.74×10^9/L, PLT 163×10^9/L, RBC 3×10^{12}/L, HG 82g/L, CRP 15mg, LDH 444 U/L, TG 5.06mmol/L	EBV-CV-IgG EBV-CV-IgM EBV PCR 5.42×10^6copies/ml	5, Alleviation
9	F/5y	24	Fever, Lymphadenopathy, Hepatosplenomegaly, hemophagocytic lymphohistiocytosis	WBC 21.2×10^9/L, PLT 426×10^9/L, RBC 4.64×10^{12}/L, HG106g/L, CRP 48mg, AST 52.4U/L, ALT536U/L	EBV-CV-IgG EBV PCR 2.81×10^8copies/ml	1,Dead
10	M/4y	2	Fever, Lymphadenopathy, hemophagocytic lymphohistiocytosis	WBC 2.15×10^9/L, PLT62$\times10^9$/L, RBC 3.15×10^{12}/L, CRP 12mg	EBV-CV-IgG EBV PCR 1.02×10^3copies/ml	2, Alleviation
11	M/7y	6	Fever, Lymphadenopathy, Hepatosplenomegaly, hemophagocytic lymphohistiocytosis	WBC 6.44×10^9/L, PLT 145×10^9/L, RBC 4.45×10^{12}/L, CRP<8mg	EBV PCR 6.57×10^7copies/ml	1, Alleviation

Case No.	Structure destruction	Components of cells	Atypia	Necrosis	Diagnosis	CD3	CD20	CD56	TIA-1	GRB	CD4	CD8	Ki67	EBER(/HPF)
1	Yes	M	H	Yes	CAEBV-T/LPD A3	++	-	-	-	-	++	+	30%	>100
2	Yes	M	H	Yes	CAEBV-T/LPD A3	++	-	-	+	+	+	+	40%	>100
3	Yes	M	H	Yes	CAEBV-T/LPD A2	++	-	-	+	+	++	+	40%	50-100
4	Yes	L	H	No	CAEBV-T/LPD A3	++	-	+/-	+	+	+	+	50%	>100
5	No	M	M	No	CAEBV-T/LPD A1	++	-	-	-	-	+	+	10%	50-100
6	Yes	L	H	Yes	CAEBV-T/LPD A2	++	-	-	-	-	+	+	70%	>100
7	No	M	M	No	CAEBV-T/LPD A1	++	-	-	-	-	+	+	10%	50-100
8	Yes	M	H	No	CAEBV-B/LPD A2-3	+	++	-	-	-	+	+	80%	>100
9	No	M	M	Yes	CAEBV-T/LPD A2	++	-	-	+	+	++	+	35%	50-100
10	Yes	L	H	No	CAEBV-T/LPD A3	++	-	-	+	+	+	+	80%	50-100
11	Yes	M	H	Yes	CAEBV-T/LPD A3	++	-	-	-	-	++	+	40%	>100

Conclusions: Most of children's CAEBV diseases presenting initially with HLH are T/NK-LPD. The prognosis of this disease is variable and is not necessarily related to the histological grade. Some patients can progress over a long-term clinical course after supportive treatment and HLH therapy.